e-ISSN: 2149-3189

European Research Journal

Volume 12 Supplement 1 March 2026

Available at https://www.eurj.org.tr

The European Research Journal

Aim and Scope

The European Research Journal (EuRJ) is an international, independent, double-blind peer reviewed, Open Access and online publishing journal, which aims to publish papers on all the related areas of basic and clinical medicine.

Editorial Board of the European Research Journal complies with the criteria of the International Council of Medical Journal Editors (ICMJE), the World Association of Medical Editors (WAME), and Committee on Publication Ethics (COPE).

The journal publishes a variety of manuscripts including original research, case reports, invited review articles, technical reports, how-to-do it, interesting images and letters to the editor. The European Research Journal has signed the declaration of the Budapest Open Access Initiative. All articles are detected for similarity or plagiarism. Publication language is English.

EuRJ recommends that all of our authors obtain their own ORCID identifier which will be included on their article.

The journal is published (January, February, March, April, May, June, July, September, October, November and December).

Abstracting and Indexing

The journal is abstracted and indexed with the following: ULAKBIM TR Index (ULAKBİM TR DİZİN), NLM Catalog (NLM ID: 101685727), Google Scholar (h-index: 15), EMBASE, ProQuest Central, EBSCO Academic Search Ultimate, J-Gate, EZB, TURK MEDLINE, Turkish Citation Index, ResearhGate, SOBIAD, ScienceGate, Publons, (Clarivate Web of Science)

Publisher

The European Research Journal (EuRJ)
Nicaea Medical Publishing
Konak Mh. Kudret Sk. Şenyurt İş Mrk. Blok No:6 İç kapı no: 3 Nilüfer/Bursa-Türkiye
info@nicaeamp.com

https://dergipark.org.tr/en/pub/eurj
https://www.nicaeamp.com
Note: The European Research Journal has changed publishers with its March 2026 issue

e-ISSN: 2149-3189

EDITORIAL BOARD

EDITOR-IN-CHIEF

EDITORS

OWNER ON BEHALF OF THE NICAEA MEDİCAL PUBLISHING

ASSISTANT EDITOR

Dear Colleagues,

We are pleased to invite you to the 6th Uludağ Cardiology Summit, to be held at the Karinna Hotel Uludağ between March 26-29, 2026.

This year's congress will feature registered entries for both theoretical and practical presentations on the latest developments in cardiology policy. Developments in the field of cardiology will be discussed with expert participation. The congress aims to evaluate current advancements in the diagnostic and treatment spectrum. Oral presentations will allow for the presentation of research and projects in the field of cardiology, and the sharing of experiences.

The success of the congress depends on your active participation. We look forward to meeting you in the winter of 2026 and wish you a successful and productive congress...

Prof.Dr.Hasan ARI
Congress President

6th Uludag Cardiology Summit Organizing Committee

Congress President
Prof.Dr.Hasan ARI

Congress General Secretary
Prof.Dr.Hakan ERKAN

Congress Secretary
Prof.Dr.Alparslan BİRDANE

Bursa Uludag University, Faculty of Medicine,
Department of Cardiology

Prof.Dr.Tunay ŞENTÜRK
Prof.Dr.Sümeyye GÜLLÜLÜ
Prof.Dr.Dilek YEŞİLBURSA
Prof.Dr.Bülent ÖZDEMİR
Prof.Dr.Mustafa YILMAZ
Doç.Dr.Şeyda Günay POLATJKAN

University of Health Sciences, Bursa Faculty of Medicine
Bursa Yüksek İhtisas Training and Research Hospital,
Department of Cardiology

Prof.Dr.Fahriye VATANSEVER AĞCA
Doç.Dr.Mehmet MELEK
Doç.Dr.Ahmet TÜTÜNCÜ

Bursa City Hospital
Department of Cardiology

Prof.Dr.Mehmet DEMİR
Doç.Dr.Mustafa Adem YILMAZTEPE
Doç.Dr.Selma KENAR TİRYAKİOĞLU

Scientific Committee Members

Prof.Dr.Hasan ARI

Prof.Dr.Hakan ERKAN

Prof.Dr.Alparslan BİRDANE

Prof.Dr.Tunay ŞENTÜRK

Prof.Dr.Sümeyye GÜLLÜLÜ

Prof.Dr.Dilek YEŞİLBURSA

Prof.Dr.Bülent ÖZDEMİR

Prof.Dr.Mustafa YILMAZ

Doç.Dr.Şeyda Günay POLATJKAN

Prof.Dr.Fahriye VATANSEVER AĞCA

Doç.Dr.Mehmet MELEK

Doç.Dr.Ahmet TÜTÜNCÜ

Prof.Dr.Mehmet DEMİR

Doç.Dr.Mustafa Adem YILMAZTEPE

Doç.Dr.Selma KENAR TİRYAKİOĞLU

Scientific Programme

6. Uludağ Kardiyoloji Zirvesi
Bilimsel Programı

Saat	Salon	Program
		26 Mart 2026 Perşembe
16:00 - 17:00	A SALONU	PANEL KILAVUZLARDA GÜNCELLEME - 1 Oturum Başkanları: Mustafa Kemal Erol - Mahmut Açıkel 16:00 - 16:15 Gebelik ve Kalp Hastalıkları Kılavuzu - Çağlar Kaya 16.15-16.30 Kalp Kapak Hastalıkları Kılavuzu - Muhammet Gürdoğan 16.30-16.45 Miyokardit ve Perikardit Kılavuzu - Selda Murat 16.45-17.00 Tartışma
16:00 - 17:00	B SALONU	SÖZLÜ BİLDİRİ OTURUMU - 1 Oturum Başkanları: Ali Aydınlar - Sümeyye Güllülü - Saim Sağ Primer Perkütan Koroner Girişim Uygulanan STEMI Hastalarında Sol Ventrikül Yeniden Şekillenmesini Öngörmede HALP Skorunun Prognostik Değeri - Vedat Hekimsoy Vazospastik Anjina: Ergonovin ile Doğrulanan Koroner Spazm Olgusu - Ömer Fatih Savcı ST Eleve Miyokard Enfarktüsü ile Prezente Olan Koroner Vazospazm - Veysel Macit Koroner Arter Ektazisini Tahmin Etmede Intermountain Risk Skoru'nun Rolü - Şahhan Kılıç Primer PKG Uygulanan STEMI Hastalarında No-Reflow Gelişiminin Öngörülmesinde Pan-Immune-Inflammation Değerinin (PIV) Prognostik Rolü - Ali Sezgin NSTEMI Hastalarında Ürik Asit/Albümin Oranı ile No-Reflow Fenomeni Arasındaki İlişki - M. Mücahit Tiryaki Koroner Arter Stentlemesi Sonrası Kolşisin Kullanımı: Bir Yıllık Takip Sonuçları - Sherzod Akhmedov
17:00 - 17:30		KAHVE ARASI
17:30 - 18:45	A SALONU	PANEL KILAVUZLARDA GÜNCELLEME - 2 Oturum Başkanları: Nizamettin Toprak - Sinan Aydoğdu 17.30-17.45 Ruh Sağlığı ve Kardiyovasküler Hastalıklar Kılavuzu - Ferit Böyük 17.45-18.00 Disipidemi Kılavuzu - Erdal Belen 18.00-18.15 ACC/AHA Akut Koroner Sendromu Kılavuzu - Can Yücel Karabay 18.15-18.30 Ulusal Hipertansiyon Uzlaşı Raporu - Mehmet Akif Düzenli 18.30-18.45 Tartışma
Saat	**Salon**	**Program**
17:30 - 18:45	B SALONU	SÖZLÜ BİLDİRİ OTURUMU - 2 Oturum Başkanları: Tahsin Bozat - Ufuk Aydın - Yusuf Ata Minimal Semptom, Maksimum Risk: 81 mm Asendan Aort Anevrizmasına Eşlik Eden Gizli Tip A Diseksiyon - Yakup Han Yılmaz Gözden Kaçan Bir Fenotip: Görme Kaybı ile Ortaya Çıkan Yaygın Nonkalsifik Ateroskleroz - Nuray Mammadova Perkütan Koroner Girişim (PCI) Sırasında Radyal Spazm ve Komplikasyonların Önlenmesinde Farmakolojik Kokteyllerin Rolü: Klinik Bir Çalışma - Javokhir Akhrorov İskemik İnme Sonrası Kırılganlığın Öngörülmesinde PNI'nin Rolü: Orta Dönem Klinik Izlem Verileri - Eda Özcan Diseke Lezyon İçinde Sıyrılan Stent Vakasının Yönetimi - Veysel Macit Kolşisinin Tekrarlayan Kalp Pili Cep Enflamasyon Yönetimine Katkısı:Olgu Sunumu - Tolga Koşmaz Safen Bypass Greft Anevrizmasının Amplatzer ASD Kapama Cihazı ile Kapatılması - Hamza Baha Kandemir Anjinanın Beklenmedik Nedeni: Internal Mammary Arter-Sol Atriyum Fistülünün Başarılı Perkütan Kapatılması - Ecem Gürses
19:30 - 21:30		AKŞAM YEMEĞİ
Saat	**Salon**	**Program**
		27 Mart 2026 Cuma
09:00 - 10:00	A SALONU	PANEL HER YÖNÜYLE MİTRAL KAPAK Oturum Başkanları: Saide Aytekin - Omaç Tüfekçioğlu 09:00 - 09:12 Mitral Darlığının Değerlendirilmesi - Türkan Seda Tan 09:12 - 09:24 Mitral Yetmezliğinde Etiyolojik Değerlendirme ve Ciddiyetin Değerlendirilmesi - Pelin Karaca Özer 09:24 - 09:36 Atriyal MY 'yi Nasıl Tanıyalım, Nasıl Yönetelim? - Demet Menekşe Gerede 09:36 - 09:48 MY Hastasında Mitral TEER - Sinem Özbay 09.48 - 10.00 Tartışma
09:00 - 10:00	B SALONU	SÖZLÜ BİLDİRİ OTURUMU - 3 Oturum Başkanları: Erhan Tenekecioğlu - Enbiya Aksakal - Tezcan Peker Kalp Yetersizliği Hastalarında SGLT-2 İnhibitörlerinin Ortalama Trombosit Hacmi Üzerine Etkisi - Ferhat Perk Sirozda Subklinik Miyokard Disfonksiyonunun 4D Strain ile Değerlendirilmesi - Mahmut Kapsız Karotis Arter Stentleme Uygulanan Hastalarda Hastane İçi İskemik İnme Gelişimini Öngörmede Aterojenik İndeks Plazmanın Kullanılabilirliği - Tuba Unkun ST Yükselmeli Miyokard İnfarktüsünde Reperfüzyonu Öngörebilir miyiz? - Gülümser Sevgin Halil Bir İmplantasyon, İki Sınav: Anatomik Zorluk ve Post-Cardiac Injury Sendromu - Orkhan Yunisli Genç Erişkin Bireylerde Trigliserid/HDL Kolesterol İndeksi ile Hipertansiyon Arasındaki İlişki - Ahmet Yılmaz ST Elevasyonu Olmayan Miyokard Enfarktüsü Hastalarında Total Oklüzyonu Öngörmede Plazma Aterojenik İndeksinin Klinik Önemi - Enes Çelik
10:00 - 10:20		KAHVE ARASI
10:20 - 11:00	A SALONU	UYDU SEMPOZYUMU - 1 UYDU SEMPOZYUMU - ASTRA ZENECA Oturum Başkanı: Erdal Belen Kalp Yetersizliği Tedavisinde Forziga - Erdal Belen, Selma Tiryakioğlu

Saat	Salon	Program
10:20 - 11:00	B SALONU	SÖZLÜ BİLDİRİ OTURUMU - 4 Oturum Başkanları: Hakan Özkan - İbrahim Baran - Hasan Arı Selektif Sol Dal Pacingin Prediktörleri ve Kısa Dönem Klinik Sonuçları - Davut Davutoğlu Gecikmiş QRS Geçiş Bölgesi ve Diyabet Mellitus Arasındaki İlişki - Yakup Han Yılmaz Kronik Piretiroid Maruziyetinin Kardiyak Etkileri - Safa Oktay Ventriküler Aritmiyle Prezente Olan Bir Long QT Sendromu Olgusu - Davut Davutoğlu Kardiyak Defibrilatör İmplantasyonu Sırasında Gelişen Hemoptizi: Nadir Bir Komplikasyon - Yasin Aktaş
11:00 - 11:20		KAHVE ARASI
11:20 - 12:20	A SALONU	PANEL KALP YETERSİZLİĞİ Oturum Başkanları: Yüksel Çavuşoğlu - Mehmet Birhan Yılmaz 11:20 - 11:32 Kalp Yetersizliği Neden mi? Sonuç mu? Etiyolojik Araştırma Nereye Kadar? - Ahmet Çelik 11:32 - 11:44 Kalp Yetmezliği İlaç Tedavisindeki Güncel Durum - Hakkı Kaya 11:44 - 11:56 İleri Kalp Yetmezliği Hastasını Nakil için Ne Zaman Yönlendirelim? Sağ Ventrikülü Gözden mi Kaçıyoruz? - Umut Kocabaş 11:56 - 12:08 Kalp Yetmezliğinde Cihaz Tedavilerini Abartıyor muyuz? - Erol Tülümen 12.08 - 12.20 Tartışma
11:20 - 12:20	B SALONU	SÖZLÜ BİLDİRİ OTURUMU - 5 Oturum Başkanları: Bülent Özdemir - Fatih Levent - Fatih Koca Anaflaksi Sonrası Akut Koroner Sendrom Vakası:Kounis Sendromu - Adem Yarar Kardiyak Lenfoma: Nadir Görülen Bir Olgu Sunumu - Abdulsamet Arslan Spironolakton-Hidroklorotiyazid Kullanan Orta Yaşlı Bir Kadında Hiponatremik Nöbet - Mehmet Zafer Aydın Nondiabetik ve Nonobez Bireylerde İzole Nokturnal Hipertansiyonun Öngördürücüleri - Çağdaş Kaynak Güncel Kılavuzlara Uygun Tedavinin Enfektif Endokarditte Hastane İçi Sonuçlara Etkisi - Mustafa Kara Kronik Total Oklüzyonlar İçin Sadece İlaç Kaplı Balon (DCB) Stratejisi: 48 Hastalık Prospektif, İki Merkezli Çalışma - Sherzod Akhmedov Akut Miyokard İnfarktüsü ile Başvuran Hastalarda Frontal QRS-T Açısının Koroner Trombüs Yükünü Öngördürme Değeri - Yakup Han Yılmaz
12:20 - 14:00		ÖĞLE YEMEĞİ
13:00 - 14:00	B SALONU	IVUS KURSU Eğitmenler - Emrah Erdoğan, Alper Karakuş

Saat	Salon	Program
14:00 - 15:00	A SALONU	PANEL GİRİŞİMSEL KARDİYOLOJİ : KORONER STENTLEME SANATI Oturum Başkanları: Cevat Kırma - Vedat Aytekin 14:00 - 14:12 İntrakoroner Görüntüleme - Neryan Özgül Özden 14:12 - 14:24 Koroner Plak Modifikasyonu - Kadriye Kılıçkesmez 14:24 - 14:36 Koroner Stent Seçimi - Serkan Kahraman 14:36 - 14:48 Koroner İlaçlı Balonlar - Hasan Ali Barman 14.48 - 15.00 Tartışma
14:00 - 15:00	B SALONU	SÖZLÜ BİLDİRİ OTURUMU - 6 Oturum Başkanları: Hakan Erkan - Emre Erkuş - Bedrettin Boyraz Dirençli Radial Arter Spazmında İntraarteriyel Lidokain Kullanımı - Yasin Aktaş Kapama Bir Engel Haline Geldiğinde: Kompleks Bir Mitral Paravalvüler Kaçağın Yönetimi - Fatih Cihat Büyükbaş Transkateter Aort Kapak İmplantasyonu Sonrası Yüksek Dereceli Atriyoventriküler Blok Gelişimini Öngören Rutin Klinik ve Lipid Parametreler: Tek Merkezli Pragmatik Bir Çalışma - Mert Şentürkün Çoklu Membranöz Ventriküler Septal Defektlere Perkütan Tedavi Yaklaşımı - Sena Tokatlı Tropoinin Pozitifliğinde Tip 2 Miyokard İnfarktüsü İle Miyokard Hasarı Ayrımı: Retrospektif Klinik Sınıflama ve 30 Günlük Prognoz - Muhammet Geneş Transradyal Girişim Sonrası Akut Aksiller Arter Oklüzyonu: Olgu Sunumu - Serdar Enes Akcan Karotis Arter Stentleme Sonrası Kontrast Maddeye Bağlı Nefropatiyi Tahmin Etmek İçin Çok Alanlı Risk Kümesi - Aibek Orozbaev
15:00 - 15:20		KAHVE ARASI
15:20 - 16:00	A SALONU	UYDU SEMPOZYUMU - 2 UYDU SEMPOZYUMU - MERIL Oturum Başkanı: Engin Bozkurt Myval Octacor Optimal İmplantasyon Teknikleri - Teoman Kılıç

Saat	Salon	Program
15:20 - 16:00	B SALONU	SÖZLÜ BİLDİRİ OTURUMU - 7 Oturum Başkanları: Mustafa Yılmaz - Tolga Doğan - Mehmet Tuğrul Göncü Kardiyak AL Amiloidozunda Tanısal Zorluklar: Görüntüleme, Serum Biyobelirteçlerinden Daha Önemli Olduğunda - Burak Yaman Akut Ekstremite İskemisinde Tromboembolektomi Sonrası Akut Böbrek Hasarı ile Preoperatif Serum Magnezyum Düzeyleri Arasındaki İlişki - Fuat Ahmet Bilyay Koroner Arter Bypass Greftleme Ameliyatı Geçirecek Diyabetik Hastalarda Eş Zamanlı Karotis Arter Hastalığının Öngörülmesinde Ekzokrin Pankreas Yetersizliğinin Rolü - Abdulkerim Özkan TASC II Lezyon Şiddeti ile Karotis Arter Darlığı Arasındaki İlişki: Kesitsel Bir Analiz - Çağlar Alp Mekanik Kapak Trombozunda Görüntüleme Rehberli Tromboliz ile Acil Cerrahinin Önlenmesi - Mert Şentürkün
16:00 - 16:20		KAHVE ARASI
16:20 - 17:20	A SALONU	PANEL GİRİŞİMSEL İŞLEMLERDE GÖRÜNTÜLEME Oturum Başkanları: Teoman Kılıç - Faruk Ertaş 16:20 - 16:32 İnteratriyal Septum Değerlendirmesi - Selcen Yakar Tülüce 16:32 - 16:44 Sol Atriyal Apendiks Kapama - Münevver Sarı 16:44 - 16:56 PVL'de Görüntüleme - Hatice Tolunay 16:56 - 17:08 İntraoperatif Transözefageal Ekokardiyografi - Fulya Avcı Demir 17:08 - 17:20 Tartışma
16:20 - 17:20	B SALONU	SÖZLÜ BİLDİRİ OTURUMU - 8 Oturum Başkanları: Dilek Yeşilbursa - Dursun Topal - Burhan Aslan Hemodiyaliz Hastalarında Volüm Yükünün Ventrikülo-Arteriyel Coupling Üzerine Etkisi - Seray Yazgan Sistemik Koagülasyon İnflamasyon İndeksi Karotis Endarterektomi Sonrası Daha Kötü Sonuçların Bir Göstergesi Olabilir mi? - Mehmet Sadık Akpınar Akut Dekompanse Kalp Yetmezliğinde CONUT Skoru ve Hastanede Kalış Süresi - Çağatay Tunca Kronik Böbrek Yetmezliği Olan Hastalarda Kardiyovasküler Mortalitenin Bağımsız Bir Öngörücüsü Olarak Miyokardiyal Kontraksiyon Fraksiyonu - Oğuz Kağan Şentürk Koroner Full Metal Ceket Olgularında Cerrahi Stentektomi ve Bypass - Demir Çetintaş Ozaki Prosedürü - Mustafa Selçuk Atasoy Koroner BT Anjiyografinin İnvaziv Koroner Anjiyografiye Göre Tanısal Performansı ve Koroner Kalsiyum Skorunun Etkisi: Tek Merkezli Gerçek Yaşam Çalışması - Shokhzod Atashev
17:20 - 17:40		KAHVE ARASI
17:40 - 18:00	A SALONU	AÇILIŞ TÖRENİ

Saat	Salon	Program
18:00 - 18:30	A SALONU	PANEL MESLEKİ TECRÜBELER, DENEYİMLER VE GELECEK VİZYONU Konuşmacılar - Kemalettin Aydın, Feridun Yılmaz, Mehmet Demir, Soner Cander
18:00 - 18:30	B SALONU	AKILCI İLAÇ KULLANIMI Oturum Başkanı: Ahmet Tütüncü Konuşmacı - Sencer Çamcı
19:30 - 21:30		AKŞAM YEMEĞİ

Saat	Salon	Program
		28 Mart 2026 Cumartesi
09:00 - 10:00	A SALONU	PANEL KORONER ARTER HASTALIĞI Oturum Başkanları: Mustafa Karaca - Kürşat Tigen Kalsifik Koroner Vakası - Nihat Kalay, Serkan Kahraman
09:00 - 10:00	B SALONU	SÖZLÜ BİLDİRİ OTURUMU - 9 Oturum Başkanları: Osman Akın Serdar - Tunay Şentürk - Mehmet Melek Persistan Atriyal Fibrilasyonda Tek ve İki Defibrilatör ile Ortogonal Elektriksel Kardiyoversiyonun Etkinliğinin Karşılaştırılması - Esra Akpınar Postpartum KMP Gelişen bir c-TGA Hastasında AV Blok: Sağ Taraflı Kardiyak Resenkronizasyon Tedavisi - Rauf Samet Gençgün Septal Occluder Cihazı İçinden Transseptal Geçişle Af-Ablasyon Yapılan Bir Olgu - Semih Babacan Transkateter Aort Kapak Implantasyonu Geçiren Hastalarda Hastane İçi Majör Kardiyak Olayların Öngörücüsü Olarak Fragmente QRS - Özkan Bekler INOCA'nın Öngörülmesinde Sistemik İmmün-İnflamasyon İndeksinin Prognostik Değeri - Mustafa Ferhat Keten
10:00 - 10:20		KAHVE ARASI
10:20 - 11:00	A SALONU	UYDU SEMPOZYUMU - 3 UYDU SEMPOZYUMU - MEDINTEK Oturum Başkanı: Mehmet Melek Allegra Kapak İmplantasyonu - Can Yücel Karabay
10:20 - 11:00	B SALONU	SÖZLÜ BİLDİRİ OTURUMU - 10 Oturum Başkanları: Vedat Koca - Feyzullah Beşli Mekanik Mitral Kapak Replasmanı Sonrası Gelişen Mitral Paravalvuler Kaçağın Transkatater Yöntemle Kapatılması: Olgu Sunumu - Şirin Şebnem Önür Yanlış Extravasasyon Tanısı: Stent Malpozisyonu ve Çözümü - Mehmet Mert Dönmez Sigara Kullanımı ile Miyokardiyal Performans Arasındaki İlişkide Kalp Hızının Aracılık Edici Rolü - İsmail Balaban LIMA Grefti Olan Hastada Trombotik Subklavyen Oklüzyona Bağlı STEMI - Yasin Aktaş Kateter Laboratuvarında Kabus: LMCA Diseksiyonu - M. Nusret Akın
11:00 - 11:20		KAHVE ARASI

Saat	Salon	Program
11:20 - 12:10	A SALONU	PANEL PULMONER HİPERTANSİYON Oturum Başkanları: Serdar Küçükoğlu - Mehmet Akbulut 11:20 – 11:30 Doğru PCWP Ölçümü - Kartal Emre Aslanger 11:30 - 11:40 Grup 1-2 Ayırıcı Tanısında Yol Ayrımları - Çağlar Çağlayan 11:40 - 11:50 Bağ Dokusu Hastalarında Grup 1-3 Tanısında Yol Ayrımları - Dilek Çiçek Yılmaz 11:50 - 12:00 Her ASD'yi Kapatmalı mıyız? - Barış Kaya 12:00 - 12:10 Tartışma
11:20 - 12:10	B SALONU	PANEL KARDİYAK YOĞUN BAKIM HEMŞİRELİĞİ- 1 Oturum Başkanları: Mesut Engin - Sevil Tecir - Öznur Acar Kalp Yetersizliğinde Hastaneye Tekrar Yatışları Önlemede Kendi Kendilerine Bakım Yönetimi ve Hasta Eğitimi - Ramazan Tek Kardiyoloji Yoğun Bakım Hemşirelerinde Merhamet Yorgunluğu ve Tükenmişlikle Baş Etme Yolları - Esma Aydoğdu İmplante Edilen Kardiyoverter Defibrilatörü Olan Hastalarda Hemşirelik Yönetimi - Kader Eren Kardiyak Yoğun Bakım Ünitesinde Terminal Dönem Hasta Bakımı ve "Onurlu Ölüm" Kavramında Hemşirenin Etik Sorumlulukları - Hamide Baykan Karataş İnotrop Desteği Altındaki Hastada Hemşirelik Yönemi - Gökhan Kalkan
12:10 - 12:30		KAHVE ARASI
12:20 - 14:00		ÖĞLE YEMEĞİ
12:30 - 13:00	A SALONU	PANEL SAĞLIKTA GELECEK Oturum Başkanları: Mehmet Birhan Yılmaz - Ayhan Olcay Kardiyolojide İnnovasyon - Ayhan Olcay Kardiyolojide Klinik Araştırma Vizyonu - Mehmet Birhan Yılmaz
13:00 - 14:00		ÖĞLE YEMEĞİ
13:20 - 14:10	B SALONU	MITRAKLIP KURSU Eğitmenler - Hakan Uçar, Sinem Özbay

Saat	Salon	Program
14:00 - 15:20	A SALONU	PANEL HER TELDEN KARDİYOLOJİ Oturum Başkanları: Cihan Ören - Engin Bozkurt 14:00 - 14:08 MI Sonrası Betabloker Ne Kadar Süreyle Verelim? - Davran Çiçek 14:08 - 14:16 İnflamasyon ve Kalp - Ahmet Barutçu 14:16 - 14:24 Koroner Arter Hastalığında Yeni Antitrombotik Stratejiler - Taner Şen 14:24 - 14:32 Obezite ve Kalp - Metin Güçlü 14:32 - 14:40 Yapay Zeka ve Kardiyoloji - Evrim Şimşek 14:40 - 14:48 Kalp Hastalıklarında Genetik Tarama - Şebnem Sağ 14:48 - 14:56 Mitral Yetersizliği Cerrahisi Olacak AF'li Hastada AF Ablasyonu/LAA Kapama Önerelim mi? - Başar Candemir 14:56 - 15:20 Tartışma
14:20 - 15:20	B SALONU	PANEL KATETER LABORATUVARI HEMŞİRELİĞİ-1 Oturum Başkanları: Ömer Furkan Demir - Ercan Karabey Kalp mi Kırık, Yoksa Ruh mu?, Takotsuba Kardiyomiyopatisi - Hatice Özyıldırım Radyasyon Güvenliği Ve Çalışan Sağlığı - Uğur Güneş Supraventriküler Taşikardilerin Fizyolojisi - Doğukan Dülker Primer PCI Vakalarında Anjiyo Hemşireliği - Halil Emre Gündoğan TAVI Vakalarında Hasta ve Salon Hazırlığı - Yüksel Çiçek Katater Labratuvarında ECMO Uygulaması - Harun Karaoğlu
15:20 - 15:40		KAHVE ARASI
15:40 - 16:20	A SALONU	UYDU SEMPOZYUMU – 4 UYDU SEMPOZYUM – BİOTRONİK Oturum Başkanı: Uğur Canpolat İleti Sistemi Pacing - Uğur Canpolat, Enes Elvin Gül

Saat	Salon	Program
15:40 - 16:20	B SALONU	PANEL KARDİYAK YOĞUN BAKIM HEMŞİRELİĞİ- 2 Oturum Başkanları: Selma Arı - Eylem Paslı Gürdoğan İABP Destekli Hastada Hemşirenin Kritik Rolü - Merve Aslan TAVI Hastasında Hemşirelik Bakımı - Yeter Esen STEMI Hastasında Dakikalarla Yarış, Acil Hemşiresinin Zaman Yönetimindeki Kritik Rolü - Zozan Kahraman Akut Kalp Yetmezliğinde İlk Saat Yönetimi, Acil Hemşiresinin Rolü - Feyza Akyüz
16:20 - 16:40		KAHVE ARASI
16:40 - 17:40	A SALONU	PANEL ARİTMİ Oturum Başkanları: Dursun Aras - Sedat Köse 16:40 - 16:52 İleti Sistemi Pacing - Selçuk Kanat 16:52- 17:04 Leadless Pacemaker - Fethi Kılıçaslan 17:04 - 17:16 Sık VES'i Olan Hastaya Yaklaşım - Kutay Vurgun 17:16-17:28 Non-invaziv Ritm Değerlendirmesi - Abdulkadir Uslu 17:28-17:40 Tartışma
16:40 - 17:40	B SALONU	KATETER LABORATUVARI HEMŞİRELİĞİ-2 Oturum Başkanları: Çetin Alak - Zülfiye Tay Göven - Dudu Biler IVUS vakalarında Hasta ve Salon Hazırlığı - Gamze Gelen FFR Vakalarında Hasta ve Salon Hazırlığı - Mustafa Demir Perkütan Mitral Balon Valvüloplasti Vakasında Hasta ve Salon Hazırlığı - Lütfiye Taşkın Perkütan ASD Kapama Vakasında Hasta ve Salon Hazırlığı - Yasin Oruç
17:40 - 18:00		KAHVE ARASI
18:00 - 19:00	A SALONU	PANEL BİLİMSEL YAZI YAZMA VE EDİTÖRE KABUL ETTİRME SANATI Moderatörler: Bilgin Timuralp - Şenol Yavuz Konuşmacı: - Servet Altay
19:30 - 21:30		AKŞAM YEMEĞİ

Saat	Salon	Program
		29 Mart 2026 Pazar
09:00 - 10:00	A SALONU	PANEL GİRİŞİMSEL İŞLEMLERDE KOMPLİKASYON YÖNETİMİ: İLGİNÇ VAKA VE KOMPLİKASYON OTURUMU YARIŞMASI Oturum Başkanları: Mehmet Ertürk - Levent Korkmaz 09:00 - 09:12 Olgularla Pacemaker Komplikasyonları - Kıvanç Yalın 09:12 - 09:24 Olgularla Koroner Komplikasyon - Eyüp Avcı 09:24 - 09:36 Olgularla Yapısal Komplikasyon - Serkan Aslan 09:36 - 09:48 Olgularla Periferik Komplikasyon - Bektaş Murat 09:48 - 10:00 Tartışma
09:00 - 10:00	B SALONU	SÖZLÜ BİLDİRİ OTURUMU - 11 Oturum Başkanları: Fahriye Vatansever Ağca - Berat Uğuz - İsmet Zengin Perimiyokardit Gölgesinde Malign RCA - Ayşe Nilgün Kara Gebeliğin Bedeli mi? IVF Sonrası Peripartum Kardiyomiyopati - Ayşe Nilgün Kara Enfektif Endokarditin Karanlık Yolu: Multimodalite Görüntüleme ile Aydınlatılan Protez Kapak Endokarditi ve Komplikasyonları - Muhammed Yahya Demirel LFLG-AS Hastalarında CAR Düzeyinin TAVI Sonrası In-Hospital Mortaliteyi Öngördürmedeki Rolü - Doğancan Çeneli Stuck Kapakta Mortalite Prediktörü: Occluder Pozisyonu - Hüseyin Sefa İnce TAVI'de Myval, Portico ve Evolut-R Kapaklarının VARC-3 Sonuçları - Ümit Bulut
10:00 - 10:20		KAHVE ARASI
10:20 - 11:30	A SALONU	PANEL KARDİYOLOJİ'DE 2025 YILI GÜNCELLEMESİ: 2025 YILI TOP 10 ÇALIŞMALAR Oturum Başkanları: Yekta Gürlertop - İbrahim Halil Kurt 10:20 - 10:28 2025'de Kardiyo Onkoloji - Cafer Zorkun 10:28 - 10:36 2025'de Aritmiler - Mehmet Özgeyik 10:36 - 10:44 2025'de Koroner Arter Hastalığı - Kadir Uğur Mert 10:44 - 10:52 2025'de Kapak Hastalıkları - Ali Rıza Akyüz 10:52 - 11:00 2025'de Girişimsel Kardiyoloji - Hakan Güllü 11:00 - 11:08 2025'de Kalp Yetersizliği - Gönenç Kocabay 11:08 - 11:16 2025'de Kardiyak Görüntüleme - Bilge Duran Karaduman 11:20 - 11:30 Tartışma

Saat	Salon	Program
10:20 - 11:30	B SALONU	SÖZLÜ BİLDİRİ OTURUMU - 12 Oturum Başkanları: Alparslan Birdane - Aysel Aydın Kaderli Rutin Antikolinerjik Ön Tedavi Olmaksızın Yapılan Karotis Arter Stentlemenin Güvenlik ve Etkinliği - İbrahim Aktaş Radyal Yolla Yapılan Koroner Anjiyografide Fraksiyone Olmamış Heparin Uygulama Zamanının Radiyal Arter Spazmı ve Oklüzyonuna Etkisi - Doğan Ormancı Çift TAVI Kapak Komşuluğunda Gelişen Ciddi Paravalvular Kaçağın Perkütan Kapatılması - Buse Çuvalcıoğlu Embolizan Ajanla Adhezyona Bağlı Mikrokateter Fraktürü: Endovasküler Snare ile Girişim - Sena Tokatlı Opere Fallot Tetralojisi Hastasında Rezidü Ventriküler Septal Defektin Perkütan Kapatılması - İsmail Adsız Gerçek LCx-OM Bifurkasyon Lezyonunda (Medina 1.1.1) Sadece İlaç Salan Balon (DCB) Stratejisi: 12 Aylık Takipli Olgu Sunumu - Jurayev Ilkhom Şiddetli Kalsifik LAD In-Stent Under-Expansion'da Başarısız Litotripsi ve Cerrahi Revaskülarizasyon - İsmail Adsız
11:30 - 11:45	A SALONU	KAPANIŞ OTURUMU KAPANIŞ TÖRENİ

6th Uludag Cardiology Summit

March 26-29, 2026, Bursa, Türkiye

MEETING ABSTRACTS

Oral Presentations

Eur Res J. 2026;12(Suppl 1):S1-S135
DOI: https://doi.org/10.18621/eurj.1260

MEETING ABSTRACTS

Meeting Abstracts of the 6th Uludag Cardiology Summit, March 26-29, 2026, Bursa, Türkiye

MEETING ABSTRACTS

Submitted: March 15, 2026; **Accepted:** March 27, 2026; **Published Online:** March 27, 2026

e-ISSN: 2149-3189

OP-01.
Prognostic Value of the HALP Score for Predicting Left Ventricular Remodeling in STEMI Patients Undergoing Primary PCI

Vedat Hekimsoy[1], Çağatay Tunca[1]

[1]*Department of Cardiology, Ankara Etlik City Hospital, Ankara, Türkiye*

Objectives: Left ventricular remodeling (LVR) after ST-elevation myocardial infarction (STEMI) is a major determinant of adverse outcomes and remains an important clinical challenge. Identification of patients at risk for remodeling is crucial for early intervention. The Hemoglobin, Albumin, Lymphocyte, and Platelet (HALP) score is a novel index reflecting both nutritional and inflammatory status, yet its prognostic significance in STEMI has not been fully clarified. To evaluate the prognostic value of the HALP score in predicting LVR after primary percutaneous coronary intervention (PCI) in STEMI patients and to compare its performance with conventional inflammatory and nutritional indices.
Methods: A total of 240 consecutive STEMI patients who underwent successful primary PCI were retrospectively analyzed. Echocardiography was performed at baseline and at 3-month follow-up. LVR was defined as a ≥20% increase in left ventricular end-diastolic volume. HALP, neutrophil-to-lymphocyte ratio (NLR), lymphocyte-to-monocyte ratio (LMR), platelet-to-lymphocyte ratio (PLR), and prognostic nutritional index (PNI) were calculated at admission. Independent predictors were identified using logistic regression, and receiver operating characteristic (ROC) analysis compared the predictive performance of the indices.
Results: LVR developed in 57 (23.7%) patients. Patients with LVR had significantly lower HALP scores compared with those without LVR (22±7 vs. 35±8, P<0.001) (Table 1). In multivariate analysis, HALP was an independent predictor of LVR (OR: 1.42, 95% CI: 1.15–1.74, P<0.001) (Table 2). ROC analysis demonstrated superior prognostic accuracy of HALP (AUC=0.72) compared with NLR (0.64), LMR (0.60), PLR (0.61), and PNI (0.68) (Table 3, Figure 1).
Conclusion: HALP score, by incorporating both nutritional and inflammatory components, provides a more comprehensive risk assessment than traditional indices. Its ability to independently predict LVR highlights its potential role in guiding clinical decision-making and tailoring follow-up strategies in STEMI patients.
Keywords: HALP score, Left Ventricular Remodeling, ST-Elevation Myocardial

TABLE 1. Baseline Demographic, Clinical, Laboratory, Echocardiographic and Treatment Characteristics According to Left Ventricular Remodeling Status in STEMI Patients

Parameter	Total (n=240)	LVR (n=57)	No LVR (n=183)	P-value
Age (years)	59±10	60±9	58±10	0.21
Male sex (%)	176 (73.3)	43 (75.4)	133 (72.7)	0.68
BMI (kg/m²)	26.1±3.4	27.2±3.2	25.7±3.5	0.03
Hypertension (%)	102 (42.5)	26 (45.6)	76 (41.5)	0.55
Diabetes Mellitus (%)	58 (24.1)	18 (31.6)	40 (21.9)	0.04
Oral antidiabetic use (%)	36 (15.0)	11 (19.3)	25 (13.7)	0.24
Smoking (%)	124 (51.7)	31 (54.4)	93 (50.8)	0.64
Family history CAD (%)	62 (25.8)	17 (29.8)	45 (24.6)	0.42
Systolic BP (mmHg)	128±18	125±16	129±18	0.17
Diastolic BP (mmHg)	77±10	76±9	78±11	0.29
Heart rate (bpm)	79±13	82±12	78±13	0.08
Killip class ≥ II (%)	29 (12.1)	11 (19.3)	18 (9.8)	0.04
Anterior MI (%)	152 (63.3)	42 (73.7)	110 (60.1)	0.05
Multivessel disease (%)	72 (30.0)	20 (35.1)	52 (28.4)	0.33
Glucose (mg/dL)	106±22	113±25	104±20	0.01
Triglyceride (mg/dL)	161±52	175±54	156±50	0.03
Total cholesterol (mg/dL)	201±35	206±36	199±34	0.18
HDL (mg/dL)	39±7	37±6	40±7	0.04
LDL (mg/dL)	131±30	136±31	129±29	0.16
Creatinine (mg/dL)	1.0±0.3	1.1±0.3	1.0±0.3	0.21
NT-proBNP (pg/mL)	510 (280–1700)	720 (300–1680)	460 (270–1340)	**<0.001**
Peak troponin I (ng/mL)	11.2 (2–28)	15.0 (4–28)	9.8 (2–25)	**<0.001**
HALP score	32±9	22±7	35±8	**<0.001**
NLR	3.1±1.4	3.6±1.5	2.9±1.2	0.01
LMR	2.7±0.8	2.4±0.7	2.9±0.8	0.02
PLR	145±55	160±60	140±50	0.04
PNI	47±5	44±6	48±5	0.01
Baseline LVEF (%)	38±7	35±6	39±7	0.01
Baseline LVEDV (mL)	110±28	115±26	108±29	0.15
Baseline LVESV (mL)	45±12	47±11	44±12	0.04
Follow-up LVEF (%)	47±9	39±7	50±8	**<0.001**
Follow-up LVEDV (mL)	120±30	143±28	113±27	**<0.001**
Follow-up LVESV (mL)	52±14	61±12	49±13	**<0.001**
Beta-blocker (%)	222 (92.5)	52 (91.2)	170 (92.9)	0.69
ACEi/ARB (%)	228 (95.0)	54 (94.7)	174 (95.1)	0.92
Statin (%)	232 (96.7)	55 (96.5)	177 (96.7)	0.94
Aspirin (%)	238 (99.2)	57 (100)	181 (98.9)	0.32
P2Y12 inhibitor (%)	240 (100)	57 (100)	183 (100)	—

Data are shown as mean±standard deviation or n (%) where appropriate. BP, blood pressure; CAD, coronary artery disease; HALP, hemoglobin, albumin, lymphocyte, and platelet; LMR, lymphocyte-to-monocyte ratio; LVEDV, left ventricular end-diastolic volume; LVEF, left ventricular ejection fraction; LVESV, left ventricular end-systolic volume; LVR, left ventricular remodeling; NLR, neutrophil-to-lymphocyte ratio; PLR, platelet-to-lymphocyte ratio; PNI, prognostic nutritional index. Statistically significant values are shown in bold.

TABLE 2. Multivariate Logistic Regression Analysis for Predictors of Left Ventricular Remodeling in STEMI Patients

Variable	OR	95% CI	P-value
HALP score	1.42	1.15–1.74	**<0.001**
NLR	1.11	0.98–1.26	0.092
LMR	0.89	0.74–1.08	0.221
PLR	1.01	0.99–1.02	0.145
PNI	0.94	0.88–1.01	0.076
Diabetes mellitus	1.30	0.80–2.10	0.28

HALP, hemoglobin, albumin, lymphocyte, and platelet; LMR, lymphocyte-to-monocyte ratio; NLR, neutrophil-to-lymphocyte ratio; PLR, platelet-to-lymphocyte ratio; PNI, prognostic nutritional index. Statistically significant value is shown in bold.

Table 3. ROC Analysis for Prediction of Left Ventricular Remodeling in STEMI Patients

Index	AUC	Cut-off (sensitivity/specificity)
HALP	0.72	24 (71%/65%)
NLR	0.64	3.2 (63%/60%)
LMR	0.60	2.5 (58%/55%)
PLR	0.61	150 (60%/57%)
PNI	0.68	46 (66%/62%)

HALP, hemoglobin, albumin, lymphocyte, and platelet; LMR, lymphocyte-to-monocyte ratio; NLR, neutrophil-to-lymphocyte ratio; PLR, platelet-to-lymphocyte ratio; PNI, prognostic nutritional index.

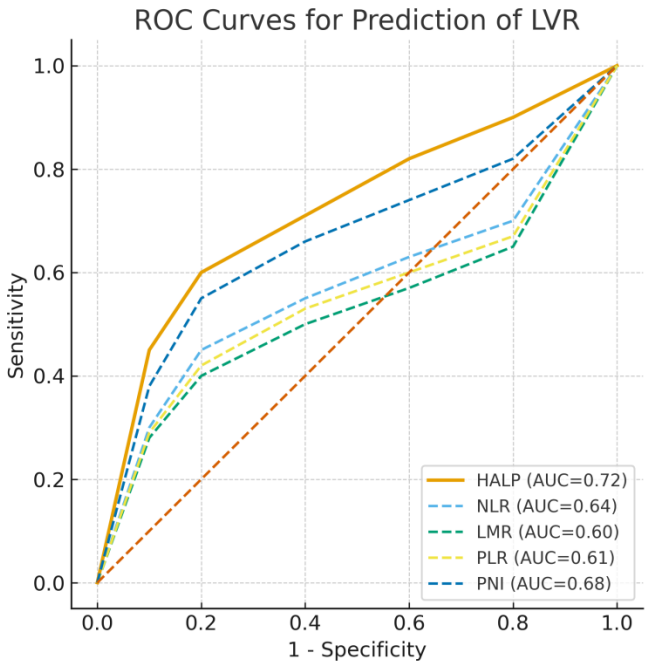

FIGURE 1. ROC curves comparing indices for prediction of left ventricular remodeling in STEMI patients.

OP-02.
Short Term Clinical Outcomes and Predictors of Selective Left Bundle Branch Pacing

Fatih Levent[1], Ahmet Tütüncü[1], Özlem Karakurt[1], Gökhan Özmen[1], Kübra Severgün[1], Mustafa Kinik[1], Fatih Koca[1], Davut Davutoğlu[1]

[1]Department of Cardiology, University of Health Sciences, Bursa Yüksek İhtisas Training and Research Hospital, Bursa, Türkiye

Objectives: Since right ventricular apex pacing in patients with permanent pacemakers causes adverse outcomes such as heart failure and increased mortality due to electrical and mechanical ventricular asynchrony, left bundle branch pacing (LBBP) methods, have recently been developed. In this study, we investigated the short-term outcomes of selective left bundle branch pacing patients and the predictors of selective left bundle branch pacing.
Methods: The study was a single-center, observational study. Patients over the age of 18 who were scheduled for LBBP between January 2024-June 2024 were identified. Patients with severe chest deformities and poor echocardiographic image quality were excluded. All patients' pre-procedure electrocardiographic characteristics (baseline rhythm, bundle branch block), clinical and demographic characteristics, laboratory parameters, and New York Heart Association (NHYA) functional capacity levels were recorded. In addition to baseline 2D echocardiographic measurements, the aortic septal angle (ASA) was assessed on echocardiography in all patients. (Figure 1) Follow-up echocardiographic parameters were measures on all patients at 1 month and compared with baselines parameters. LBBP was performed according to the current expert report of the European Heart Rhythm Association (EHRA) Selective LBBP were referred as obtaining a time from the stimulus to the peak time of the R wave in lead V6 on the electrocardiogram (ECG) of 75 ms or less whereas obtaining a time above 75 ms were considered as non-selective LBBP
Results: Clinical laboratory findings of the patients are shown in Tables 1 and 2. Only a history of myocardial infarction was a predictor of failure in selective left bundle branch pacing (OR=0.222, CI: 0.052-0.949, P=0.042). Baseline and 1-month comparisons are shown in Figure 2. While NHYA exercise capacity improved in all groups, left ventricular ejection fraction (LVEF) increased in the selective left branch pacing group only. At 6 months, mortality was observed in 3 (5.7%) patients. The cause of death was infective endorcarditis in 1 patient, myocardial infarction in 1 patient, and the cause remained unexplained in 1 patient.
Discussion: In our study, the selective LBBP rate was found to be 51.9%. This rate is below the 60-90% rate reported in the literature. This may be due to differences in the population and the criteria used. 6-month mortality rates are similar to those in the literature. In our study, the increased exercise capacity in each patient was related to increased chronotropy. In our study, LVEF increased only in the selective left branch pacing group. However, no difference in LVEF was found between the selective and nonselective left branch pacing groups in the literature. The fact that only a history of MI was found to be a factor affecting selective LBBP failure may be due to increased scarring at the pacing site. The aortic septal angle did not affect the success of selective LBBP
Conclusions: Selective LBBP provides greater improvement in left ventricular systolic function in the acute phase. LBBP failure is not affected by echocardiographic parameters, while a history of MI is the only independent predictor of selective LBBP.
Keywords: Aortic Septal Angle, Left Bundle Branch Pacing, Left Ventricular Ejection Fraction, Myocardial Infarction, Selective Left Bundle Branch Pacing, V6 R Wave Peak Time.

TABLE 1. The Comparisons of the Demographic and Clinic Characteristics Between two Groups

Total patients			52
Selective left bundle pacing (%)			51.9%
Male gender (%)			65.4%
Age (years)			70.7±10.2
Indications, n (%)			
Third-degree atrioventricular (AV) block			33 (63.5%)
Mobitz type 2 AV bloc			9 (17.3%)
Advanced first-degree AV block			2 (3.8%)
Others (sinoatrial block, atrial fibrillation with slow ventricular response, sinus syndrome, AV node ablation, trifascicular block)			8 (15.3%)
Pneumothorax, n (%			1 (1.9%)
Hematoma, n (%			3 (5.7%)
Septal perforation, n (%			4 (7.6%)
Procedural mortality, n (%			0 (0.0%)
Variable	**sLBBP group (n=27)**	**nsLBBP group (n=25)**	**P-value**
Age (years)	71.5±7.8	69.8±12.4	0.553
Male, n (%	18 (66.7)	16 (64.0)	0.840
BMI (kg/m^2)	28.1±4.5	27.6±3.8	0.671
Diabetes, n (%	12 (44.4)	7 (28.0)	0.219
CAD, n (%	9 (33.3)	11 (44.0)	0.430
Hypertension, n (%	23 (85.2)	23 (92.0)	0.442
Prior MI, n (%	3 (11.1)	9 (36.0)	**0.033**
Heart failure, n (%	10 (37.0)	11 (44.0)	0.609
Pacemaker types, n (%			0.572
DDD-R	25 (92.6)	22 (88.0)	
VVI-R	0 (0.0)	(4.0)	
CRT-P	2 (7.4)	(8.0)	

Data are shown as mean±standard deviation or n (%) where appropriate. AF, atrial fibrillation; AV, atrioventricular; BMI, body mass index; CAD, coronary artery disease; MI, myocard infarction; N, number; nsLBBP, nonselective left bundle branch pacing; sLBBP, selective left bundle branch pacing. Statistically significant value is shown in bold.

TABLE 2. The Comparison of the Laboratory and Echocardiographic Characteristics Between two Groups

Variable	sLBBB group (n=27)	nsLBBB group (n=25)	P-value
Hemoglobin (g/dL)	11.91±1.67	12.5±1.67	0.163
Lymphocytes (×10^9/L)	1.86±0.69	1.86±0.74	0.993
Creatinine (mg/dL)	1.28±0.89	1.28±1.03	0.994
CRP (mg/L)	3.64 (3.11–29.8)	4.19 (3.13–20.30)	0.454
Potassium (mEq/L)	4.42±0.50	4.53±0.61	0.514
Baseline LVEF (%)	50.40±10.31	46.12±13.66	0.205
SHF*, n (%)	12 (44.4)	14 (56.0)	0.405
Baseline LVEDD (mm)	50.14±5.74	51.52±7.68	0.467
Baseline RVD (mm)	38.14±5.36	38.72±6.22	0.723
Tricuspid annulus (mm)	38.59±4.94	37.28±6.48	0.414
IVS (mm)	12.03±2.42	11.72±2.13	0.620
Baseline TR grade	1 (1–2)	1 (1–2)	0.485
Aortoseptal angle)	111.37±10.01	113.52±10.96	0.463
LBBB, n (%)	4 (14.8)	6 (24.0)	0.401
RBBB, n (%)	12 (44.4)	13 (52.0)	0.586
Baseline QRS duration (ms	121.48±28.94	129.40±30.27	0.340
Paced QRS duration (ms)	122.18±21.40	128.24±20.50	0.303
R wave amplitude (mV)	9.91±2.56	11.20±3.53	0.138
Pacing threshold (V)	0.56±0.11	0.65±0.15	**0.030**
V6 RWPT (ms)	68.25±3.12	90.24±10.46	**<0.001**

Data are shown as mean±standard deviation or n (%) or median (25th–75th) where appropriate. CRP, C-reactive protein; IVS, interventricular septum; LBBB, left bundle branch block; LVEDD, left ventricular end-diastolic diameter; LVEF, left ventricular ejection fraction; mV, millivolt; nsLBBB, non-selective left bundle branch pacing; RBBB, right bundle branch block; RVD, right ventricular diameter; SHF, systolic heart failure; sLBBB, selective left bundle branch pacing; TR, tricuspid regurgitation; TSH, thyroid-stimulating hormone; V, volt; V6RWPT, V6 R wave peak time.

Statistically significant values are shown in bold.

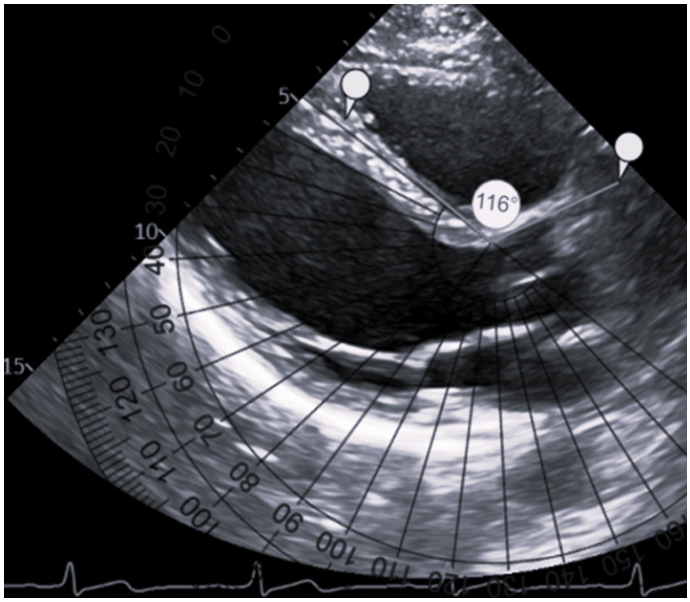

FIGURE 1. Measurement of aortoseptal angle in 2D echocardiography.

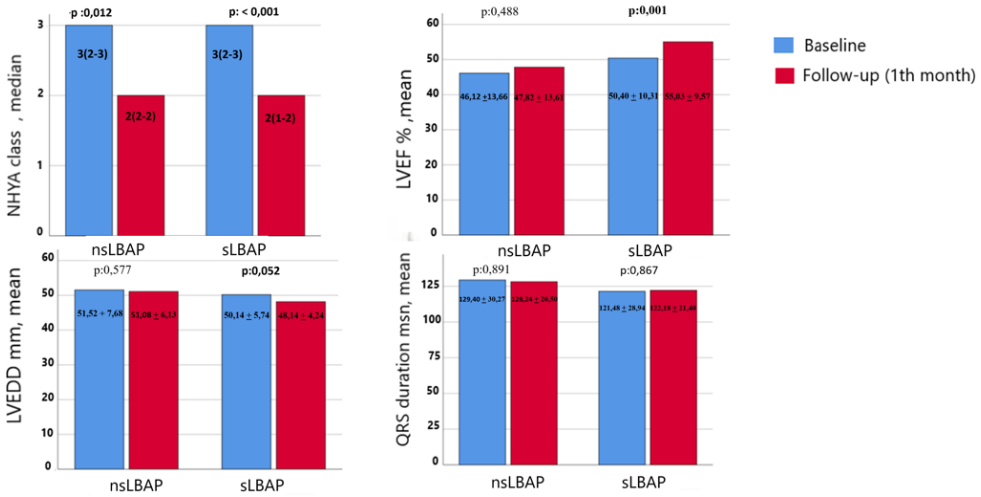

FIGURE 1. The comparisons of the basal and 1-month parameters.

OP-03.
Association Between Delayed QRS Transition Zone and Diabetes Mellitus

Yakup Han Yilmaz[1], Özge Turgay Yildirim[1], Mehmet Özgeyik[1]

[1]Department of Cardiology, Eskişehir City Hospital, Eskişehir, Türkiye

Objectives: The QRS transition zone on a standard 12-lead electrocardiogram (ECG) is defined as the precordial lead where the amplitudes of the R and S waves are nearly equal, commonly occurring between leads V3 and V4. A delayed QRS transition zone refers to the shift of this transition to more lateral leads (V5 or V6). This phenomenon can be associated with left ventricular hypertrophy, conduction disease, chronic pulmonary disease, obesity, or anatomical changes, as well as with increased subclinical cardiac risk even in patients without overt heart disease. Understanding the transition zone is important because delay may serve as a non-invasive indicator of subtle cardiac alterations. Diabetes mellitus is known to contribute to both structural and electrophysiological remodeling of the heart, leading to cardiac fibrosis, autonomic dysfunction, and conduction disturbances. Despite this, the relationship between diabetes and delayed QRS transition zone remains underexplored.
Methods: This retrospective study included 200 consecutive patients who presented to the cardiology outpatient clinic. Patients under 18 years, and those with acute coronary syndrome, prior myocardial infarction, history of cardiac surgery or heart failure, atrial fibrillation, bundle branch block, pacemaker rhythm, or high-degree atrioventricular block were excluded. Demographic characteristics, diabetes status, and ECG findings were recorded. The presence of delayed QRS transition zone was evaluated by a blinded cardiologist. Clinical and demographic data are compared between diabetics and non-diabetics using Chi-square and t-tests as appropriate.
Results: Of the 200 patients analyzed, 96 (48%) had diabetes mellitus (Table 1). Delayed QRS transition zone was observed in 55 (57.3%) of diabetic patients, compared to 35 (33.6%) of non-diabetic patients, with a statistically significant difference (P=0.001). Diabetic patients were older (mean age: 61.7 vs. 57.6 years, P=0.007), and had a higher prevalence of hypertension (66 vs. 24 cases, P<0.001). No significant differences were detected concerning peripheral vascular disease, COPD, stroke, chronic kidney disease, or malignancy.
Conclusions: Delayed QRS transition zone is significantly more common in patients with diabetes mellitus, independent of other major comorbidities. This electrocardiographic feature may reflect diabetes-induced myocardial remodeling or conduction system involvement. Recognizing delayed transition zone in ECGs could serve as a simple tool for identifying diabetic patients at heightened risk for underlying cardiac disturbances. Prospective studies are needed to clarify the prognostic implications and potential role of delayed QRS transition zone in clinical risk stratification for diabetes mellitus.
Keywords: Diabetes Mellitus, Delayed QRS Transition Zone, Electrocardiography

TABLE 1. **Demographic Characteristics of the Study Population**

Variables	Diabetes Mellitus Patients (n=96)	Non-diabetic patients (n=104)	P-value
Age (years)	61.7±11.2	57.6±10.5	**0.007**
Gender (Male)	41	75	**<0.001**
Hypertension	66	24	**<0.001**
Periferic vascular disease	3	2	0.595
Chronic obstructive pulmonary disease	4	5	0.815
Stroke	1	0	0.299
Chronic kidney disease	4	2	0.360
Malignancy	1	1	0.960

Data are shown as mean±standard deviation or number where appropriate.
Statistically significant values are shown in bold.

OP-04.
Vasospastic Angina: A Case of Coronary Spasm Confirmed by Ergonovine

Ömer Fatih Savci[1], Ömer Faruk Kahraman[1], Adem Yarar[1], Doğan Ormanci[1], Rauf Samet Gençgün[1], Mücahit Yarar[1], Mehmet Melek[1]

[1]Department of Cardiology, Bursa Yüksek İhtisas Training and Research Hospital, Bursa, Türkiye

Case Presentation: A 39-year-old male patient presented to the cardiology outpatient clinic with recurrent, intense, non-exertional chest pain that occurred mainly in the morning and evening hours. He had no known comorbidities and denied smoking or substance use. A coronary angiography performed at another center 2.5 months earlier had been reported as normal. The patient had been prescribed isosorbide-5-mononitrate 20 mg once daily, diltiazem 90 mg twice daily, acetylsalicylic acid 100 mg, and colchicine 0.5 mg once daily. Due to persistent anginal symptoms, he was admitted with a preliminary diagnosis of vasospastic angina. On the second night of hospitalization, at 03:30 a.m., he experienced severe chest pain. Electrocardiography (ECG) revealed anterior ST-segment elevation consistent with acute coronary syndrome (Figure 1). Intravenous nitroglycerin infusion was initiated, after which the ST elevations regressed. Transthoracic echocardiography showed a left ventricular ejection fraction of 60%, normal right heart structures, and mild mitral and tricuspid regurgitation. Laboratory results were within normal limits (Table 1). An ergonovine provocation test was performed during coronary angiography. The test induced total vasoconstriction in the proximal left anterior descending (LAD) artery, accompanied by chest pain and ST-segment elevation (Figure 2). The vasospasm completely resolved after intracoronary nitrate administration (Figure 3). The patient was started on diltiazem 120 mg in the morning and 240 mg in the evening, isosorbide-5-mononitrate 50 mg daily, and low-dose alprazolam. No further anginal episodes occurred during follow-up, and he was discharged on the sixth day with medical therapy.

Discussion: Vasospastic angina (VSA) is characterized by transient myocardial ischemia resulting from coronary artery spasm in the absence of significant atherosclerotic obstruction. It typically occurs at rest and may be triggered by smoking, alcohol, emotional stress, cold exposure, cocaine, or certain medications. VSA accounts for approximately 2–5% of patients undergoing coronary angiography for angina, with a higher prevalence among men aged 40–60 years. Diagnosis is usually based on clinical features and ECG findings; however, in uncertain cases, provocation tests such as ergonovine or acetylcholine challenge may be employed. These tests directly demonstrate coronary vasospasm and confirm reversibility with nitrates.

Management involves lifestyle modification and avoidance of precipitating factors. Pharmacologic therapy relies primarily on calcium channel blockers, which are the most effective long-term treatment. Sublingual nitroglycerin is highly effective for acute attacks, while oral nitrates are used for chronic symptom control.

Conclusions: This case highlights a patient who presented with acute coronary syndrome secondary to vasospastic angina, in whom coronary spasm was confirmed by ergonovine testing. It emphasizes the importance of recognizing VSA as a reversible cause of myocardial ischemia and the effectiveness of prompt diagnosis and appropriate pharmacologic therapy in preventing recurrent ischemic episodes.

Keywords: Vasospastic Angina, Ergonovine Test, Coronary Artery Spasm, Acute Coronary Syndrome

TABLE 1. Laboratory Findings

Laboratory	21 Oct	23 Oct	24 Oct	27 Oct
Hemogram (g/dL)	16		16.3	16
Creatinine (mg/dL)	0.8		0.7	0.7
Troponin T (ng/mL)	8	7	6.5	4.7
CK-MB (ng/mL)	1	0.6	0.6	0.5
Pro-BNP (pg/mL)	51			62

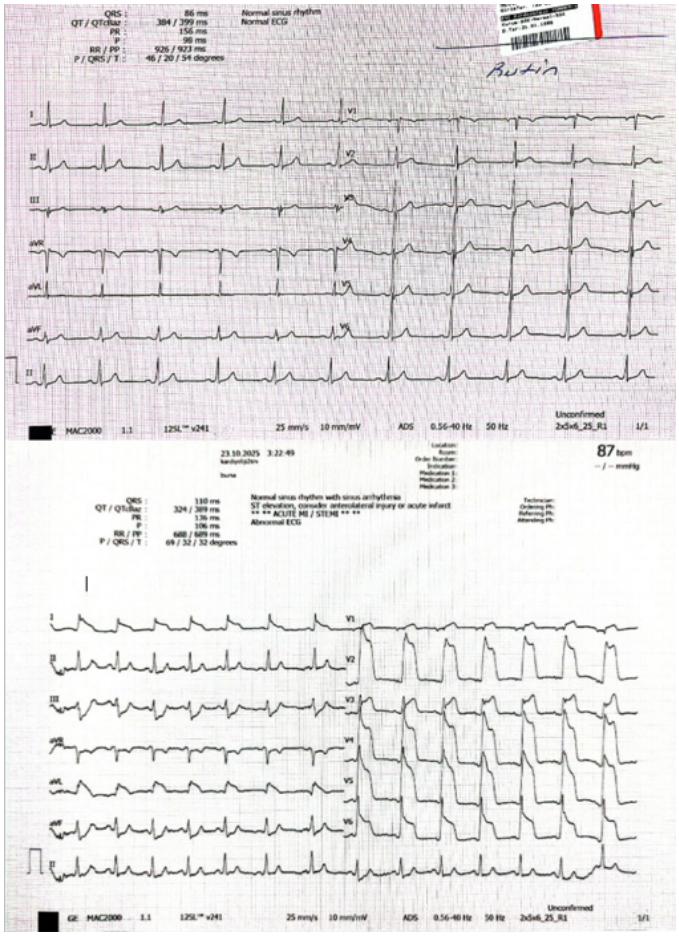

FIGURE 1. Electrocardiography reveals anterior ST-segment elevation consistent with acute coronary syndrome.

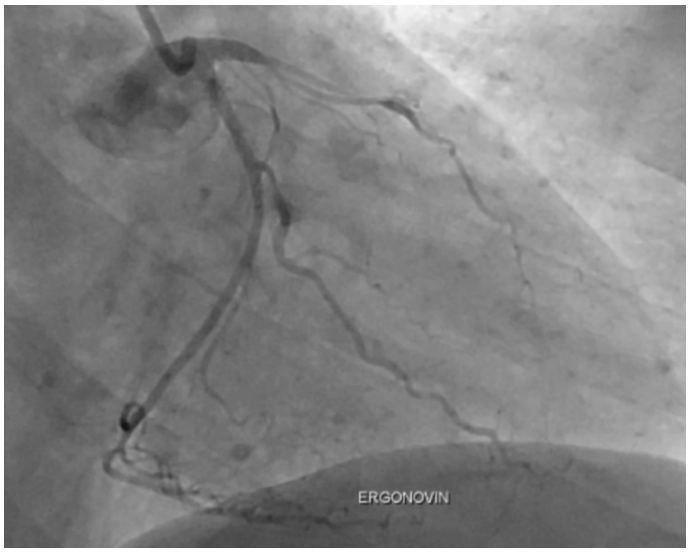

FIGURE 2. Ergonovine provocation test induces total vasoconstriction in the proximal left anterior descending (LAD) artery.

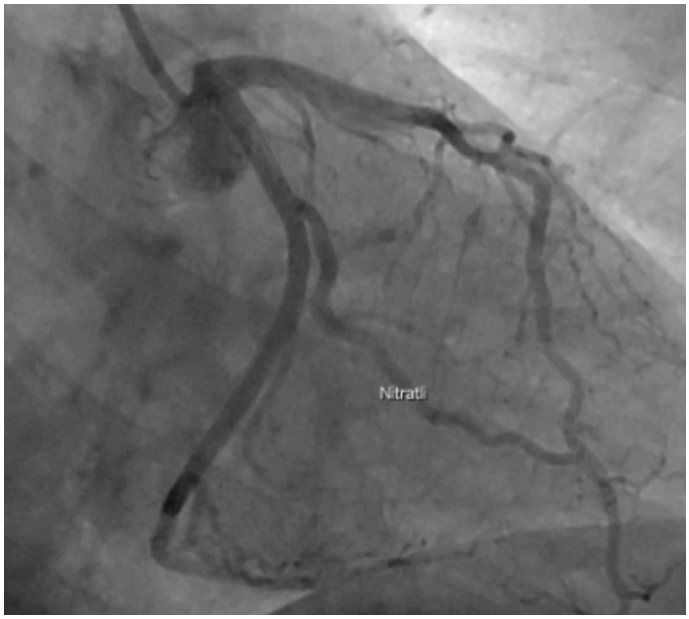

FIGURE 3. Intracoronary nitrate administration appears to completely resolve coronary vasospasm.

OP-05.
Cardiac Effects of Chronic Pyrethroid Exposure

Safa Oktay[1], Ayşe Dilara Balyimez[1], Ömer Fatih Savci[1], Sanatbek Rustembakov[1], Doğan Ormanci[1], Rauf Samet Gençgün[1], Adem Yarar[1], Veysel Macit[1], Mehmet Melek[1], Hasan Ari[1]

[1]Department of Cardiology, University of Health Sciences, Bursa Yüksek İhtisas Training and Research Hospital, Bursa, Türkiye

Case Presentation: A 46-year-old male presented to the emergency department with newly-onset fatigue, weakness, and dizziness. He was admitted to the coronary intensive care unit after an electrocardiogram (ECG) performed at an outside facility revealed atrioventricular (AV) block. The patient had no known comorbidities or medication use but reported a 50 pack-year smoking history. He denied consumption of herbal teas or honey. A farmer for 26 years, the patient had a recent history of agricultural pesticide exposure before admission. ECGs obtained in the intensive care unit showed variable-degree AV block (Figures 1–3). Vital signs were stable, consciousness was clear, and physical examination was unremarkable. Transthoracic echocardiography (Videos 1–3) demonstrated normal cardiac structures with an ejection fraction of 65%. Laboratory results (Table 1) were within normal limits. During 48 hours of coronary care follow-up, the patient's AV block resolved spontaneously around the 36th hour, with restoration of sinus rhythm. A 48-hour Holter ECG performed on the fifth hospital day showed normal rhythm without conduction abnormalities. The Bruce protocol exercise test demonstrated an adequate chronotropic response, and no further arrhythmias were observed (Figure 4). Coronary angiography (Figures 5–8) was performed after recovery of sinus rhythm, as the patient had no prior angiographic evaluation. It revealed a critical (80%) stenosis in the right coronary artery (RCA) and mild plaques in the circumflex (Cx) and left anterior descending (LAD) arteries. A 3.5×44 mm everolimus-eluting stent (DES) was implanted in the RCA. The patient was discharged after completing all investigations, with follow-up planned one week later. At control, a 48-hour Holter showed only nocturnal sinus bradycardia without pathological findings. The patient had been exposed to a deltamethrin-containing insecticide (Demond EC 2.5, synthetic pyrethroid) and subsequently developed variable-degree AV block. Based on the clinical, electrocardiographic, and laboratory findings, the conduction disturbance was attributed to transient cardiotoxicity secondary to deltamethrin exposure, consistent with reversible conduction system toxicity.

Discussion: Deltamethrin, a pyrethroid insecticide, usually has low systemic toxicity; however, high-dose or chronic exposure may affect both neurological and cardiac conduction systems. It prolongs the opening of voltage-gated sodium channels, leading to neuronal hyperexcitability. Similar effects on myocardial sodium and calcium channels can cause conduction delay, bradycardia, or AV block, particularly at the sinoatrial and atrioventricular nodes. Although rare, pyrethroid-associated conduction abnormalities such as QT prolongation, sinus bradycardia, and AV block have been reported. Singh et al. (Cardiology, 2016) described a reversible complete AV block secondary to pyrethroid exposure. Another case in the American Journal of Industrial Medicine (2020) required pacemaker implantation for pyrethroid-induced complete AV block. In our patient, AV block developed after pesticide exposure without laboratory evidence of organophosphate poisoning and resolved spontaneously within 48 hours. This suggests a reversible ion channel dysfunction induced by deltamethrin. No specific antidote exists; thus, close cardiac monitoring and supportive care remain the mainstay of treatment.

Conclusions: This case highlights that pyrethroid exposure may affect not only the nervous system but also the cardiac conduction system, underscoring the importance of clinical vigilance in similar

Keywords: Deltamethrin, Pyrethroid, Cardiac Effects Caused by Insecticides

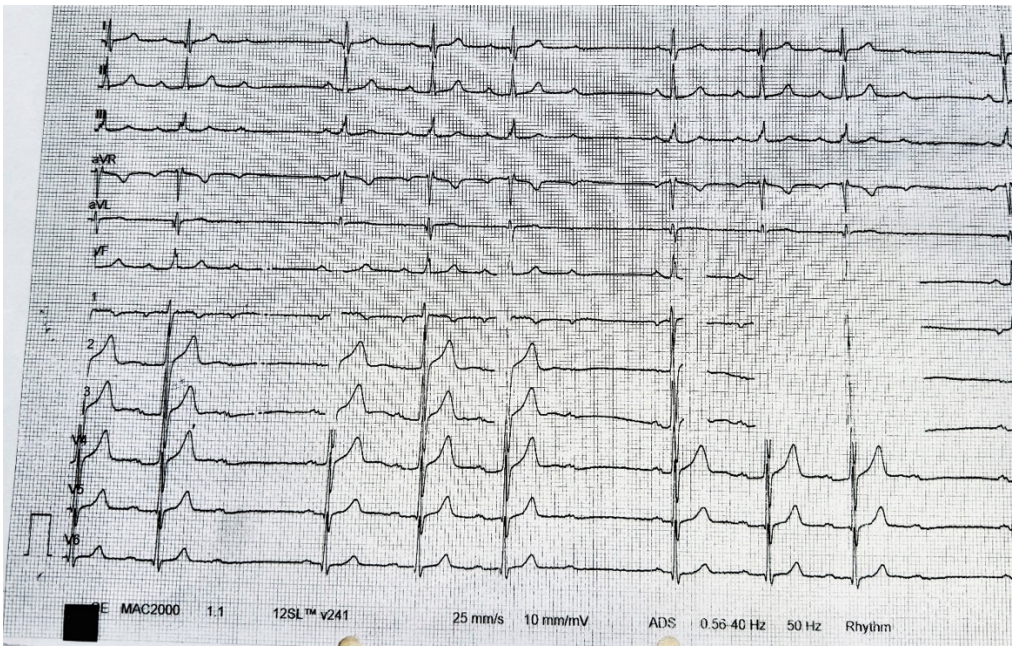

FIGURE 1. **Variable-degree AV block.**

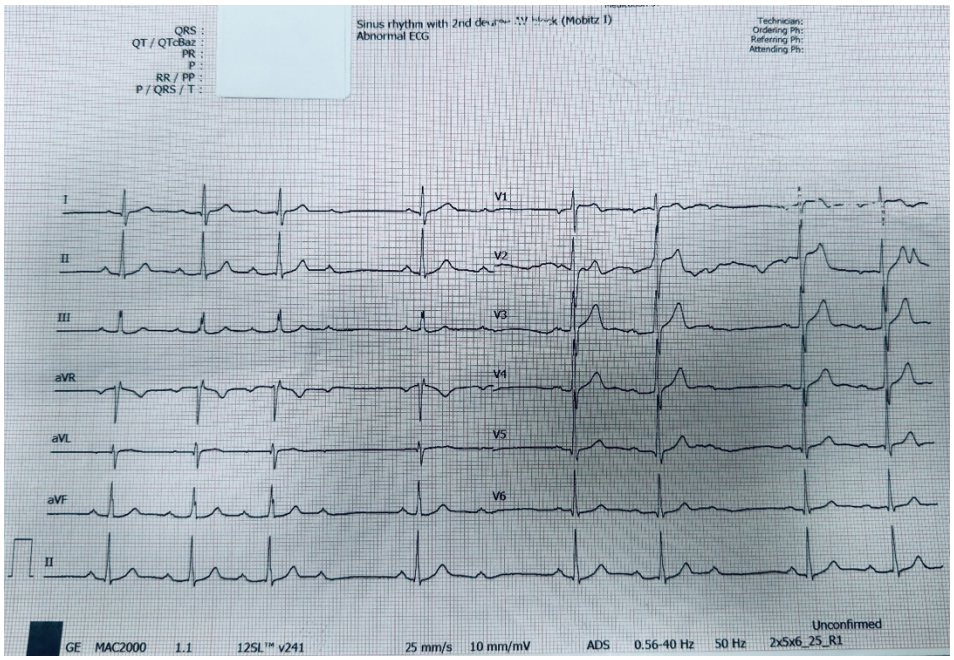

FIGURE 2. **Variable-degree AV block.**

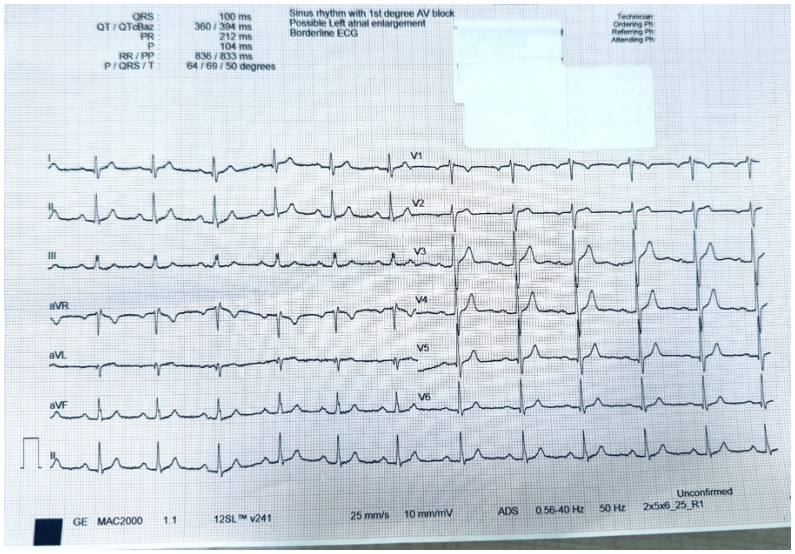

FIGURE 3. **Variable-degree AV block.**

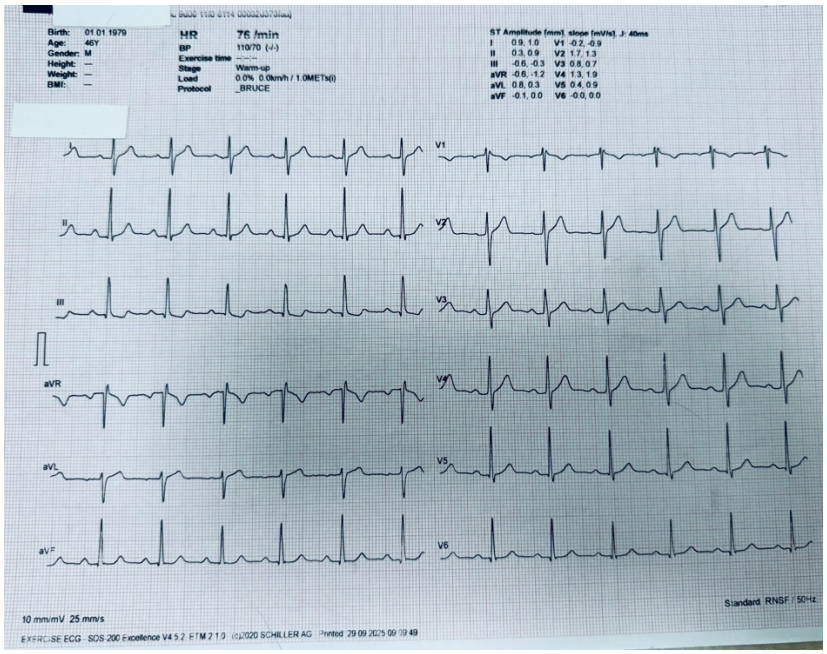

FIGURE 4. **Sinus rhythm.**

TABLE 1. Laboratory results

Laboratory results	Day 1	Day 2	Day 3	Day 4	Day 5	Reference Values
Sodium (mEq/L)	140	142.5	140	143	139.2	135-145
Potassium (mEq/L)	4.12	4.38	4.15	4.55	5.1	3.5-5.5
Calcium (mg/dL)	8.8	9				8.5-10.5
Magnesium (mg/dL	2.06	2.04				1.6-2.6
Chloride (mEq/L)	106.4	107.7	105.3	103.3	102.1	96-106
Glucose (fasting blood) (mg/dL)	95					70-100
Albumin (g/L)	40.2	39.5				34-54
Creatinine (mg/dL)	0.7	0.72	0.87	0.64	0.7	0.6-1.2
Glomerular filtration rate (mL/min)	116	106	107	119	117	90-122
Blood urea nitrogen (mg/dL)	13.13	15	16.73	13.7	12.01	6-20
Uric acid (mg/dL)	3.5					1.6-6.5
Brain natriuretic peptide (pg/mL)	22.3					0-100
Aspartate aminotransferase (U/L)	13	18				8-33
Alanine aminotransferase (U/L)	11	16				0-55
C-reactive protein (mg/L)	0.67	1.1				0-5
Total bilirubin (mg/dL)	0.27	0.31				0.2-1.2
Direct bilirubin (mg/dL)	0.13	0.09				0-0.5
Troponin I (hsTn-I) (ng/mL)	4.5	4.23				0-15.6
Creatine kinase-MB (ng/mL)	1.48	1.73				0-3.4
White blood cell (10^3/mL)	7.3	7.64	6.72	7	7.1	3.5-10.5
Red blood cell (RBC) (10^6/mL)	5.71	5.83	5.46	5.62	5.24	3.9-5.3
Neutrophil (10^3/mL)	3.49	4.5	4.1	4.6	5.4	1.9-8
Eosinophil (10^3/mL)	0.3	0.1	0.3	0.3	0.4	0-0.5
Basophil (10^3/mL)	0.2	0.1	0.3	0.2	0.1	0-0.5
Lymphocyte (10^3/mL)	2.41	2.49	2.5	2.6	2.2	1.2-3.9
Monocyte (10^3/mL)	0.4	0.5	0.4	0.45	0.6	0.3-0.9
Platelets (10^3/mL)	206	215	220	230	300	150-450
Hemoglobin (g/dL)	14.9	13.8	15.1	15.5	13.8	12-15.5
Hematocrit (%)	44.9	42.2	44.4	41.5	46	34.9-45.2
Digoxin level (ng/mL)	0.36	0.3				0.5-2
LDL (mg/dL)	124.2					<130
HDL (mg/dL)	32.9					>45
VLDL (mg/dL)	19					<50
Triglyceride (mg/dL)	92					<150
Total cholesterol (mg/dL)	176					<200
Pseudocholinesterase (U/L)	8883					5320-12920

LDL, low-density lipoprotein; HDL, high-density lipoprotein; VLDL, very low-density lipoprotein.

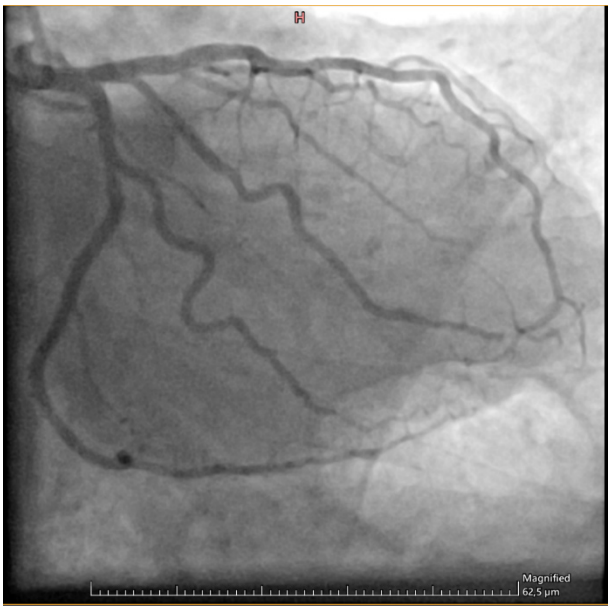

FIGURE 5. Coronary angiography

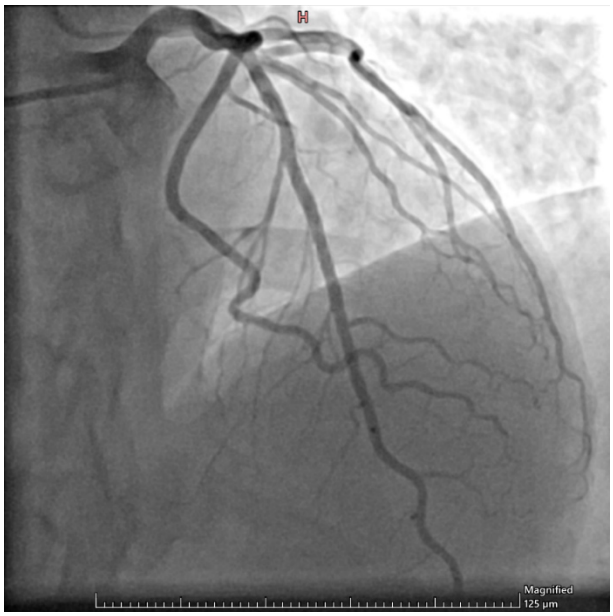

FIGURE 6. Coronary angiography

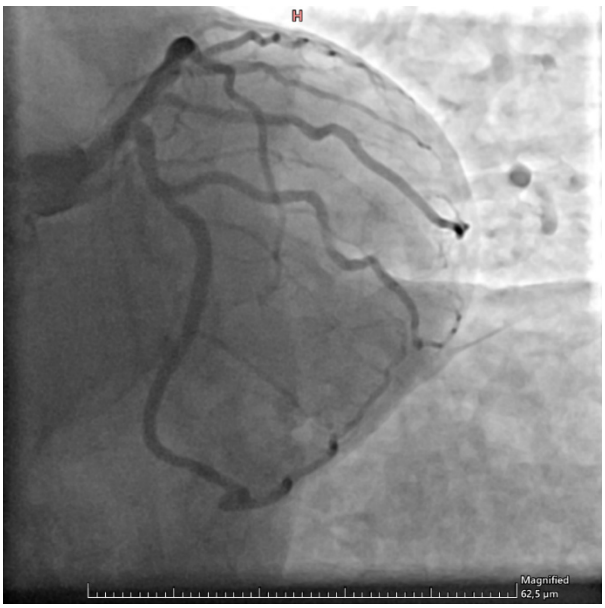

FIGURE 7. Coronary angiography

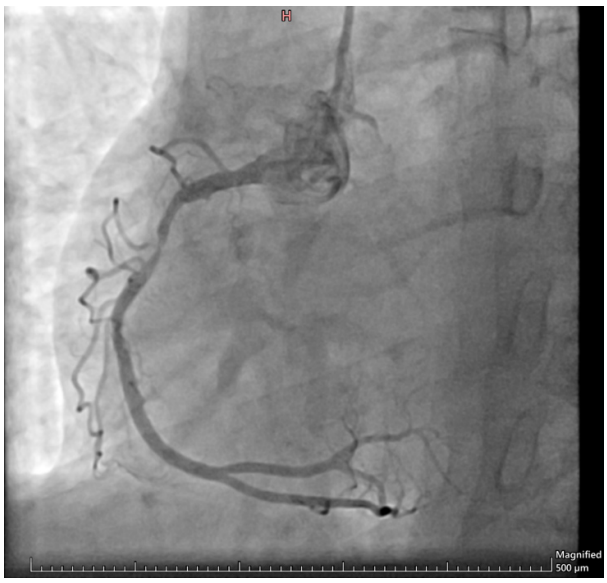

FIGURE 8. Coronary angiography

OP-06.
Effect of SGLT-2 Inhibitors on MPV in Heart Failure Patients

Hüseyin Orta[1], Cihan Aydin[1], Ferhat Perk[1], Yunus Salih Aslan[1]

1Department of Cardiology, Tekirdağ Namık Kemal University Hospital, Tekirdağ, Türkiye

Objectives: Heart failure (HF), particularly heart failure with reduced ejection fraction (HFrEF), is a chronic cardiovascular disease associated with high morbidity and mortality, and new therapeutic targets continue to be explored. Sodium-glucose cotransporter-2 (SGLT-2) inhibitors have gained prominence in HF treatment due to their cardiovascular benefits. Mean platelet volume (MPV), a parameter reflecting platelet activity, has been associated with cardiovascular diseases such as atherosclerosis, diabetes, and heart failure. This study aimed to evaluate the effect of SGLT-2 inhibitor therapy on MPV in patients diagnosed with HFrEF and to investigate whether this effect is independent of the drugs' cardioprotective properties.
Methods: A total of 80 patients diagnosed with HFrEF between January 2023 and December 2024 were retrospectively analyzed. All patients were on optimal guideline-directed medical therapy (according to ESC guidelines) when SGLT-2 inhibitor therapy was initiated, and no treatment changes were made for 6 months. Complete blood count and biochemical parameters were evaluated at baseline and at the end of the 6th month. Changes in hematological parameters, particularly MPV, were statistically analyzed.
Results: After SGLT-2 inhibitor therapy, MPV values showed a significant decrease ($P<0.05$). Additionally, a significant increase in platelet (PLT) count was observed, while hemoglobin (HGB) and hematocrit (HCT) levels increased without reaching statistical significance. No significant differences were found in biochemical parameters such as LDL, triglycerides (TG), creatinine, and urea. All patients were evaluated under maximally tolerated medical therapy.
Discussion: The findings suggest that SGLT-2 inhibitors may exert beneficial effects not only metabolically but also hematologically. The decrease in MPV may indicate reduced platelet activity, potentially contributing to the prevention of cardiovascular events. There are limited studies in the literature investigating the effect of SGLT-2 inhibitor therapy on MPV in HFrEF patients. Therefore, this study sheds light on the potential utility of MPV as a biomarker in heart failure.
Conclusions: SGLT-2 inhibitor therapy reduces MPV levels and increases platelet count in patients with HFrEF. These hematological changes may contribute to the cardiovascular benefits of this drug class. Further prospective, randomized, and controlled studies are needed to better understand these findings and their clinical implications.
Keywords: SGLT-2 Studies, Mean Platelet Volume, Heart Time, Hematological Effect, Platelet Activities, Contraction Risk

OP-01.
Evaluation of Subclinical Myocardial Dysfunction in Cirrhosis Using 4D Strain Analysis

Mahmut Kapsiz[1], **Dilek Yeşilbursa**[2]

[1]*Department of Cardiology, University of Health Sciences, Bursa Yüksek İhtisas Training and Research Hospital, Bursa, Türkiye;*
[2]*Department of Cardiology, Bursa Uludağ University, Faculty of Medicine, Bursa, Türkiye*

Objectives: Liver cirrhosis is associated with hyperdynamic circulation and cirrhotic cardiomyopathy, both of which affect the cardiovascular system. Although conventional echocardiography findings are often normal at rest in cirrhotic patients, subclinical myocardial dysfunction may go unnoticed. Two-dimensional (2D) and four-dimensional (4D) strain imaging techniques, which quantify myocardial deformation, offer high sensitivity for detecting this "silent" phase. This prospective case–control study aimed to evaluate the role of 4D strain analysis in the early detection of subclinical left ventricular systolic dysfunction in cirrhotic patients and to compare it with 2D global longitudinal strain (GLS). The findings were reported in comparison with healthy controls.

Case Presentation: Between March and December 2020, twenty patients with liver cirrhosis and twenty-five age- and sex-matched healthy controls were enrolled at the Department of Cardiology, Uludağ University Faculty of Medicine. Patients with cardiac pathology, arrhythmia, systemic hypertension, significant valvular disease, or diabetes mellitus were excluded. All participants underwent standard echocardiographic examination supplemented with 2D GLS and 4D strain analyses. Images were acquired using a GE Vivid E95 system and analyzed offline with EchoPAC software (GE Healthcare). In the 4D analysis, global longitudinal, radial, and circumferential peak strain (GPSL, GPSR, GPSS) parameters were calculated. The results were compared between groups to evaluate the sensitivity of 4D strain in detecting subclinical left ventricular systolic dysfunction.

Discussion: The cirrhosis and control groups were similar in age, sex distribution, and left ventricular ejection fraction (EF) ($P>0.05$). EF values were within normal limits in both groups; however, 2D GLS values were significantly lower in the cirrhosis group (−18.1±2.3% vs. −20.9±1.8%, $P=0.021$). Similarly, 4D global longitudinal strain (GPSL) was reduced in cirrhotic patients (−17.8±2.4% vs. −20.9±2.0%, $P=0.021$). No significant differences were found in 4D radial (GPSR) or circumferential (GPSS) strain values between the two groups ($P>0.05$). A strong positive correlation was observed between 2D GLS and 4D GPSL in the cirrhosis group ($r=0.81$, $P<0.001$). These findings indicate that subclinical left ventricular systolic dysfunction can be demonstrated in cirrhotic patients even when EF is preserved. The 4D strain technique provided complementary information to 2D GLS, suggesting its potential utility for early detection of cirrhotic cardiomyopathy.

Conclusions: Despite preserved left ventricular ejection fraction, subclinical myocardial dysfunction can be identified in cirrhotic patients using strain imaging. In this study, 4D strain analysis showed a strong correlation with 2D GLS and offered additional diagnostic insight. The results suggest that 4D strain imaging may serve as a valuable tool for the early detection of cirrhotic cardiomyopathy; however, larger studies are needed to confirm these findings.

Keywords: Liver Cirrhosis, Subclinical Myocardial Dysfunction, Global Longitudinal Strain, 4D Strain, Cirrhotic Cardiomyopathy

OP-08.
The Role of the Intermountain Risk Score in Predicting Coronary Artery Ectasia

Şahhan Kiliç[1], Süha Asal[1], Mert Babaoğlu[2], Samet Yavuz[2], Mohaddeseh Davoudi Bilehsavar[3], Hatice Altinişik[2], Yusuf Turan Gül[2], Mustafa Oğuz[2], Selami Doğan[4], Ahmet Lütfullah Orhan[2]

[1]Department of Cardiology, Çorlu State Hospital, Tekirdağ, Türkiye; [2]Department of Cardiology, Sultan Abdülhamid Han Training and Research Hospital, İstanbul, Türkiye; [3]Department of Cardiology, University of Health Sciences, Hamidiye Faculty of Medicine, İstanbul, Türkiye; [4]Department of Cardiology, VM Medical Park Maltepe Hospital, İstanbul, Türkiye

Objectives: Coronary artery ectasia (CAE) represents a distinct form of coronary artery pathology characterized by abnormal dilatation exceeding 1.5 times the diameter of adjacent normal segments. Despite its notable prevalence among patients undergoing coronary angiography, CAE remains underrecognized, and its clinical implications are incompletely defined. Given the lack of standardized risk stratification tools, this study aimed to investigate the relationship between the Intermountain Risk Score (IMRS)—a composite index derived from demographic and routine laboratory parameters—and the presence of CAE. The objective was to evaluate whether IMRS can serve as an independent predictor of CAE and assist in identifying individuals at elevated risk.
Methods: This retrospective, observational study included patients who underwent invasive coronary angiography at Sultan 2. Abdülhamid Han Training and Research Hospital between January 2019 and January 2024. Patients diagnosed with CAE, defined as ≥1.5-fold dilation of a coronary segment compared with an adjacent normal area, were compared with age- and sex-matched controls without ectasia. Individuals with ≥50% coronary stenosis, congenital anomalies, or previous revascularization were excluded. Demographic data, cardiovascular risk factors, and laboratory findings were collected. IMRS values were calculated using standardized methods and categorized into three risk strata (green, yellow, red). Statistical analyses included chi-square, t-test or Mann–Whitney U test, and multivariate logistic regression. Receiver operating characteristic (ROC) curves were used to assess discriminatory performance.
Results: A total of 446 patients were included (226 with CAE, 220 controls). The ectatic group had a higher proportion of men (77% vs. 67.7%, P=0.029) and more frequent smoking history (19.2% vs. 7.3%, P<0.001) (Table 1). Laboratory comparisons showed significantly elevated red cell distribution width (RDW: 14.3% vs. 13.4%, P<0.001), mean platelet volume (MPV: 9.8 vs. 9.3, P<0.001), and monocyte counts (0.51 vs. 0.47 $\times 10^3/\mu L$, P=0.047) in the ectatic group (Tables 2 and 3). Mean IMRS was higher among CAE patients (10 vs. 8.5, P=0.011), and more individuals were classified in higher IMRS risk categories (P=0.002) (Table 2). Multivariate analysis identified smoking (HR: 3.744, P=0.045), mean corpuscular volume (HR: 1.105, P=0.019), and IMRS color category (HR: 5.255, P=0.016) as independent predictors of CAE (Table 3). ROC analysis revealed moderate discriminative capacity (AUC=0.617 for IMRS score, 0.627 for IMRS category) (Figure 1).
Discussion: This study demonstrates that IMRS may predict CAE by reflecting systemic inflammation and hematologic changes. Elevated RDW, MPV, and monocyte levels support the inflammatory and rheologic basis of ectasia, while smoking contributes through endothelial damage. Despite its moderate accuracy, IMRS is a practical, cost-effective tool for early identification and management of patients at risk for CAE.
Conclusions: Patients with CAE exhibit distinct inflammatory and hematologic profiles, alongside elevated IMRS values, which independently predict the presence of ectasia. IMRS, derived from routine laboratory data, offers a feasible means for early risk stratification in clinical settings. Smoking cessation and tailored

surveillance strategies may mitigate CAE-related complications. Prospective multicenter studies are warranted to validate these findings and determine whether IMRS-guided management can improve cardiovascular outcomes in patients predisposed to CAE.

Keywords: Coronary Artery Ectasia, Intermountain Risk Score, Inflammation

TABLE 1. Demographic Properties of Groups.

	Ectasia (-) n=220	Ectasia (+) n=226	P-value
Age (years)	62±10	62±10	0.915
Gender (male) n (%)	149 (67.7%)	174 (77%)	**0.029**
Hypertension, n (%)	120 (54.5%)	114 (50.9%)	0.441
Diabetes mellitus, n (%)	55 (25%)	51 (22.8%)	0.581
Hyperlipidemia, n (%)	90 (41%)	101 (44.7%)	0.385
Smoking, n (%)	16 (7.3%)	43 (19.2%)	**<0.001**

Data are shown as mean±standard deviation or n (%) where appropriate.
Statistically significant P-values are shown in bold.

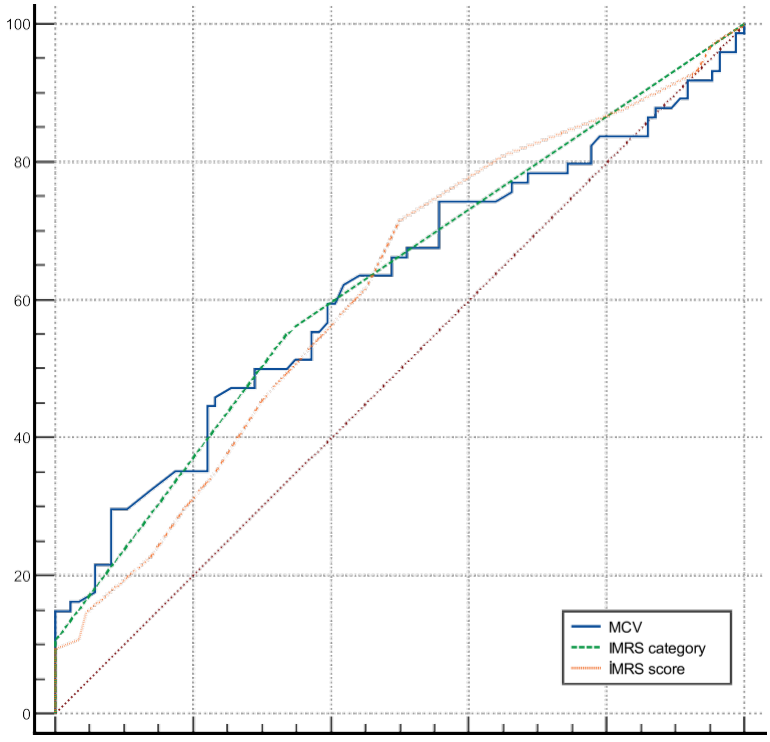

	Cutoff value.	Specificity	Sensitivity	AUC (Confidence Interval)
MCV	>89	69	45	0.548
IMRS score	>9	62	55	0.617
IMRS category	>1	66	55	0.627

MCV: Mean corpuscular volume, **IMRS:** Intermountain Mortality Risk Score, **IMRS category:** IMRS category

FIGURE 1. Analysis of the ROC (Receiver Operating Characteristics) Curves

TABLE 2. Examination of Laboratory and Indices.

Laboratory	Ectasia (-) n=220	Ectasia (+) n=226	P-value
WBC (10^3/µL)	8.03±2.49	8.11±2.68	0.761
Hemoglobin (g/dL)	13.6±1.6	13.8±1.9	0.126
Hematocrit (%)	40.7±4.7	41.6±5.03	0.069
MCV (fL)	87±5.1	87.5±5.8	0.129
MCHC (g/dL)	33.2±1.42	33.2±1.47	0.889
RDW (%)	13.4±1.2	14.3±3.02	**<0.001**
MPV (fL)	9.3 (8.5–10.2)	9.8 (9.1–10.6)	**<0.001**
Platelet count (10^3/µL)	234 (194–274)	236 (200–281)	0.316
Neutrophils (10^3/µL)	4.6 (3.7–5.7)	4.5 (3.8–5.5)	0.881
Lymphocytes (10^3/µL)	2.1 (1.7–2.5)	2.3 (1.7–2.8)	0.067
Monocyte (10^3/µL)	0.47 (0.37–0.62)	0.51 (0.41–0.62)	**0.047**
Creatinine (mg/dL)	0.95 (0.84–1.15)	0.98 (0.79–1.12)	0.839
Sodium (mmol/L)	139±3	139±3	0.963
Potassium (mmol/L)	4.4±0.4	4.45±0.47	0.951
Calcium (mg/dL)	9.4±0.6	9.3±0.53	**0.001**
Bicarbonate (mmol/L)	25.8±2.7	25.7±3.6	0.816
Glucose (mg/dL)	104 (93–133)	104 (92–127)	0.708
CRP (mg/dL)	2.4 (2–5.1)	3 (2–10)	0.385
ESR	20 (12–34)	16 (8–32)	0.244
Albumin (g/L)	42±4.6	41±4.1	0.269
Total cholesterol (mg/dL)	186 (152–223)	192 (160–218)	0.822
LDL-C (mg/dL)	111 (84–141)	117 (89–143)	0.205
HDL-C (mg/dL)	41 (35–53)	41 (34–49)	0.375
Triglyceride (mg/dL)	150 (101–208)	132 (100–176)	0.049
Indices			
NLR	2.09 (1.7–2.82)	1.98 (1.61–2.78)	0.177
LMR	4.5 (3.44–5.86)	4.5 (3.33–5.62)	0.589
PLR	111 (84–140)	106 (81–138)	0.416
PNI	53.6 (49.3–56.9)	53.5 (48.5–57.7)	0.891
SII index	485 (352–699)	455 (347–694)	0.468
CAR	0.57 (0.45–1.25)	0.72 (0.43–2.14)	0.284
IMRS score	8.5 (7–11)	10 (8–13)	**0.011**
IMRS category	1 (1–2)	2 (1–2)	**0.002**
TyG index	1.29 (0.88–1.85)	1.21 (0.83–1.71)	0.296

Data are shown as mean±standard deviation or n (%) or median (interquartile range) where appropriate. WBC, white blood cell, MCV, mean corpuscular volume; MCHC, mean corpuscular hemoglobin concentration; RDW, red cell distribution width; MPV, mean platelet volume; CRP, C-reactive protein; ESR, erythrocyte sedimentation rate, LDL-C, low-density lipoprotein cholesterol, HDL-C, high-density lipoprotein cholesterol; NLR, neutrophil-to-lymphocyte ratio; LMR, lymphocyte-to-monocyte ratio; PLR, platelet-to-lymphocyte ratio; PNI, prognostic nutritional index; SII, systemic immune-inflammation index; CAR, C-reactive protein-to-albumin ratio; IMRS, intermountain risk score; TyG, Triglyceride-glucose. Statistically significant P-values are shown in bold.

TABLE 3. Independent Predictors of Angiographic Ectasia in Univariate and Multivariate Logistic Regression Analysis.

	Univariate regression analysis			Multivariate regression analysis		
	HR	**%95 Cl**	**P-value**	**HR**	**%95 Cl**	**P-value**
Gender (male)	0.627	0.412–0.953	**0.028**			
Smoking	3.014	1.641–5.535	**<0.001**	3.744	1.026–13.653	**0.045**
Hemoglobin	1.086	0.976–1.209	0.125			
Hematocrit	1.036	0.997–1.077	0.068			
MCV	1.027	0.992–1.063	0.129	1.105	1.016–1.202	**0.019**
RDW	1.406	1.204–1.642	**<0.0001**			
MPV	0.991	0.956–1.027	0.611			
Lymphocytes	1.207	0.965–1.508	0.093			
Monocytes	2.786	0.964–8.050	**0.025**			
Calcium	0.556	0.386–0.801	**0.001**			
Triglyceride	0.998	0.996–1.000	0.186			
NLR	0.957	0.872–1.050	0.352			
IMRS score	1.138	1.034–1.252	**0.006**			
IMRS category	2.656	1.502–4.695	**<0.001**	5.255	1.349–20.464	**0.016**

MCV, mean corpuscular volume; RDW, red cell distribution width; MPV, mean platelet volume; NLR, neutrophil-to-lymphocyte ratio; IMRS, intermountain risk score.

Statistically significant P-values are shown in bold.

OP-09.
Association Between Uric Acid to Albumin Ratio and No-Reflow Phenomenon in Patients with NSTEMI

Cemalettin Yilmaz[1], Muhammet Mücahit Tiryaki[2]

[1]Department of Cardiology, Yalova University, Yalova, Turkiye; [2]Department of Cardiology, Muş State Hospital, Muş, Turkiye

Objectives: The no-reflow (NR) phenomenon following percutaneous coronary intervention (PCI) in non–ST-elevation myocardial infarction (NSTEMI) is a significant determinant of adverse outcomes, including infarct expansion, heart failure, and mortality. Oxidative stress and systemic inflammation are major contributors to microvascular dysfunction. The uric acid-to-albumin ratio (UAR) has recently emerged as a novel biomarker reflecting both oxidative and inflammatory burden. This study aimed to investigate the association between UAR and the NR phenomenon in NSTEMI patients undergoing coronary angiography.
Methods: A total of 213 consecutive NSTEMI patients who underwent coronary angiography between January 2025 and June 2025 were retrospectively analyzed. Patients were classified into two groups based on the presence (n=35) or absence (n=178) of angiographic no-reflow, defined as final TIMI flow ≤2 despite successful epicardial vessel opening. Baseline demographic, clinical, and laboratory data were recorded. The UAR was calculated as serum uric acid (mg/dL) divided by serum albumin (g/dL). Data were expressed as median (interquartile range). Variables with P<0.10 in univariate analysis were included in multivariable logistic regression.
Results: The median age of the study population was 60 (55–67) years, and 72.8% were male. The prevalence of diabetes mellitus was significantly higher in the NR group (68.6% vs. 24.7%, P<0.001). Compared with patients without NR, those with NR had higher serum uric acid levels [6.1 (5.7–6.7) vs. 5.7 (4.4–6.5) mg/dL, P=0.029] and lower albumin levels [3.7 (3.2–3.9) vs. 3.8 (3.6–4.1) g/dL, p=0.008]. Accordingly, UAR values were significantly higher in the NR group [1.76 (1.44–1.92) vs. 1.48 (1.17–1.70), P<0.001]. In multivariable analysis, diabetes mellitus (OR 8.02, 95% CI 3.26–19.76, P<0.001), peak troponin (OR 1.19, 95% CI 1.04–1.35, P=0.010), and UAR (OR 2.25, 95% CI 1.17–4.35, P=0.015) were independent predictors of no-reflow.
Discussion: Our findings demonstrate that a higher uric acid-to-albumin ratio is associated with the occurrence of no-reflow in NSTEMI patients. Both elevated uric acid and reduced albumin reflect systemic oxidative stress, endothelial dysfunction, and inflammatory activation—pathophysiological mechanisms known to impair coronary microcirculation. The independent predictive value of UAR suggests its potential role as an integrated biomarker combining these processes. This easily measurable parameter may aid in pre-procedural risk stratification for microvascular complications during PCI.
Conclusions: An increased uric acid-to-albumin ratio is independently associated with the no-reflow phenomenon in NSTEMI patients undergoing PCI. UAR may serve as a practical, inexpensive, and readily available marker to identify patients at higher risk for impaired myocardial reperfusion. Prospective studies are warranted to validate its predictive value and explore its clinical utility in guiding preventive strategies.
Keywords: No-reflow, Uric acid, Albumin, NSTEMI

TABLE 1. Baseline Characteristics by No-Reflow Status

Variables	Overall n=213	No-Reflow (+) n=35	No-Reflow (-) n=178	P-value
Age, years (IQR)	60 (55-67)	62 (55.5-65.5)	59 (55-67)	**0.709**
Male sex, n (%)	155 (72.8)	23 (65.7)	132 (74.2)	0.305
LVEF, % (IQR)	50 (40-55)	50 (40-55)	50 (40-55)	0.975
Hypertension, n (%)	135 (63.4)	25 (71.4)	110 (61.8)	0.280
Diabetes Mellitus, n (%)	68 (31.9)	24 (68.6)	44 (24.7)	**<0.001**
COPD, n (%)	19 (8.9)	3 (8.6)	16 (9)	0.937
Smoking, n (%)	93(43.7)	13 (37.1)	80 (44.9)	0.395
Sinus Rhythm, n (%)	205 (96.2)	1 (3.8)	7 (3.9)	0.760
Culprit Lesion, n (%)				0.394
LAD	86 (40.4)	17 (48.6)	68 (38.7)	
CX	90 (42.3)	15 (42.9)	75 (42.1)	
RCA	37 (17.4)	3 (8.6)	34 (19.1)	
WBC (10^9/L)	9.9 (8.6-12.7)	11.9 (9-15.7)	9.9 (8.2-11.8)	**0.002**
Neutrophils (10^9/L)	6.5 (4.8-9.3)	8.7 (6-10.4)	6.2 (4.8-8.9)	**0.004**
Hemoglobin (g/dL)	12.7 (11.6-13.7)	13.1 (12.1-13.6)	12.7 (11.6-13.7)	0.893
Platelet (10^9/L)	262 (214-312)	250 (225-299)	263 (214-317)	0.673
Glucose (mg/dL)	111 (95-134)	136 (71-229)	107 (75-170)	0.205
Creatinine (mg/dL)	0.73 (0.6-0.94)	0.73 (0.64-1.1)	0.73 (0.59-0.84)	0.095
BUN (mg/dL)	22 (16-36.4)	31 (16-34)	22 (16-42)	0.071
eGFR (mL/min/1.73m^2)	76 (65-92)	75.5 (65-91.3)	81 (64.8-96.8)	0.169
Uric Acid (mg/dL)	6 (4.7-6.7)	6.1 (5.7-6.7)	5.7 (4.4-6.5)	**0.029**
Albumin (g/dL)	3.8 (3.6-4.1)	3.7 (3.2-3.9)	3.8 (3.6-4.1)	**0.008**
CRP (mg/L)	5.7 (2.9-9)	5.7 (2.7-9)	5.6 (3.1-14)	0.410
Total Cholesterol (mg/dL)	191 (158-225)	193 (158-225)	177 (156-212)	0.247
Triglycerides (mg/dL)	197 (132-237)	198 (101-298)	193 (134-237)	0.879
HDL (mg/dL)	33 (22-40)	28 (19-41)	33 (24-40)	0.078
LDL (mg/dL)	127 (101-162)	127 (107-161)	122 (81-165)	0.391
Peak Troponin (ng/mL)	1.21 (0.41-4.83)	5.4 (0.8-10)	1.1 (0.4-4.2)	**<0.001**
TSH (µIU/mL)	1.43 (1-2.1)	1.56 (1-3)	1.43 (0.97-2.1)	0.458
UAR	1.57 (1.2-1.8)	1.76 (1.44-1.92)	1.48 (1.17-1.7)	**<0.001**

BUN, blood urea nitrogen; COPD, chronic obstructive pulmonary disease; CRP, C-reactive protein; CX, circumflex artery; eGFR, estimated glomerular filtration rate; HDL, high-density lipoprotein cholesterol; LAD, left anterior descending artery; LVEF, Left ventricular ejection fraction; LDL, low-density lipoprotein cholesterol; RCA, right coronary artery; TSH, thyroid stimulating hormone; UAR, uric acid to albumin ratio; WBC, white blood cell count. Data are presented as median (interquartile range). Statistically significant P-values are shown in bold.

TABLE 2. Multivariable Logistic Regression for No-Reflow Status

Variables	OR	95% CI (lower-upper)	P-value
Age (year)	1.02	0.98-1.06	0.322
Sex (male)	1.08	0.49-2.72	0.859
Diabetes mellitus (yes)	8.02	3.26-19.76	**<0.001**
WBC (10^9/L)	1.05	0.96-1.15	0.264
Peak troponin (ng/mL)	1.19	1.04-1.35	**0.010**
UAR	2.25	1.17-4.35	**0.015**

WBC, white blood cell count; UAR, uric acid to albumin ratio.
Statistically significant P-values are shown in bold.

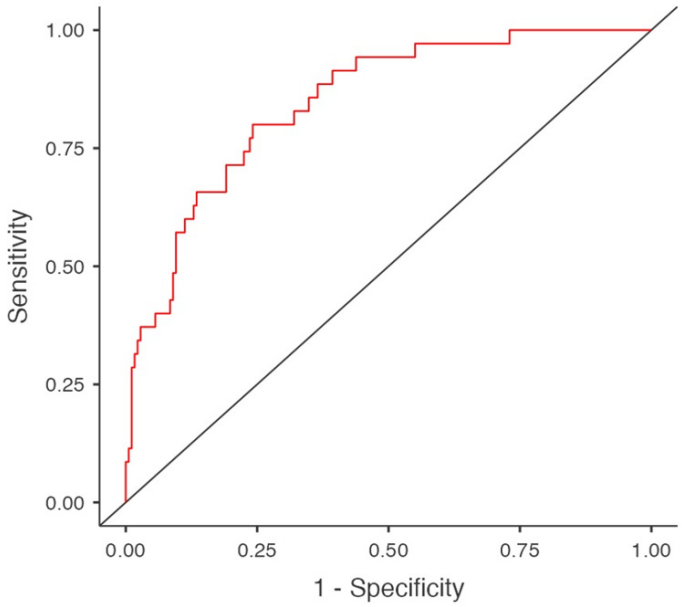

FIGURE 1. Receiver operating characteristic (ROC) rurve for the multivariable logistic regression model predicting no-reflow phenomenon (AUC=0.847).

OP-10.
Coronary Vasospasm Presenting as ST-Elevation Myocardial Infarction: A Case Report

Veysel Macit[1], Doğan Ormanci[1], Ayşe Dilara Balyimez[1], Sanatbek Rustambakov[1], Rauf Samet Gençgün[1], Safa Oktay[1], Adem Yarar[1], Ömer Fatih Savci[1], Mehmet Melek[1], Hasan Ari[1]

[1]Department of Cardiology, University of Health Sciences, Bursa Yüksek İhtisas Training and Research Hospital, Bursa, Türkiye

Case Presentation: A 58-year-old male presented to the emergency department with typical anginal chest pain radiating bilaterally to the arms, originating from the midsternal area, lasting 10–15 minutes, and recurring for one week. He had no known comorbidities or smoking history. Coronary angiography performed seven years earlier revealed a normal left anterior descending artery (LAD), 50% plaque in the circumflex artery (Cx), and a normal right coronary artery (RCA). An electrocardiogram (ECG) showed anterior ST-segment elevation myocardial infarction (STEMI), and the patient was immediately taken to the catheterization laboratory (Figure 1). Before the procedure, the ST elevation regressed and the chest pain resolved. Coronary angiography revealed 50% stenosis in the LAD and a normal Cx, while diffuse spasm was observed in the RCA, which resolved after intracoronary nitroglycerin administration (Figure 2). The lesion in the LAD was interpreted as vasospasm, and the patient was admitted to the coronary intensive care unit (ICU). Echocardiography showed an ejection fraction of 55% and mild left ventricular hypertrophy. The patient received standard acute coronary syndrome treatment, diltiazem 60 mg twice daily, and intravenous nitroglycerin (5–10–15 µg/min). During ICU follow-up, he remained asymptomatic with stable ECG findings and normal laboratory results (Table 1). After 30 hours, he was transferred to the ward and started on oral isosorbide-5-mononitrate 40 mg twice daily. However, he later developed recurrent chest pain with anterior ST elevation on ECG. Intravenous nitroglycerin was restarted, and the patient was readmitted to the ICU. Following treatment, symptoms and ST elevation resolved. To confirm the suspected diagnosis of vasospastic angina, a methylergometrine provocation test was performed after 24 hours of intravenous nitroglycerin therapy. During the test, vasospasm was induced in the left coronary system, which completely regressed after nitrate administration (Figure 3). The diagnosis of vasospastic angina was confirmed. The patient was discharged with verapamil 120 mg twice daily, oral nitrate therapy, and nitroglycerin spray, along with standard medication and lifestyle recommendations.

Discussion: Vasospastic angina (VSA) results from transient coronary artery spasm leading to reversible myocardial ischemia, independent of atherosclerosis. It accounts for approximately 2–5% of patients undergoing coronary angiography for angina and typically occurs between 40 and 60 years of age, particularly among smokers.

Diagnosis is established using provocation tests such as the ergonovine, acetylcholine, hyperventilation, or cold pressor tests. Treatment includes lifestyle modification and pharmacological therapy. Calcium channel blockers are the first-line and most effective long-term agents, while sublingual nitroglycerin provides rapid relief during acute attacks. Long-acting nitrates are recommended for long-term prevention.

Conclusions: This case demonstrates that coronary vasospasm can mimic STEMI, emphasizing the importance of recognizing this condition to prevent unnecessary interventions and recurrent ischemic episodes through appropriate medical therapy.

Keywords: Vasospasm, ST Elevation, Vasospastic Angina, Vasodilator

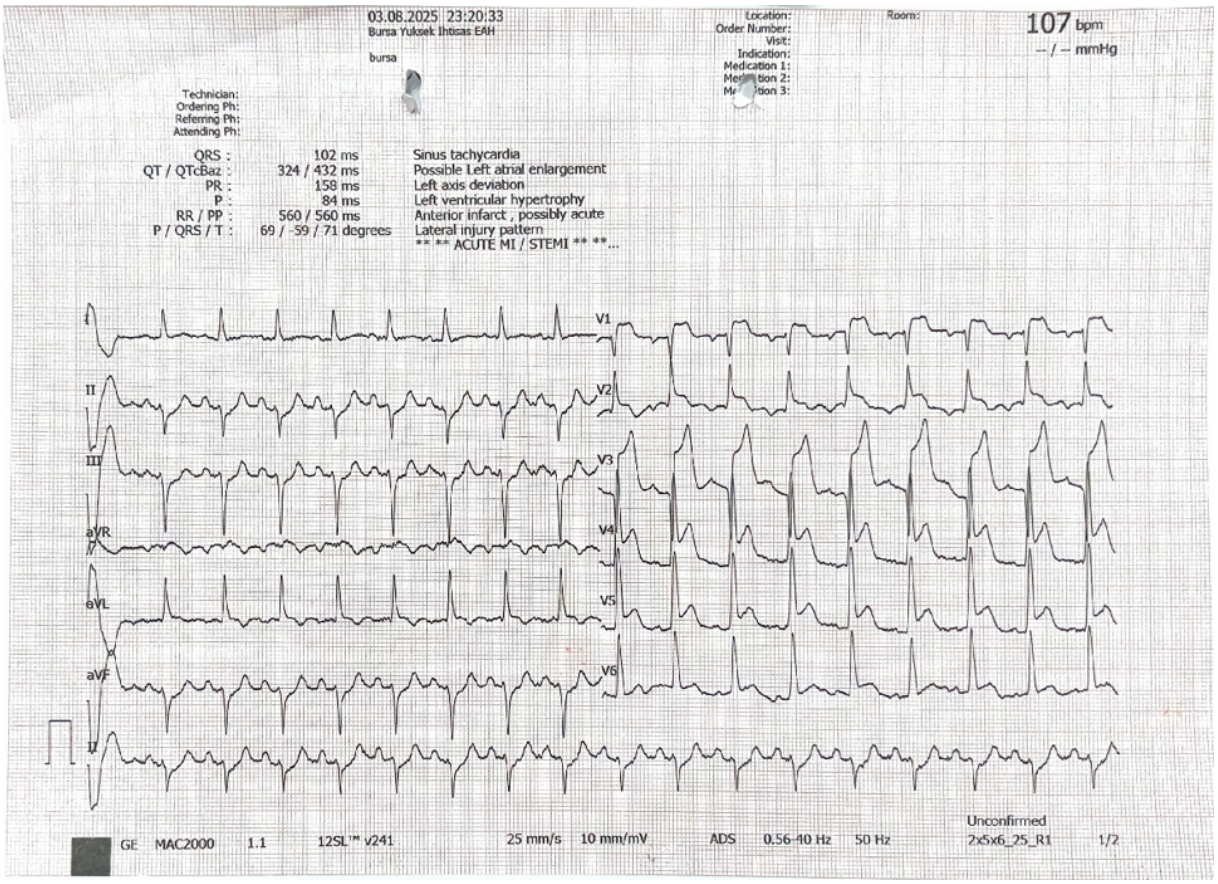

FIGURE 1. **An electrocardiogram (ECG) shows anterior ST-segment elevation myocardial infarction (STEMI).**

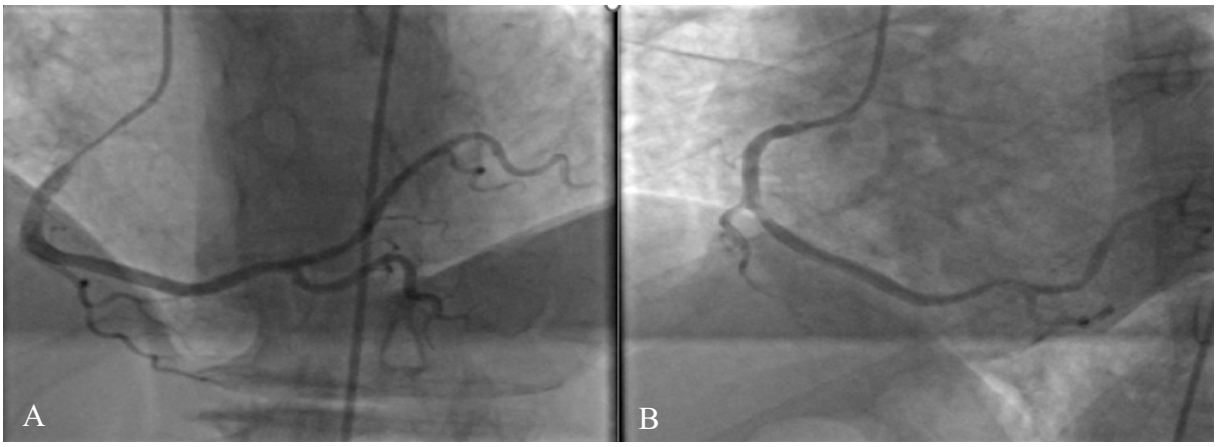

FIGURE 2. **(A) Coronary angiography reveals diffuse spasm in the RCA. (B) It has been observed that coronary spasm resolves after intracoronary administration of nitroglycerin.**

TABLE 1. Laboratory Findings

	Day 1	Day 2	Day 3	Day 4	Day 5
Hemoglobin (g/dL)	15.8	16.3	16		14.5
Creatine kinase (mg/dL)	0.6	0.8	0.8	0.8	1.07
CK-MB (ng/dL)	9.5-15.5	23.3-11.3	8.5		
Troponin-T (pg/dL)	436-260	396-529	378		

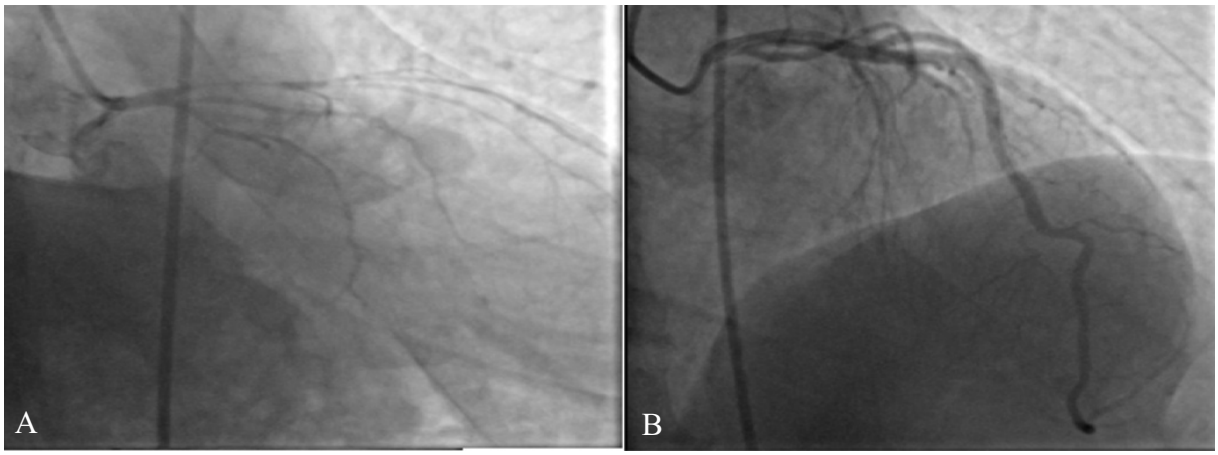

FIGURE 3. During the ergonovine test, vasospasm was induced in the left coronary system (A), which completely regressed after nitrate administration (B).

OP-11.
Management of a Stripped Stent within a Dissected Coronary Lesion

Veysel Macit[1], Doğan Ormanci[1], Ayşe Dilara Balyimez[1], Sanatbek Rustambakov[1], Rauf Samet Gençgün[1], Safa Oktay[1], Adem Yarar[1], Ömer Fatih Savci[1], Mehmet Melek[1], Hasan Ari[1]

[1]Department of Cardiology, University of Health Sciences, Bursa Yüksek İhtisas Training and Research Hospital, Bursa, Türkiye

Objectives: Although coronary angiography and percutaneous coronary interventions (PCI) are routinely performed procedures, they require great precision and are prone to serious complications. In this report, we present the management of a stripped stent within a dissected coronary artery in a patient who presented with acute myocardial infarction (MI).

Case Presentation: A 65-year-old male presented to the emergency department with typical chest pain persisting for two days and worsening over the past 30 minutes. The electrocardiogram (ECG) revealed findings consistent with acute inferior myocardial infarction (Figure 1). The patient was urgently transferred to the catheterization laboratory. Coronary angiography demonstrated 50% stenosis in the LAD, 50% in the circumflex artery, and two significant lesions (99% and 80%) in the right coronary artery (RCA) (Figure 2). After wiring the RCA with a 0.014-inch guidewire, balloon predilatation was performed, during which a coronary dissection developed (Figure 3) To seal the dissection, a 3.0 × 37 mm drug-eluting stent was advanced, but it failed to cross the lesion. A Guideliner catheter was introduced to facilitate delivery, but during withdrawal of the deformed Guideliner, it became entangled with the balloon and guidewire, leading to stent stripping from the balloon shaft. (Figure 4) As the RCA flow became sluggish, an attempt was made to retrieve the stripped stent using a snare; however, the snare could not pass through the dissected segment. A new guidewire was then advanced, confirming re-entry into the true lumen. Gentle balloon dilatation restored distal flow. Subsequently, two 3.0×12 mm and one 3.0×24 mm everolimus-eluting stents were deployed sequentially, embedding the stripped stent between the vessel wall and the newly implanted stents. Final angiography showed successful lesion sealing without residual dissection and restoration of TIMI 3 flow (Figure 5).

Discussion: Coronary artery dissection can occur spontaneously or iatrogenically during coronary catheterization, angioplasty, or stent implantation. It may lead to abrupt vessel closure, hemodynamic instability, ischemic ECG changes, and, in cases of aortic extension, life-threatening complications. When dissection is localized and coronary flow is preserved, conservative management may be considered. However, if flow is compromised or the left main coronary artery is involved, immediate interventional or surgical treatment is required. Stent stripping or dislodgement is a rare but potentially catastrophic complication during PCI. It can occur when the stent fails to properly engage the vessel wall, during withdrawal of a balloon or guiding device, or if the guidewire becomes entangled around the stent. Consequences may include stent embolization, thrombosis, or vessel occlusion. Retrieval options include snare extraction, multi-wire or balloon trapping techniques, or, in selected cases, surgical removal. However, no standardized management algorithm exists.

Conclusions: In the present case, the decision to embed the stripped stent within the dissected segment using additional stents successfully restored flow and sealed the dissection, avoiding the need for surgical intervention. This case highlights the importance of rapid recognition, careful device handling, and adaptability during complex PCI to manage rare but critical complications such as stent stripping within a dissected coronary artery.

Keywords: Coronary Dissection, Stent Stripping, Percutaneous Coronary Intervention, Complication Management, RCA Dissection

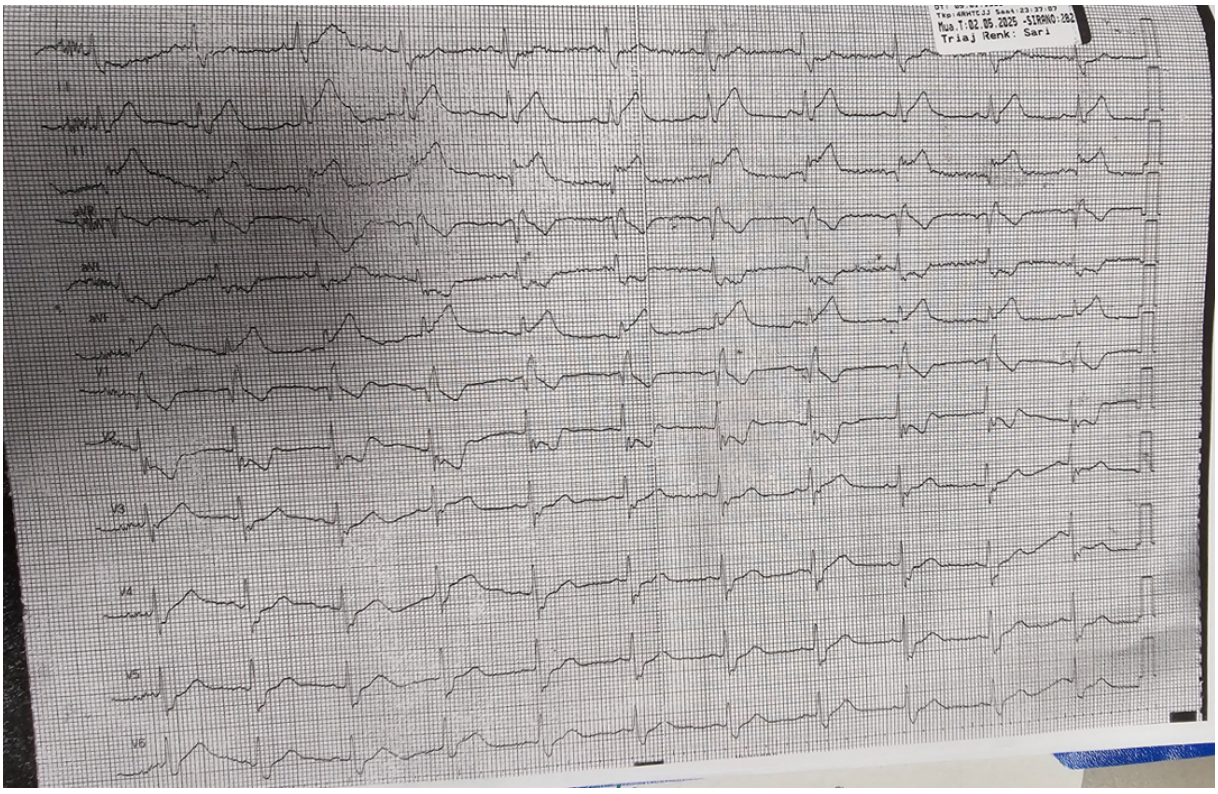

FIGURE 1. The electrocardiogram (ECG) shows findings consistent with acute inferior myocardial infarction.

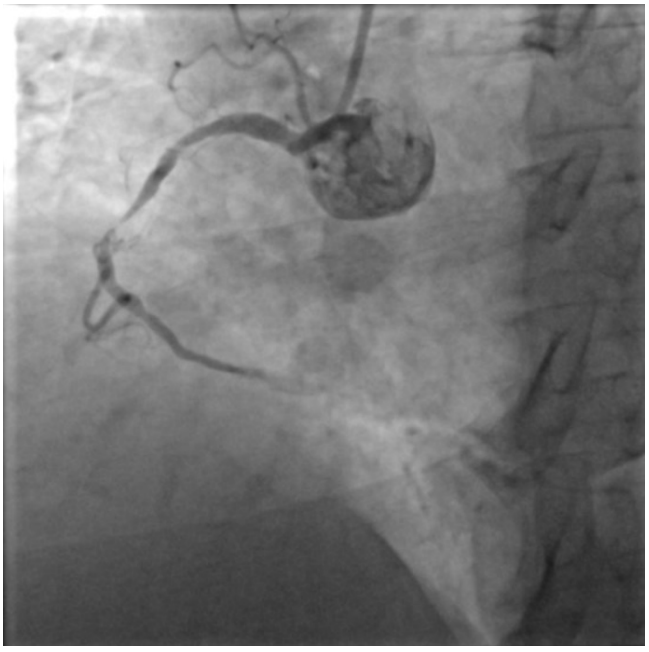

FIGURE 2. Coronary angiography demonstrating two significant lesions (99% and 80%) in the right coronary artery (RCA).

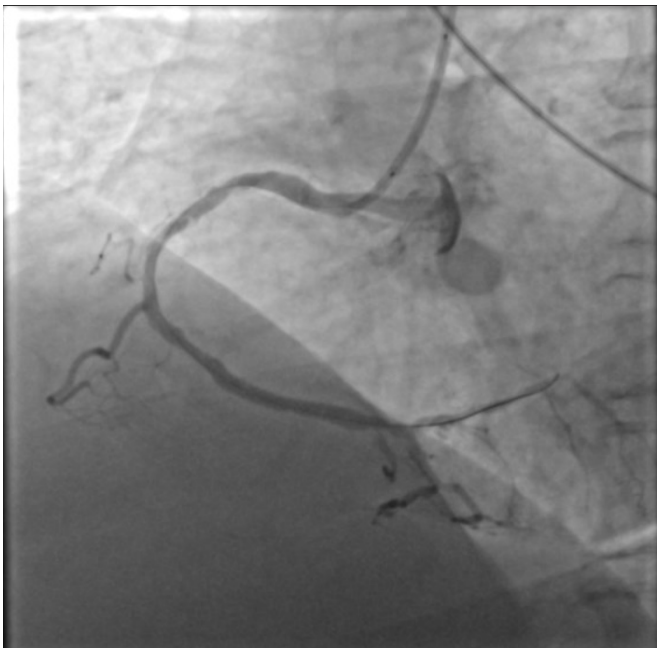

FIGURE 3. Coronary angiography demonstrating dissection line on the right coronary artery following predilatation.

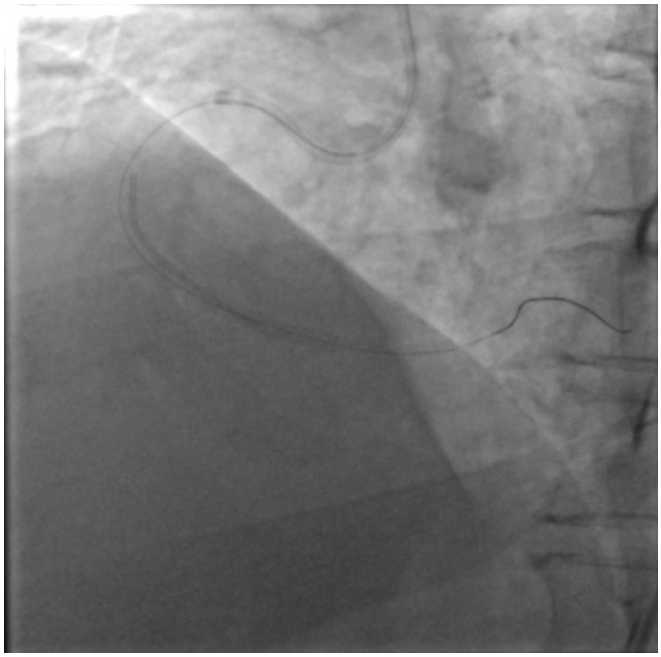

FIGURE 4. **Image of detached stent**

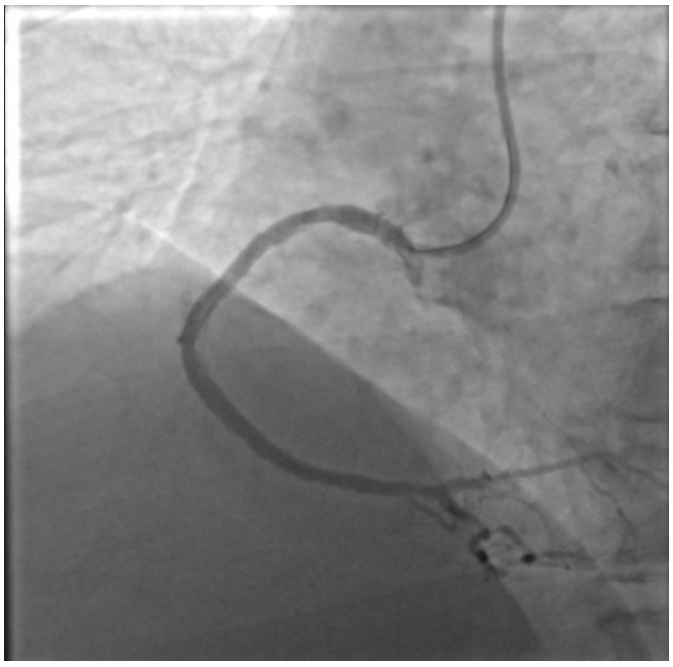

FIGURE 5. **Final angiography shows successful lesion sealing without residual dissection and restoration of TIMI 3 flow.**

OP-12.
Prognostic Utility of the Pan-Immune-Inflammation Value (PIV) in Predicting No-Reflow Among Patients Undergoing Primary PCI for STEMI

Ali Sezgin[1], Çağatay Tunca[1]

[1]*Department of Cardiology, Ankara Etlik City Hospital, Ankara, Türkiye*

Objectives: No-reflow following primary percutaneous coronary intervention (PCI) in patients with ST-segment elevation myocardial infarction (STEMI) represents a critical therapeutic challenge, as it is associated with adverse myocardial recovery, ventricular dysfunction, larger infarct size, and increased short- and long-term morbidity and mortality. Despite advances in interventional techniques and pharmacotherapy, the incidence of no-reflow remains substantial, underscoring the importance of early risk stratification. Systemic inflammation plays a pivotal role in microvascular obstruction and ischemia–reperfusion injury. Conventional inflammatory indices such as neutrophil-to-lymphocyte ratio (NLR), platelet-to-lymphocyte ratio (PLR), lymphocyte-to-monocyte ratio (LMR), and systemic immune-inflammation index (SII) have been associated with impaired microvascular reperfusion; however, comparative evidence evaluating more comprehensive inflammatory markers is limited. The pan-immune-inflammation value (PIV), incorporating neutrophils, lymphocytes, monocytes, and platelet counts, recently emerged as a composite marker reflecting cumulative inflammatory and immune burden. This study aimed to assess the role of PIV in predicting no-reflow following primary PCI for STEMI and compare its diagnostic performance with established hematologic inflammatory biomarkers.
Methods: This retrospective single-center cohort included 356 consecutive STEMI patients who underwent primary PCI within 12 hours of symptom onset between January 2022 and December 2024. Detailed clinical, angiographic, and laboratory data were analyzed. No-reflow was defined as post-procedural Thrombolysis in Myocardial Infarction (TIMI) flow grade ≤2 despite successful epicardial vessel recanalization. PIV and other inflammatory indices were calculated using admission complete blood count parameters. Multivariable logistic regression was performed to evaluate independent determinants of no-reflow, adjusting for age, diabetes, left ventricular ejection fraction, ischemia-to-balloon time, peak troponin, albumin, and C-reactive protein. Receiver operating characteristic (ROC) analyses assessed the discriminatory capacity of each index.
Results: No-reflow occurred in a clinically meaningful proportion of patients. Admission PIV levels were significantly elevated in the no-reflow group compared with patients achieving optimal reperfusion (Table 1). In multivariable analysis, PIV remained an independent predictor of no-reflow, whereas NLR, PLR, LMR, and SII did not demonstrate independent significance after adjustment (Table 2). ROC analysis revealed that PIV achieved the highest discriminatory performance (AUC ~0.70), modest yet superior to other indices including NLR (AUC ~0.68), PLR (AUC ~0.66), SII (AUC ~0.65), and LMR (AUC ~0.64) (Figure 1). Sensitivity analyses across infarct territories and clinical subgroups yielded consistent results, reinforcing the robustness of these findings.
Discussion: PIV independently predicts no-reflow in STEMI patients undergoing primary PCI and demonstrates superior predictive performance compared with other routinely used hematologic inflammatory indices. As an easily obtainable and cost-effective biomarker, PIV may support early risk stratification, allowing identification of high-risk patients who may benefit from individualized pharmacological strategies, intracoronary vasodilators, or adjunctive microvascular protection therapies. Prospective multicenter studies

are warranted to validate these results and elucidate whether PIV-guided clinical decision pathways can improve outcomes in STEMI care.

Conclusions: PIV is a practical and effective biomarker for predicting no-reflow in STEMI patients undergoing primary PCI, outperforming traditional inflammatory indices. Its use may enhance early risk assessment and guide targeted interventions, but further prospective studies are needed to confirm its clinical utility.

Keywords: STEMI; No-Reflow, Primary PCI, Inflammation, PIV, NLR, PLR, SII, LMR, Risk Stratification, Microvascular Obstruction.

TABLE 1. Baseline Characteristics of the Study Population According to No-Reflow Status

Variable	Normal (n=285)	No-reflow (n=71)	P-value
Age (year)	54 (45–62)	60 (53–67)	**<0.001**
Male (%)	158 (55.4%)	53 (75.2%)	0.33
Hypertension (%)	158 (55.4%)	43 (60.1%)	0.089
DM (%)	113 (39.5%)	28 (40.0%)	0.815
Dyslipidemia (%)	38 (13.3%)	12 (17.1%)	0.318
CAD (%)	54 (19.0%)	18 (24.7%)	0.655
Smokers (%)	137 (48.2%)	33 (46.6%)	0.354
LVEF (%)	39.2±6.9	31.8±5.1	**<0.001**
Killip III–IV (%)	13 (4.4%)	6 (8.2%)	0.062
BMI (kg/m^2)	26.5 (23.6–30.8)	28.4 (26–31)	**<0.001**
GFR	85.3±39.4	81.9±37.2	0.17
Glucose	109.3±68.6	129.5±34.5	0.144
Total cholesterol	156.3 (132–179)	175 (141–210)	0.291
HDL	39 (29–47)	37 (31–45)	0.713
LDL	101 (79–135)	106 (82–176)	0.645
Triglyceride	129 (83–211)	144 (91–233)	0.536
Albumin	4.2 (3.5–4.4)	3.9 (3.5–4.1)	0.021
Hemoglobin	14.2 (13.3–15.2)	14.3 (12.9–15.1)	0.883
Platelet	220 (188–263)	227 (187–257)	0.716
WBC	7.4 (5.8–8.9)	12.3 (9.6–16.9)	**<0.001**
Neutrophil	4.1 (3.3–5.6)	7 (4.5–15.3)	**<0.001**
Neutrophil %	67.2 (45.2–75.3)	81.9 (66.9–89.1)	**<0.001**
Lymphocyte	1.8 (1.3–2.5)	1.7 (1.3–2.3)	0.168
CRP	3.2 (2–4.6)	5 (3.6–8)	**<0.001**
NLR	2.1 (1.5–3)	4.6 (2.9–9.6)	**<0.001**
NPAR	16.32±4.14	21.01±3.65	**<0.001**
CAR	0.75 (0.59–1.7)	1.1 (0.74–2.1)	**<0.001**
PIV	298.4 (182.7–448.6)	561.2 (401.5–754.3)	**<0.001**

Data are shown as mean±standard deviation or mean (minimum-maximum) or n (%) or median (interquartile range) where appropriate. DM, diabetes mellitus; CAD, coronary artery disease; LVEF; left ventricular ejection fraction; BMI, body mass index; GFR, glomerular filtration rate; HDL, high density lipoprotein; LDL, low density lipoprotein; WBC, white blood cell; CRP, C-reactive protein; NLR, neutrophil-to-lymphocyte ratio; NPAR, neutrophil percentage-to-albumin ratio; CAR, C-reactive protein-to-albumin ratio; PIV, pan-immune-inflammation value. Statistically significant P values are shown in bold.

TABLE 2. Univariate and Multivariate Predictors of No-Reflow

Variable	Unadj OR	Unadj. P-value	Adj OR	Adj. P-value
Age	1.05	**<0.001**	1.052	0.002
LVEF	0.94	**0.003**	0.95	0.006
Ischemia-to-balloon	1.006	**0.004**	1.005	0.01
Albumin	0.61	**0.002**	0.72	0.04
PIV	1.82	**0.002**	1.71	0.005
NLR	1.32	**0.003**	—	—
PLR	1.21	**0.04**	—	—
SII	1.18	0.05	—	—
LMR	1.15	0.08	—	—

LVEF, left ventricular ejection fraction; PIV, pan-immune-inflammation value; NLR, neutrophil-to-lymphocyte ratio; PLR, platelet-to-lymphocyte ratio; SII, systemic immune-inflammation index; LMR, lymphocyte-to-monocyte ratio, OR, odds ratio. Statistically significant P values are shown in bold.

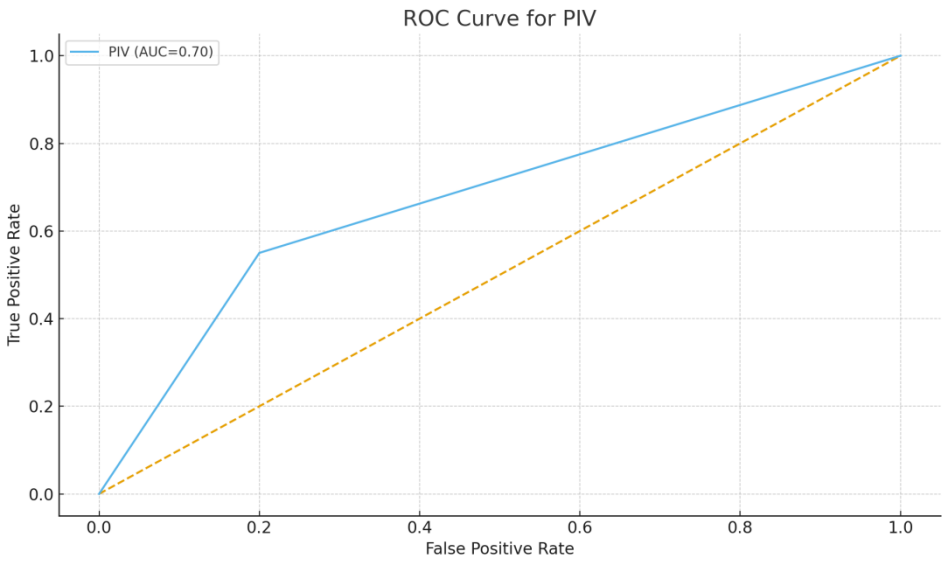

FIGURE 1. ROC curve for PIV in predicting no-reflow. PIV, pan-immune-inflammation value.

OP-13.
VARC-3 Outcomes of Myval, Portico, and Evolut-R in TAVI

Serkan Aslan[1], Ümit Bulut[1], Mehmet Ertürk[1]

1Department of Cardiology, University of Health Sciences, Istanbul Mehmet Akif Ersoy Thoracic and Cardiovascular Surgery Training and Research Hospital, İstanbul, Türkiye

Objectives: To compare baseline, procedural, and clinical outcomes of patients undergoing transcatheter aortic valve implantation (TAVI) with Myval, Portico, and Evolut-R valves.
Methods: A total of 445 patients (Myval=179, Portico=166, Evolut-R=100) who underwent transfemoral TAVI between 2019 and 2024 were retrospectively analyzed. Baseline characteristics and imaging parameters were recorded. Procedural and hemodynamic variables were compared (Table 1). Composite endpoints including device success, early safety, and clinical efficacy were defined according to the Valve Academic Research Consortium-3 (VARC-3) criteria (Table 2).
Results: The Portico group had higher mean age and left ventricular ejection fraction compared with other groups (P=0.007 and P=0.004, respectively), while other demographic and clinical variables were similar. Annular dimensions and valve-to-annulus oversizing ratios differed significantly among valve types (P<0.05), reflecting differences in device design and sizing strategies. The procedure time was shortest with Myval (70±34 min, P=0.005). Predilatation was least frequent with Myval (16.2%) and most frequent with Portico (81.9%) (P<0.001). Postdilatation was performed in 47% of Portico cases (P<0.001), and a second valve was required in 8.4% (P<0.001). Postprocedural gradients were slightly higher with Myval (8.7±4.1 mmHg, P=0.011) without clinical impact. Technical success exceeded 90% across all valve types, though correct positioning rates were slightly lower for Portico (91.6%, P<0.001). According to VARC-3 criteria, 30-day device success rates were comparable and satisfactory (Myval 83.8%, Portico 76.5%, Evolut-R 79.0%; P=0.230). Early safety, including death, stroke, bleeding, vascular, and renal events, was similar among devices (Myval 63.7%, Portico 56.6%, Evolut-R 57.0%; P=0.345), with no significant differences in major vascular complications, moderate-to-severe aortic regurgitation, or new pacemaker implantation. At one-year follow-up, freedom from death, stroke, or valve-related rehospitalization was high and comparable across groups (Myval 79.9%, Portico 76.5%, Evolut-R 76.0%; P=0.671).
Discussion: TAVI has become an established therapeutic option for severe aortic stenosis, providing a less invasive alternative to surgery in patients at intermediate or high surgical risk. However, comparative real-world data for new-generation transcatheter valves remain limited. Understanding procedural and clinical differences among valve platforms is essential for optimizing patient selection and long-term outcomes.
In this study, Myval, Portico, and Evolut-R valves showed high technical success and similar VARC-3–defined composite outcomes. The absence of significant differences in early safety or one-year efficacy suggests that outcomes are influenced more by anatomical and operator factors than by valve design. Myval demonstrated shorter procedural times and fewer balloon interventions, while Portico required more frequent postdilatation and second-valve use. Despite these procedural variations, all three valves provided consistent clinical performance and safety.
Conclusions: TAVI procedures using Myval, Portico, and Evolut-R valves achieved high technical success with comparable early and long-term outcomes. These findings support the reliability and effectiveness of all three valve systems in contemporary TAVI practice.
Keywords: Clinical Outcomes, Transcatheter Aortic Valve Implantation, Transcatheter Heart Valves, VARC-3 Criteria

TABLE 1. Baseline and Procedural Characteristics

Parameters	Total (n=445)	Myval (n=179)	Portico (n=166)	Evolut R (n=100)	P-value
Demographic and clinical characteristics					
Age (years)	78.07±7.23	77.39±6.32	79.46±6.74	76.99±9.03	**0.007**
Men	192 (43.1)	77 (43.0)	63 (38.0)	52 (52.0)	0.081
Systemic hypertension	337 (75.7)	144 (80.4)	119 (71.7)	74 (74.0)	0.149
Diabetes mellitus	201 (45.2)	91 (50.8)	68 (41.0)	42 (42.0)	0.141
Coronary artery disease	325 (73.0)	140 (78.2)	115 (69.3)	70 (70.0)	0.129
Coronary bypass	96 (21.6)	35 (19.6)	37 (22.3)	24 (24.0)	0.660
Stroke/TIA	33 (7.4)	11 (6.1)	9 (5.4)	13 (13.0)	0.052
Chronic kidney disease	120 (27.0)	47 (26.3)	48 (28.9)	25 (25.0)	0.755
Pulmonary disease	91 (20.4)	29 (16.2)	41 (24.7)	21 (21)	0.146
Pacemaker	16 (3.6)	6 (3.4)	6 (3.6)	4 (4.0)	0.962
Atrial fibrillation	84 (18.9)	31 (17.3)	32 (19.3)	21 (21.0)	0.742
STS score	6 (4–7)	6 (5–7)	6 (4–8)	6 (4–8)	0.625
Echocardiographic characteristics					
LVEF (%)	55 (45–60)	55 (45–60)	60 (50–60)	55 (36–60)	**0.004**
Aortic valve area (cm^2)	0.71±0.15	0.71±0.15	0.72±0.14	0.70±0.18	0.538
Aortic mean pressure gradient (mmHg)	46.6±13.0	46.1±14.0	46.9±11.4	46.8±14.0	0.846
Aortic peak systolic velocity (m/s)	4.3±0.67	4.2±0.65	4.3±0.67	4.3±0.58	0.534
Computed tomography characteristics					
Left main height (mm)	14.35±3.13	13.83±3.03	14.75±3.08	14.39±3.30	0.053
Right coronary artery height (mm)	17.07±3.44	16.60±3.87	17.52±3.25	16.96±2.94	0.083
Annulus perimeter (mm)	76.86±7.66	78.01±8.53	75.79±5.90	77.11±8.95	0.054
Annulus, perimeter derived diameter (mm)	24.45±2.41	24.86±2.67	24.13±1.87	24.52±2.85	0.053
Annulus area (mm^2)	455.91±92.36	470.58±104.5	441.95±68.58	459.42±107.7	0.034
Annulus, area derived diameter (mm)	23.89±2.62	24.35±2.66	23.65±1.84	23.74±3.64	0.089
Oversizing (%)	12.28±8.31	6.77±8.60	12.69±4.54	20.32±6.52	**<0.001**
Minimum iliofemoral lumen diameter (mm)	7.0±3.5	7.1±4.8	6.9 ±1.2	7.0±1.8	0.944
Procedural Characteristics					
Implanted valve size, mm	26.91±3.08	25.34±2.76	27.09±1.86	29.43±3.51	**<0.001**
Conscious anesthesia	348 (78.2)	135 (75.4)	136 (81.9)	77 (77.0)	0.325
Procedure time* (min)	75±31	70±34	81±27	77±30	**0.005**
Pre-dilatation	196 (44.0)	29 (16.2)	136 (81.9)	31 (31.0)	**<0.001**
Post-dilatation	160 (36.0)	42 (23.5)	78 (47.0)	40 (40.0)	**<0.001**
Need for second valve	17 (3.8)	2 (1.1)	14 (8.4)	1 (1.0)	**<0.001**
Cardiac structure perforation	9 (2.0)	4 (2.2)	1 (0.6)	4 (4.0)	0.157
Converted to open surgery	4 (0.9)	2 (1.1)	0 (0.0)	2 (2.0)	0.227
Coronary artery occlusion	2 (0.4)	1 (0.6)	1 (0.6)	0 (0.0)	0.746
Cardiac tamponade	9 (2.0)	2 (1.1)	5 (3.0)	2 (2.0)	0.458
Postop AF	25 (5.6)	7 (3.9)	14 (8.4)	4 (4.0)	0.138
Postop mean pressure gradient (mmHg)	8.1±4.0	8.7±4.1	7.8±4.0	7.2±3.5	**0.011**

Data are shown as mean±standard deviation or n (%) or median (interquartile range) where appropriate. LVEF, left ventricular ejection fraction; STS, society of thoracic surgeons; TIA, transient ischemic attack.

*Procedure time was defined as the time from arterial puncture, until vascular closure.

Statistically significant P values are shown in bold.

TABLE 2. Composite endpoints.

Parameters	Total (n=445)	Myval (n=179)	Portico (n=166)	Evolut R (n=100)	P-value
Technical success, n (%)	407 (91.5)	167 (93.3)	146 (88.0)	94 (94.0)	0.122
Absence of procedural mortality	434 (97.5)	176 (98.3)	159 (95.8)	99 (99.9)	0.177
Successful access, delivery, deployment, system retrieval	438 (98.4)	177 (98.9)	163 (98.2)	98 (98.0)	0.812
Correct positioning of one valve in proper location	428 (96.2)	177 (98.9)	152 (91.6)	99 (99.0)	<0.001
Absence of surgery or intervention related to device or to a major vascular or access-related, or cardiac structural complication	21 (95.3)	169 (94.4)	160 (96.4)	95 (95.0)	0.681
Device success (at 30 days) n (%)	356 (80.0)	150 (83.8)	127 (76.5)	79 (79.0)	0.230
Technical success	407 (91.5)	167 (93.3)	146 (88.0)	94 (94.0)	0.122
Absence of surgery or intervention related to device or to a major vascular or access-related, or cardiac structural complication	405 (91.0)	167 (93.3)	147 (88.6)	91 (91.0)	0.306
Intended valve performance*	421 (94.6)	171 (95.5)	155 (93.4)	95 (95.0)	0.662
Early safety (at 30 days), n (%)	265 (59.6)	114 (63.7)	94 (56.6)	57 (57.0)	0.345
All stroke	17 (3.8)	6 (3.4)	5 (3.0)	6 (6.0)	0.428
VARC type 2–4 bleeding	96 (21.6)	35 (19.6)	43 (25.9)	18 (18.0)	0.220
Major vascular complications	35 (7.9)	11 (6.1)	17 (10.2)	7 (7.0)	0.345
Acute kidney injury stage 3 or 4	27 (6.1)	7 (3.9)	9 (5.4)	11 (11.0)	0.054
Moderate or severe aortic regurgitation	17 (3.9)	5 (2.9)	8 (4.9)	4 (4.0)	0.625
New permanent pacemaker	91 (20.4)	42 (23.5)	32 (19.3)	17 (17.0)	0.392
Repeat procedure for valve dysfunction	4 (0.9)	2 (1.1)	0 (0.0)	2 (2.0)	0.227
Clinical efficacy (at 1 year and thereafter), n (%)	346 (77.8)	143 (79.9)	127 (76.5)	76 (76.0)	0.671
All-cause mortality	86 (19.3)	29 (16.2)	36 (21.7)	21 (21.0)	0.388
All stroke	22 (4.9)	8 (4.5)	7 (4.2)	7 (7.0)	0.557
Hospitalization for procedure- or valve-related causes	8 (1.8)	5 (2.8)	2 (1.2)	1 (1.0)	0.428

#at exit from procedure room.

*intended valve performance based on discharge echo included mean aortic valve gradient <20 mmHg, peak velocity <3 m/s, no moderate/severe prosthetic valve regurgitation.

OP-14.
Colchicine Aiding Recurrent Pacemaker Pocket Inflammation Management: A Case Report

Tolga Koşmaz[1], Ahmet Özderya[2], Muhammed Raşit Sayin[3], Ezgi Kalaycioğlu[1]

[1]Department of Cardiology, Ahi Evren Chest, Heart and Vascular Surgery Training and Research Hospital, Trabzon, Türkiye; [2]Department of Cardiology, Trabzon Kanuni Training and Research Hospital, Trabzon, Türkiye; [3]Department of Cardiology, Medical Park Yıldızlı Hospital, Trabzon, Türkiye

Objectives: Cardiac implantable electronic device (CIED) infections are an important clinical problem due to their increasing incidence and tendency to recur. This report presents a patient with recurrent CIED infections despite multiple system extractions and reimplantations. Histopathological evaluation revealed a foreign-body giant-cell reaction, suggesting that inflammatory mechanisms might play a key role. Colchicine was added to the treatment regimen for its potential anti-inflammatory effects, and no infection recurrence was observed during long-term follow-up.

Case Presentation: A 56-year-old male patient with hypertension and diabetes mellitus presented with redness and itching at the pacemaker pocket site. The patient's clinical course, laboratory findings, imaging results, surgical procedures, and histopathological data were retrospectively reviewed. The clinical outcome after the addition of colchicine was assessed. The patient underwent DDD + LBBP pacemaker implantation on May 5, 2023, due to complete atrioventricular block. On June 16, 2023, localized infection was suspected because the lead was unaffected, and pocket revision was performed. Persistent infection required complete system removal on July 31, 2023. A contralateral DDD-KPM pacemaker was implanted on August 7, 2023. On January 12, 2024, the system was again removed for recurrent infection. Subsequently, a new DDD pacemaker (Medtronic) with a TYRX antibacterial envelope was implanted on March 18, 2024. During follow-up, the patient represented with local erythema and itching. Laboratory inflammatory parameters were within normal limits. Ultrasonography showed a loculated collection, and both transthoracic and transesophageal echocardiography revealed no vegetation. On April 30, 2024, localized infection was again suspected, and pocket revision was performed. Histopathological analysis demonstrated chronic inflammation with multinucleated giant-cell reaction, while all blood and tissue cultures were sterile (Figure 1). Colchicine 0.5 mg twice daily was added to the discharge regimen. At 14-month follow-up, the patient remained asymptomatic with no clinical or laboratory evidence of infection recurrence.

Discussion: This case demonstrates that recurrent CIED infections can occur despite optimal surgical and antimicrobial therapy. The absence of bacterial growth and the presence of a foreign-body giant-cell reaction suggested that a non-infectious inflammatory process might contribute to recurrence. Colchicine, a potent anti-inflammatory agent, acts mainly by inhibiting neutrophil activation, chemotaxis, and inflammatory cytokine release. Its efficacy in conditions characterized by exaggerated inflammatory responses is well documented. In this patient, the addition of colchicine appeared to contribute to infection-free survival over 14 months. Nevertheless, this observation is based on a single case and cannot be generalized. Further studies with larger cohorts and prospective, controlled designs are required to determine whether colchicine has a consistent role in managing recurrent or inflammation-dominant CIED infections.

Conclusions: In recurrent pacemaker infections, the possibility of a foreign-body giant-cell reaction should be considered alongside microbial causes. Given its anti-inflammatory properties, colchicine may serve as an adjunctive therapeutic option in managing such inflammation-related CIED pocket complications.

Keywords: CIED, Colchicine, Device infection, Pacemaker

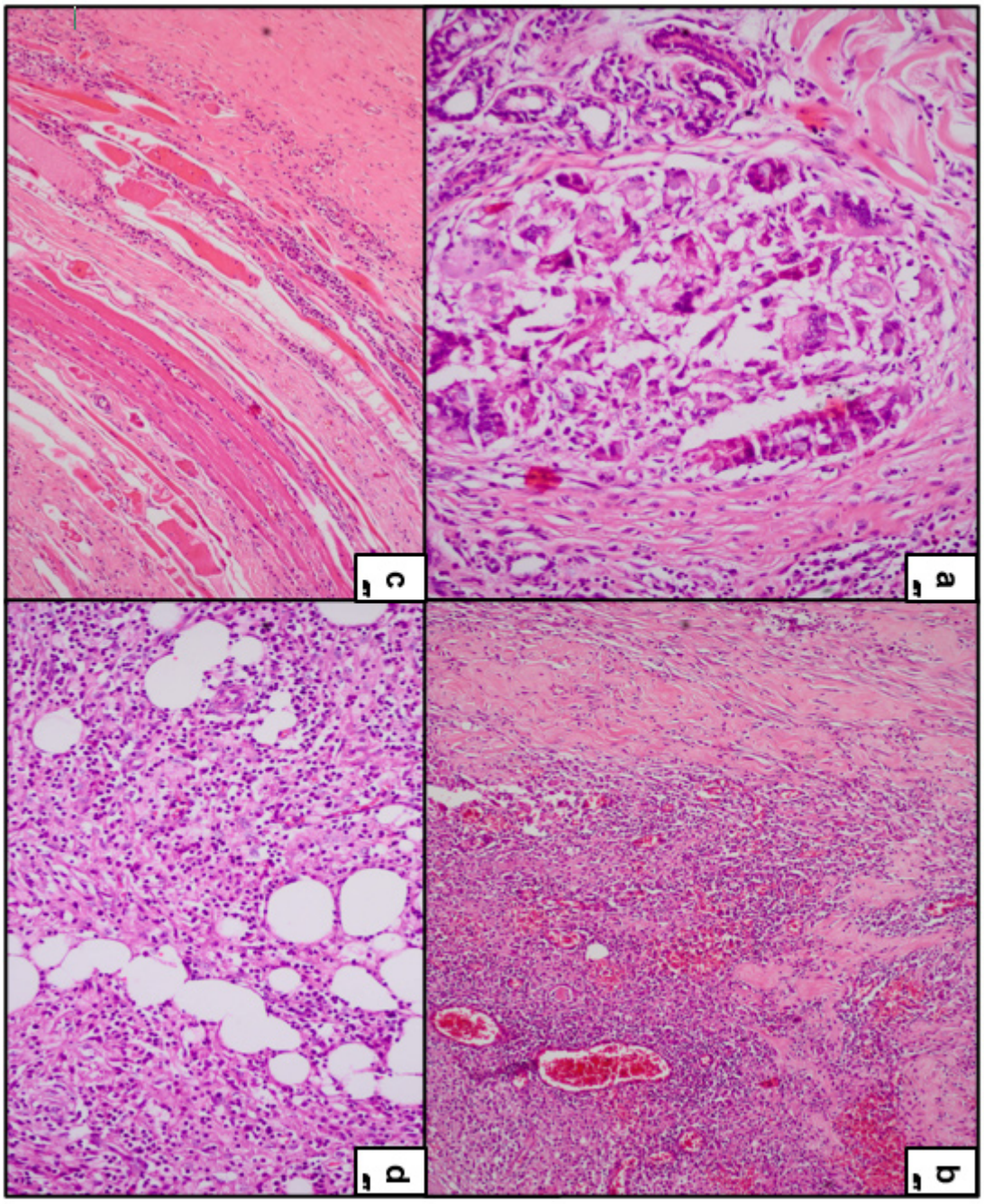

FIGURE 1. **a) Foreign body-type multinucleated giant cell formation (H&E, ×200). b) Severe active-chronic inflammation, congestion, and fibrosis (H&E, ×100). c) Chronic inflammatory cell infiltration rich in lymphocytes, also affecting striated muscle fibers (H&E, ×100). d) Areas of fat necrosis and lipogranulomatous inflammation (H&E, ×200).**

OP-15.
Colchicine Use After Coronary Artery Stenting: One-Year Follow-Up Results

Sherzod Akhmedov[1], Javokhir Akhrorov[2], Jurayev Ilkhom[2], Abror Abdullajonov[3], Nizomov Asror[4], Bobur Maxmudov[5]

[1]Department of Cardiology, Ezgu Niyat Tashkent, Carmen+ Bukhara, Uzbekistan; [2]Department of Cardiology, Carmen+ Bukhara, Uzbekistan; [3]Department of Cardiology, American Hospital, Uzbekistan; [4]Department of Cardiology, Ezgu Niyat Tashkent, Uzbekistan 5Department of Cardiology, Neurocenter Tashkent, Uzbekistan

Objectives: Restenosis following coronary artery stenting remains a significant clinical problem, particularly in patients with ischemic heart disease. Despite the widespread use of drug-eluting stents (DES), certain high-risk subgroups, such as those with diabetes mellitus and vascular calcification, continue to experience elevated restenosis rates. Inflammation plays a key role in this process. Colchicine, an anti-inflammatory agent known to inhibit the NLRP3 inflammasome and reduce systemic inflammatory markers, may help mitigate this risk. This study aimed to evaluate the efficacy of colchicine in reducing the incidence of in-stent restenosis one year after coronary stenting and to assess its impact on inflammatory biomarkers and clinical outcomes.

Methods: This prospective, randomized, controlled trial was conducted at Ezgu Niyat Cardiology Center and Carmen+ Clinic (Uzbekistan) between January 2021 and December 2024. A total of 120 patients with stable coronary artery disease undergoing successful elective percutaneous coronary intervention (PCI) with DES implantation were enrolled and randomized (1:1) into: Group 1 (Colchicine Group): 60 patients received colchicine 0.5 mg once daily for 12 months. Group 2 (Placebo Group): 60 patients received a matching placebo. The primary endpoint was the rate of angiographically confirmed in-stent restenosis (≥50% luminal narrowing) at 12 months. Secondary endpoints included major adverse cardiovascular events (MACE) and changes in inflammatory biomarkers (CRP, IL-6, TNF-α) from baseline to 12 months.

Results: At one-year follow-up, restenosis was significantly lower in the colchicine group compared to the placebo group (6.7% vs. 18.3%, P=0.02).

Colchicine group (n=60):

- LAD: 0/25 (0%)
- RCA: 3/20 (15%)
- LCX: 1/15 (6.7%)
- Diabetic patients: 7.3%; non-diabetic: 5.3%
- With calcification: 7.7%

Placebo group (n=60):

- LAD: 2/30 (6.7%)
- RCA: 5/20 (25%)
- LCX: 4/10 (40%)
- Diabetic patients: 16.7%; non-diabetic: 22.2%
- With calcification: 15.4%

Inflammatory markers significantly decreased in the colchicine group (all $P < 0.01$):

- **CRP:** 4.2 → 1.8 mg/L
- **IL-6:** 6.5 → 3.1 pg/mL
- **TNF-α:** 12.7 → 6.2 pg/mL

No significant changes were observed in the placebo group (P>0.05).

Discussion: Colchicine significantly reduced restenosis rates and systemic inflammation in patients undergoing coronary stenting. Its anti-inflammatory mechanism, targeting the NLRP3 inflammasome, may explain the observed vascular protection. The absence of restenosis in LAD and LCX territories further supports colchicine's beneficial effect on critical vascular segments. The drug's efficacy extended to patients with diabetes and vascular calcification—populations at inherently higher restenosis risk.

Conclusions: Daily colchicine (0.5 mg) therapy significantly reduced in-stent restenosis and inflammatory biomarkers at one-year follow-up compared with placebo. These findings support the inclusion of colchicine as an adjunct to standard post-PCI therapy, especially in high-risk patients. Larger multicenter studies are warranted to confirm these results and refine patient selection criteria.

Keywords: Colchicine, Coronary Artery Stenting, Restenosis, Inflammation, Ischemic Heart Disease, Drug-Eluting Stent, CRP, IL-6, TNF-α, MACE

OP-16.
Drug-Coated Balloon-Only Strategy for Chronic Total Occlusion: A Prospective, Two-Center Study of 48 Patients

Sherzod Akhmedov[1], Javokhir Akhrorov[2], Jurayev Ilkhom[2], Abror Abdullajonov[3], Nizomov Asror[4], Bobur Maxmudov[5], Xayrullo Saidov[2]

[1]Department of Cardiology, Ezgu Niyat Tashkent, Carmen+ Bukhara, Uzbekistan; [2]Department of Cardiology, Carmen+ Bukhara, Uzbekistan; [3]Department of Cardiology, American Hospital, Uzbekistan; [4]Department of Cardiology, Ezgu Niyat Tashkent, Uzbekistan [5]Department of Cardiology, Neurocenter Tashkent, Uzbekistan

Objectives: Drug-coated balloon (DCB) angioplasty has emerged as a promising stentless approach for coronary artery disease, offering delivery of antiproliferative drugs while avoiding permanent metallic scaffolds. Its use in chronic total occlusion (CTO) lesions remains limited, particularly in complex lesions that traditionally require stent implantation after successful recanalization. CTO PCI is challenging due to extensive lesion modification, high rates of dissection, and increased restenosis risk, making careful lesion preparation essential. Intravascular imaging, including intravascular ultrasound (IVUS) and optical coherence tomography (OCT), enables precise assessment of plaque morphology, calcium burden, vessel sizing, and dissection patterns, while physiological assessment with instantaneous wave-free ratio (iFR) identifies non–flow-limiting dissections that may not require stenting.

Methods: This prospective, two-center registry enrolled consecutive patients with de novo coronary CTO (TIMI 0 ≥3 months) treated with a DCB-only strategy between January 2023 and May 2025. CTO crossing was achieved using antegrade wire escalation, antegrade dissection–reentry, or retrograde techniques as clinically indicated. Lesion preparation involved semi-compliant, non-compliant, and cutting/scoring balloons, targeting <30% residual stenosis, TIMI 3 flow, and absence of flow-limiting dissection. IVUS or OCT assessed plaque composition, calcium severity, vessel diameter, and dissection patterns to optimize balloon sizing. Non–flow-limiting dissections were evaluated with iFR, and procedures were completed without stenting if iFR ≥0.89. All patients received a paclitaxel-coated balloon inflated ≥60 seconds at nominal pressure, sized 1:1 to the reference vessel diameter. Dual antiplatelet therapy was prescribed for ≥12 months. Clinical follow-up occurred at 1, 6, and 12 months, with repeat angiography or coronary CT for symptomatic or ischemic patients.

Results: Forty-two patients (mean age 61±9 years; 71% male) underwent DCB-only PCI. Right coronary artery lesions accounted for 52%, LAD 33%, and LCx 15%; mean J-CTO score was 2.3±0.7. Moderate-to-severe calcification was observed in 48%, and mean lesion length was 32±9 mm, with 36% in the proximal segment. Procedural success (<30% residual stenosis, TIMI 3 flow, no in-hospital MACE) was 95%. Antegrade wire escalation was used in 64% of cases, antegrade dissection–reentry in 21%, and retrograde in 15%. IVUS was performed in 30 patients and OCT in 12. Non–flow-limiting type A–C dissections occurred in 33% and were safely managed with iFR (mean 0.93±0.04), allowing stentless completion. Bail-out stenting was required in 2 patients (5%). At 12 months, CCS class improved to 0–I in 90% of patients; clinical restenosis occurred in 2 patients (4.8%), both successfully re-treated. No target vessel thrombosis occurred. MACE-free survival was 92.9%, and target lesion revascularization–free survival was 95.2%.

Conclusions: A DCB-only strategy for de novo CTO lesions is feasible, safe, and effective when combined with meticulous lesion preparation, systematic intravascular imaging, and selective physiological assessment.

Avoiding permanent metallic scaffolds may reduce late stent-related complications, preserve vessel physiology, and maintain vasomotion. Our results support the potential of stentless CTO PCI as a viable alternative to contemporary stenting strategies. Larger, randomized studies with extended follow-up are needed to validate these findings and define the optimal role of DCB-only PCI in CTO treatment.
Keywords: Chronic Total Occlusion, Drug-Coated Balloon, Percutaneous Coronary Intervention, Intravascular Imaging, Angiographic Dissection, Instantaneous Wave-Free Ratio, Stentless Therapy

OP-17.
The Role of Pharmacological Cocktails in Preventing Radial Spasm and Complications During Percutaneous Coronary Intervention (PCI): A Clinical Study

Javokhir Akhrorov[1], Sherzod Akhmedov[2], Javokhir Akhrorov[1], Jurayev Ilkhom[1], Abror Abdullajonov[3], Nizomov Asror[4], Bobur Maxmudov[5], Xayrullo Saidov[1], Jamshid Sadullayev[1]

[1]Department of Cardiology, Carmen+ Bukhara, Uzbekistan; [2]Department of Cardiology, Ezgu Niyat Tashkent, Carmen+ Bukhara, Uzbekistan; [3]Department of Cardiology, American Hospital, Uzbekistan; [4]Department of Cardiology, Ezgu Niyat Tashkent, Uzbekistan [5]Department of Cardiology, Neurocenter Tashkent, Uzbekistan

Objectives: Percutaneous coronary intervention (PCI) is a standard procedure for treating coronary artery disease, with radial artery access preferred due to reduced bleeding risk and faster recovery. However, radial artery spasm (RAS) remains a common complication that can limit procedural success and cause patient discomfort. Pharmacological cocktails, consisting of vasodilators, calcium channel blockers, and anticoagulants, have been proposed to prevent RAS and improve procedural outcomes. This study aimed to evaluate the efficacy of a pharmacological cocktail in reducing RAS and improving procedural and post-procedural outcomes during PCI. Key objectives included assessing RAS incidence, procedural success, radial artery patency, and post-procedural complications such as hematoma and radial artery occlusion (RAO).
Methods: This prospective observational study enrolled 900 patients undergoing elective PCI between January 2024 and December 2024 at a tertiary cardiac center. Patients were randomized into two groups: the Cocktail Group (n=450), which received an intra-arterial pharmacological cocktail prior to PCI, and the Control Group (n=450), which underwent PCI without the cocktail. The cocktail consisted of nitroglycerin (100 µg), verapamil (2.5 mg), and heparin (5000 IU) administered as a single dose before the procedure.
All patients underwent Doppler ultrasonography on the day following PCI to assess radial artery patency, blood flow velocity, and presence of complications. Pain and spasm severity were evaluated using a Visual Analog Scale (VAS) on the day of PCI and the following day.
Results: The incidence of RAS was significantly lower in the Cocktail Group (5%) compared to the Control Group (20%) (P<0.001). Procedural success was higher in the Cocktail Group (98%) versus the Control Group (90%) (P<0.01). Radial artery patency evaluated by Doppler was 99% in the Cocktail Group compared to 92% in the Control Group. Post-procedural complications were reduced, with RAO occurring in 1% of the Cocktail Group and 5% of the Control Group. Doppler ultrasonography showed improved flow in the Cocktail Group: mean peak systolic velocity (PSV) 45 cm/s, end-diastolic velocity (EDV) 10 cm/s, and 90% of patients with minimal flow resistance; no arterial wall thickening was observed. In the Control Group, PSV was 30 cm/s, EDV 5 cm/s, with moderate to severe flow resistance in 25% of cases and mild arterial wall thickening in 15%.
Discussion: The use of a pharmacological cocktail significantly reduces the incidence of radial artery spasm, enhances procedural success, and improves radial artery patency during PCI. Vasodilators, calcium channel blockers, and anticoagulants synergistically contribute to these benefits. The study provides strong evidence for the routine use of pharmacological cocktails to enhance patient safety and procedural efficiency.
Limitations: The observational design limits causal inference, and long-term outcomes were not assessed.
Conclusions: Intra-arterial administration of a pharmacological cocktail containing nitroglycerin, verapamil, and heparin effectively reduces radial artery spasm, increases procedural success, and decreases post-procedural

complications during PCI. Routine use of this cocktail is recommended as a preventive strategy in PCI procedures. Future studies should evaluate long-term benefits and outcomes.
Keywords: Percutaneous Coronary Intervention, Radial Artery Spasm, Pharmacological Cocktail, Radial Artery Patency, Doppler Ultrasonography, Nitroglycerin, Verapamil

OP-18.
Drug-Coated Balloon-Only Strategy in a True LCx-OM Bifurcation Lesion (Medina 1.1.1): Case Report with 12-Month Follow-Up

Jurayev Ilkhom[1], Sherzod Akhmedov[2], Javokhir Akhrorov[1], Jurayev Ilkhom[1], Abror Abdullajonov[3], Nizomov Asror[4], Bobur Maxmudov[5], Xayrullo Saidov[1], Jamshid Sadullayev[1]

[1]Department of Cardiology, Carmen+ Bukhara, Uzbekistan; [2]Department of Cardiology, Ezgu Niyat Tashkent, Carmen+ Bukhara, Uzbekistan; [3]Department of Cardiology, American Hospital, Uzbekistan; [4]Department of Cardiology, Ezgu Niyat Tashkent, Uzbekistan [5]Department of Cardiology, Neurocenter Tashkent, Uzbekistan

Objectives: True bifurcation lesions, particularly involving the left circumflex artery (LCx) and obtuse marginal branch (OM), remain a major challenge in percutaneous coronary intervention (PCI). Standard provisional stenting is associated with risks of stent thrombosis, restenosis, and impaired vessel physiology. Drug-coated balloon (DCB)-only PCI, following careful lesion preparation, offers a "leave nothing behind" strategy, which may reduce long-term complications, especially in high-risk patients such as those with diabetes mellitus, hypertension, dyslipidemia, and smoking history. Evidence from the DEBUT trial (NEJM 2019) and bifurcation registry sub-analyses (2020–2023) supports the safety and efficacy of DCB-only approaches in complex coronary lesions. ESC 2023 guidelines recommend DCB use in bifurcation PCI when adequate lesion preparation is ensured.

Case Presentation: A 55-year-old male with Type 2 diabetes mellitus (10 years), hypertension, dyslipidemia, and a smoking history presented with stable angina CCS III, worsening on exertion. Stress testing was positive for ischemia. Coronary angiography revealed a true LCx–OM bifurcation lesion (Medina 1.1.1): LCx occluded distal to OM take-off and OM ostial-to-mid-segment stenosis up to 85%. TIMI 3 flow was preserved in the proximal LCx.

Strategy Rationale: Given the patient's high-risk profile and the lesion characteristics, a DCB-only strategy was selected. Bailout two-stent PCI was planned only if residual stenosis exceeded 75%, dissection ≥Type C occurred, or TIMI flow fell below 3. This approach was chosen to avoid permanent metal implantation, preserve vessel physiology, and reduce the risk of late stent thrombosis or in-stent restenosis.

P**rocedure Details:**

•*Lesion Preparation:* Recannalization and predilatation using non-compliant balloons: LCx 2.5×20 mm and OM 2.75×20 mm, at 12–14 atm.

•*DCB Application:* Kissing DCB inflation was performed: LCx 2.75×30 mm and OM 2.5×30 mm at 8 atm for 60 seconds each. Optimal balloon sizing and inflation time were used to maximize drug delivery and minimize vessel trauma.

•*Technical Considerations:* Careful wire positioning, avoidance of over-dilatation, and angiographic monitoring were crucial to prevent dissection and preserve side-branch flow.

Results: Final angiography demonstrated TIMI 3 flow in both LCx and OM, no significant dissection, and <30% residual stenosis. The patient remained asymptomatic on clinical follow-up at 3, 6, and 12 months. Control angiography at 12 months showed patent vessels without restenosis.

Discussion: DCB-only PCI is feasible in selected true bifurcation lesions with careful preparation. Advantages include the absence of permanent metal, preservation of vessel physiology, and reduced risk of late thrombosis.

High-risk patient factors—diabetes, smoking, hypertension—did not compromise procedural success. The approach aligns with DEBUT trial findings and ESC 2023 guidelines, supporting DCB use in bifurcation PCI with adequate lesion preparation. Strict adherence to bailout criteria is essential to ensure safety.

Conclusions: In this high-risk patient with a true LCx–OM bifurcation lesion (Medina 1.1.1), a DCB-only strategy achieved excellent angiographic and clinical outcomes at 12 months. This case highlights the potential of "leave nothing behind" PCI as a safe and effective alternative in selected complex bifurcation lesions, emphasizing meticulous lesion preparation, optimal DCB sizing, and rigorous follow-up.

Keywords: Drug-Coated Balloon, Bifurcation Lesion, LCx–OM, PCI, Medina 1.1.1, Leave Nothing Behind, Diabetes Mellitus, Stable Angina, High-Risk Patient, DEBUT Trial

OP-19.
The Utility of Atherogenic Index of Plasma in Predicting in-Hospital Ischemic Stroke in Patients Undergoing Carotid Artery Stenting

Tuba Unkun[1], **Serdar Fidan**[1]

[1]*Department of Cardiology, Kartal Kosuyolu Yüksek İhtisas Training and Research Hospital, Istanbul, Türkiye*

Objectives: Carotid artery stenosis is a major preventable cause of ischemic stroke. Carotid artery stenting (CAS) is a widely employed revascularization procedure in patients with high surgical risk. Periprocedural ischemic stroke is among the most serious complications, markedly increasing both mortality and morbidity. The Atherogenic Index of Plasma (AIP) is a biomarker reflecting the balance between pro- and anti-atherogenic lipoproteins. This study aimed to evaluate the predictive value of AIP for in-hospital ischemic stroke in patients undergoing CAS.

Methods: We retrospectively analyzed 745 patients who underwent elective CAS at Kartal Koşuyolu Yuksek Ihtisas Training and Research Hospital between 2018 and 2024. Demographic, clinical, and biochemical data were obtained from hospital records. AIP was calculated using log(TG/HDL-C). Patients were categorized into two groups according to the occurrence of in-hospital ischemic stroke: stroke (n=28) and no-stroke (n=717). Statistical analyses included the chi-square test for categorical variables and Mann–Whitney U test for continuous variables, with $p<0.05$ considered significant.

Results: No significant differences were observed between groups in terms of sex, diabetes mellitus, hyperlipidemia, smoking, or coronary artery disease (Table 1). The median AIP was higher in the stroke group compared to the control group, but the difference was not statistically significant (P=0.351). Hypertension was significantly more frequent among patients who developed stroke (P=0.042). Hemoglobin, leukocyte count, HDL-C, LDL-C, and triglyceride levels were not associated with stroke occurrence (Table 2).

Discussion: Although AIP has been previously linked to cardiovascular events, it did not predict early in-hospital ischemic stroke following CAS in this study. Hypertension emerged as the only significant risk factor, highlighting the importance of strict perioperative blood pressure management. The absence of independent predictive value for AIP suggests that comprehensive risk assessment, incorporating multiple clinical factors, is necessary for identifying patients at risk.

Conclusions: Hypertension is a significant predictor of in-hospital ischemic stroke after CAS, whereas AIP alone does not provide sufficient predictive value. Larger prospective multicenter studies will clarify AIP's prognostic value.

Keywords: Atherogenic Index of Plasma, Carotid Artery Stenting, Ischemic Stroke

TABLE 1. Association of Demographic and Clinical Parameters with In-Hospital Stroke

Variables		No Stroke n (%)	Stroke n (%)	P-value
Sex	Male	517 (96.1%)	21 (3.9%)	0.737
	Female	200 (96.6%)	7 (3.4%)	
Hypertension		554 (97.0%)	17 (3.0%)	**0.042**
Diabetes mellitus		313 (95.4%)	15 (4.6%)	0.300
Hyperlipidemia		432 (96.0%9)	14 (3.1%)	0.278
Smoking		358 (95.7%)	16 (4.3%)	0.454
Coronary artery disease		492 (96.1%)	20 (3.9%)	0.753
Peripheral artery disease		88 (95.7%)	4 (4.3%)	0.751

Chi-square test, P<0.05*. Statistically significant P-value is shown in bold.

TABLE 2. Association of Laboratory Parameters with In-Hospital Stroke

Variables	No Stroke Median (min–max)	Stroke Median (min–max)	P-value
Hemoglobin (g/L)	12.7(8.0–14.2)	12.5 (11.0–9.6)	0.617
Leukocytes (×10³/µL)	8.8 (5–14.04)	7.65 (6–7.83)	0.070
Platelets (×10³/µL)	232 (91–771)	214 (122–282)	0.121
Neutrophils (×10³/µL)	3.385 (3–9.59)	2.835 (7–4.23)	0.156
HDL cholesterol (mg/dL)	39.0 (20.0–90.0)	35.5 (25.0–63.0)	0.077
LDL cholesterol (mg/dL)	122.0 (30.0–312.0)	124.5 (58.0–190.0)	0.773
Triglycerides (mg/dL)	165.0 (100.0–929.0)	166.0 (103.0–587.0)	0.996
Hemoglobin (g/L)	34.0 (1.0–774.0)	35.0 (1.0–835.0)	0.886
Leukocytes (×10³/µL)	146.5 (1.0–397.0)	92.5 (16.0–354.0)	0.250
Platelets (×10³/µL)	4.23 (1.22–29.97)	4.83 (1.79–13.00)	0.351

HDL, High-Density Lipoprotein; LDL, Low-density lipoprotein. Mann–Whitney U test, P<0.05

OP-20.
A Case of Long QT Syndrome Presenting with Ventricular Arrhythmia

Davut Davutoğlu[1], Mehmet Taşci[1], Ayşe Dilara Balyimez[1], Selma Ari[1], Ahmet Tütüncü[1], Safa Oktay[1], Tahsin Bozat[1], Hasan Ari[1]

[1]Department of Cardiology, University of Health Sciences, Bursa Yüksek İhtisas Training and Research Hospital, Bursa, Türkiye

Case Presentation: A 67-year-old male presented to the emergency department with a two-day history of nausea, dizziness, palpitations, and constipation. He was diagnosed with diabetic ketoacidosis, treated with insulin, and discharged after improvement. The following night, he experienced syncope while getting up to use the bathroom and was brought back by ambulance. Laboratory tests showed hypokalemia (3 mmol/L), and ECG revealed a QTc interval of 566 ms (Figure 1). Intravenous potassium replacement was started. During observation, the patient developed Torsades de Pointes (Figure 1), progressing to ventricular fibrillation, and required seven defibrillation shocks. Serial ECGs showed QTc prolongation up to 655 ms (Figure 1). He was transferred to our center for further evaluation. His history included type 2 diabetes mellitus, hypertension, hyperlipidemia, and anxiety–depressive disorder. It was noted that his 41-year-old son had died suddenly during sleep, suggesting possible hereditary predisposition. On examination, fine crackles were heard in both lungs, and neurological findings were normal.

The patient's medications included perindopril, metformin, linagliptin, insulin, sertraline, and atorvastatin. On admission to our center, ECG showed a QTc of 672 ms (Figure 1). Echocardiography demonstrated an ejection fraction (EF) of 30%, global hypokinesia, mild mitral and tricuspid regurgitation, left ventricular hypertrophy (IVS 1.3 cm, PW 1.2 cm), and left atrial dilatation (Figure 2). Laboratory data revealed K: 3.4 mmol/L, troponin I: 248 pg/mL, and pro-BNP: 7650 pg/mL. Despite correction of electrolyte imbalance and heart failure therapy, recurrent malignant arrhythmias persisted. Diagnostic electrophysiological study (EPS) demonstrated no inducible ventricular arrhythmia (Figure 3). Based on clinical and ECG findings, Long QT Syndrome (LQTS) was suspected, and a DDD-ICD was implanted for primary prevention. After implantation, QTc shortened slightly, and no further arrhythmic events occurred during follow-up. Coronary angiography revealed non-obstructive disease: mild plaque in LAD, 30–50% stenosis in CX, and 50–60% in distal RCA (Figure 3). Genetic testing identified a heterozygous KCNH2 mutation, confirming LQTS Type 2. In this subtype, potassium channel dysfunction delays myocardial repolarization, and arrhythmias are often triggered by sudden auditory or emotional stimuli. First-degree relatives were referred for genetic screening. At one-month follow-up, EF improved to 48% with mild residual hypokinesia and trivial valvular regurgitation (Figure 4).

Discussion: Long QT Syndrome comprises inherited or acquired disorders of cardiac repolarization predisposing to polymorphic ventricular tachycardia and sudden death. The three common genotypes—LQT1, LQT2, and LQT3—account for about 75% of congenital cases. LQT2 results from KCNH2 gene mutations reducing IKr potassium current. Although systolic dysfunction is uncommon, transient EF reduction may occur after electrical storm episodes.

Diagnosis relies on clinical findings, ECG criteria, Schwartz score, and genetic testing. Treatment includes beta-blockers, potassium supplementation, avoidance of QT-prolonging drugs, and ICD implantation in high-risk or symptomatic patients.

Conclusions: LQTS is a heterogeneous disorder caused by abnormal cardiac repolarization. Integration of clinical, electrocardiographic, and genetic data ensures accurate diagnosis and risk assessment. In genetically

confirmed LQT2, early identification, appropriate ICD therapy, and family screening are essential to prevent recurrent arrhythmias and sudden cardiac death.

Keywords: Long QT Syndrome, Torsades de Pointes, Ventricular Fibrillation

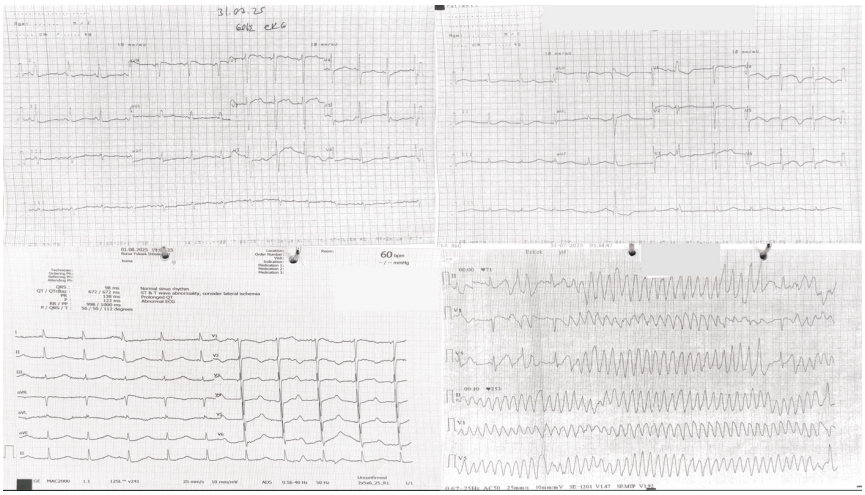

FIGURE 1. Electrocardiogram obtained at initial presentation; note the prolonged QT interval. Subsequent ECG demonstrating the development of Torsades de Pointes. Serial ECG recordings showing further prolongation of the QT interval over time.

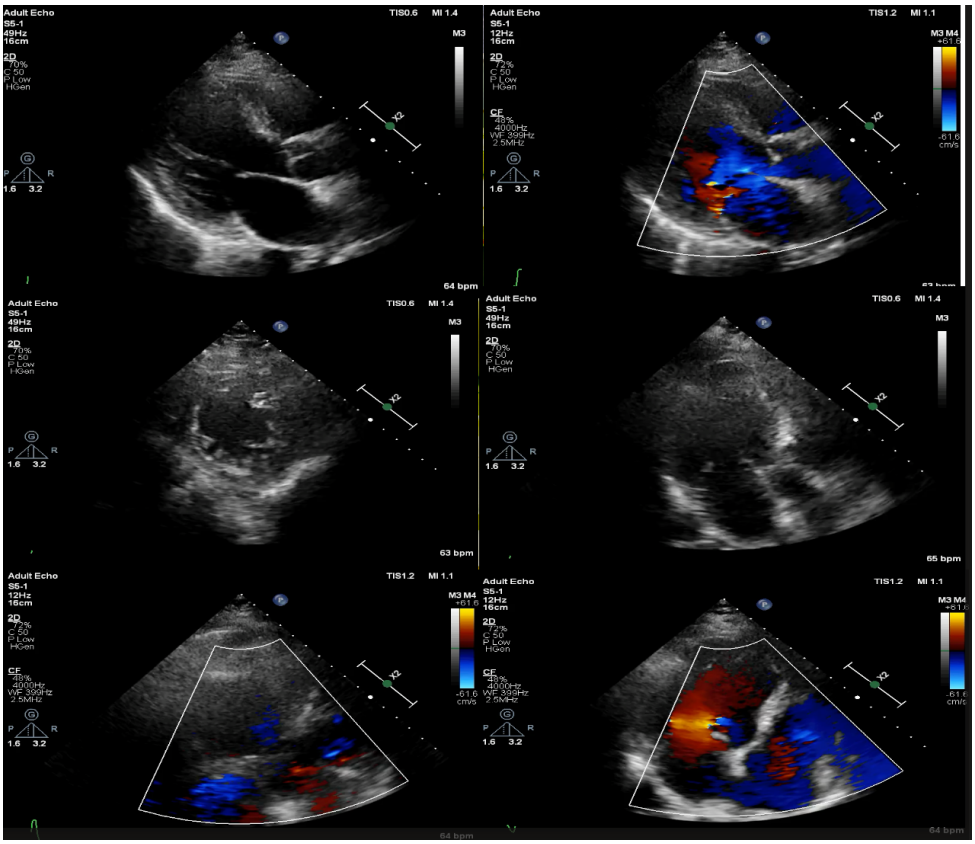

FIGURE 2. Transthoracic echocardiography performed at hospital admission.

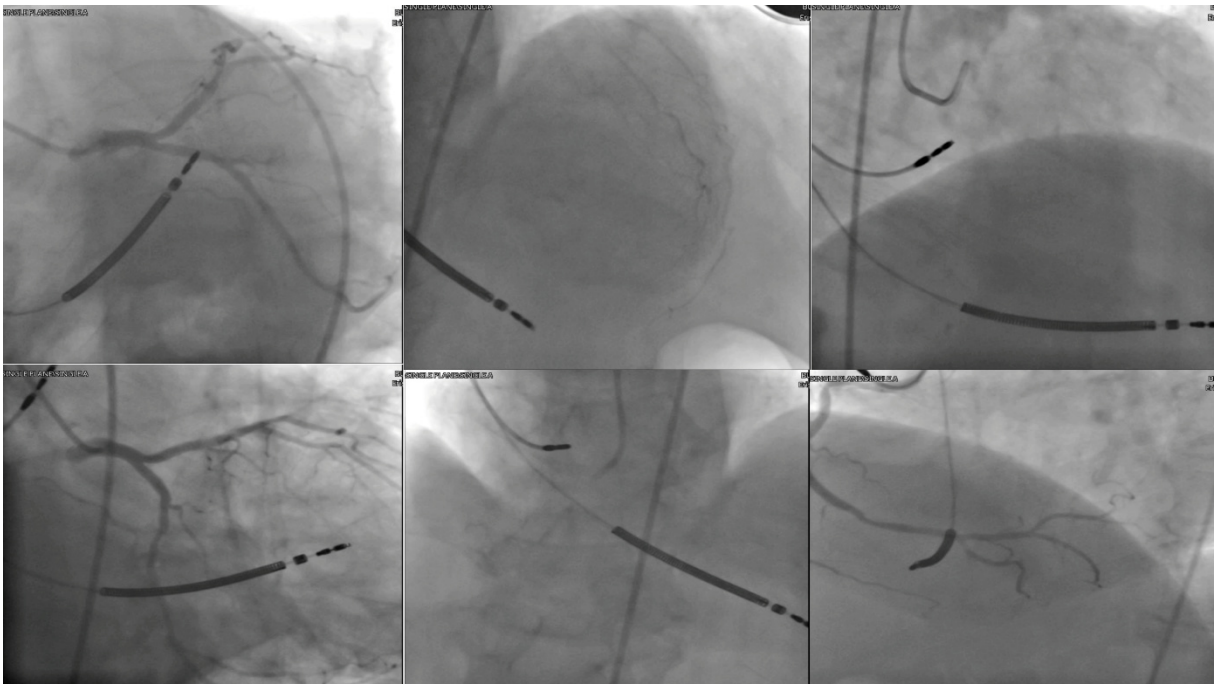

FIGURE 3. **1) Electrophysiological study, which was interpreted as normal. 2) Coronary angiography revealing no critical coronary artery disease; medical management was therefore pursued.**

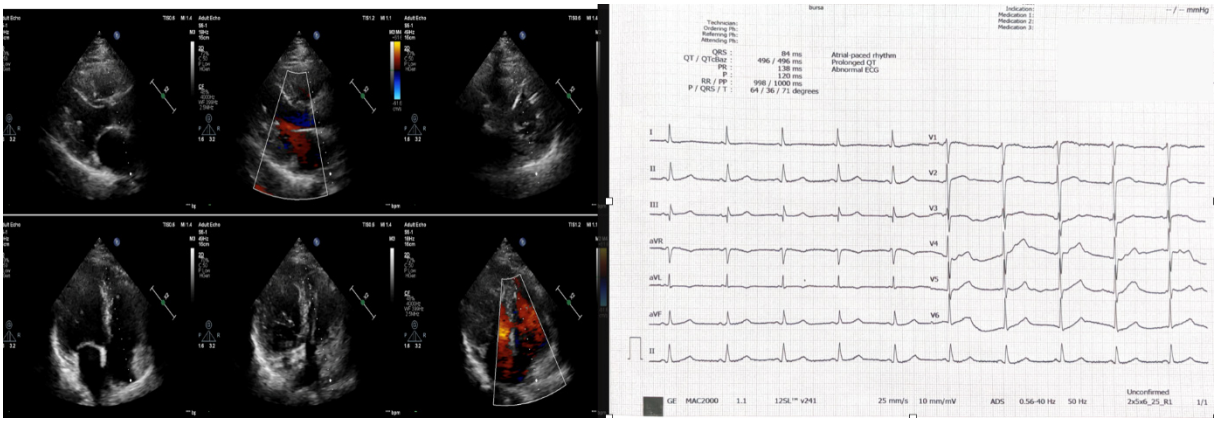

FIGURE 4. **Transthoracic echocardiography performed at 1-month follow-up after hospital discharge.**

OP-21.
Can We Predict Reperfusion in ST-Elevated Myocard Infaction?

Gülümser Sevgin Halil[1], Emir Özgür Barış Ökçün[2], Zerrin Yiğit[2]

[1]Department of Cardiology, University of Health Sciences, Kartal Koşuyolu Yuksek Ihtisas Training and Research Hospital, İstanbul, Türkiye; [2]Department of Cardiology, İstanbul University, Cerrahpaşa Institute of Cardiology, İstanbul, Türkiye

Objectives: Although percutaneous coronary intervention is the first choice in patients presenting with ST elevation myocardial infarctio, thrombolytic therapy is still used in the treatment of ST elevation myocardial infarction in some countries. for predicting success of reperfusion after thrombolytic treatment risk scores TIMI, PAMI, GRACE, and TIMI INDEX have been using and previously shown to be associated with mortality and morbidity. In our study, we aimed to compare the success of post-thrombolytic reperfusion using these risk scores with patient parameters recorded during hospital admission.
Methods: A total of 304 patients who received thrombolytic therapy between 2006 and 2012 were retrospectively included in the study. The patients' demographic characteristics were examined, and the ECG with the highest ST segment elevation at the time of hospital admission and the ECG taken at the 90th minute after thrombolytic treatment were analyzed. The criterion for successful reperfusion was defined as a resolution of ST segment elevation of more than 50% in the derivation with the highest ST segment elevation in the initial ECG.
Results: According to the risk scores, reperfusion rates were evaluated, and the TIMI risk score, GRACE risk score, and PAMI risk scale were found to be significantly higher in the non-reperfusion group. Upon evaluating the demographic and clinical parameters of the patients, it was observed that reperfusion decreased with increasing age (Age<65 (n=247),180 (%72.9), 67 (27.1%); Age 65-74 (n=44), 27 (61.4%), 17 (38.6%); Age>75 (n=13), 5 (%38.5), 8 (%61.5) in group 1 and group 2; respectively, P=0.013) and reperfusion success was also lover and statistically significant in group 1 in patients with Killip class≥ 2 (KILLIP 1 (n=249), 180 (%72.3), 69 (27.7%) (respectively); KILLIP 2-4 (n=55), 32 (58.2%), 23 (41.8%) (respectively), P=0.039. The length of symptom duration and elevated fasting blood glucose level were found to have a negative impacton reperfusion (<2 hours (n=123), 97 (78.9%), 26 (21.1%) (respectively); 2-4 hours (n=118), 82 (69.5%), 36 (30.5%) (respectively); >4 hours (n=63), 33 (52.4%), 30 (47.6%) (respectively), P=0.001). Regardless of the presence of diabetes mellitus, the incidence blood glucose levels evaluated by the patients were also divided into two groups as below and above 120 mg/dL, and significantly less reperfusion developed in the group with incidencelood glucose level than in other group (blood glucose level<120 mg/dL (n=174),130 (74.7%), 44 (25.3%); >120 mg/dL (n=129), 82 (63.6%), 47 (36.3%) (respectively), P=0.036). In the non-reperfusion group, the left ventricular ejection fraction was found to be significantly lower (LVEF% <40, (n=87), 37 (42.5%), 50 (57.5%); LVEF%≥40, (n=179), 149 (83.2%), 30 (16.8%) (respectively), P<0.001). Gender, administered thrombolytic agent, systolic blood pressure, heart rate, infarct localization, kidney glomerular filtration rate, patients' hematocrit values, and patients' history of diabetes mellitus and arterial hypertension were found to be similar in both the reperfusion and non-reperfusion groups, and it was determined that these parameters were not predictors of reperfusion. The TIMI risk score, PAMI risk score, and GRACE risk score were found to be predictors of reperfusion; however, the TIMI risk score was identified as more sensitive compared to the other scores.
Conclusion: We can predict the reperfusion success before thrombolytic therapy by calculating the TIMI risk score and recommend timely referral for primary percutaneous coronary intervention (PCI) for patients with high TIMI risk scores, if feasible, or immediate referral for a potential rescue PCI after thrombolytic therapy.
Keywords: TIMI Risk Score, ST-Elevated MI, Reperfusion

OP-22.
The Effect of Volume Overload on Ventriculo-Arterial Coupling in Hemodialysis Patients

Seray Yazgan[1], Doğan Ormanci[1], Ayşe Dilara Balyimez[1], Selma Ari1, Hasan Ari[1]

[1]Department of Cardiology, University of Health Sciences, Bursa Yüksek İhtisas Training and Research Hospital, Bursa, Türkiye

Objectives: The aim of this study was to investigate the effect of volume overload on right ventricle-pulmonary artery (RV-PA) coupling in patients undergoing hemodialysis treatment.
Methods: In this prospectively designed study, 33 patients undergoing hemodialysis (HD) for more than one year, who were admitted to the cardiology and internal medicine clinics, and 22 healthy volunteers were enrolled. Echocardiographic imaging was performed once in healthy subjects and, before and after hemodialysis sessions in HD patients. RV-PA coupling was assessed using TAPSE/SPAP, RV GLS/SPAP, and RV FAC/SPAP parameters.
Results: The mean age of HD patients was 43.6±11.6 years, compared to 37.2±13.2 years in the control group (P=0.06). RV TAPSE/SPAP ratio (1.11±0.19 vs 0.98±0.31; P=0.03) (Figure 1) and RV GLS/SPAP ratio (-0.91±0.09 vs -0.82±0.28; P=0.009) were significantly lower in HD patients compared to controls. RV TAPSE/SPAP ratio; before hemodialysis: 0.98±0.31 and after hemodialysis: 1.07±0.27; P=0.048 (Figure 2). RV GLS / SPAP ratio; before hemodialysis: -0.82±0.28 and after hemodialysis: -0.96±0.29, P=0.032 (Figure 3). FAC / SPAP ratio; before hemodialysis: 1.84±0.44 and after hemodialysis: 2.21±0.64, P=0.002 (Figure 4) these parameters significantly increased with dialysis in HD patients.
Conclusions: We found that RV-PA coupling parameters were significantly decreased in hemodialysis patients compared to the healthy control group. In hemodialysis patients, RV- PA coupling parameters improved with hemodialysis.
Keywords: Hemodialysis, Ventriculoarterial Coupling, FAC/SPAP

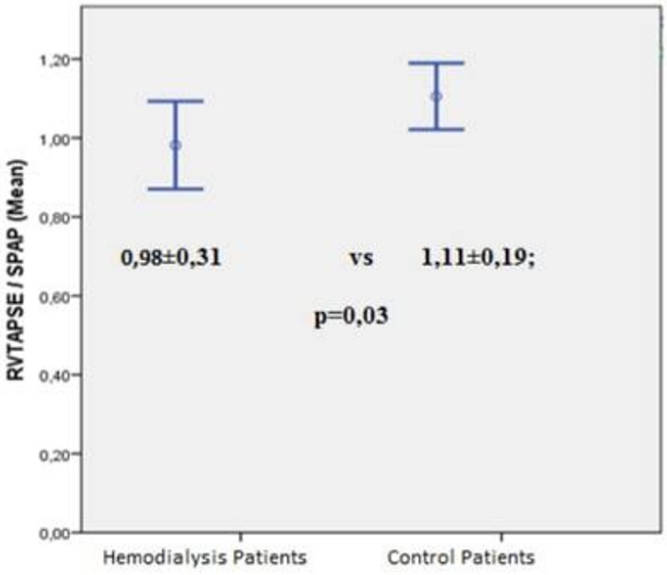

FIGURE 1. RV TAPSE/SPAP ratio of hemodialysis and control patients.

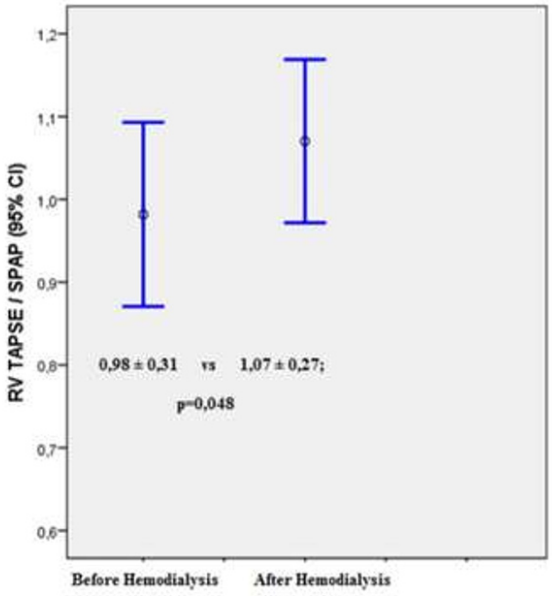

FIGURE 2. In hemodialysis patients RV TAPSE/SPAP ratio before and after hemodialysis.

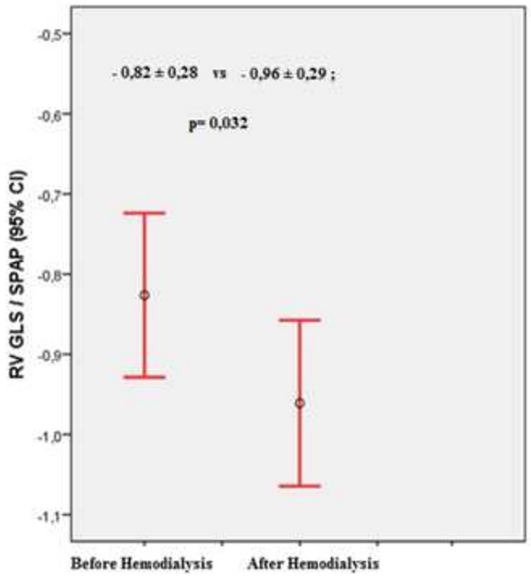

FIGURE 3. In hemodialysis patients RV GLS/SPAP ratio before and after hemodialysis

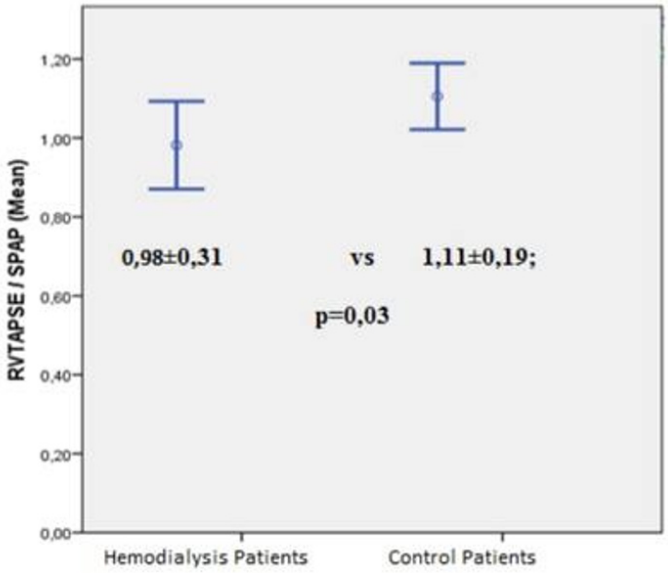

FIGURE 4. In hemodialysis patients RV FAC/SPAP ratio before and after hemodialysis.

OP-23.
Minimal Symptoms, Maximum Risk: Hidden Type A Dissection Accompanying an 81 mm Ascending Aortic Aneurysm

Yakup Han Yilmaz[1], Emre Şener[1]

[1]*Department of Cardiology, Eskişehir City Hospital, Eskişehir, Türkiye*

Objectives: Ascending aortic aneurysms usually progress silently, and when symptoms appear, they often present with rupture or dissection. When the aortic diameter exceeds 60 mm, the risk of rupture and dissection increases dramatically. Giant ascending aortic aneurysms over 80 mm are rarely reported in the literature and are generally associated with extremely high mortality. In this report, we present a case of an 81 mm giant ascending aortic dilation and Type A aortic dissection detected in a patient who presented without chest pain—complaining only of sweating and exertional fatigue. The aim is to emphasize that even patients with minimal symptoms may harbor an acute aortic syndrome.

Case Presentation: A 57-year-old male presented to the outpatient clinic with a one-week history of sweating and easy fatigability. He reported no chest pain. He had a known history of hypertension but was not taking medication. He also had a 30 pack-year smoking history (ex-smoker). On examination, blood pressure was 151/71 mmHg and pulse was 71 bpm. The electrocardiogram showed sinus rhythm and right bundle branch block (RBBB) (Figure 1). Initial laboratory tests revealed Hb 15.6 g/dL, WBC 9.21 K/µL, and platelets 154 K/µL. Renal function was normal (creatinine 0.9 mg/dL). Cardiac markers, including troponin, were within normal limits. Laboratory findings did not support acute coronary syndrome or infection and were nonspecific, consistent with the clinical picture. Transthoracic echocardiography showed a normal ejection fraction but an ascending aortic diameter of 81 mm (Figure 2). Additionally, moderate-to-severe aortic regurgitation was detected. The patient was urgently admitted to the service, and CT angiography was planned. CT imaging revealed aneurysmal dilation of the ascending aorta reaching up to 80 mm, along with a dissection flap extending from the ascending aorta to the proximal descending aorta (Figure 3). Findings were consistent with Stanford Type A aortic dissection. The patient was urgently transferred to the cardiovascular surgery team. Hemi-arch replacement and the Bentall procedure were performed. Although the surgery was technically successful, postoperative cardiac arrest occurred, and despite all interventions, the patient passed away.

Discussion: This case demonstrates that fatal acute aortic syndromes may be present even in patients who exhibit only nonspecific symptoms such as sweating or exertional fatigue, without chest pain. The absence of a visible dissection flap on echocardiography occurs in 15–20% of Type A dissections, highlighting the decisive role of CT in diagnosis. Furthermore, giant aneurysms over 80 mm carry extremely high perioperative mortality, even when surgically treated. This case underscores the need for vigilance in patients with known risk factors—such as hypertension—even when they present with mild or vague symptoms.

Conclusions: Giant ascending aortic aneurysm and Type A dissection can occur even in patients with minimal symptoms. This case emphasizes the importance of maintaining a high index of suspicion, recognizing the limitations of echocardiography, and using early CT imaging, which can be life-saving. Additionally, surgical mortality remains high in aneurysms exceeding 80 mm, despite aggressive interventions.

Keywords: Ascending Aortic Aneurysm, Type A Aortic Dissection, Aortic Regurgitation, Emergency Surgery

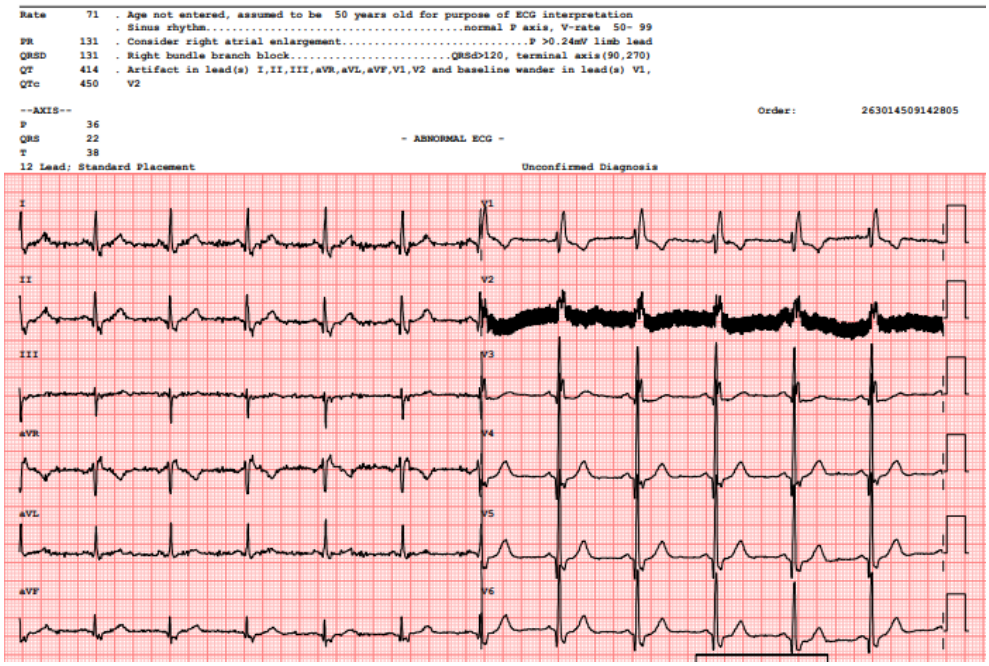

FIGURE 1. **The admission ECG shows sinus rhythm, right bundle branch block (RBBB), and a ventricular rate of approximately 71 bpm.**

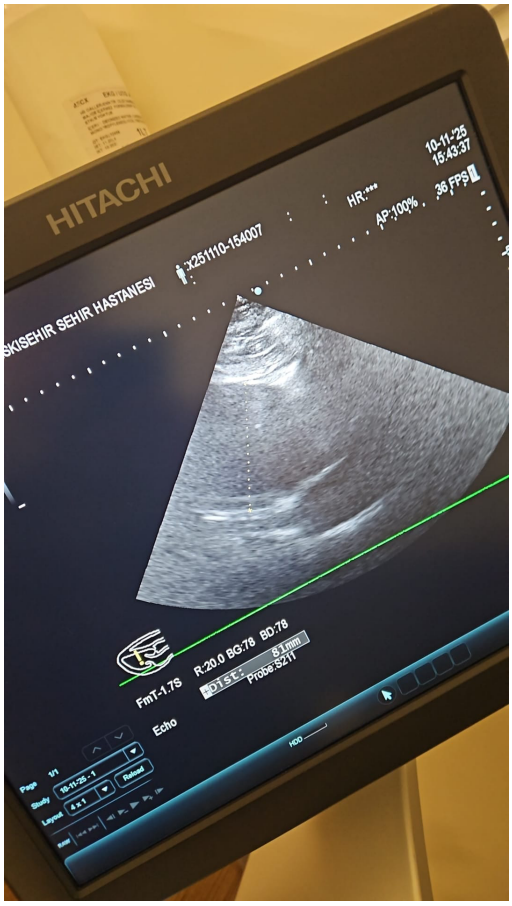

FIGURE 2. **Echocardiography shows an ascending aorta measuring 81 mm.**

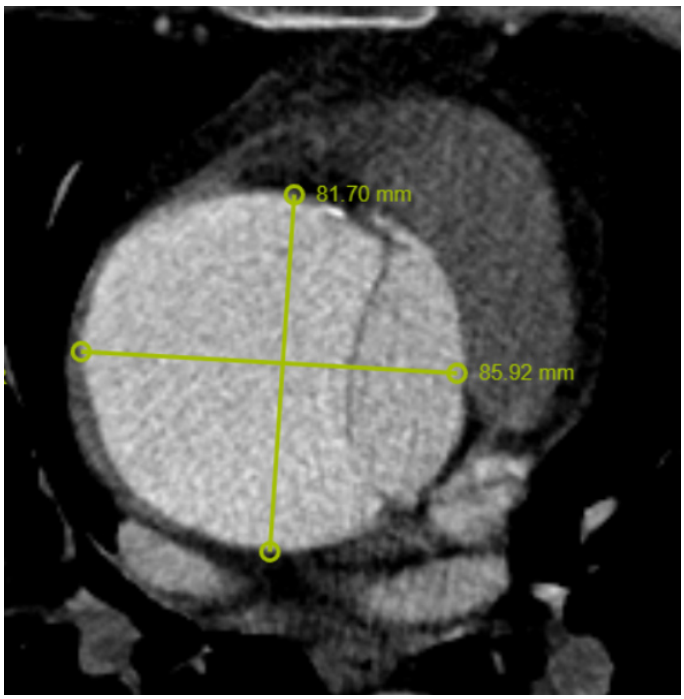

FIGURE 3. **CT shows 80–81 mm aneurysm and Type A dissection line in the ascending aorta.**

OP-24.
Comparative Efficacy of Single- and Dual-Defibrillator Orthogonal Electrical Cardioversion in Persistent Atrial Fibrillation

Esra Akpinar[1], Mehmet Can Çilğin[2], Hasan Ari[1], Ayşe Dilara Balyimez[1], Bilal Mete Ülker[1], Mehmet Taşci[1], Ahmet Tütüncü[1], Selma Ari[1], Mehmet Melek[1], Tahsin Bozat[1]

[1]Department of Cardiology, University of Health Sciences, Bursa Yüksek İhtisas Training and Research Hospital, Bursa, Türkiye; [2]Department of Cardiology, İnegöl State Hospital, Bursa, Türkiye

Objectives: Atrial fibrillation (AF) is treated with DC shocks delivered transthoracically; however, in approximately 5 to 30% of patients, these shocks fail to restore sinus rhythm (SR). In this study, we aimed to evaluate whether delivering high-energy shocks at different axes using a single-device or dual-device orthogonal configuration could improve the success of cardioversion compared with standard DC shocks to restore SR.

Methods: After TEE evaluation, 180 persistent AF patients were included in the study. In group 1, 50 patients underwent conventional DCCV; in group 2, 50 patients underwent orthogonal single-device DCCV; and in group 3, 80 patients underwent orthogonal dual-device DCCV. The conventional group DCCV electrode pads were positioned antero-lateral (Figure 1). The orthogonal single-device group DCCV electrode pads were positioned antero-lateral and antero-posterior, and these pads were connected to a single defibrillator (Figure 2). The orthogonal dual-device group DCCV electrode pads were positioned antero-lateral and antero-posterior, and these pads were connected to two defibrillators (Figure 3). Periprocedural anticoagulation was achieved with 5000 IU of unfractionated heparin administered before cardioversion, and anticoagulation was continued with either warfarin or DOAC at therapeutic dose. Amiodarone infusion was initiated (5 mg/kg IV loading dose infused over 10 minutes, followed by 1mg/min IV for 6 hours, then 0.5 mg/min IV for 18 hours) in all patients before the DCCV. In conventional group; transthoracic electrical cardioversion was performed with delivery of synchronized biphasic DC shocks of 200, 200, and 270J using antero-lateral pads (Figures 1 and 4). In orthogonal single-device group; transthoracic electrical cardioversion was performed with delivery of synchronized biphasic DC shocks of 200, 200, and 270J using antero-lateral and antero-posterior pads (Figures 2 and 4). In the orthogonal dual-device group; transthoracic electrical cardioversion was performed with delivery of synchronized biphasic DC shocks of 100 + 100, 200 + 200, and 270 + 270J using antero-lateral and antero-posterior pads (Figures 3 and 4). Cardioversion was considered successful if atrial P waves were unmistakably identified 5 min after the shock.

Results: The results of the study are shown in Figure 4. First DCCV shock success (conversion to SR) was significantly higher in group 3 than in group 1; in group 1: 70% vs in group 3: 85%; P=0.04, and in group 2; 80%. Second DCCV shock success was significantly higher in group 3 than in group 1 and 2; in group 1: 72% vs in group 3: 95 %; P<0.001, in group 2: 80% vs in group 3: 95%; P=0.007. Third DCCV shock success was significantly higher in group 2: 90% than in group 1: 74%; P=0.03, and in group 3: 97.5% than in group 1: 74%; P<0.001. CK, CK-MB, and hs-Troponin I levels were evaluated at baseline and at 6 and 12 hours after DCCV, and these parameters were similar among the three groups (P>0.05). All patients who converted to SR remained in sinus rhythm until hospital discharge.

Conclusions: Double simultaneous DC shocks in an orthogonal configuration is an effective method than

standart antero-lateral DC shocks for the cardioversion of persistant AF. These methods have similar safety.
Keywords: Atrial Fibrillation, Orthogonal, Direct Current Cardioversion, Defibrillator

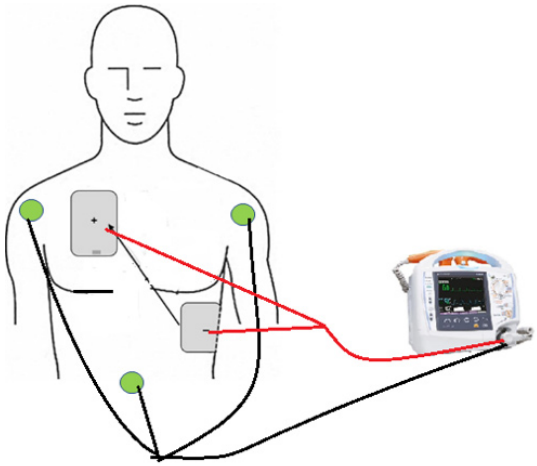

FIGURE 1. Standard antero-lateral DCCV.

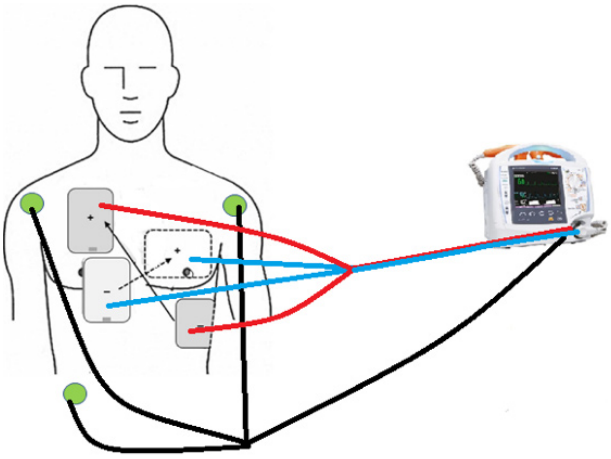

FIGURE 2. Orthogonal single-device antero-lateral and antero-posterior DCCV.

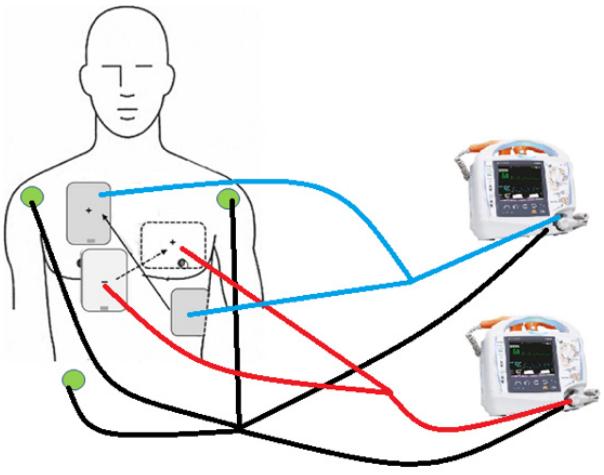

FIGURE 3. Orthogonal dual-device antero-lateral and antero-posterior DCCV.

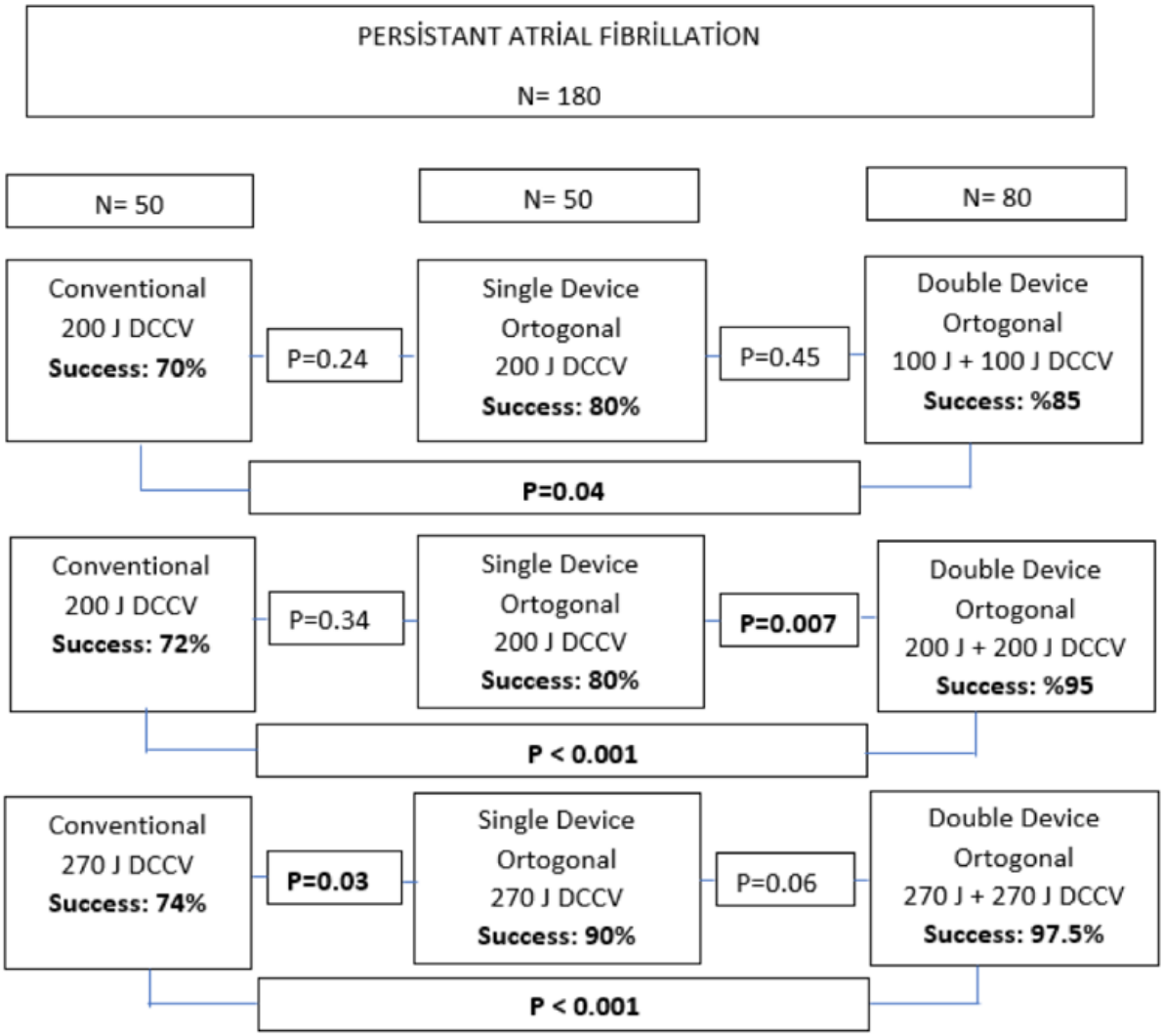

FIGURE 4. Study protocol and results.

OP-25.
Complete Atrioventricular Block and Postpartum Cardiomyopathy in a Patient With c-TGA: A Case of Right-Sided Cardiac Resynchronization Therapy

Esra Akpinar[1], Rauf Samet Gençgün[1], Ahmet Fatih Kişpinar[1], Mahmut Kapsiz[1], Ahmet Tütüncü[1], Selma Ari[1], Hasan Ari[1]

[1]Department of Cardiology, University of Health Sciences, Bursa Yüksek İhtisas Training and Research Hospital, Bursa, Türkiye

Case Presentation: A 35-year-old woman presented to the emergency department one week after cesarean delivery with orthopnea, dyspnea, and fatigue. Her medical history included corrected transposition of the great arteries (c-TGA) and surgical closure of an atrial septal defect 15 years prior. Physical examination revealed bilateral basal crackles and pretibial edema. Electrocardiogram showed complete atrioventricular block (Figure 1). Transthoracic echocardiography demonstrated c-TGA with trivial aortic and pulmonary regurgitation and mild functional mitral valve (anatomical tricuspid) regurgitation. The ejection fraction of the anatomical right ventricle (functional left ventricle) was 40% with global hypokinesia. Laboratory results showed creatinine 0.8 mg/dL, pro-BNP 7027 pg/mL, and CRP 68 mg/dL. The patient was diagnosed with postpartum cardiomyopathy and complete AV block. Heart failure therapy was initiated with perindopril 5 mg daily, spironolactone 25 mg daily, and furosemide 20 mg twice daily. Bromocriptine 2.5 mg twice daily was added for postpartum cardiomyopathy. The patient's clinical condition stabilized under medical therapy; however, complete AV block persisted, necessitating cardiac resynchronization therapy with defibrillator (CRT-D) implantation. Pre-procedural CT angiography guided the left subclavian approach. Under local anesthesia, three venous punctures were performed. An active ICD lead was positioned in the right ventricle (DF-4), followed by a lead advanced into the lateral branch of the functional left ventricle (anatomical right ventricle) via coronary sinus catheter. Another lead was positioned in the functional right ventricle (anatomical left ventricle) (Figure 2). After obtaining acceptable sensing and threshold measurements, all leads were connected to the generator and the device was implanted. The procedure was completed without complications. Post-procedural ECG showed paced rhythm with QRS duration of 138 ms (Figure 3). On follow-up, the patient was NYHA class I and was managed with medical therapy. Post-procedural echocardiography revealed an ejection fraction of 50% with mild mitral and tricuspid regurgitation (Figure 4).

Discussion: In c-TGA, the anatomical right ventricle functions as the systemic ventricle, predisposing to progressive systolic dysfunction. Pregnancy and the postpartum period impose additional hemodynamic stress, potentially triggering postpartum cardiomyopathy. Progressive AV block is common in c-TGA due to conduction system anomalies. Persistent complete AV block requiring permanent pacing increases the risk of ventricular dyssynchrony, making CRT-D implantation an appropriate choice to prevent pacing-induced dysfunction and provide protection against tachyarrhythmias. Although evidence for CRT-D in patients with systemic right ventricle is limited, observational studies show symptomatic improvement and increased ejection fraction. This case demonstrates that CRT-D may represent a feasible and effective therapeutic option in postpartum patients with systemic right ventricular dysfunction and complete AV block.

Keywords: c-TGA, Postpartum Cardiomyopathy, AV Block, CRT-D, Congenital Heart Disease

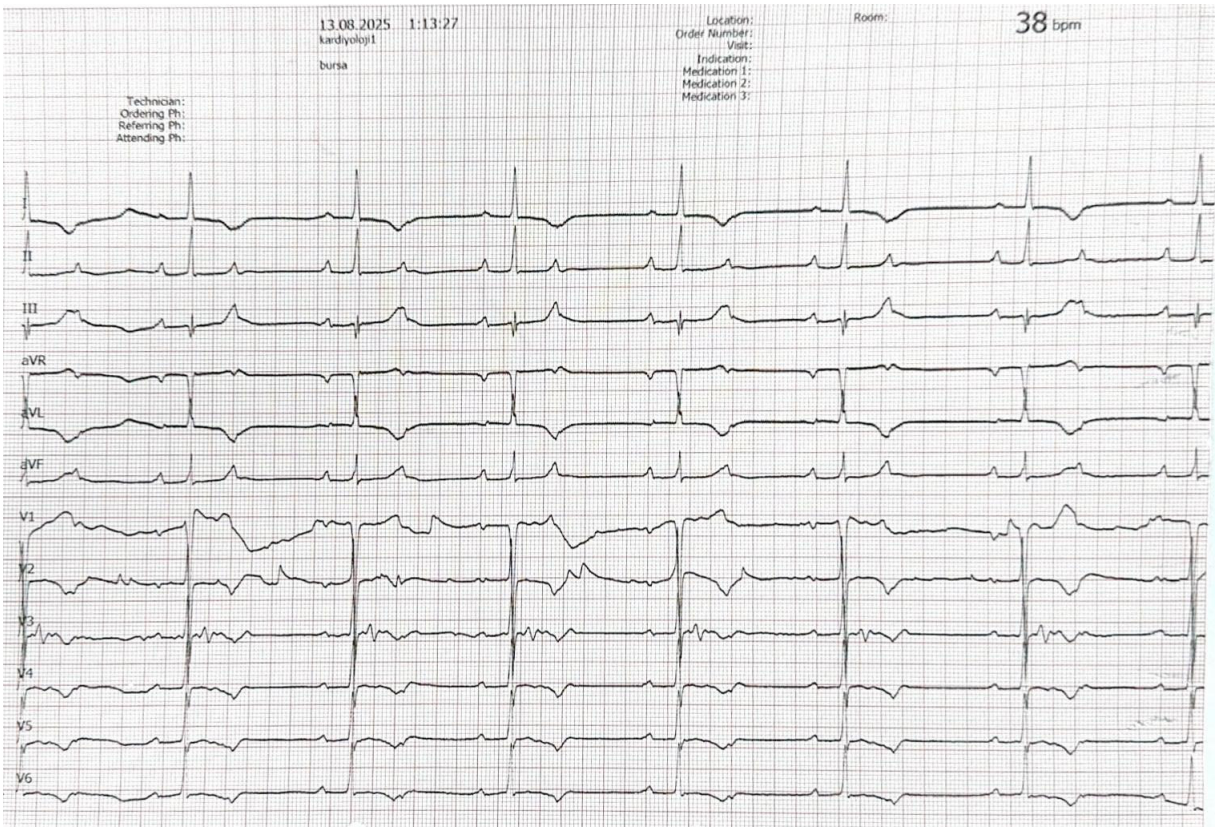

FIGURE 1. **Electrocardiogram showing complete atrioventricular block.**

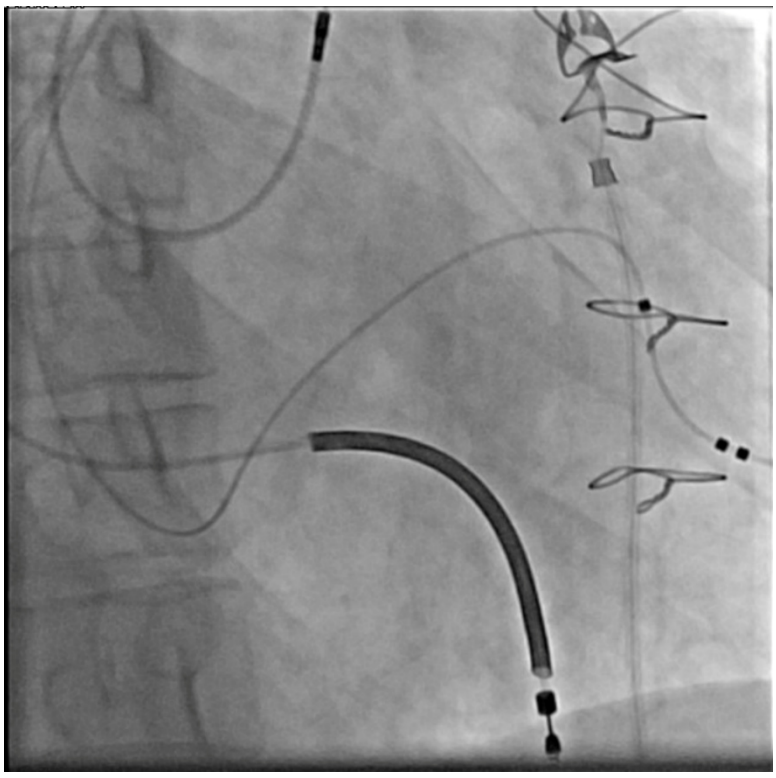

FIGURE 2. **Another lead positioning in the functional right ventricle (anatomical left ventricle).**

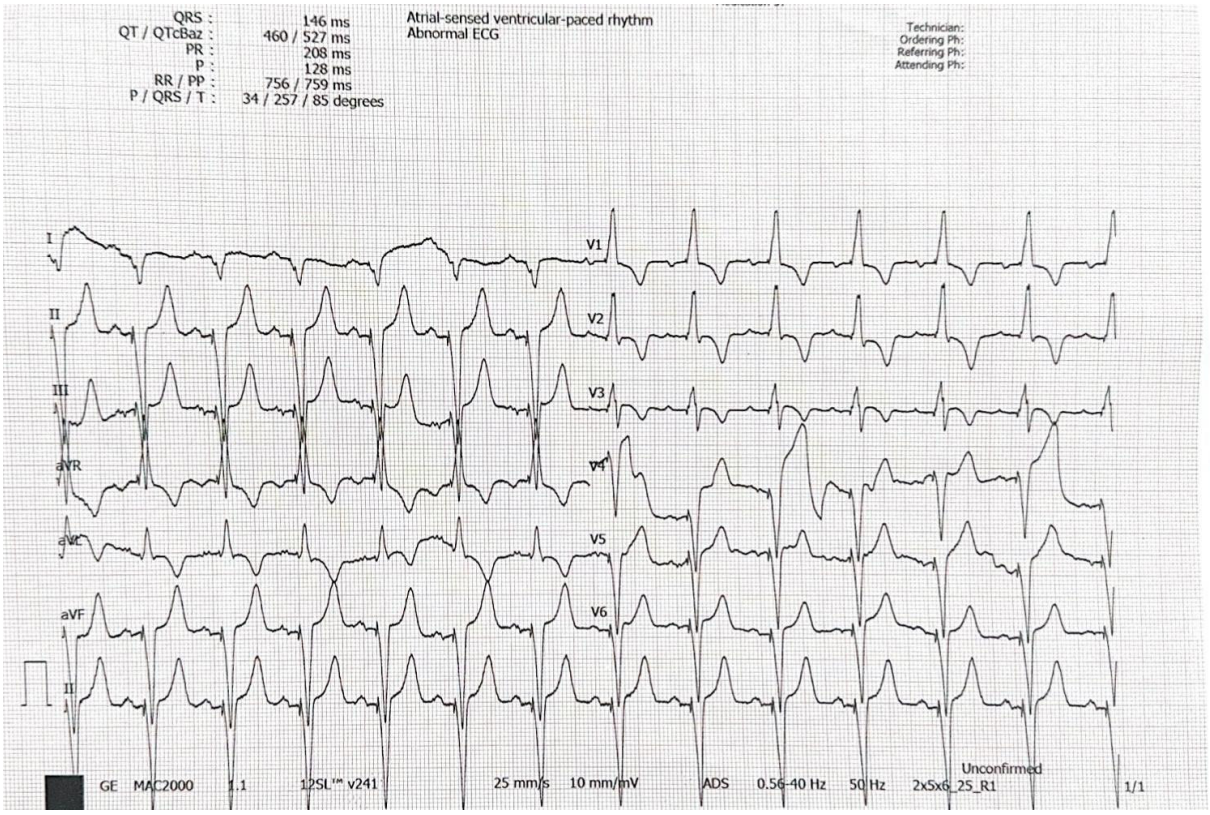

FIGURE 3. **Post-procedural ECG showing paced rhythm with QRS duration of 138 ms.**

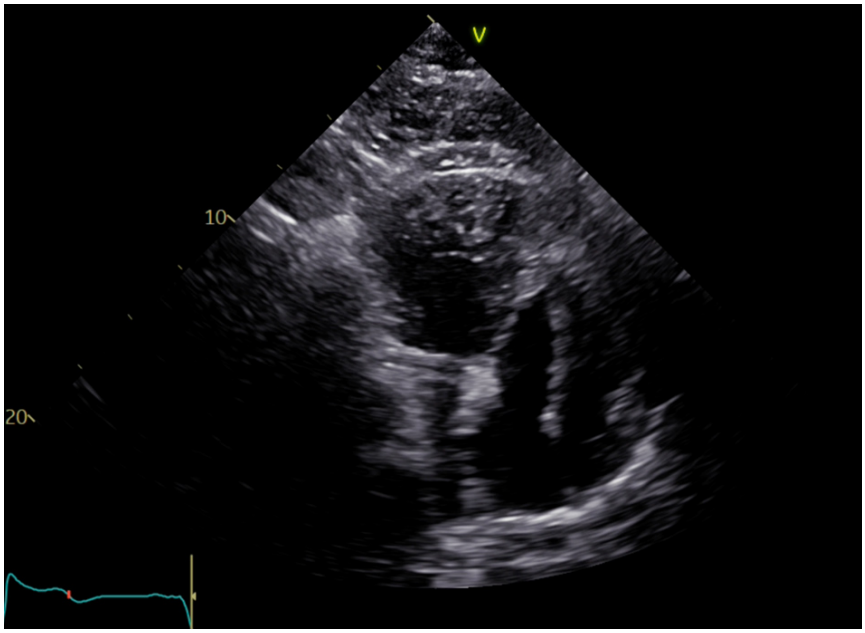

FIGURE 4. **Post-procedural echocardiography revealing an ejection fraction of 50% with mild mitral and tricuspid regurgitation.**

OP-26.
Predictive Value of Systemic Immune-Inflammation Index for INOCA

Büşra Güvendi Şengör[1], Mustafa Ferhat Keten[1]

[1]Department of Cardiology, Kartal Koşuyolu Yüksek İhtisas Training and Research Hospital, İstanbul, Türkiye

Objectives: Chronic systemic inflammation has been shown to play an important role in the development of coronary artery disease. The systemic immune-inflammation index (SII), calculated as platelets count × (neutrophil/lymphocyte ratio), has been proposed as an inflammatory biomarker. Previous studies have demonstrated that increased SII is associated with both the development and severity of CAD. The aim of this study was to investigate the association between the SII and patients with ischemia with non-obstructive coronary artery (INOCA).
Methods: This retrospective study included 145 patients who had non-obstructive coronary arteries on coronary angiography and had undergone myocardial perfusion scintigraphy (MPS) prior to procedure at our tertiary center. Patients were stratified into two groups according to the presence of ischemia based on the MPS findings. Baseline demographic, clinical, laboratory, imaging and angiographic data were obtained from the hospital database. Peripheral venous blood samples were collected 24 hours prior to the procedure.
Results: Of these 145 patients, 36 patients had ischemia on MPS and were assigned to the ischemic group while 109 patients were assigned to the non-ischemic group. The white blood cell (WBC), albumin, C-reactive protein (CRP), the left ventricular ejection fraction (LVEF) and the SII were significantly different between two groups (P=0.006, P<0.001, P<0.001, P<0.001and P=0.012; respectively). In contrast, no significant difference was observed for body mass index (BMI), hemoglobin and creatinine (P=0.650, P=0.058 and P=0,218; respectively). Ischemic group showed a higher inflammatory burden reflected by a higher WBC, CRP, SII and a lower albumin (8.56 vs. 7.51, 5.57 vs. 3.43, 546.5 vs. 439.9, 4.16 vs. 16.8; respectively. The ROC analysis was performed to determine the predictive performance of SII for ischemia in patients with non-obstructive coronary arteries. The cut-off value of SII was 363.8; however, the diagnostic performance was weak due to the low AUC value. (AUC:0.406, 95% CI: 0.661-0.361, P=0.012)
Discussion: In this study, we found that patients with INOCA who demonstrated ischemia on myocardial perfusion scintigraphy had significantly higher SII values, along with increased WBC and CRP levels and lower albumin concentrations, indicating a greater systemic inflammatory burden. These findings support the growing evidence that inflammation plays a key role in microvascular dysfunction and the pathophysiology of ischemia in the absence of obstructive coronary stenosis. Although SII showed a statistically significant association with ischemia, its diagnostic performance was limited, as reflected by the low AUC value. This suggests that SII alone may be insufficient as a standalone marker and may gain greater clinical utility when interpreted alongside other inflammatory and clinical parameters. Further prospective studies with larger cohorts are needed to clarify the prognostic and diagnostic role of SII in INOCA populations.
Conclusions: A higher SII was associated with ischemia in patients with non-obstructive coronary arteries and SII may be more useful when combined with additional inflammation markers in predicting INOCA patients.
Keywords: Systemic Immune-Inflammation Index (SII), Ischemia with Non-Obstructive Coronary Arteries (INOCA), Myocardial Perfusion Scintigraphy

OP-27.
Transcatheter Closure of Mitral Paravalvular Leak Developing After Mechanical Mitral Valve Replacement: A Case Report

Şirin Şebnem Önür[1], Ecem Gürses[1]

[1]Department of Cardiology, Bakircay University Cigli Regional Education Hospital, İzmir, Türkiye

Objectives: Paravalvular leak is a rare but significant complication following prosthetic valve replacement. It can cause recurrent heart failure and haemolysis. Treatment often requires reoperation or transcatheter intervention. Transcatheter paravalvular leak closure is emerging as a minimally invasive alternative to redo surgery in selected patients. This case report presents the clinical course of a patient who underwent transcatheter leak closure after the patient refused surgical treatment, which was recommended due to early-onset paravalvular mitral leak following simultaneous coronary bypass graft surgery with metallic mitral valve replacement. This case represents an important clinical example of the applicability and efficacy of the transcatheter approach for paravalvular regurgitation developing in the early period after mechanical valve replacement, particularly in patients with high surgical risk or who refuse redo surgery.
Case Presentation: A 50-year-old male patient who had undergone mitral valve replacement and simultaneous coronary bypass graft surgery 4 months prior presented to the outpatient clinic with dyspnoea and symptoms similar to those experienced before the operation. Echocardiography revealed moderate-to-severe paravalvular mitral regurgitation. Although the cardiac team recommended redo surgery, the patient declined surgery. At the patient's request, percutaneous paravalvular leak closure was performed at an external centre. Follow-up echocardiography after the procedure revealed a functional mitral valve, left atrial dilatation, and a mobile echogenic mass at the left ventricular apex; no paravalvular mitral regurgitation was observed. No haemolytic anaemia was detected in the patient.
Conclusions: Transcatheter leak closure can be considered an applicable method in high-risk patients who refuse redo surgery. Monitoring haemoglobin and LDH levels for haemolytic anaemia associated with residual leakage is important in the period following transcatheter paravalvular leak closure. This case demonstrates that transcatheter paravalvular leak closure is a feasible and effective treatment option in patients with high surgical risk. In patients who refuse redo surgery or are at high risk, the transcatheter approach emerges as a safe and minimally invasive alternative method.
Keywords: Mitral Paravalvular Leak, Transcatheter Repair, Transesophageal Echocardiography, Prosthetic Valve Complication, Case Report, Paravalvular Leak

OP-28.
Acute Coronary Syndrome After Anaphylaxis: Kounis Syndrome Case

Adem Yarar[1], Ahmet Tütüncü[2], Bilal Mete Ülker[2], Ayşe Dilara Balyimez[2], Veysel Macit[2], Ömer Fatih Savci[2], Hasan Ari[2]

[1]Bursa Yüksek İhtisas Training and Research Hospital, Bursa, Türkiye; [2]Department of Cardiology, University of Health Sciences, Bursa Yüksek İhtisas Training and Research Hospital, Bursa, Türkiye

Case Presentation: A 69-year-old man presented to an outside emergency department after being stung on the head and neck by approximately 15 bees when he fell onto a beehive while working in the field. Shortly after arrival, he developed retrosternal pressure-like chest pain and dizziness. Electrocardiography revealed an acute inferior myocardial infarction accompanied by complete atrioventricular block (Figure 1), and he was transferred to our center for further management. His medical history included hypertension, a 45-pack-year smoking history, and coronary stent implantation following acute coronary syndrome 10 years earlier. During transfer to the catheterization laboratory, the patient developed ventricular fibrillation. He was successfully defibrillated, but subsequently progressed to asystole. Cardiopulmonary resuscitation (CPR) was initiated, the patient was intubated, and spontaneous circulation was restored after 15 minutes. Coronary angiography demonstrated a totally thrombotic occlusion within the right coronary artery (RCA) stent (Figure 2), 80% stenosis of the circumflex artery (Cx), and a patent left anterior descending (LAD) stent with a 50% pre-stent lesion. Thrombus aspiration and intracoronary abciximab were administered to the RCA, followed by percutaneous transluminal coronary angioplasty with a 2.0×15 mm balloon for the distal lesion. Complete revascularization of the RCA was achieved, and elective intervention for the Cx was planned. Two hours after admission to the coronary intensive care unit, the patient demonstrated meaningful neurological recovery and was extubated. Follow-up ECGs showed resolution of ST-segment elevation (Figure 3). On day 3, he was transferred to the ward without active complaints. During hospitalization, sequential implantation of a 2.5×23 mm sirolimus-eluting stent and a 2.75×24 mm everolimus-eluting stent was performed in the Cx, achieving full revascularization. The patient was discharged in good condition with optimized medical therapy and outpatient allergy–immunology follow-up.

Discussion: Hypersensitivity reactions can trigger numerous systemic responses, including life-threatening coronary vasospasm. Acute coronary syndrome occurring in the context of allergic hypersensitivity or anaphylaxis is known as Kounis syndrome. Mast-cell activation leads to the release of histamine, tryptase, prostaglandins, platelet-activating factor, and various pro-inflammatory mediators, which may cause coronary vasospasm, rupture of an atheromatous plaque, or stent thrombosis, ultimately resulting in myocardial ischemia. Three variants of Kounis syndrome are recognized:

Type I: Coronary vasospasm in patients without underlying coronary disease.

Type II: Acute ischemia triggered by allergic-mediator–induced plaque destabilization in patients with established atherosclerosis.

Type III: Stent thrombosis or restenosis secondary to a severe allergic reaction in patients with previous percutaneous coronary intervention.

Diagnostic evaluation includes serum histamine, tryptase, troponin, and eosinophil levels. Echocardiography can assess regional wall-motion abnormalities, while coronary angiography remains critical for evaluating vasospasm and coronary lesions. Therapeutic management may include nitrates, calcium-channel blockers,

antihistamines, and corticosteroids. Beta-blockers should be avoided due to their potential to worsen vasospasm.
Conclusions: In this case, bee-sting–induced Type III Kounis syndrome resulted in stent thrombosis and cardiogenic arrest but was successfully managed with prompt resuscitation and revascularization.
Keywords: Bee, Anaphlaxis, Kounis

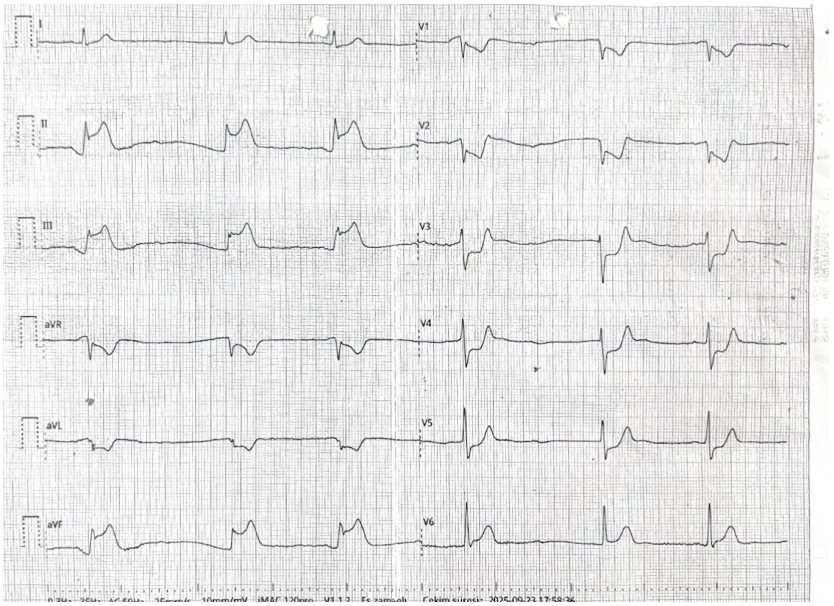

FIGURE 1. Electrocardiography revealing an acute inferior myocardial infarction accompanied by complete atrioventricular block.

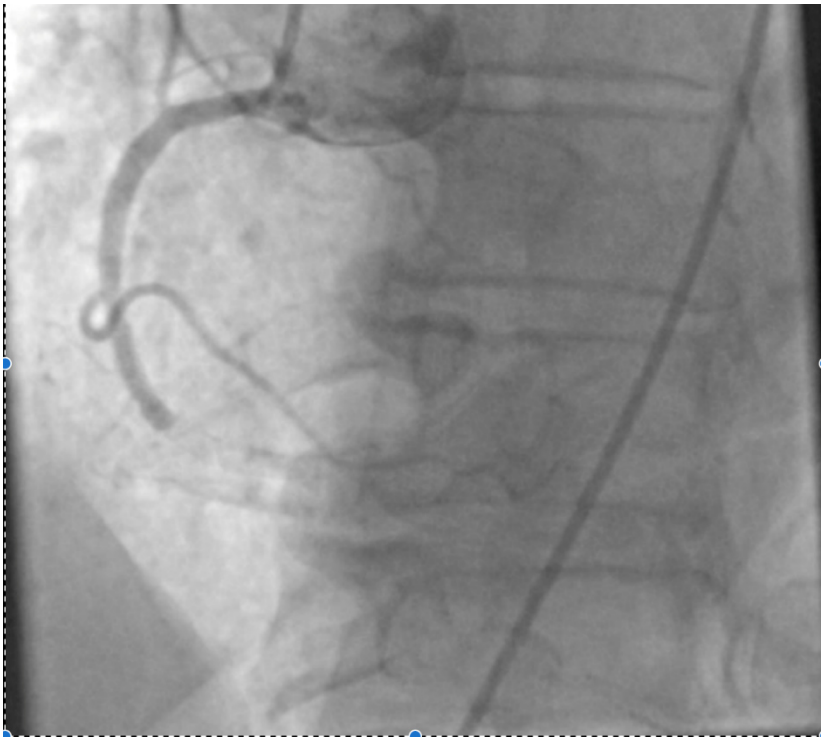

FIGURE 1. Coronary angiography demonstrating a totally thrombotic occlusion within the right coronary artery (RCA) stent.

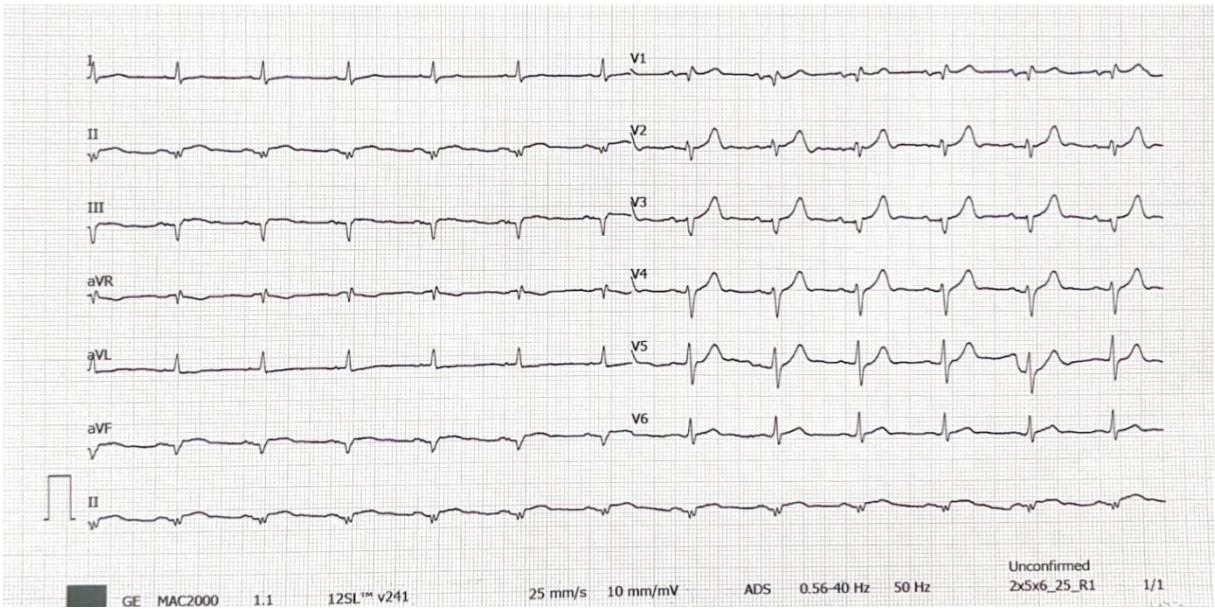

FIGURE 1. Follow-up ECG showing resolution of ST-segment elevation.

OP-29.
Cardiac Lymphoma: A Rare Case Report

Hasan Ari[1], Fahriye Vatansever Ağca[1], Selma Ari[1], Ayşe Dilara Balyimez[1], Abdulsamet Arslan[1], Mustafa Kani Gözcü[1], Hülya Haksever[1]

[1]Department of Cardiology, University of Health Sciences, Bursa Yüksek İhtisas Training and Research Hospital, Bursa, Türkiye

Objectives: Primary cardiac lymphomas are exceptionally rare among malignant cardiac tumors and most frequently involve the right atrium or right ventricle. Clinical manifestations may vary depending on the location and size of the tumor within the heart. Diagnosis is often delayed, and prognosis is generally poor.
Case Presentation: A 69-year-old male with a known history of chronic obstructive pulmonary disease was admitted to the emergency department due to exertional dyspnea. Physical examination revealed no significant cardiac murmur on auscultation, and no peripheral edema was observed. Transthoracic echocardiography demonstrated a left ventricular ejection fraction of 60%, mild-to-moderate mitral and tricuspid regurgitation, and left atrial dilatation. A pericardial effusion surrounding the heart without signs of compressive physiology was noted, measuring 0.8 cm around the right ventricle and 1.4 cm around the right atrium. In addition, an intracardiac mass associated with the atrial chambers was identified. Transesophageal echocardiography revealed a heterogeneous mass measuring approximately 80×55 mm, involving the roofs of both the right and left atria and destructing the interatrial septum. The mass encased the pulmonary artery, superior vena cava, pulmonary veins, and aortic root, and internal blood flow was demonstrated within the lesion using color Doppler imaging (Figure 1). Thoracic and abdominal computed tomography revealed a mediastinal mass with a cardiac component. PET-CT demonstrated a hypermetabolic mass filling the right atrium and extending into the left atrium, encasing the pulmonary artery and superior vena cava, and surrounding the aortic root. The lesion measured 10×8×12 cm at its maximum dimensions and exhibited a SUVmax of 25.7, consistent with malignancy (Figure 2). The preliminary diagnosis was angiosarcoma. Cardiac magnetic resonance imaging demonstrated a contrast-enhancing, lobulated mass measuring 14×10×12 cm, involving both atria as well as the proximal aorta, pulmonary arteries, and pulmonary veins (Figure 3). The findings were interpreted as being more consistent with a mass secondary to lymphoma involvement. Additionally, a 24 mm pericardial effusion and bilateral pleural effusions, more pronounced on the left side, were detected. A diagnostic cardiac biopsy was obtained under transesophageal echocardiographic and fluoroscopic guidance (Figure 4). Histopathological examination confirmed the diagnosis of diffuse large B-cell lymphoma (Figure 5). The patient received four cycles of R-CHOP chemotherapy, consisting of rituximab, cyclophosphamide, doxorubicin, vincristine, and prednisone. Follow-up evaluations revealed no significant reduction in the size of the mass. The patient died six months after the diagnosis.
Conclusions: Cardiac lymphomas are rare tumors, predominantly affecting elderly male patients and should be considered in the differential diagnosis of cardiac masses. Clinical presentation is dyspnea, chest pain, palpitations, or pericardial effusion. Diagnosis is usually established using multimodality imaging such as echocardiography, computed tomography, magnetic resonance imaging, and PET-CT, while definitive diagnosis requires histopathological confirmation. Systemic chemotherapy, most commonly the R-CHOP regimen, is the preferred treatment; however, prognosis remains poor. A multidisciplinary approach involving cardiology, oncology, radiology, and pathology is essential in the management of cardiac lymphoma cases.
Keywords: Diffuse Large B-Cell Cardiac Lymphoma, Primer Cardiac Tumor, Multimodality Imaging

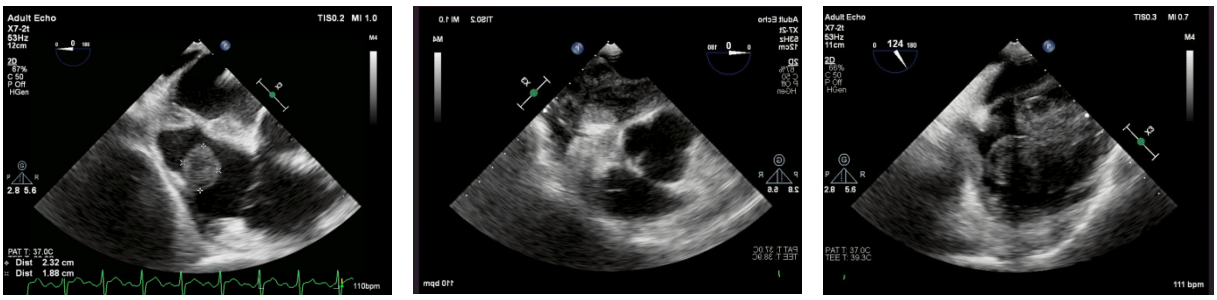

FIGURE 1. TEE image.

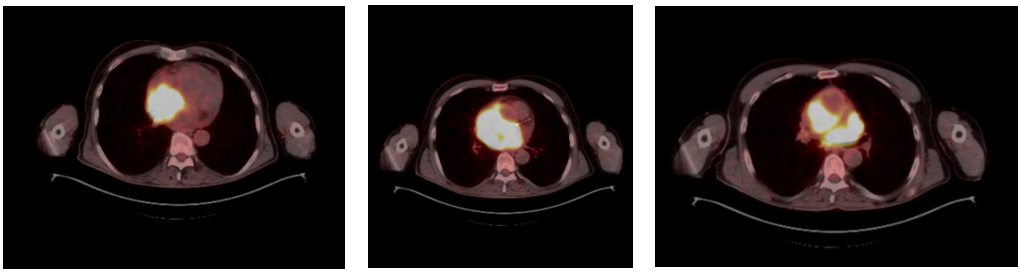

FIGURE 2. PET CT.

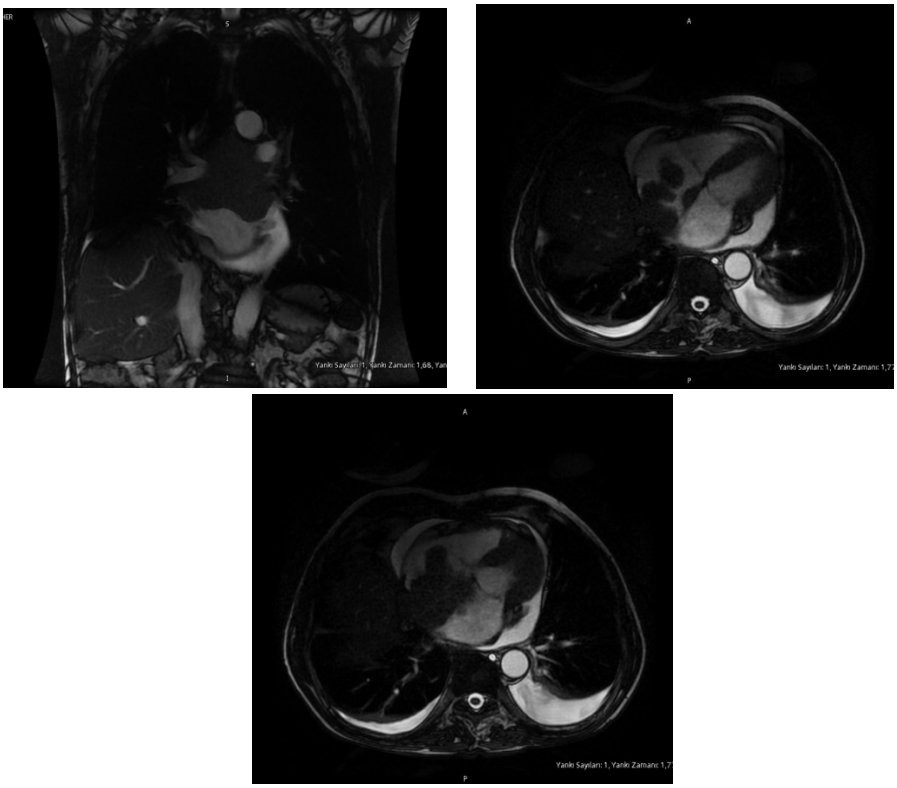

FIGURE 2. MR.

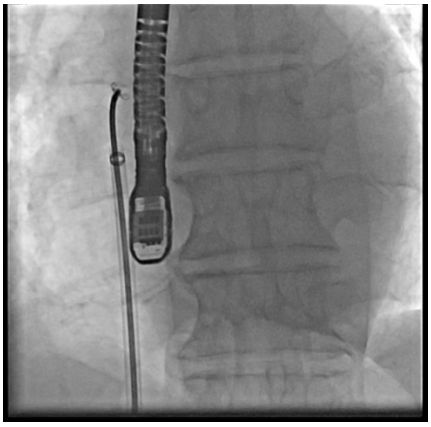

FIGURE 4. Fluoroscopy.

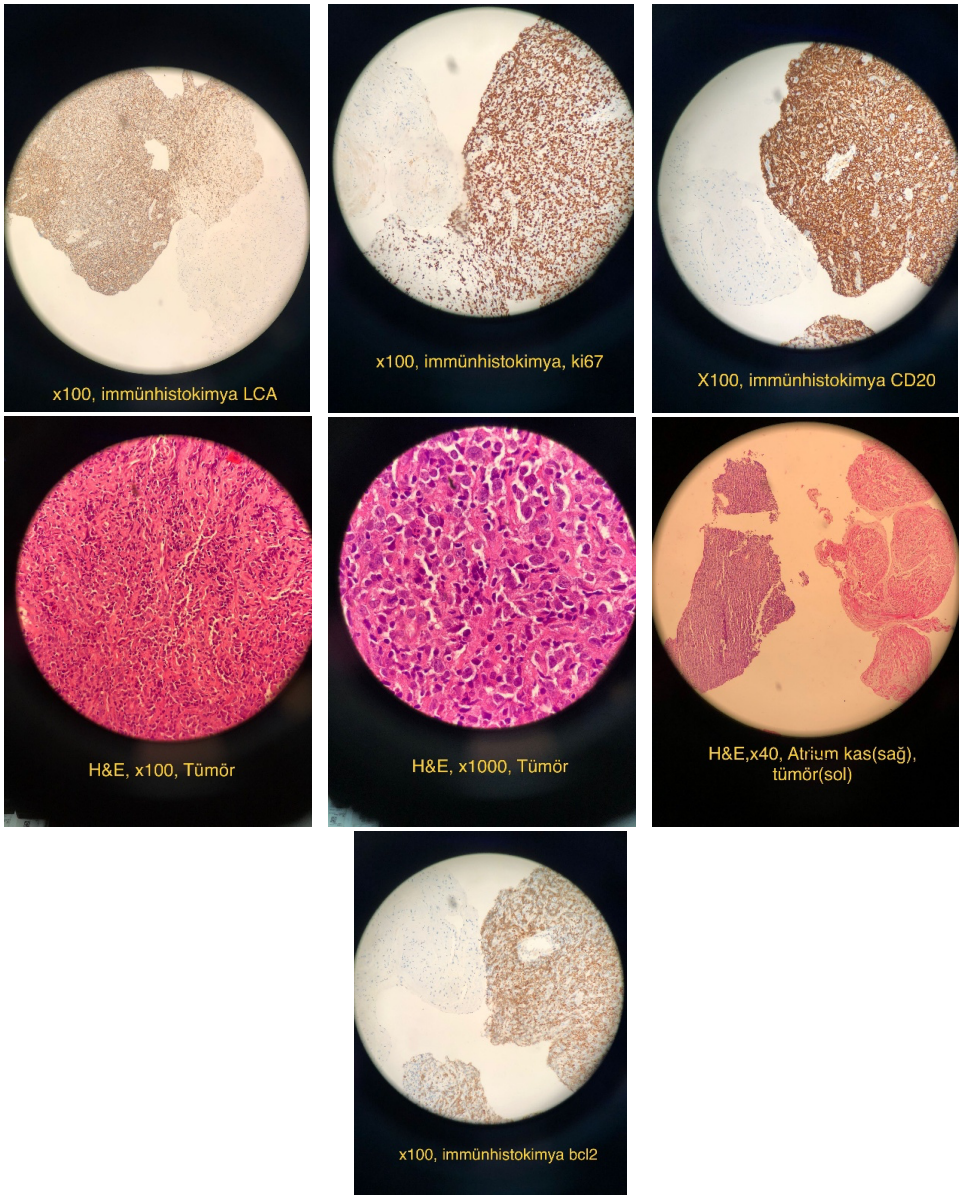

FIGURE 5. Pathology.

OP-30.
The Clinical Significance of the Plasma Atherogenic Index in Predicting Total Occlusion in Patients with Non-ST Elevation Myocardial Infarction

Enes Çelik[1], Hakan Güneş[2], Musa Dağli[3], Murat Kerkütlüoğlu[4]

[1]Department of Cardiology, Bilecik Şeyh Edebali University, Faculty of Medicine, Bilecik, Türkiye; [2]Department of Cardiology, University of Health Sciences, Izmir Tepecik Training and Research Hospital, İzmir, Türkiye; [3]Department of Cardiolog, Konya Akşehir State Hospital, Konya, Türkiye; [4]Department of Cardiology, Kahramanmaraş Sütçü İmam University, Faculty of Medicine, Kahramanmaraş, Türkiye

Objectives: Non-ST-elevation myocardial infarction (NSTEMI) is a heterogeneous clinical presentation often associated with incomplete arterial obstruction. However, some patients exhibit total occlusion (TO) in the infarct-related artery, which adversely affects cardiovascular outcomes. The plasma atherogenic index (AIP) is a biomarker that can be used in cardiovascular risk prediction. The aim of this study was to investigate the predictive value of AIP for the presence of TO in NSTEMI patients.
Methods: This retrospective study included 155 NSTEMI patients hospitalized between 2021 and 2022. Patients were divided into two groups based on the presence of total occlusion: the TO group (n=79$) and the Non-TO group (n=76). AIP was calculated by taking the logarithm of the ratio of plasma triglyceride (TG) level to HDL-cholesterol (HDL-C) level [log(TG/HDL-C)]. Baseline clinical characteristics, laboratory findings, and coronary artery involvement were compared between the groups (Table 1). The performance of AIP in predicting TO was evaluated using ROC curve analysis.
Results: AIP was found to be significantly higher in the TO group compared to the Non-TO group (0.756±0.154 vs. 0.57±0.104; P<0.001) (Figure 1). The area under the curve (AUC) for AIP in predicting TO was calculated as 0.784 (95% CI: 0.712–0.856) as a result of the ROC curve analysis (Figure 2). Hypertension, high LDL cholesterol, triglycerides, and platelet count were more common in the TO group. Regarding the distribution of coronary artery involvement, right coronary artery lesions were dominant in the TO group, while left circumflex and left anterior descending artery lesions were more frequently observed in the Non-TO group.
Discussion: In this study, it was demonstrated that AIP is significantly associated with total occlusion in patients with NSTEMI. Our findings are consistent with previous studies suggesting that AIP may be related to coronary artery occlusion, as it reflects an atherogenic lipid profile. The higher prevalence of hypertension, elevated LDL cholesterol, and triglyceride levels in the TO group supports the presence of a more pronounced atherosclerotic burden in these patients. Additionally, the differences in coronary artery involvement patterns between the groups highlight the heterogeneous pathophysiology of NSTEMI. The strong predictive performance of AIP in the ROC analysis further reinforces its potential as a low-cost and easily applicable risk marker in clinical practice. However, the retrospective design and limited sample size restrict the generalizability of our results.
Conclusions: AIP was found to be significantly associated with the presence of total occlusion in NSTEMI patients, demonstrating its potential as a predictive biomarker. As an easily applicable and low-cost index, AIP may strengthen risk stratification and contribute to early intervention in high-risk patients. However, larger-scale prospective studies are needed to confirm its prognostic value.
Keywords: NSTEMI, Total Occlusion (TO), Plasma Atherogenic Index (AIP), Coronary Artery Disease, Triglyceride/HDL Ratio

TABLE 1. Key Features

	TO n=79	Non-TO n=76	P-value
Hypertension, n (%)	56 (70.9)	39 (51.3)	**0.012**
COPD, n (%)	17 (21.5)	8 (10.5)	0.062
Smoking (n (%)	48 (60.8)	43 (56)	0.600
Stroke History (n (%)	6 (7.6)	7 (9.2)	0.719
Gender (male) n (%)	44 (57.9)	54 (68.4)	0.180
Age (years)	67 ±12	64 ±12	0.921
Diabetes mellitus, n (%)	27 (34.2)	35 (46.1)	**0.045**
Laboratory findings			
Glukoz (mg/dL)	141±49.31	155±61.41	0.122
BUN (mg/dL)	22.6±11.84	20.3±15.82	0.294
Kreatin mg/dL	0.93±0.31	0.91±0.35	0.423
WBC ($\times 10^9$/L)	9.93±2.84	9.43±2.5	0.255
Hemoglobin (g/dL)	14.27±4.88	15.7±7.68	0.167
Hematokrit (%)	39.4±6.81	37.67±11.51	0.241
Platelet ($\times 10^6$/µL)	266.2±56.63	227.06±42.61	**<0.001**
MPV (fL)	11.74±10.66	10.48±10	0.306
LDL (mg/dL)	128.1±36.10	104.82±33.03	**<0.001**
HDL (mg/dL)	(23-79)40.46	(25-65)41	0.183
Trigliserid (mg/dL)	223.77±79.08	165.19±74.06	**<0.001**
AIP	0.756±0.15	0.57±0.104	**<0.001**
Responsible lesion, n (%)			
Left circumflex artery	24 (30.4)	35(46.1)	**0.045**
Left anterior descending artery	19(24.1)	32(42.1)	**0.006**
Right coronary artery	36(45.6)	4(5.3)	**<0.001**

Data are shown as mean±standard deviation or n (%) where appropriate. TO, total occlusion; COPD, chronic obstructive pulmonary disease; BUN, blood urea nitrogen, WBC, white blood cell; MPV, mean platelet volume; LDL, low-density lipoprotein; HDL, high-density lipoprotein; AIP, plasma atherogenic index.

Statistically significant P-values are shown in bold.

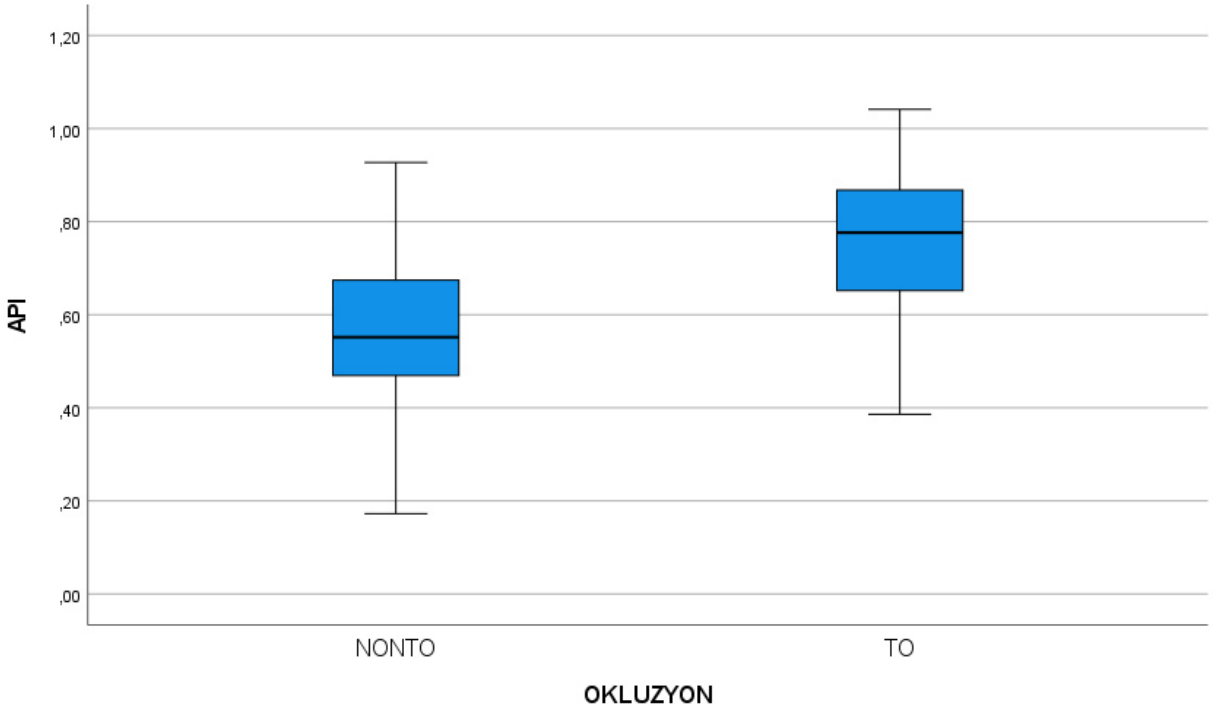

FIGURE 1. **AIP are significantly higher in the TO group compared to the Non-TO group (P<0.001)**

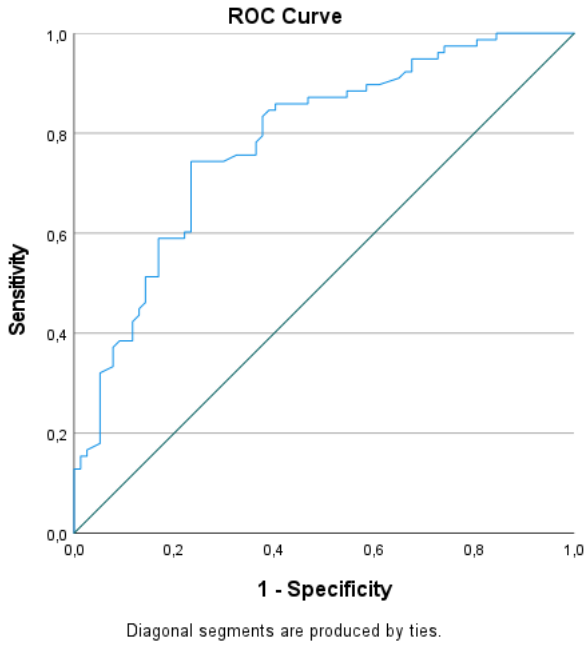

FIGURE 2. **ROC curve analysis.**

OP-31.
Prognostic Nutritional Index and Frailty After Ischemic Stroke: Mid-Term Follow-Up Results

Eda Özcan[1], **Sibel Çatalkaya**[1]

[1]*Department of Cardiology, Bursa City Hospital, Bursa, Türkiye*

Objectives: The Prognostic Nutritional Index (PNI), a biomarker reflecting systemic inflammation and nutritional status, has been associated with morbidity and mortality in oncology, cardiology, and critical care settings. Frailty, characterized by reduced physiological reserve and heightened vulnerability to stressors, is a well-established predictor of adverse outcomes after stroke. While frailty has been shown to affect both early and long-term recovery and survival after stroke, its association with PNI in patients with ischemic stroke remains underexplored. This study aimed to investigate the relationship between PNI measured at the time of stroke and mid-term frailty status assessed during follow-up.
Methods: We retrospectively analyzed patients admitted with ischemic stroke between 2021 and 2023. Patients with malignancies or chronic systemic diseases were excluded. PNI was calculated at admission using the formula: PNI=10 × serum albumin (g/dL) + 0.005 × total lymphocyte count (/mm³). Patients were stratified into two groups based on a literature-based PNI cutoff value of 49.75: malnourished (PNI ≤ 49.75) and well-nourished (PNI > 49.75). Frailty was assessed during outpatient visits or via structured telephone interviews using the Frailty Scale (FS), a 0–5 scoring tool evaluating daily activity, mobility, and general health. A score ≥3 was defined as frail.
Results: A total of 86 patients (mean age: 66±11.1 years; 64.6% male) were included, with a median follow-up duration of 16 months (range: 3–25 months). The prevalence of comorbidities was high, including hypertension (77.9%), diabetes (45.4%), and coronary artery disease (36.1%). Frailty was significantly more common among patients with lower PNI values (35.3% vs. 15.7%; P=0.047). Similarly, mean frailty scores were higher in the malnourished group (2.1±1.6 vs. 1.3±1.5; P=0.017). There was an inverse and statistically significant correlation between PNI and frailty scores (Spearman r=- 0.53; P<0.001). Patients with low PNI also exhibited higher neutrophil and CRP levels and lower hemoglobin, triglyceride, and albumin values (Detailed estimates are presented in Table 1).
Discussion: Lower PNI at stroke onset was significantly associated with higher mid-term frailty. This suggests that systemic inflammation and reduced nutritional reserves contribute to poorer functional resilience after stroke. PNI, derived from routine laboratory parameters, may serve as an early, objective indicator of vulnerability. Identifying patients at risk could guide targeted interventions, such as intensive rehabilitation, nutritional optimization, or closer post-discharge monitoring. Furthermore, integrating PNI assessment into routine stroke care could help prioritize patients for multidisciplinary management, including physical therapy, dietary counseling, and social support. Prospective studies are needed to confirm these findings, explore the causal mechanisms linking nutrition and inflammation to frailty, and assess whether interventions targeting these pathways can mitigate functional decline and improve long-term outcomes.
Conclusions: PNI at admission predicts mid-term frailty in ischemic stroke patients. Given its simplicity, low cost, and objectivity, PNI may be a valuable tool for early risk stratification in clinical practice.
Keywords: Ischemic Stroke, Frailty, Malnutrition, Prognostic Nutritional Index

OP-32.
Diagnostic Challenge in Cardiac AL Amyloidosis: When Imaging Speaks Louder Than Serum Biomarkers

Burak Yaman[1], Çetin Alak[1], Fazıl Çağrı Hunutlu[2], Osman Akın Serdar[1]

[1]Department of Cardiology, Uludağ University, Faculty of Medicine, Bursa, Türkiye; [2]Department of Internal Medicine, Uludağ University, Faculty of Medicine, Bursa, Türkiye

Objectives: Cardiac amyloidosis, particularly the AL (light chain) subtype, is an underrecognized cause of heart failure with preserved or mildly reduced ejection fraction. This case highlights the diagnostic utility of cardiac imaging and tissue biopsy in a patient with strong clinical suspicion but normal serum biomarkers.
Case Presentation: A 65-year-old male with a one-year history of recurrent hospitalizations due to decompensated heart failure presented with exertional dyspnea and orthopnea. On physical examination, bilateral pretibial edema, jugular venous distension, and hepatomegaly were noted. ECG revealed sinus rhythm with diffusely low QRS voltages (Figure 1). Transthoracic echocardiography (TTE) showed concentric left ventricular hypertrophy with normal chamber size, ejection fraction of 38%, and biatrial enlargement. Mild mitral and moderate tricuspid regurgitation were noted with a pulmonary artery systolic pressure of 43 mmHg. Inferior vena cava was 24 mm in diameter with <50% inspiratory collapse. TAPSE was reduced to 13 mm (Figure 2). Cardiac magnetic resonance imaging (MRI) revealed concentric LV hypertrophy with mildly reduced ejection fraction (41%). Global hypokinesia, basal and mid-septal akinesia, and biatrial enlargement were noted. Late gadolinium enhancement (LGE) sequences demonstrated diffuse subendocardial enhancement without evidence of myocardial edema. T1 mapping indicated prolonged native T1 relaxation time. Pericardial and bilateral pleural effusions were present (Figure 3). Neurological evaluation showed autonomic dysfunction with orthostatic hypotension, raising suspicion for systemic involvement. Serum and urine protein electrophoresis with immunofixation did not detect monoclonal protein. Free light chain (FLC) testing revealed a kappa value of 1.67 g/L and lambda 3.85 g/L with a kappa/lambda ratio of 0.43, within reference range yet suggestive of lambda excess. Due to strong clinical suspicion, a bone marrow biopsy was performed.
Bone marrow histopathology revealed >10% clonal plasma cells expressing monotypic lambda light chains. Congo red staining of the bone marrow was weakly positive, confirming amyloid deposition. Abdominal fat pad biopsy was negative. Positron emission tomography (PET/CT) did not show hypermetabolic lesions or lytic bone lesions. Serum calcium level was 9.2 mg/dL. Thus, the patient did not meet CRAB or SLiM criteria for multiple myeloma. The plasma cell dyscrasia was classified within the spectrum of monoclonal gammopathy with amyloidogenic potential (MGUS/smoldering myeloma).
Discussion: This case illustrates the diagnostic complexity of AL amyloidosis when conventional serum markers are non-contributory. The diagnosis hinged on imaging modalities and bone marrow findings. The patient did not fulfill hematologic criteria for multiple myeloma, yet imaging findings and clonal plasma cell infiltration supported the diagnosis of AL cardiac amyloidosis. Weakly positive Congo red staining in bone marrow biopsy emphasizes the importance of evaluating multiple tissue sites. The normal serum FLC ratio also highlights the potential for non-secretory or low-burden disease. This case underscores the necessity of integrating clinical findings, imaging, and histology in suspected amyloidosis.
Conclusion: AL cardiac amyloidosis must be considered in patients with heart failure, low ECG voltages, and increased ventricular wall thickness—even when routine serum and urine tests are negative. Cardiac MRI and bone marrow biopsy remain crucial tools in confirming diagnosis in such complex presentations.

Keywords: AL Amyloidosis, Cardiac MRI, Bone Marrow Biopsy, Low Voltage ECG, Heart Failure, Plasma Cell Dyscrasia, Congo Red Staining

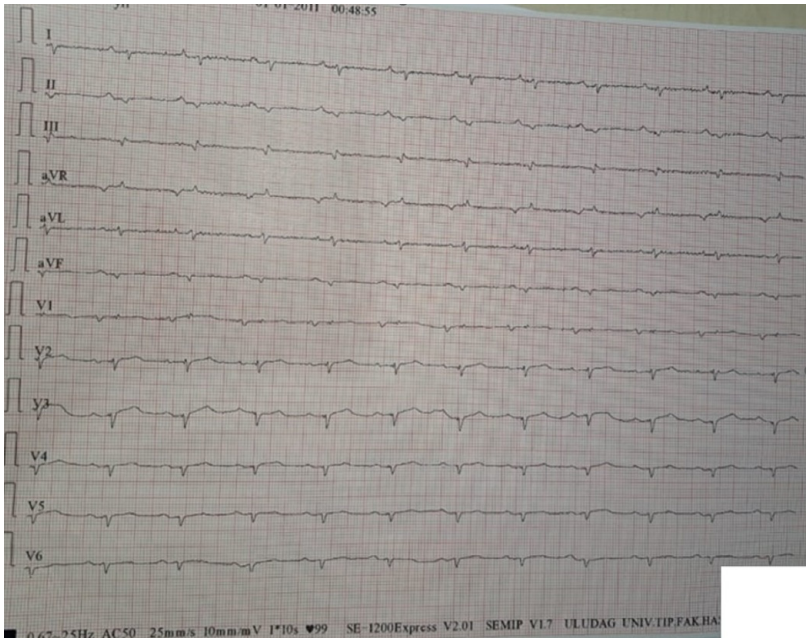

FIGURE 1. **Twelve-lead electrocardiogram (ECG) demonstrating sinus rhythm with diffuse low QRS voltages in limb and precordial leads. This pattern is suggestive of cardiac amyloidosis in the appropriate clinical context and is notably discordant with the echocardiographic evidence of increased left ventricular wall thickness.**

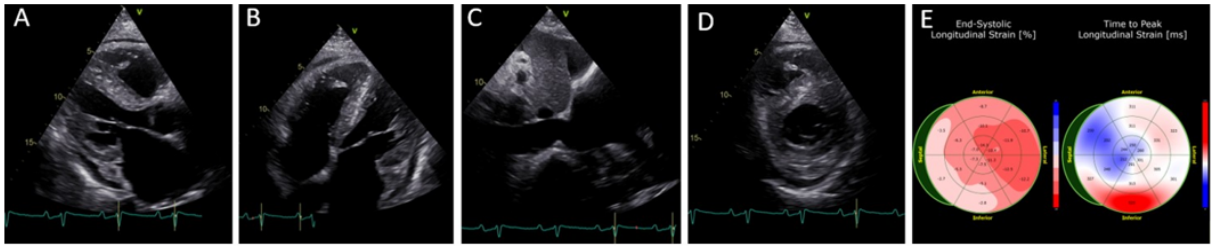

FIGURE 2. **Transthoracic echocardiographic features consistent with cardiac AL amyloidosis. (A) Parasternal long-axis view demonstrating concentric left ventricular hypertrophy with increased myocardial echogenicity and mild pericardial effusion. (B) RV-focused apical four-chamber view showing biatrial enlargement and right ventricular wall thickening, suggestive of biventricular involvement. (C) Subcostal view highlighting pericardial effusion and plethoric inferior vena cava, consistent with elevated right atrial pressure. (D) Parasternal short-axis view at mid-papillary level demonstrating symmetric thickening of the ventricular walls with a granular sparkling appearance. (E) Bull's eye plot showing significantly reduced global longitudinal strain (−8.6%) with relative apical sparing pattern (apical-to-basal ratio >1), highly specific for cardiac amyloidosis. The right panel illustrates delayed time-to-peak longitudinal strain in basal and mid-segments, supporting mechanical dispersion and infiltration.**

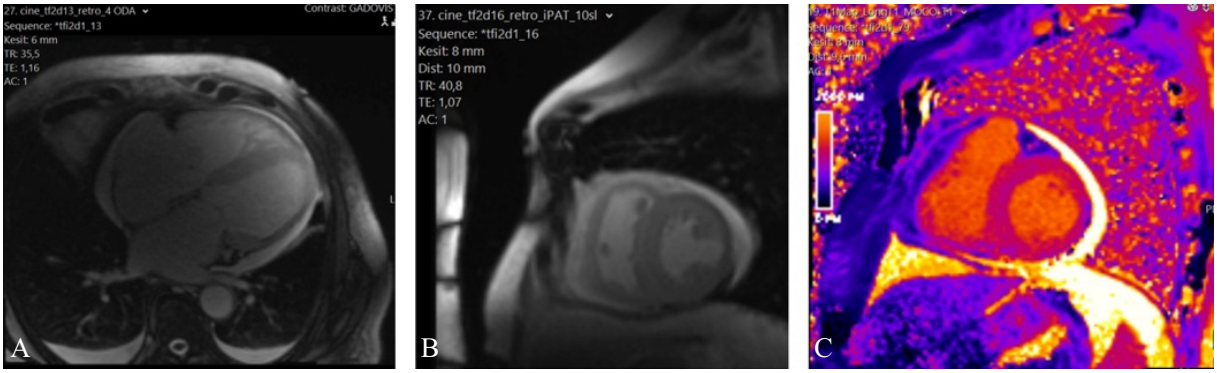

FIGURE 3. Cardiac magnetic resonance imaging findings consistent with cardiac AL amyloidosis. (A) Four-chamber steady-state free precession (SSFP) cine image demonstrating concentric left ventricular hypertrophy, biatrial enlargement, and a small pericardial effusion. Bilateral pleural effusions are also noted. (B) Short-axis SSFP cine view revealing symmetric myocardial thickening with global hypokinesia. (C) Native T1 mapping reveals diffusely prolonged myocardial T1 relaxation times, consistent with diffuse amyloid infiltration and interstitial expansion, in the absence of myocardial edema.

OP-33.
Nightmare in the Cath Lab: LMCA Dissection

Hasan Ari[1], Hüseyin Akdoğan[1], Ayaşe Dilara Balyimez[1], Muhammed Nusret Akin[1]

[1]Department of Cardiology, University of Health Sciences, Bursa Yüksek İhtisas Training and Research Hospital, Bursa, Türkiye

Case Presentation: A 56-year-old male patient presented to the cardiology outpatient clinic with a one-month history of persistent chest pain. His medical history revealed hypertension (HT). Transthoracic echocardiography showed an ejection fraction (EF) of 65%, left ventricular hypertrophy (IVS: 1.4 cm, PW: 1.3 cm), Grade 1 diastolic dysfunction, and mild mitral regurgitation (MR +1). Myocardial Perfusion Scintigraphy (MPS) demonstrated findings consistent with ischemia, and the patient was hospitalized for a planned coronary angiography (CAG). Coronary imaging was performed via the right radial artery. Coronary angiography revealed critical lesions in the right coronary artery (RCA) and the circumflex artery (Cx). In the same session, the RCA lesion was crossed with a guidewire, and PTCA was performed using a 2.0×15 mm balloon. Two everolimus-eluting stents (3.0×38 mm and 3.0×12 mm) were implanted, followed by overlap and post-dilatation with 3.5×15 mm and 3.5×10 mm non-compliant (NC) balloons (Figure 1). Subsequently, the Cx-OM2 lesion was crossed with a guidewire using a left guiding catheter. After PTCA with 2.0×15 mm and 2.5×25 mm balloons, a 2.5×38 mm everolimus-eluting stent was implanted (Figure 2). During this intervention, a dissection of the left main coronary artery (LMCA) occurred. Without removing the guiding catheter and guidewire positioned in Cx-OM from the right radial artery, a 7F sheath was inserted via the right femoral artery using the ping-pong technique. A left guiding catheter was then used to urgently advance a guidewire from the LMCA into the LAD (Figure 3). Stents measuring 4.0×16 mm (LMCA–Cx) and 4.0×24 mm (LMCA–LAD) were advanced through separate pathways and deployed using the crush technique (Figure 4). As the patient's clinical condition deteriorated, he was intubated, and an intra-aortic balloon pump (IABP) was inserted. POT was performed in the LMCA using a 5.0×6 mm NC balloon. After reevaluating the Cx, PTCA with 2.0×15 mm and 3.0×17 mm balloons were performed, followed by implantation of a 2.5×20 mm stent in distal Cx and a 3.0×28 mm stent in the mid-segment. A second POT was performed in the LMCA with a 5.0×6 mm NC balloon, followed by kissing balloon inflations in the LAD (4.0×10 mm) and Cx (4.0×10 mm) (Figure 5). A final POT was applied to the LMCA ostium with a 5.0×6 mm NC balloon, achieving near-complete luminal patency (Figure 6). After the successful procedure, the patient stabilized during intensive care follow-up and was discharged without complications.

Discussion: Iatrogenic LMCA dissection typically occurs due to catheter manipulation, guidewire misdirection, high-pressure contrast injection, or non-coaxial cannulation. Early diagnosis, rapid stenting of the true lumen, and mechanical support (IABP/Impella) significantly reduce mortality. When LMCA dissection occurs, keeping the initial catheter and guidewire in place and employing the ping-pong technique to introduce a second guiding catheter are crucial for procedural success.

Conclusions: LMCA dissection is a rare but potentially fatal complication. Early identification, prompt stenting, and appropriate mechanical support improve survival. Operator experience and meticulous technical execution are key protective factors.

Keywords: LMCA Dissection, Ping-Pong Technique, Crush Technique

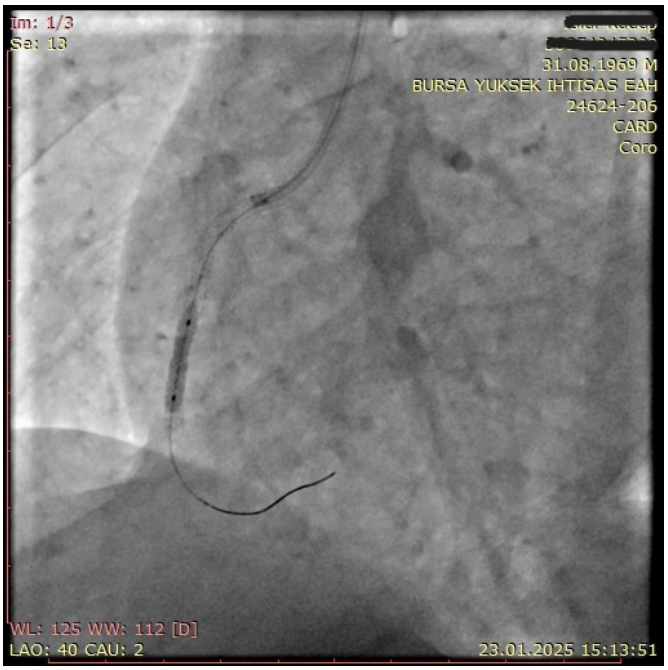

FIGURE 1. RCA after stenting

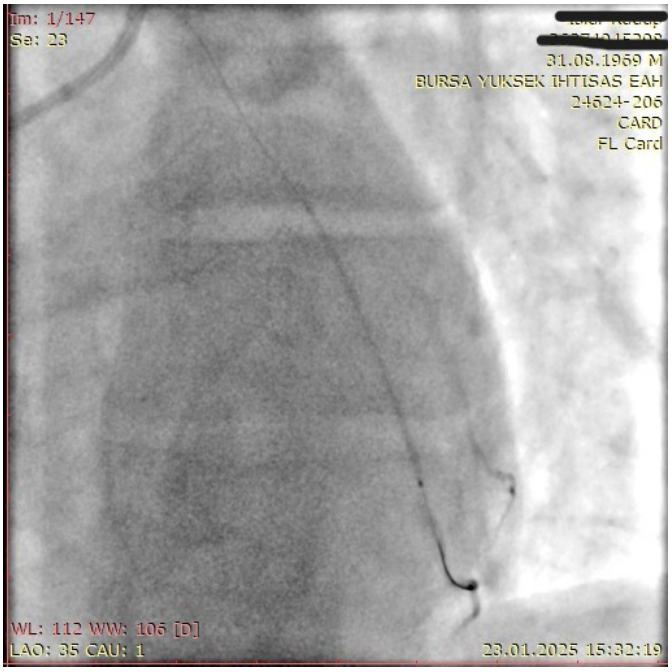

FIGURE 2. Cx OM2 was stent implanted

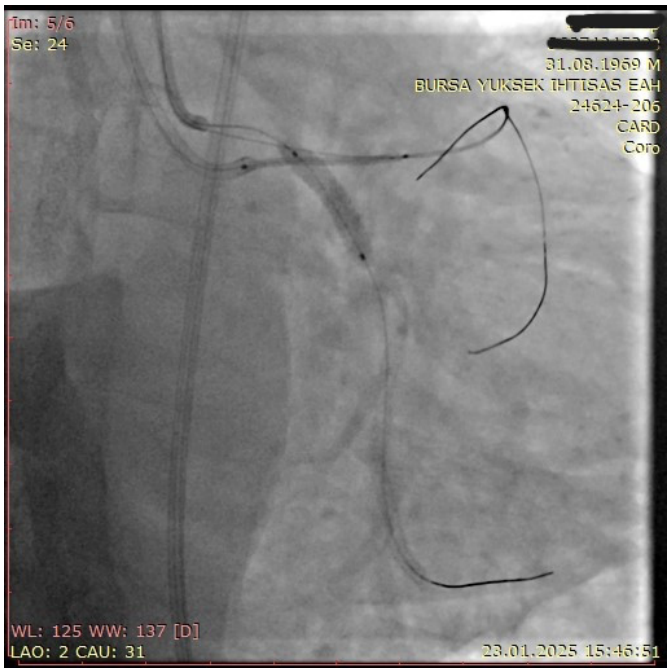

FIGURE 3. Ping-pong technique

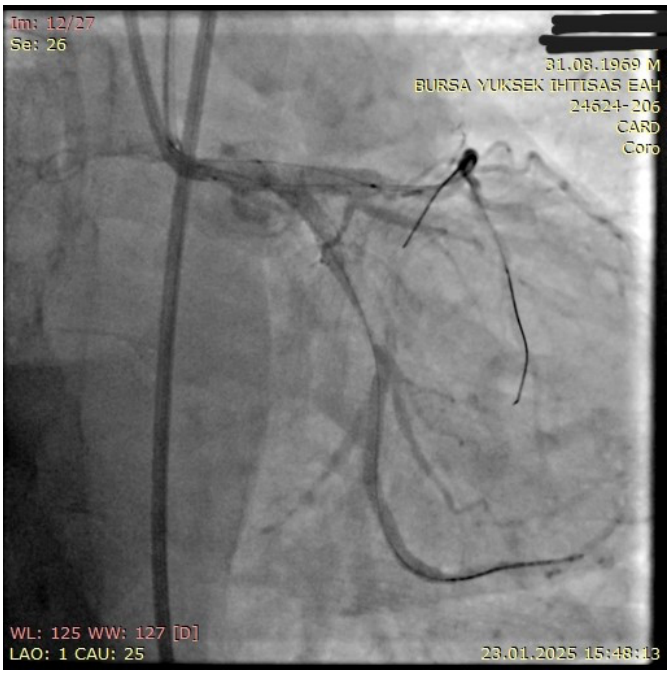

FIGURE 4. **Stenting of LMCA-CX and LMCA-LAD using the crush technique**

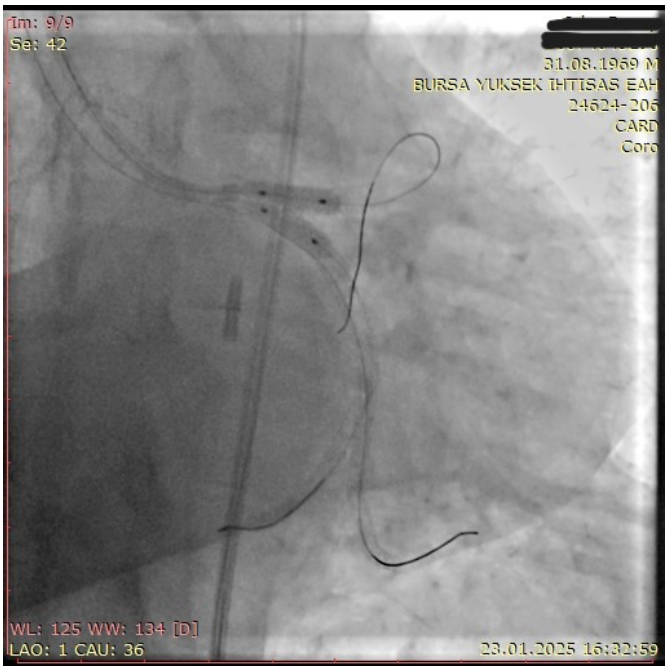

FIGURE 5. **Kissing ballon inflations in the LAD and CX**

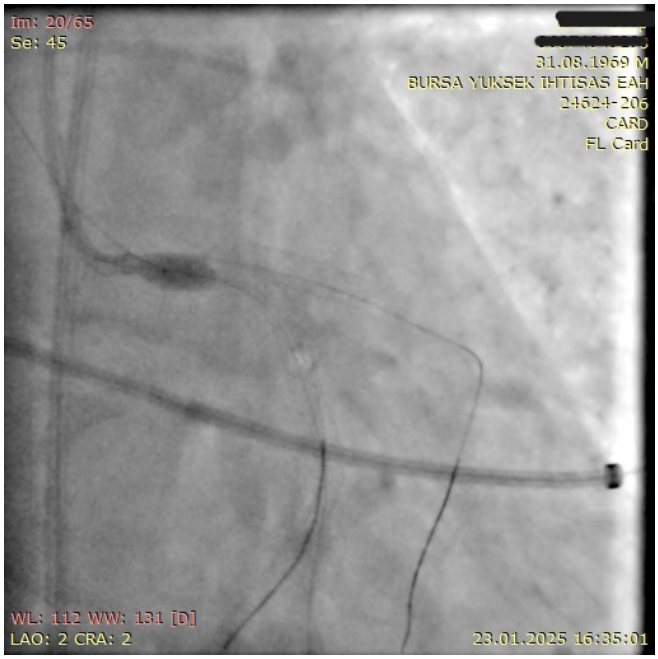

FIGURE 6. **Final POT was applied to the LMCA ostium**

OP-34.
Association of Preoperative Serum Magnesium Levels and Acute Kidney Injury Following Thromboembolectomy in Acute Limb Ischemia

Mesut Engin[1], Ahmet Kağan As[1], Fuat Ahmet Bilyay[1], Ufuk Aydin[1], Yusuf Ata[1], Şenol Yavuz[1]

[1]Department of Cardiovascular Surgery, University of Health Sciences, Bursa Yüksek İhtisas Training and Research Hospital, Bursa, Türkiye

Objectives: Acute lower extremity ischemia (ALI) is an important cardiovascular emergency. Acute kidney injury (AKI) after surgical embolectomy prolongs hospitalization and increases treatment costs. Low blood magnesium (Mg) levels were shown to be associated with renal dysfunction. In this study, we aimed to investigate the relationship between preoperative magnesium values and AKI.
Methods: Patients who underwent a surgical embolectomy for ALI between January 2016 and June 2024, were consecutively included in this retrospective study. After the exclusion criteria, patients were divided into two groups: those who developed AKI in the postoperative period (Group 1) and those who did not (Group 2).
Results: The 69 patients in Group 1 and the 403 patients in Group 2 had median ages of 67 (35-89) and 64 (39-95), respectively (P=0.098). The two groups shared similar characteristics concerning the history of past cerebrovascular events, gender, hypertension, diabetes mellitus, hyperlipidemia, rates of coronary artery disease and peripheral arterial disease. As a result of the multivariate analysis, HbA1c >9 (OR: 1.350, CI 95%: 1.110-1.984, P=0.028), high creatinine (OR: 2.945, CI 95%: 1.837-3.682, P<0.001) and low Mg (OR: 0.695, CI 95%: 0.550-0.869, P=0.014) values, were determined as independent predictors for predicting AKI.
Discussion: AKI after vascular surgical operations is an important problem due to the associated prolonged hospitalization and mortal-morbid consequences. Therefore, it is imperative to identify the risk factors and to take precautions, whenever possible. In our current study, we have shown that preoperative low Mg levels are an independent predictor of AKI risk. In light of these findings, preoperative Mg replacement may be performed in patient groups considered at risk, however the former need to be supported by prospective multicenter studies.
Conclusions: In our current study, we have shown that preoperative low Mg levels may be an independent predictor of AKI risk
Keywords: Magnesium, Revascularization, Lower Extremity Ischemia, Risk Factor

OP-35.
Could the Systemic Coagulation Inflammation Index Be a Predictor of Worse Outcomes After Carotid Endarterectomy?

Mesut Engin[1], Ahmet Kağan As[1], Mehmet Sadik Akpinar[1], Orhan Güvenç[1], Ufuk Aydin[1], Yusuf Ata[1], Şenol Yavuz[1]

1Department of Cardiovascular Surgery, University of Health Sciences, Bursa Yüksek İhtisas Training and Research Hospital

Objectives: Stroke is a significant disease which results in high mortality and morbidity rates and one of its most significant causes is the presence of carotid artery stenosis (CAS). Although endovascular applications have increased in the treatment of CAS, carotid endarterectomy (CEA) surgeries remain prominent. The Systemic Coagulation Inflammation Index (SCII) has emerged as an important marker indicating coagulation and inflammation status.In this study, we aimed to investigate the effect of SCII value on mortality and stroke in a 30-day follow-up, in patients to whom we applied CEA.
Methods: This study consecutively included patients who underwent carotid endarterectomy at our clinic between January 1, 2020 and June 1, 2025. Patients who did not develop worse outcomes within the first 30 days after surgery were assigned to Group 1 and those who did were assigned to Group 2. Worse outcomes in the study were defined as stroke, myocardial infarction and death.
Results: A total of 594 patients underwent elective CEA surgery. The 546 patients in Group 1 and the 48 patients in Group 2 had median ages of 71 (44-88) and 69 (41-91), respectively (P=0.185). As a result of the multivariate analysis, the presence of CAD (OR: 1.690, CI 95%: 1.210-1.984, P=0.032), and high SCII (OR: 1.780, CI 95%: 1.270-2.894, P<0.001) were determined as independent predictors for predicting worse outcomes, after CEA surgery.
Discussion: The prognostic value of parameters currently obtained from routine blood tests has been widely investigated. In our study, we examined the effect of SCII values, currently being researched as a predictor in various cardiovascular diseases, on early prognosis after CEA. Our results indicated that high SCII values were associated with worse outcomes within 30 days after CEA.
Conclusions: In patients undergoing CEA, SCII values can be calculated preoperatively to identify at-risk patient groups, therefore measures can be taken for patient management and follow-up in the postoperative period.
Keywords: Carotid Artery Stenosis, Carotid Endarterectomy, Inflammation

OP-36.
The Role of Exocrine Pancreatic Insufficiency in Predicting Concomitant Carotid Artery Disease in Diabetic Patients Scheduled to Undergo Coronary Artery Bypass Grafting

Mesut Engin[1], Abdulkerim Özkan[1], Ufuk Aydin[1], Yusuf Ata[1], Şenol Yavuz[1]

[1]Department of Cardiovascular Surgery, University of Health Sciences, Bursa Yüksek İhtisas Training and Research Hospital

Objectives: Preoperative identification of the presence of concomitant carotid artery stenosis (CAS) in patients planning coronary artery bypass graft (CABG) surgery is crucial. Exocrine pancreatic insufficiency (EPI) is a condition particularly common in diabetic patients and can lead to significant problems. In this study, we aimed to investigate the role of EPI in predicting CAS in diabetic patients scheduled to undergo CABG.
Methods: Diabetic patients scheduled for CABG surgery at our clinic between September 10, 2025, and November 10, 2025, were consecutively included in this study. Emergency operations, those who did not wish to participate in the study, patients scheduled for additional cardiac surgery, and patients with malignancy were excluded. After the exclusion criteria, 75 patients were included in the study. Patients were divided into two groups: those with EPI (Fecal elastase <200 µg/g) and those without EPI (200 µg/g and above).
Results: There were 32 patients in the EPI (+) group and 43 patients in the EPI (-) group. There was no difference between the groups in terms of hypertension frequency, gender, and chronic obstructive pulmonary disease frequency (P>0.005). The groups were similar in terms of age, left ventricular ejection fraction, SYNTAX score I, albumin, creatinine, and C-reactive protein values (P>0.005). HbA1c values were statistically significantly higher in patients with EPI (+) (8.4±2.2 vs 7.6±1.2, P=0.045). The number of patients with at least unilateral carotid artery stenosis of 50% or more was also statistically significantly higher in patients with EPI (+) (11.6% vs. 40.6%, P=0.004).
Discussion: Pancreatic fecal elastase-1 (FE-1) levels are an inexpensive and effective way to detect exocrine pancreatic insufficiency. A study in the cardiovascular field showed that FE-1 levels were decreased in patients with decompensated heart failure. Similarly, a significant relationship between cardiovascular diseases and FE-1 levels was found in patients with chronic pancreatitis. In our current research, we showed that exosomal pancreatic insufficiency may indicate the presence of CAS in diabetic patients scheduled for CABG.
Conclusions: Diabetes mellitus is an important risk factor and prognostic marker for cardiovascular diseases. EPI is also frequently seen in these patients. Based on the data we obtained, FE-1 levels may indicate the presence of additional CAS in diabetic patients scheduled for CABG.
Keywords: Coronary Artery Disease, Diabetes Mellitus, Fecal Elastase, Carotid Artery Stenosis

OP-37.
Relationship Between TASC II Lesion Severity and Carotid Artery Stenosis: A Cross-Sectional Analysis

Çağlar Alp[1], **Hüseyin Kandemir**[1]

[1]*Department of Cardiology, Kırıkkale University, Faculty of Medicine, Kırıkkale, Türkiye.*

Objectives: Peripheral arterial disease represents a systemic manifestation of atherosclerosis and is frequently accompanied by carotid artery involvement, which increases the risk of adverse cardiovascular outcomes. Although the Trans-Atlantic InterSociety Consensus (TASC II) classification is commonly used to describe peripheral lesion complexity, its association with the severity of carotid artery stenosis remains insufficiently explored. The present study aimed to investigate the relationship between TASC II lesion categories and the degree of right and left carotid artery stenosis, as well as to compare demographic, clinical, and laboratory characteristics between patients with lower and higher TASC II lesion classes.
Methods: This study included 95 patients who were stratified into two groups according to TASC II classification: A–B lesions (n=51) and C–D lesions (n=44). Baseline demographic data, smoking status, laboratory findings, and carotid artery stenosis percentages were recorded and compared between groups (Table 1). Continuous variables were summarized using mean±standard deviation or median (interquartile range), depending on data distribution, while categorical variables were presented as frequencies and percentages. Associations between TASC II class and carotid artery stenosis were assessed using Spearman correlation analysis. Partial correlation analysis was subsequently performed to adjust for potential confounders, including age, smoking status, and glucose levels.
Results: Patients classified as TASC II C–D were significantly older and demonstrated a higher prevalence of smoking compared with those in the TASC II A–B group. Both right and left carotid artery stenosis percentages were markedly higher in the TASC II C–D group. Correlation analyses revealed a positive association between increasing TASC II class and the severity of carotid artery stenosis on both sides (Figures 1 and 2). After adjustment for age, smoking status, and glucose levels, TASC II classification remained weakly but significantly correlated with right and left carotid artery stenosis (Table 2). Moreover, a strong positive relationship was observed between right and left carotid artery stenosis measurements.
Discussion: The findings indicate that more advanced TASC II lesion classes are associated with greater carotid artery stenosis severity, independent of major clinical confounders. This suggests that TASC II classification may reflect the overall systemic atherosclerotic burden rather than being limited to peripheral arterial lesion complexity. Assessment of carotid artery involvement may therefore provide additional clinical value in patients with advanced TASC II lesions.
Conclusions: Higher TASC II lesion classes are independently associated with increased severity of right and left carotid artery stenosis. These results support the notion that TASC II classification reflects not only peripheral arterial lesion complexity but also the extent of systemic atherosclerosis. Incorporating carotid artery assessment into the evaluation of patients with advanced TASC II lesions may contribute to improved cardiovascular risk stratification and clinical decision-making.
Keywords: Carotid Artery Stenosis; TASC II Classification; Peripheral Arterial Disease

TABLE 1. Demographic, Clinical and Laboratory Characteristics of Patients

	TASC II A-B lesion n=51	TASC II C-D lesion n=44	P-value
Demographic characteristics			
Male, n (%)	46 (90.2)	31 (70.5)	**0.014**
Female, n (%)	5 (9.8)	13 (29.5)	**0.014**
Age (years)	64.04±8.55	67.66±8.91	**0.046**
Smoker, n (%)	20 (39.2)	35 (79.5)	**0.001**
Laboratory characteristics			
Hemoglobin (g/dL)	13.19±1.92	12.59±2.28	0.16
WBC (×10³/µL)	9.55 ±2.34	9.65 ±3.22	0.86
Neutrophil count (×10³/µL)	6.49±2.05	6.52 ±2.77	0.95
Platelet count (×10³/µL)	244.1±75.19	279.4±87.7	0.56
Total cholesterol (mg/dL)	176.5±52.72	164.58±63.3	0.33
LDL-C (mg/dL)	103.6±41.9	91.5±44.9	0.18
HDL-C (mg/dL)	40.2±12.1	41.5±13.9	0.62
Triglyceride (mg/dL)	158.5 (110.5-242.5)	119 (85.5-188)	0.051
Creatinin (mg/dL)	1.1±0.63	1.28 ±0.93	0.27
Glucose (mg/dL)	137±43.9	160.4 ±68.5	**0.05**
C-reactive protein (mg/L)	10.9 (4.2-31)	10.2 (3.7-33.3)	0.06
Carotid artery stenosis			
Right carotid (%)	22.3±13.6	33.6±14.4	**0.001**
Left Carotid (%)	24.1±12.8	33.8±14.3	**0.001**

Data are shown as mean±standard deviation or n (%) or median (interquartile range) where appropriate. HDL-C, high density lipoprotein cholesterol; LDL-C, low density lipoprotein cholesterol; WBC, white blood cells; TASC, Trans-Atlantic Inter Society Consensus.

Statistically significant P-values are shown in bold.

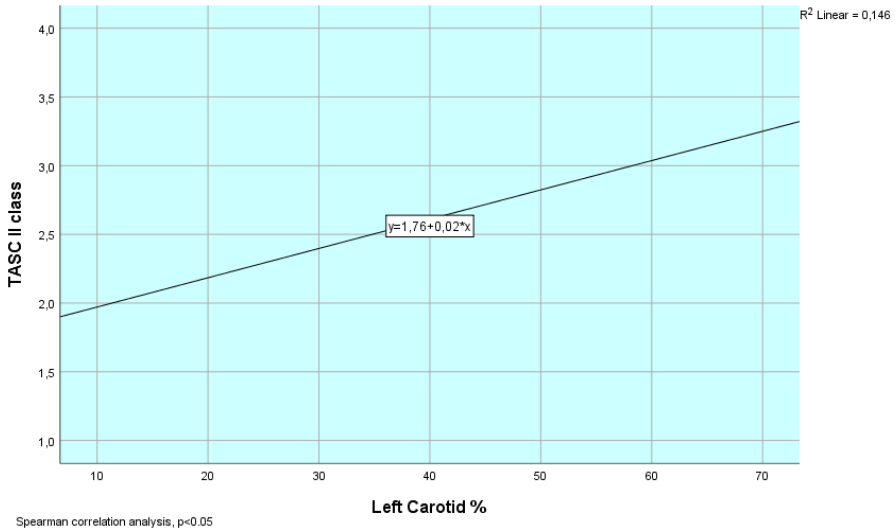

FIGURE 1. The association between left carotid artery stenosis (%) and TASC II lesion class.

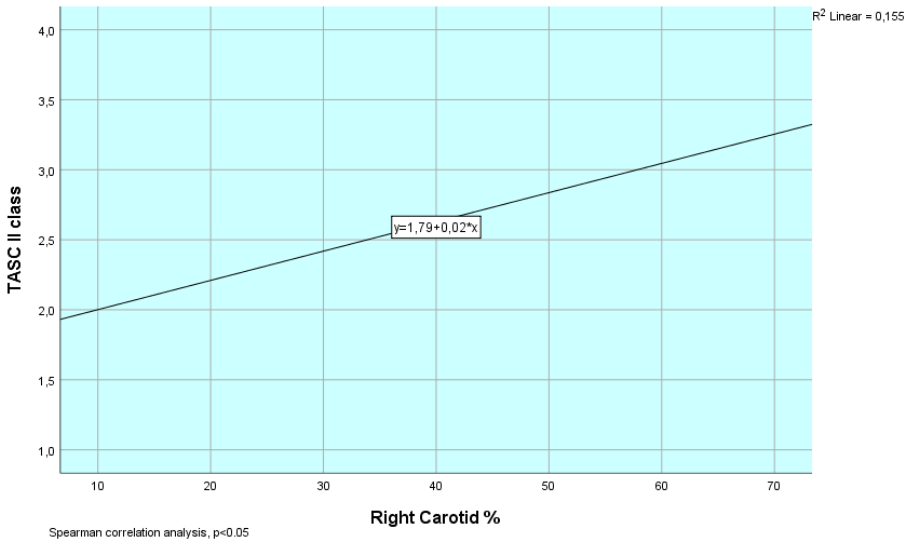

FIGURE 1. **The association between left carotid artery stenosis (%) and TASC II lesion class.**

TABLE 2. **Partial Correlation Analysis Between TASC II Classification and Right–Left Carotid Artery Stenosis After Adjustment for Age, Smoking Status and Glucose Levels.**

Control Variables			TASC II Class	Right Carotid (%)	Left Carotid (%)
Age, Smoker and Glucose	TASC II Class	Correlation	1.000	0.203*	0.228*
		Significance (2-tailed)	.	0.050	**0.031**
	Right Carotid (%)	Correlation	0.203*	1.000	0.667**
		Significance (2-tailed)	0.050	.	**<0.001**
	Left Carotid (%)	Correlation	0.228*	0.667**	1.000
		Significance (2-tailed)	**0.031**	**<0.001**	.

Values are partial correlation coefficients (r). Analyses were adjusted for age, smoking status, and glucose levels

*Correlation is significant at 0.05 level

**Correlation is significant at 0.01 level

OP-38.
Hyponatremic Seizure in a Middle-Aged Woman on Spironolactone-Hydrochlorothiazide

Mehmet Zafer Aydin[1], Mehmet Kamil Teber[1], Zülfiye Kuzu[1], Mustafa Gök[1]

[1]Department of Cardiology, Kayseri City Hospital, Kayseri, Türkiye

Objectives: Thiazide-induced hyponatremia (TIH) is a well-recognized adverse effect of hydrochlorothiazide-containing medications, typically occurring in elderly individuals. Severe acute hyponatremia presenting with seizures in middle-aged adults is uncommon. Combination therapy with spironolactone–hydrochlorothiazide may increase susceptibility to rapid electrolyte shifts.
Case Presentation: A 52-year-old woman presented with a generalized tonic–clonic seizure. Three days earlier, she had started a spironolactone–hydrochlorothiazide combination for hypertension. Her sodium level prior to starting the medication was 131 mg/dL. On admission, she was hemodynamically stable with a GCS of 15. Laboratory testing revealed severe hyponatremia (115 mg/dL), hypokalemia, and hypochloremia. CT and MRI were normal. Controlled correction with 3% hypertonic saline resulted in progressive normalization of sodium levels without complications, and the patient recovered fully. The spironolactone–hydrochlorothiazide combination was discontinued permanently.
Discussion: This case demonstrates that acute symptomatic hyponatremia can develop rapidly following initiation of thiazide-containing therapy, even in non-elderly adults. The combination of spironolactone and hydrochlorothiazide may have synergistic natriuretic effects that heighten susceptibility to rapid sodium decline. Early neurological symptoms, including seizures, may be the first clinical sign. The absence of thyroid, adrenal, or renal dysfunction supports a drug-induced mechanism.
Conclusions: Clinicians should monitor electrolytes closely during the initial days of therapy with spironolactone–hydrochlorothiazide combinations. Early detection of hyponatremia can prevent serious neurological complications such as seizures.
Keywords: Hyponatremic Seizure, Thiazide-Induced Hyponatremia, Middle-Aged Woman

OP-39.
An Unexpected Cause of Angina: Successful Percutaneous Closure of an Internal Mammary Artery-Left Atrium Fistula

Ecem Gürses[1], **İlker Gül**[1]

[1]*Department of Cardiology, Bakırçay University, İzmir, Türkiye*

Objectives: Coronary artery fistulas are rare vascular anomalies that may present with myocardial ischemia and angina despite the absence of significant obstructive coronary artery disease. We aimed to present a rare case of an internal mammary artery–left atrium (IMA–LA) fistula presenting with angina and successfully treated by percutaneous coil embolization.
Methods: A 48-year-old female patient with no known chronic medical conditions presented to the cardiology outpatient clinic with typical chest pain. An exercise stress test was positive for ischemia, and myocardial perfusion scintigraphy demonstrated ischemia in the posterior and lateral myocardial walls. Based on these findings, coronary angiography was performed. Coronary angiography revealed normal left main coronary artery; mild non-obstructive atherosclerotic changes in the left anterior descending artery with 30% stenosis in the mid and distal segments; a non-dominant circumflex artery arising from a separate ostium with atherosclerotic plaques; and 20% stenosis in the mid right coronary artery. In addition, an anomalous fistulous connection between the internal mammary artery and the left atrium was identified. After multidisciplinary heart team evaluation, percutaneous closure of the fistula was planned. During the procedure, the IMA–LA fistula was crossed using a PT2 guidewire, followed by advancement of a microcatheter. Coil embolization was performed using coils measuring 3×6 mm, 4×8 mm, 4×15 mm, and two 5×8 mm Interlock coils.
Results: Post-procedural angiography demonstrated complete occlusion of the fistula with no residual shunt. The procedure was completed successfully without any complications. The patient was discharged after optimization of medical therapy. During follow-up at the cardiology outpatient clinic, the patient reported marked improvement in anginal symptoms with significant reduction in ischemic complaints.
Discussion: IMA–LA fistulas are extremely rare and may cause myocardial ischemia through a coronary steal phenomenon, even in the absence of significant coronary artery stenosis. Non-invasive ischemia testing plays a crucial role in identifying clinically relevant fistulas. Percutaneous coil embolization represents a safe and effective treatment option, offering symptom relief and avoiding surgical intervention in selected patients.
Conclusions: This case highlights a rare cause of angina and myocardial ischemia due to an internal mammary artery–left atrium fistula. Percutaneous coil embolization is a feasible, safe, and effective therapeutic approach, resulting in complete fistula closure and significant clinical improvement.
Keywords: Internal Mammary Artery Fistula, Left Atrium Fistula, Coronary Artery Fistula, Angina Pectoris, Myocardial Ischemia, Percutaneous Coil Embolization

OP-40.
Predictors of Isolated Nocturnal Hypertension in Non-obese Non-diabetic Individuals

Cagdas Kaynak[1]

[1]*Departmant of Cardiology, Siirt Training and Research Hospital, Siirt, Türkiye*

Objectives: Isolated nocturnal hypertension (INH) is a distinct blood pressure (BP) phenotype that can only be detected by ambulatory blood pressure monitoring (ABPM). Despite normal daytime BP values, elevated nocturnal BP has been associated with increased cardiovascular risk. However, data regarding the predictors of INH in nonobese, nondiabetic individuals, in whom major metabolic confounding factors are minimized, remain limited.
The objective of this study was to evaluate clinical, biochemical and ABPM–related predictors of INH in nonobese, nondiabetic individuals.
Methods: This retrospective observational study included 158 non-obese, non-diabetic individuals who underwent 24-hour ABPM. Participants were classified into two groups according to the presence (n=81) or absence (n=77) of INH. Demographic characteristics, laboratory parameters and detailed ABPM indices were compared between groups. Variables demonstrating significant or borderline associations were further evaluated using multivariable logistic regression analysis to identify independent predictors of INH.
Results: The prevalence of chronic kidney disease, dyslipidemia and current smoking was significantly higher in individuals with INH compared with the control group (P<0.05) (Table 1). Individuals with INH had significantly higher daytime (P<0.001) and nighttime (P<0.001) BP load, reduced nocturnal systolic (P<0.001) and diastolic (P<0.001) dipping (%), higher body mass index (BMI) (P=0.008), elevated triglyceride–glucose (TyG) index (P<0.001), increased atherogenic index of plasma (AIP) (P<0.001) and higher C-reactive protein (CRP) levels (P<0.001) compared with the control group (Table 1). In multivariable logistic regression analysis, higher CRP levels (OR=8.37, 95% CI=3.24–21.61, P<0.001), reduced nocturnal diastolic dipping (OR=0.81, 95% CI=0.67–0.99, P=0.036), higher BMI (OR=1.54, 95% CI=1.13–2.10, P=0.007) and presence of dyslipidemia (OR=6.77, 95% CI=1.14–40.25, P=0.035) emerged as independent predictors of INH (Table 2).
Discussion: The present findings suggest that INH in non-obese, non-diabetic individuals is not merely a benign BP phenotype but reflects underlying pathophysiological mechanisms. The strong association with elevated CRP levels highlights the potential role of subclinical inflammation, while impaired nocturnal BP dipping indicates circadian dysregulation of BP control. In addition, the association with dyslipidemia and higher BMI within the non-obese range suggests that subtle metabolic alterations may contribute to nocturnal BP abnormalities even in the absence of overt metabolic disease.
Conclusions: In non-obese, non-diabetic individuals, INH is independently associated with subclinical inflammation, impaired nocturnal BP dipping, subtle increases in adiposity and the presence of dyslipidemia, underscoring the importance of ABPM for early risk identification in apparently low-risk populations.
Keywords: Isolated Nocturnal Hypertension, Ambulatory Blood Pressure Monitoring, Inflammation, Nocturnal Dipping, Non-obese, Non-diabetic

OP-41.
The Impact of Guideline-based Treatment on In-hospital Outcomes in Infective Endocarditis

Mustafa Kara[1], **Okan Korun**[2], **Gönenç Kocabay**[1]

[1]Department of Cardiology, Kartal Kosuyolu Yüksek İhtisas Training and Research Hospital, Istanbul, Türkiye; [2]Department of Cardiology, Dr. Burhan Nalbantoglu State Hospital, Nicosia, Cyprus

Objectives: Infective endocarditis (IE) is a serious disease with high mortality requiring a multidisciplinary approach. The 2023 ESC guidelines have made significant updates, particularly regarding surgical indications. This study aimed to compare the in-hospital outcomes of patients diagnosed with infective endocarditis who received treatment according to the current guidelines and those who did not.
Methods: The study was designed retrospectively. A total of 140 patients diagnosed with infective endocarditis according to the modified Duke criteria at Istanbul Kartal Koşuyolu Yüksek İhtisas Training and Research Hospital between 2019 and 2023 were included in the study. Patients were divided into two groups: those who received treatment according to current ESC guidelines and those who did not. In-hospital mortality was determined as the primary endpoint. Univariate and multivariate logistic regression analyses were applied.
Results: Thirty-one (22.1%) patients were treated according to current guidelines, and 109 (77.9%) were treated inconsistently. Vegetation diameter and preoperative antibiotic treatment duration were significantly shorter in patients treated according to current guidelines (P<0.001). No significant difference was found between the two groups in terms of in-hospital mortality. In multivariate logistic regression analysis, surgical treatment (OR: 0.077, P=0.002) and prolonged antibiotic treatment duration (OR: 0.44, P=0.003) reduced mortality, while increased blood high sensitive (hs) CRP and LDH levels increased the risk of mortality.
Discussion: In patients with infective endocarditis, surgical intervention significantly prolongs in-hospital mortality. Although current rates of appropriate treatment and vegetation size have increased, no significant difference in in-hospital mortality was found between groups that followed and those that did not follow the guidelines. Furthermore, the increase in blood hs-CRP and LDH levels, which may contribute to mortality progression, supports the prognostic development of these markers.
Conclusions: Surgical treatment and adequate antibiotic treatment duration reduce in-hospital mortality in infective endocarditis. Blood hs-CRP and LDH are valuable biomarkers in predicting mortality. Multicenter studies are needed to evaluate the impact of current guidelines on clinical practice.
Keywords: Infective Endocarditis, Surgery, Blood LDH level

OP-42.
The Effect of Unfractionated Heparin Administration Timing on Radial Artery Spasm and Occlusion in Radial Coronary Angiography

Doğan Ormanci[1], Tolga Doğan[1], Hasan Ari[1], Ömer Faruk Kahraman[1], Ayşe Dilara Balyimez[1], Bilal Mete Ülker[1], Esra Akpinar[1], Haydar Selçuk Demiray[1], Ahmet Fatih Kişpinar[1], Muhammed Bilal Aknur[1]

[1]Department of Cardiology, University of Health Sciences, Bursa Yüksek İhtisas Training and Research Hospital

Objectives: In this study, we aimed to investigate whether administering unfractionated heparin at a dose of 100 IU/kg directly through the radial sheath versus administering it into the ascending aorta via a coronary catheter has an effect on radial artery occlusion and spasm.
Methods: In this prospectively designed study, 200 patients who presented to the cardiology outpatient clinic and were scheduled for elective angiography were enrolled and randomly assigned to study groups. Prior to angiography, physical examination findings, cardiovascular risk factors, height, weight, complete blood count parameters, and biochemical characteristics were recorded. Radial and ulnar artery diameters and flow velocities were measured. During angiography, the presence or absence of arterial spasm was additionally documented. Radial and ulnar ultrasonography was performed one day and thirty days after the procedure to assess the presence of occlusion, and vessel diameters and flow velocities were measured.
Results: No statistically significant differences were observed between the control group (patients receiving heparin via the radial sheath) and the study group (patients receiving heparin into the ascending aorta) with respect to age, sex, body mass index, smoking status, hypertension, diabetes mellitus, or coronary artery disease (P>0.05). RAS was significantly higher in the control group compared with the study group (45.9% vs. 25.3%; P=0.002). RAO on day 1 was significantly more frequent in the control group (33.7% vs. 17.2%; P=0.008), whereas no statistically significant difference was observed between the groups with respect to RAO at day 30 (10.2% vs. 4.0%; P=0.092). In logistic regression analysis, RAS (OR: 7.03, 95% CI: 3.02–16.36; P<0.001), radial artery diameter (OR: 0.11, 95% CI: 0.03–0.39; P=0.001), and β-blocker therapy (OR: 0.34, 95% CI: 0.14–0.81; P=0.01) were identified as independent predictors of RAO development. Although the group variable was a significant factor for RAO development in univariate logistic regression analysis (OR: 0.40, 95% CI: 0.20–0.79; P=0.009), it was not independently associated with RAO in multivariate analysis (OR: 0.74, 95% CI: 0.34–1.62; P=0.46).
Conclusions: The results of this study indicate that administration of heparin into the aorta significantly reduces radial artery spasm. The reduction in spasm significantly decreases the development of occlusion. However, due to the systemic effect of heparin, no significant difference was observed in occlusion rates on the thirtieth day.
Keywords: Radial Angiography, Heparin, Spasm, Occlusion

OP-43.
The Mediating Role of Heart Rate in the Relationship Between Smoking and Myocardial Performance

Hakan İskender[1], İsmail Balaban[1]

[1]Deartment of Cardiology, Kartal Koşuyolu Yüksek İhtisas Training and Research Hospital, İstanbul, Türkiye

Objectives: To investigate whether heart rate serves as a functional mediator in the relationship between smoking and myocardial performance in a healthy population.
Methods: Healthy volunteers without known cardiovascular disease were enrolled and categorized according to smoking status. MPI was calculated using tissue Doppler echocardiography. Resting heart rate and blood pressure were recorded under standardized conditions. The indirect effect of heart rate on the association between smoking and MPI was examined using mediation analysis. Group comparisons and correlation analyses were performed, and key findings were illustrated graphically.
Results: MPI values were numerically higher in smokers than in non-smokers; however, the direct association did not reach statistical significance (P=0.147). Smoking status was significantly associated with resting heart rate (β=−0.39; 95% CI: −0.72 to −0.05; P=0.029). Heart rate showed a consistent relationship with MPI, indicating a tendency toward higher MPI values with increasing heart rate (β=−0.35; 95% CI: −0.72 to 0.02; P=0.056). Importantly, mediation analysis demonstrated that the association between smoking and MPI was largely explained by an indirect pathway through heart rate. No significant effect modification by age or sex was observed (P>0.05).
Discussion: These findings suggest that heart rate may function as an early functional bridge linking smoking to subclinical myocardial impairment, even in the absence of overt cardiovascular disease. Nicotine-related sympathetic activation may increase heart rate, shorten diastolic filling time, and thereby influence MPI—offering a mechanistically plausible explanation for the observed indirect effect. While a significant total effect of smoking on MPI was not detected, the identification of a heart rate–mediated pathway highlights a potentially important early signal. In this context, heart rate may represent one of the earliest modifiable physiological markers linking smoking exposure to myocardial functional alterations. Given that heart rate is both easily measurable and modifiable, this parameter may provide incremental value in the early assessment of smoking-related cardiac effects in otherwise healthy individuals.
Conclusions: This study suggests that smoking may influence myocardial performance indirectly through heart rate rather than through a direct effect. Heart rate may be useful in assessing early smoking-related cardiac effects in healthy individuals.
Keywords: Heart Rate, Myocardial Performance Index, Smoking

OP-44.
Avoiding Emergency Surgery with Imaging-Guided Thrombolysis in Mechanical Valve Thrombosis

Fahrettin Tuğrul Çitekçi[1], Hüseyin Sefa İnce[1], Fatma Kayaaltı Esin[1], Cem Nazli[1], Mert Şentürkün[1]

[1]Department of Cardiology, Katip Celebi University Ataturk Training and Research Hospital, İzmir, Türkiye

Objectives: Obstructive mechanical prosthetic valve thrombosis (PVT) is an uncommon but potentially life-threatening complication, most frequently associated with subtherapeutic anticoagulation. Clinical presentation depends on the degree of leaflet immobilization and hemodynamic compromise and may range from progressive exertional dyspnea to acute pulmonary edema or cardiogenic shock. Prompt diagnosis and appropriate management are essential, as delayed treatment is associated with increased morbidity and mortality. Accurate differentiation between thrombus and pannus is critical, since therapeutic strategies differ substantially and include thrombolytic therapy or emergency surgery. In this context, advanced imaging modalities play a pivotal role in defining prosthetic valve hemodynamics, leaflet motion, and the underlying mechanism of obstruction.

Case Presentation: A 53-year-old man with a bileaflet mechanical aortic valve implanted in 2018 presented with acute worsening dyspnea following a one-month history of progressive exertional symptoms. He reported irregular adherence to warfarin therapy. On admission, the patient was tachycardic, tachypneic, and hypoxemic. Laboratory evaluation revealed a markedly subtherapeutic international normalized ratio, suggesting thrombotic prosthetic valve dysfunction. Transthoracic echocardiography demonstrated preserved left ventricular systolic function (ejection fraction 45%) and severely elevated transprosthetic aortic gradients (maximum velocity 4.3 m/s, peak gradient 75 mmHg, mean gradient 48 mmHg), consistent with obstructive prosthetic valve dysfunction. To clarify the mechanism, multimodality imaging was performed. Cinefluoroscopy showed near-complete restriction of both mechanical valve leaflets. Transesophageal echocardiography (TEE) identified a mobile hypoechoic mass consistent with thrombus and severe aortic regurgitation due to impaired leaflet coaptation,indicating a reversible thrombotic process. After multidisciplinary Heart Team evaluation, emergency surgery was deferred. Given the subtherapeutic anticoagulation status, mobile thrombus morphology, and favorable imaging features, low-dose thrombolytic therapy was initiated. Tissue plasminogen activator (tPA) was administered at 25 mg as a slow continuous infusion over 24 hours. Because residual leaflet restriction persisted, a second identical 24-hour tPA infusion was given, resulting in a cumulative dose of 50 mg over 48 hours.

Post-treatment cinefluoroscopy demonstrated complete restoration of leaflet mobility. Follow- up echocardiography showed marked hemodynamic improvement, with peak and mean gradients reduced to 26 mmHg and 16 mmHg, respectively, and regression of aortic regurgitation to mild severity. No thromboembolic or hemorrhagic complications occurred, and the patient was discharged on optimized antithrombotic therapy consisting of warfarin combined with low-dose acetylsalicylic acid.

Discussion: This case highlights the importance of multimodality imaging in the mechanism-based management of obstructive mechanical aortic valve thrombosis. Beyond confirming obstruction, cinefluoroscopy and TEE provided critical insight into leaflet immobilization, thrombus morphology, and reversible functional aortic regurgitation, supporting differentiation between thrombus and pannus and guiding therapeutic decision-making. In carefully selected patients, low-dose, slow-infusion thrombolytic therapy represents an effective alternative to surgery. In the present case, therapeutic success was defined not only by

reduction in transprosthetic gradients but also by objective restoration of prosthetic valve physiology without hemorrhagic or embolic complications.
Conclusions: Multimodality imaging and effective low-dose thrombolytic therapy in selected patients with obstructive mechanical aortic valve thrombosis were essential for identifying a reversible thrombotic mechanism and achieving complete physiological restoration of prosthetic valve function while avoiding high-risk surgery.
Keywords: Mechanical Valve Thrombosis, Thrombolytic Therapy, Multimodality Imaging

OP-45.
Predictive Value of the Frontal QRS-T Angle for Coronary Thrombus Burden in Patients Presenting with Acute Myocardial Infarction

Yakup Han Yilmaz[1], Özge Turgay Yildirim[1], Mehmet Özgeyik[1]

1Department of Cardiology, Eskişehir City Hospital, Eskişehir, Türkiye

Objectives: Acute coronary syndrome (ACS) remains one of the leading causes of cardiovascular mortality worldwide. Intracoronary thrombus formation following plaque rupture plays a central role in the pathophysiology of ACS, and an increased thrombus burden is associated with adverse procedural outcomes such as no-reflow phenomenon, distal embolization, and procedural failure during percutaneous coronary intervention (PCI). Therefore, identifying simple, non-invasive, and readily available markers that can predict thrombus burden prior to coronary angiography is of significant clinical importance. The aim of this study was to investigate the predictive value of the frontal QRS-T angle (fQRSTa), calculated from admission electrocardiography (ECG), for angiographically assessed coronary thrombus burden in patients with acute myocardial infarction (AMI) undergoing primary PCI.

Methods: This retrospective, single-center observational study included 160 consecutive patients diagnosed with ST-segment elevation myocardial infarction (STEMI) or non-ST-segment elevation myocardial infarction (NSTEMI) who underwent primary PCI between June 2025 and December 2025. Twelve-lead ECGs obtained at admission were analyzed, and the frontal QRS-T angle was automatically calculated as the absolute difference between the QRS axis and T-wave axis. Angiographic thrombus burden was assessed using the TIMI thrombus grading system, and patients were categorized into low thrombus burden (grade 0–2) and high thrombus burden (grade 3–5) groups. Clinical, laboratory, angiographic, and electrocardiographic variables were compared between groups. Independent predictors of high thrombus burden were evaluated using multivariate logistic regression analysis. The predictive performance of fQRSTa was assessed by receiver operating characteristic (ROC) curve analysis.

Results: Of the study population, 67 (42%) patients were classified into the low thrombus burden group, while 93 (58%) patients had a high thrombus burden. Patients with high thrombus burden had significantly higher white blood cell counts (12.5±4.1 vs. 9.8±3.4 $\times 10^3/\mu L$; P=0.008) and a wider frontal QRS-T angle (68.2±30.4° vs. 43.2±28.6°; P<0.001). In multivariate logistic regression analysis, frontal QRS-T angle, SYNTAX score, and white blood cell count were identified as independent predictors of high thrombus burden. ROC analysis demonstrated that an fQRSTa cut-off value >44° predicted high thrombus burden with a sensitivity of 78.7% and a specificity of 54.7% in the overall population (AUC=0.655; P<0.001). Notably, the predictive value of fQRSTa was more pronounced in patients with NSTEMI.

Conclusions: The frontal QRS-T angle is an independent, non-invasive, and easily obtainable electrocardiographic parameter for predicting high coronary thrombus burden in patients presenting with acute myocardial infarction. Measurement of fQRSTa from a simple admission ECG may aid in pre-angiographic risk stratification and help guide interventional strategies during primary PCI.

Keywords: Acute Myocardial Infarction, Frontal QRS-T Angle, Coronary Thrombus Burden, Electrocardiography, Percutaneous Coronary Intervention

OP-46.
STEMI Caused by Thrombotic Subclavian Occlusion in LIMA Grafted Patient

Yasin Aktaş[1]

[1]*Department of Cardiology, Bursa City Hospital, Bursa, Türkiye*

Objectives: Subclavian steal syndrome (SSS) is characterized by reduced or reversed blood flow in the ipsilateral vertebral artery due to stenosis or occlusion of the proximal subclavian artery. In patients in whom the left internal mammary artery (LIMA) is used during coronary artery bypass grafting (CABG), this condition is defined as coronary–subclavian steal syndrome (CSSS) and may result in myocardial ischemia. While CSSS most commonly presents with exertional stable angina pectoris, presentation as an acute coronary syndrome (ACS) is rare. In particular, ST-segment elevation myocardial infarction (STEMI) caused by acute thrombotic occlusion of the subclavian artery has been reported in a very limited number of cases in the literature. In this case report, we present a rare CSSS case presenting with acute anterior STEMI secondary to thrombotic subclavian artery occlusion, together with its diagnostic, therapeutic, and clinical course.
Case Presentation: A 62-year-old male presented to the emergency department with sudden-onset severe chest pain accompanied by pain and numbness in the left arm. His medical history was notable for four-vessel CABG performed in 2020. Electrocardiography revealed significant ST-segment elevation in the anterior leads, and the patient was diagnosed with acute anterior STEMI. Emergency coronary angiography demonstrated complete occlusion of the left subclavian artery by a large thrombus at the level of the LIMA origin, distal to the vertebral artery takeoff (Figure 1). Attempts to access the LIMA graft using both femoral and left radial approaches were unsuccessful. Given the acute myocardial infarction setting and the high risk of complications such as distal embolization, cerebrovascular events, and graft loss associated with aggressive intervention, a limited endovascular strategy was adopted. Careful balloon dilatation using balloons of different diameters was performed at the thrombus site, resulting in partial restoration of distal flow. Following relief of chest pain, intensive antiplatelet and anticoagulant therapy was initiated. During follow-up, recurrent chest pain and reappearance of ST-segment elevations on electrocardiography prompted repeat coronary angiography, which revealed TIMI-2 flow in the distal subclavian artery and the LIMA graft (Figure 2).
Discussion: Proximal subclavian artery occlusion may lead to a wide spectrum of clinical manifestations, ranging from asymptomatic disease to upper extremity ischemia, vertebrobasilar insufficiency, and CSSS. In patients with a LIMA graft, acute thrombotic occlusion of the subclavian artery may cause a sudden reduction in myocardial perfusion through the graft, resulting in extensive myocardial ischemia. Presentation with STEMI is rare, and the diagnosis may be overlooked during standard STEMI management algorithms. In cases where no acute thrombotic lesion is identified in the native coronary arteries during angiography, subclavian artery pathology should be considered. Treatment strategies should be individualized according to hemodynamic status, thrombus burden, risk of cerebral embolization, and graft preservation. In selected patients, a combination of limited endovascular intervention and intensive medical therapy may be safer than more aggressive approaches.
Conclusions: Acute myocardial infarction secondary to thrombotic occlusion of the proximal subclavian artery in CABG patients with a LIMA graft is a rare but life-threatening condition. Early diagnosis, careful angiographic evaluation, and patient-tailored treatment strategies are crucial for improving clinical outcomes.
Keywords: Coronary Subclavian Steal Syndrome, ST-Segment Elevation Myocardial Infarction, Left Internal Mammary Artery

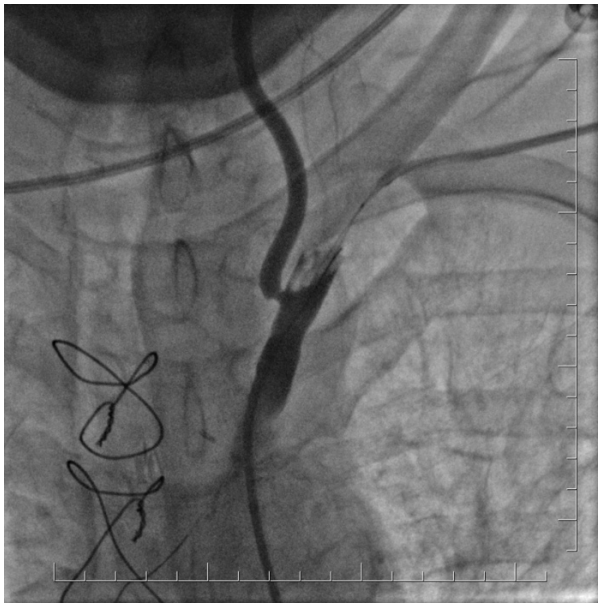

FIGURE 1. Subclavian thrombus.

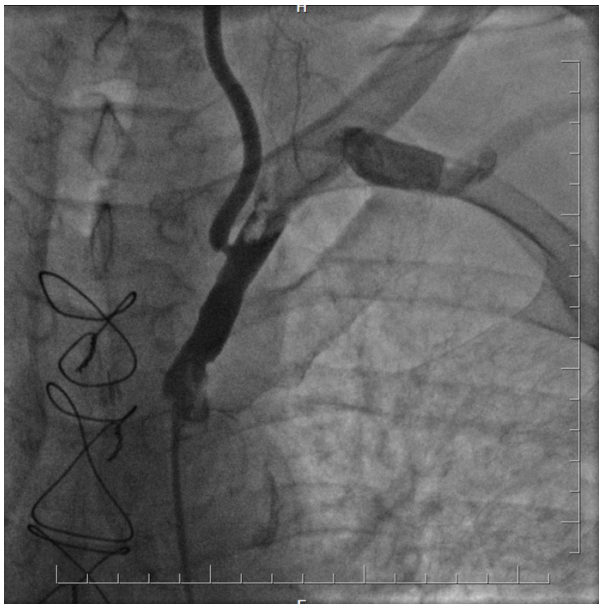

FIGURE 2. Subclavian thrombus 2.

OP-47.
Hemoptysis During Cardioverter-Defibrillator Implantation: A Rare Complication

Yasin Aktaş[1]

[1]*Department of Cardiology, Bursa City Hospital, Bursa, Türkiye*

Objectives: Implantation of cardiac pacemakers and implantable cardioverter-defibrillators (ICDs) has become increasingly common in the management of cardiovascular diseases. Despite advances in technique and operator experience, procedure-related complications may still occur, some of which can be life-threatening. Commonly reported complications include infection, hematoma, lead dislodgement, and pneumothorax. Pneumothorax related to subclavian vein puncture is a well-known complication. However, localized lung parenchymal injury and alveolar hemorrhage without pneumothorax are extremely rare. We present a case in which sudden hemoptysis during ICD implantation played a pivotal role in identifying a rare pulmonary complication.

Case Presentation: A 72-year-old male patient underwent percutaneous coronary intervention for an acute inferior myocardial infarction four months prior to presentation. Due to residual coronary lesions, coronary artery bypass grafting was planned. Three months after surgery, transthoracic echocardiography revealed a left ventricular ejection fraction of 30%, and primary prevention ICD implantation was indicated. The patient was asymptomatic at admission, with stable vital signs. After prophylactic antibiotic and analgesic administration, venous access via the subclavian vein was attempted following venography. The first three attempts were unsuccessful. Immediately after the fourth puncture attempt, the patient developed sudden and significant hemoptysis. Continuous monitoring was initiated, and supplemental oxygen was administered via nasal cannula. Oxygen saturation remained above 93%, and no hemodynamic instability occurred. As no additional acute complications were observed, ICD implantation was successfully completed, and the patient was transferred to the coronary intensive care unit. Bedside echocardiography excluded cardiac tamponade and pneumopericardium. A posteroanterior chest radiograph demonstrated increased opacity near the left apical region without clear evidence of pneumothorax. Due to ongoing hemoptysis, thoracic computed tomography was performed. CT imaging revealed a focal ground-glass opacity and infiltrative changes in the anterior segment of the left upper lobe, corresponding to the venous puncture site and consistent with localized lung parenchymal injury and alveolar hemorrhage. Serial hemoglobin measurements showed no significant decline, and bilateral pleural effusions were attributed to underlying heart failure. Conservative management with close clinical monitoring was adopted. Over the following days, hemoptysis gradually resolved, and follow-up imaging demonstrated marked regression of the pulmonary lesion. The patient was discharged without further complications.

Discussion: Complications during pacemaker or ICD implantation most commonly arise during venous access. The intrathoracic course of the subclavian vein increases the risk of pulmonary injury, particularly in cases requiring multiple puncture attempts. While pneumothorax is the most frequently recognized pulmonary complication, parenchymal lung injury without pneumothorax may occur and can be easily overlooked.

In this case, sudden hemoptysis during the procedure prompted immediate evaluation for potentially life-threatening conditions. Advanced imaging ruled out pneumothorax and hemothorax, allowing accurate diagnosis of alveolar hemorrhage. This emphasizes the importance of recognizing hemoptysis as a key clinical sign that may guide diagnostic decision-making.

Conclusions: Sudden hemoptysis during cardiac device implantation is an uncommon but clinically significant event. In addition to excluding pneumothorax, clinicians should consider localized lung parenchymal injury and alveolar hemorrhage even in the absence of radiographic pneumothorax. Prompt recognition and appropriate imaging enable effective conservative management and favorable outcomes.

Keywords: Hemoptysis, Implantable Cardioverter-Defibrillator, Alveolar Hemorrhage

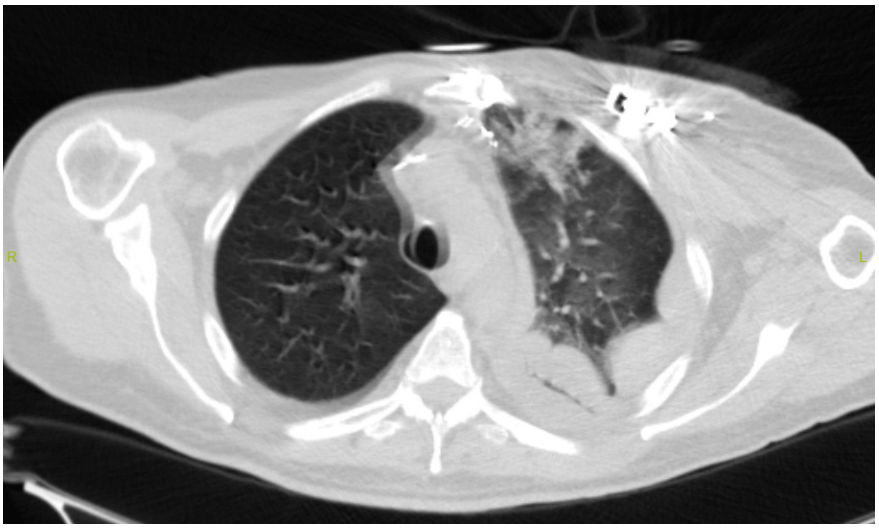

FIGURE 1. **Pulmonary injury.**

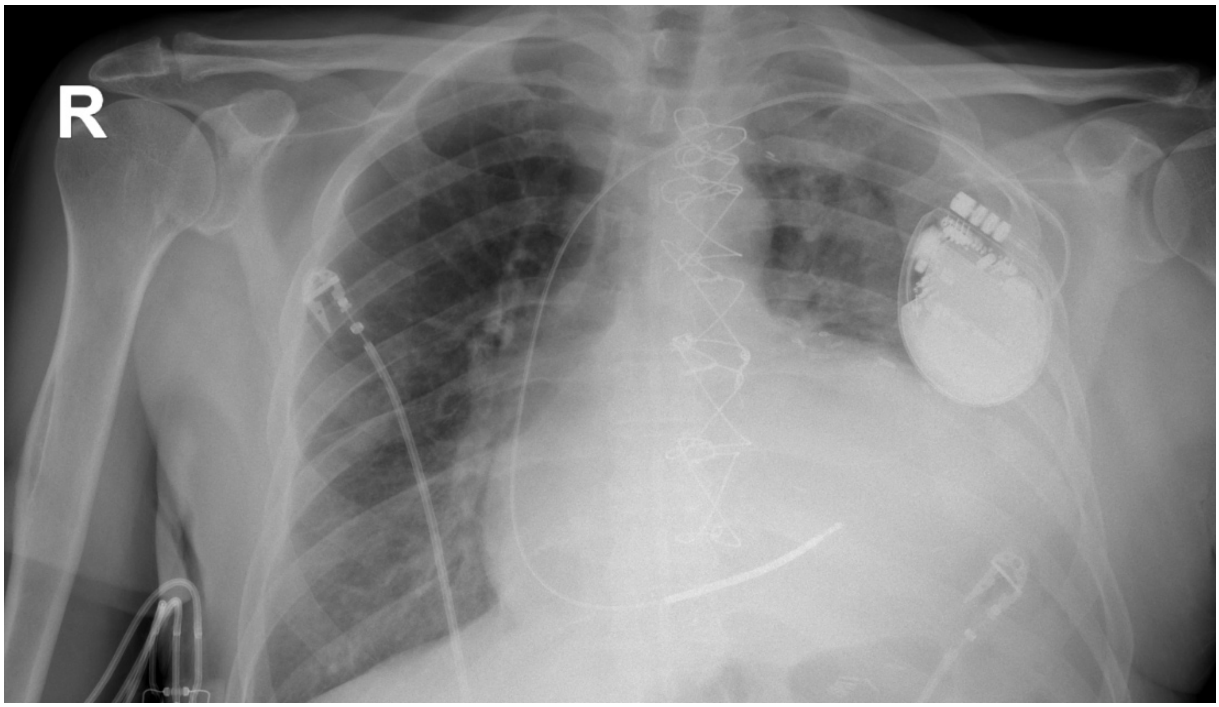

FIGURE 2. **Pulmonary injury.**

OP-48.
Intra-Arterial Lidocaine for Resistant Radial Artery Spasm

Yasin Aktaş[1]

[1]*Department of Cardiology, Bursa City Hospital, Bursa, Türkiye*

Objectives: The transradial approach is widely used for coronary angiography and interventions because it offers a low risk of bleeding, early mobilization, and improved patient comfort. Despite these advantages, radial artery spasm remains one of the most common complications associated with transradial procedures and may lead to prolonged procedural time, difficulty in catheter manipulation, and, in rare cases, serious clinical consequences. Current literature recommends intra-arterial nitrates and calcium channel blockers combined with adequate analgesia and sedation as the standard treatment for radial artery spasm. However, in some patients—particularly when the spasm extends into proximal arterial segments—these standard strategies may be insufficient, and alternative therapeutic approaches may be required. In this report, we present a case of diffuse radial/brachial artery spasm refractory to conventional therapy, successfully resolved with intra-arterial lidocaine administered via an alternative vascular route.

Case Presentation: A 47-year-old woman was admitted for elective diagnostic coronary angiography. The procedure was planned via the right radial artery. Prior to arterial puncture, local anesthesia was achieved with subcutaneous lidocaine infiltration, and a 5 French vascular sheath was inserted. Coronary angiography of the left and right coronary arteries was completed using Judkins catheters. During withdrawal of the right Judkins catheter, marked resistance was encountered, and the catheter could not be retrieved. The patient developed severe arm pain accompanied by agitation and hypotension. Intravenous atropine and midazolam were administered. After hemodynamic stabilization, intra-arterial nitroglycerin was delivered through the radial sheath; however, catheter retrieval remained unsuccessful. Consequently, access was obtained via the right femoral artery, and the right subclavian artery was cannulated. Angiography revealed severe and diffuse spasm extending from the axillary artery throughout the brachial artery, resulting in catheter entrapment (Figure 1). External local warming was applied along the brachial artery. Additional treatment included intra-arterial nitroglycerin and diltiazem administered toward the brachial artery via the subclavian route, together with intravenous morphine and midazolam. Despite these comprehensive measures, catheter removal was still unsuccessful. Before proceeding to general anesthesia or surgical intervention, intra-arterial lidocaine was considered as a final option. A total dose of 40 mg of 2% lidocaine was administered into the right subclavian artery via the femoral catheter. Following lidocaine administration, catheter resistance markedly decreased, allowing slow and controlled withdrawal (Figure 2). The procedure was completed successfully, and the patient was discharged without complications.

Discussion and Conclusions: Radial artery spasm is primarily related to mechanical irritation, catheter manipulation, and increased sympathetic activity triggered by pain and anxiety. Diffuse spasm involving the axillary and brachial arteries and refractory to standard vasodilator therapy is uncommon and poses a significant management challenge. Lidocaine, through its potent analgesic properties and suppression of peripheral sympathetic nerve transmission, may interrupt the spasm–pain–sympathetic activation cycle, leading to indirect vasodilation. This case suggests that intra-arterial lidocaine may serve as an effective and safe rescue therapy in selected patients, potentially avoiding surgical intervention or general anesthesia.

Keywords: Radial Artery Spasm, Transradial Angiography, Lidocaine

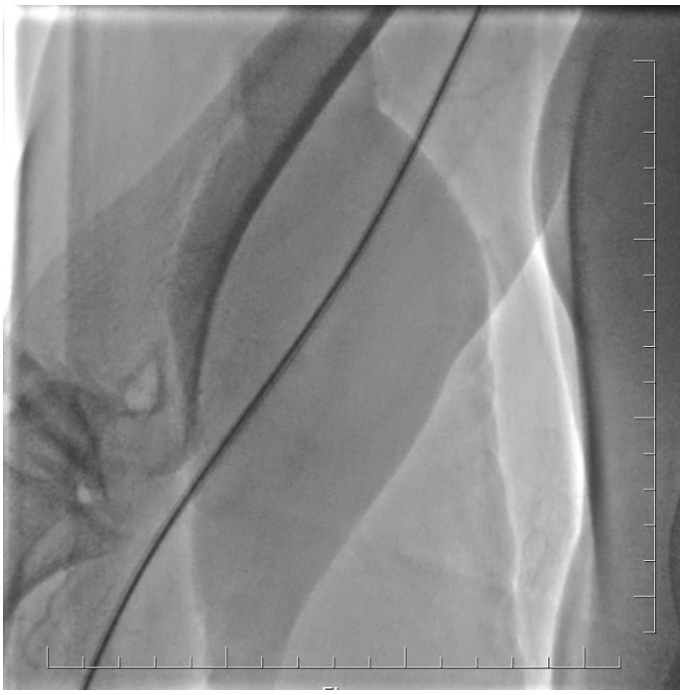

FIGURE 1. **Complete entanglement of the catheter by the brachial artery due to spasm.**

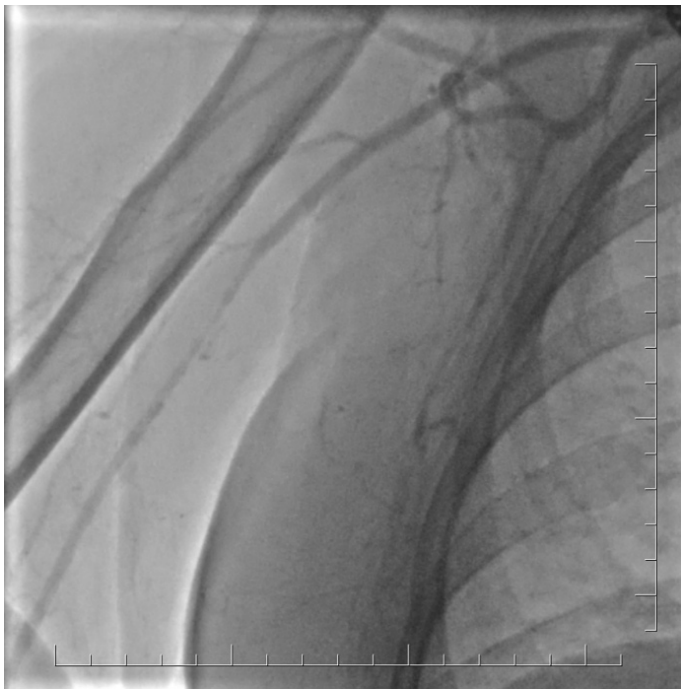

FIGURE 2. **Image after catheter removal.**

OP-49.
Routine Clinical and Lipid Parameters Predict High-Grade Atrioventricular Block After Transcatheter Aortic Valve Implantation: A Pragmatic Single-Center Study

Aykan Çelik[1], Sefa İnce[2], Mert Şentürkün[2]

[1]Department of Cardiology, Atatürk Training and Research Hospital, İzmir, Türkiye; [2]Department of Cardiology, Katip Çelebi University, Faculty of Medicine, Atatürk Training and Research Hospital, İzmir, Türkiye

Objectives: High-grade atrioventricular block (AVB) is one of the most frequent conduction disturbances following transcatheter aortic valve implantation (TAVI), and often necessitates permanent pacemaker implantation. Previous studies have mainly focused on procedural and anatomical predictors such as baseline conduction abnormalities, implantation depth, and valve type. However, these parameters are not routinely available in all centers and may vary considerably across institutions. The identification of universally accessible predictors may improve real-world risk stratification. This study aimed to evaluate whether routinely available clinical, echocardiographic, and biochemical parameters could predict the development of high-grade AVB within 30 days after TAVI.

Methods: This retrospective single-center study included 376 consecutive patients who underwent TAVI between January 2017 and December 2023. Patients were categorized according to the occurrence of high-grade AVB within 30 days of the procedure. Demographic characteristics, comorbidities, baseline laboratory parameters, and echocardiographic findings were obtained from the electronic medical records. Categorical variables were compared using the chi-square test and continuous variables were compared using the independent samples t-test. Variables with a P-value <0.10 in univariate logistic regression were entered into a multivariate logistic regression model. Statistical significance was defined as p <0.05. The baseline characteristics, laboratory findings, echocardiographic parameters, and regression analyses are presented in Tables 1–4.

Results: High-grade AVB occurred in 55 (14.6%) patients. Patients who developed AVB had higher rates of hypertension (81.8% vs. 64.2%, P=0.010), diabetes mellitus (45.5% vs. 31.2%, P=0.037), and smoking history (7.3% vs. 2.2%, P=0.038) (Table 1). Echocardiographic evaluation demonstrated significantly higher mean and peak aortic valve gradients in the AVB group (mean gradient: 48.96±12.87 vs. 44.78±14.02 mmHg, P=0.039; peak gradient: 79.8±19.9 vs. 73.5±21.0 mmHg, P=0.041) (Table 3). Total cholesterol and low-density lipoprotein cholesterol levels were also significantly higher in the patients who developed AVB (Table 2). Inflammatory indices, including the systemic immune-inflammation index, neutrophil-to-lymphocyte ratio, platelet-to-lymphocyte ratio, and lymphocyte-to-monocyte ratio, did not differ between groups. In multivariate analysis, hypertension (odds ratio [OR] 2.15, 95% confidence interval [CI] 1.01–4.55, P=0.047) and total cholesterol (OR 1.007 per mg/dL, 95% CI 1.002–1.013, P=0.010) emerged as independent predictors of high-grade AVB (Table 4).

Discussion: Our findings suggest that hypertension and elevated total cholesterol—two routinely assessed clinical parameters—are independently associated with high-grade AVB after TAVI. These factors may reflect chronic vascular and myocardial remodeling, potentially increasing vulnerability of the cardiac conduction system. Incorporating such readily available parameters into preprocedural evaluation may help identify patients at higher risk and guide closer postprocedural rhythm monitoring.

Conclusions: Hypertension and elevated total cholesterol were independently associated with the development of high-grade atrioventricular block after TAVI. These routinely available parameters may help identify patients at increased risk and guide closer postprocedural rhythm monitoring.

Keywords: Transcatheter Aortic Valve Implantation, Atrioventricular Block, Hypertension, Cholesterol

TABLE 1. Demographic and Clinical Characteristics of Patients by High-Grade Atrioventricular Block Status

Characteristics	AVB – (n=321)	AVB + (n=55)	P-value
Age (years)	76.37±8.12	77.78±7.39	0.228
Gender (female)	159 (49.5%)	31 (56.4%)	0.349
DM	100 (31.2%)	25 (45.5%)	0.037
HT	206 (64.2%)	45 (81.8%)	0.010
Dyslipidemia	88 (27.4%)	11 (20%)	0.249
Smoking	7 (2.2%)	4 (7.3%)	0.038
CAD	271 (84.4%)	45 (81.8%)	0.626
History of heart valve surgery	10 (3.1%)	2 (3.6%)	0.839
Heart failure	72 (22.4%)	6 (10.9%)	0.052
Previous stroke	23 (7.2%)	2 (3.6%)	0.332
CKD	86 (26.8%)	16 (29.1%)	0.723
GFR (mL/min)	59.30±18.75	60.38±18.65	0.691
LDL (mg/dL)	99.75±36.42	113.72±47.35	0.041
HDL (mg/dL)	44.84±12.44	42.56±11.10	0.204
TG (mg/dL)	121.32±95.09	161.18±183.73	0.121
Cholesterol (mg/dL)	167.81±48.14	187.63±58.57	0.007
WBC (10^3/uL)	7.40±2.38	7.73±2.50	0.357
PLT (10^3/uL)	221.36±83.65	201.05±79.53	0.095
HG (g/dL)	11.87±1.73	11.19±1.94	0.691
NEU (10^3/uL)	6.10±2.87	6.49±2.70	0.348
LYM (10^3/uL)	1.40±0.64	1.50±1.14	0.506
MONO (10^3/uL)	0.74±1.81	0.70±0.25	0.899
SII	1145±895	1091±815	0.680
NLR	5.51±4.61	5.58±3.43	0.925
PLR	182.98±95.62	169.93±98.67	0.352
LMR	2.43±1.43	2.28±1.23	0.463
LVEF (%)	53.47±10.88	55.01±10.85	0.330
Aort mean gradient (mmHg)	44.78±14.02	48.96±12.87	0.039

Data are shown as mean±standard deviation or n (%) where appropriate. DM, diabetes mellitus; HT, hypertension; CAD, coronary artery disease; CKD, chronic kidney disease; GFR, glomerular filtration rate; LDL, low density lipoprotein; HDL, high density lipoprotein; TG, triglyceride; WBC, white blood cell; PLT, platelet; Hg, hemoglobin; NEU, neutrophile; LYM, lymphocyte; Mono, monocyte; SII, systemic immune inflammation index; NLR, neutrophil-to-lymphocyte ratio; PLR, platelet-to-lymphocyte ratio; LMR, lymphocyte-to-monocyte ratio; LVEF, left ventricular ejection fraction.

TABLE 2. Baseline Laboratory Parameters of Patients by High-Grade Atrioventricular Block Status

Characteristics	AVB – (n=321)	AVB + (n=55)	P-value
Creatine (mg/dL)	1.13±0.66	1.21±0.93	0.494
GFR (mL/min)	59.30±18.75	60.38±18.65	0.691
AST (U/L)	23.05±15.30	26.97±23.80	0.243
ALT (U/L)	16.78±16.57	26.35±44.57	0.121
LDL (mg/dL)	99.75±36.42	113.72±47.35	0.041
HDL (mg/dL)	44.84±12.44	42.56±11.10	0.204
TG (mg/dL)	121.32±95.09	161.18±183.73	0.121
Cholesterol (mg/dL)	167.81±48.14	187.63±58.57	0.007
WBC (10^3/uL)	7.40±2.38	7.73±2.50	0.357
PLT (10^3/uL)	221.36±83.65	201.05±79.53	0.095
HG (g/dL)	11.87±1.73	11.19±1.94	0.691
NEU (10^3/uL)	6.10±2.87	6.49±2.70	0.348
LYM (10^3/uL)	1.40±0.64	1.50±1.14	0.506
MONO (10^3/uL)	0.74±1.81	0.70±0.25	0.899
SII	1145±895	1091±815	0.680
NLR	5.51±4.61	5.58±3.43	0.925
PLR	182.98±95.62	169.93±98.67	0.352
LMR	2.43±1.43	2.28±1.23	0.463

Data are shown as mean±standard deviation. GFR, glomerular filtration rate; AST, aspartate aminotransferase; ALT, alanine transaminase; LDL, low density lipoprotein; HDL, high density lipoprotein; TG, triglyceride; WBC, white blood cell; PLT, platelet; Hg, hemoglobin; NEU, neutrophile; LYM, lymphocyte; Mono, monocyte; SII, systemic immune inflammation index; NLR, neutrophil-to-lymphocyte ratio; PLR, platelet-to-lymphocyte ratio; LMR, lymphocyte-to-monocyte ratio.

TABLE 3. Echocardiographic Characteristics of Patients by High-Grade Atrioventricular Block Status

Characteristics	AVB – (n=321)	AVB + (n=55)	P-value
LVEF (%)	53.47±10.88	55.01±10.85	0.330
Aort peak gradient (mmHg)	73.53±21.04	79.80±19.86	0.041
Aort mean gradient (mmHg)	44.78±14.02	48.96±12.87	0.039
BAV, n (%)	51 (15.9%)	7 (12.7%)	0.549
AR, n (%)			0.625
Mild	213 (66.4%)	41 (74.5)	
Moderate	66 (20.6%)	8 (14.5%)	
Severe	4 (1.2%)	1 (1.8%)	
MR, n (%)			0.138
Mild	195 (60.7%)	33 (60%)	
Moderate	107 (33.3%)	16 (29.1%)	
Severe	10 (3.1%)	1 (1.8%)	
LA (mm)	44.12±6.75	43.85±6.24	0.786
sPAP (mmHg)	38.62±12.62	38.85±13.12	0.902

Data are shown as mean±standard deviation or n (%) where appropriate. LVEF, left ventricular ejection fraction; BAV, bicuspid aortic valve; AR, aortic regurgitation; MR, mitral regurgitation; LA, left atrium; sPAP, systolic pulmonary artery pressure.

TABLE 4. Univariate and Multivariate Logistic Regression Results for High-Grade Atrioventricular Block

	Univariate			Multivariate		
Variable	**OR**	**95% CI**	**P-value**	**OR**	**95% CI**	**P-value**
Diabetes Mellitus	1.84	1.30 – 3.30	**0.039**	1.64	0.89 – 3.03	0.116
Hypertension	2.51	1.22 – 5.18	**0.012**	2.15	1.012 – 4.55	**0.047**
Smoking	5.19	1.00 – 12.45	0.051	3.35	0.882 – 12.74	0.076
Cholesterol	1.007	1.002 – 1.013	**0.008**	1.007	1.002 – 1.013	0.010

OR, odds ratio; CI, confidence interval.
Statistically significant P-values are shown in bold.

OP-50.
CONUT Score and Length of Hospital Stay in Acute Decompensated Heart Failure

Meltem Altinsoy[1], Çağatay Tunca[1]

[1]*Department of Cardiology, Ankara Etlik City Hospital, Ankara, Türkiye*

Objectives: Acute decompensated heart failure (ADHF) is a leading cause of hospitalization and is associated with substantial morbidity and healthcare resource utilization. Length of hospital stay (LOS) is a clinically relevant in-hospital outcome reflecting disease severity and response to treatment. Nutritional status plays a key role in heart failure pathophysiology and may influence recovery during hospitalization. The Controlling Nutritional Status (CONUT) score, derived from serum albumin, total lymphocyte count, and total cholesterol levels, provides an objective assessment of nutritional and immune status. However, evidence regarding the relationship between admission CONUT score and hospital LOS in ADHF is limited. To evaluate whether the admission CONUT score predicts hospital length of stay and prolonged hospitalization in patients admitted with acute decompensated heart failure.

Methods: This retrospective, single-center study included consecutive patients hospitalized with ADHF between January 2024 and March 2025. The CONUT score was calculated using laboratory parameters obtained within the first 24 hours of admission. Patients were classified into low (CONUT 0–4) and high (CONUT ≥5) nutritional risk groups. The primary outcome was hospital length of stay, analyzed as both a continuous variable and as prolonged hospitalization, defined as a length of stay of ≥7 days. Multivariable regression analyses were performed to identify independent predictors of prolonged hospitalization. Receiver operating characteristic (ROC) curve analysis assessed the discriminative ability of the CONUT score.

Results: A total of 300 patients with ADHF were analyzed. The median hospital length of stay was 6 days (interquartile range 4–9 days). Patients with high CONUT scores experienced significantly longer hospital stays compared with those with low CONUT scores, and prolonged hospitalization occurred more frequently in the high CONUT group (Table 1). After adjustment for age, renal function, systolic blood pressure at admission, left ventricular ejection fraction, and natriuretic peptide levels, high CONUT score remained independently associated with prolonged hospitalization (Table 2). ROC analysis demonstrated fair discriminatory performance of the admission CONUT score for predicting prolonged LOS, with an area under the curve of approximately 0.72 (Figure 1).

Discussion: This study demonstrates that the admission CONUT score is independently associated with hospital length of stay in patients hospitalized with acute decompensated heart failure. Patients with higher CONUT scores experienced longer hospitalization and a greater likelihood of prolonged hospital stay, even after adjustment for major clinical covariates.

Malnutrition and immune-inflammatory dysregulation are common in heart failure and may delay recovery during acute decompensation. As the CONUT score incorporates serum albumin, lymphocyte count, and total cholesterol, it reflects both nutritional and inflammatory status and may identify a vulnerable patient subgroup. ROC analysis showed a modest but significant ability of CONUT to discriminate prolonged hospitalization, supporting its role as a complementary risk stratification tool.

Conclusions: The admission CONUT score is a simple and readily available predictor of hospital length of stay in patients hospitalized with acute decompensated heart failure. Early identification of patients at risk for prolonged hospitalization using CONUT may support optimized in-hospital management and resource utilization.

Keywords: Conut Score, Heart Failure, Malnutrition

TABLE 1. Baseline Characteristics According to CONUT Score

Parameter	Low CONUT (0–4)	High CONUT (≥5)	P-value
Age (years)	66±11	72±10	**<0.001**
Male sex (%)	63	68	0.39
Body mass index (kg/m²)	27.1±4.3	24.8±4.1	**0.002**
Hypertension (%)	61	74	**0.03**
Diabetes mellitus (%)	34	48	**0.04**
Chronic kidney disease (%)	22	41	**0.002**
Atrial fibrillation (%)	29	47	**0.006**
Ischemic etiology (%)	52	69	**0.01**
Prior HF hospitalization (%)	38	59	**0.004**
NYHA class III–IV (%)	46	71	**<0.001**
Systolic BP at admission (mmHg)	128±21	115±19	**<0.001**
Heart rate (bpm)	82±15	90±17	**0.01**
Hemoglobin (g/dL)	13.2±1.8	11.8±1.9	**<0.001**
White blood cell count (×10⁹/L)	8.1±2.4	9.3±2.7	**0.01**
Total lymphocyte count (×10⁹/L)	1.9±0.6	1.2±0.4	**<0.001**
Platelet count (×10⁹/L)	238±64	214±58	**0.02**
Albumin (g/L)	37±4	31±5	**<0.001**
Total cholesterol (mg/dL)	182±36	146±31	**<0.001**
Creatinine (mg/dL)	1.1±0.4	1.6±0.6	**<0.001**
eGFR (mL/min/1.73m²)	68±21	46±18	**<0.001**
Sodium (mmol/L)	138±4	134±5	**<0.001**
CRP (mg/L)	9 (4–18)	32 (18–65)	**<0.001**
NT-proBNP (pg/mL)	3200 (1600–6100)	7600 (4100–12200)	**<0.001**
Left ventricular EF (%)	31±6	26±7	**<0.001**
LVEDD (mm)	60±7	64±8	**0.01**
Moderate–severe MR (%)	28	46	**0.01**
TAPSE (mm)	18.1±3.4	15.9±3.2	**0.002**
sPAP (mmHg)	38±12	47±15	**0.001**
ACEi/ARB or ARNI use (%)	86	69	**0.003**
Beta-blocker use (%)	88	83	0.29
MRA use (%)	62	57	0.48
SGLT2 inhibitor use (%)	24	18	0.33
IV loop diuretic dose (mg)	40 (20–80)	80 (40–120)	**<0.001**
ICU admission (%)	9	22	**0.005**
Length of stay (days)	5 (4–7)	9 (6–13)	**<0.001**
Prolonged LOS ≥7 days (%)	28	56	**<0.001**

Data are shown as mean±standard deviation or percent or median (interquartile range) where appropriate. CONUT, controlling nutritional status; eGFR, estimated glomerular filtration rate; CRP, C-reactive protein, LVEDD, left ventricular end-diastolic diameter; MR, mitral regurgitation; TAPSE, tricuspid annular plane systolic excursion; sPAP, systolic pulmonary artery pressure; MRA, magnetic rezonance angiography; SGLT2, sodium-glucose co-transporter 2; IV, intravenous; ICU, intensive care unit; LOS, length of stay. Statistically significant P-values are shown in bold.

TABLE 2. Regression Analyses for Prolonged Hospital Stay (≥7 days)

Variable	Univariable OR (95% CI)	P	Multivariable OR (95% CI)	P-value
Age (per year)	1.03 (1.01–1.05)	0.004	1.02 (1.00–1.04)	**0.04**
Chronic kidney disease	2.21 (1.39–3.50)	0.001	1.61 (0.98–2.66)	**0.06**
NYHA class III–IV	2.84 (1.78–4.53)	<0.001	2.02 (1.21–3.36)	**0.007**
Systolic BP (per 10 mmHg ↓)	1.28 (1.10–1.50)	0.001	1.19 (1.01–1.40)	**0.04**
LVEF (per 5% ↓)	1.34 (1.12–1.61)	0.001	1.22 (1.01–1.48)	**0.04**
NT-proBNP (log)	1.41 (1.19–1.67)	<0.001	1.26 (1.03–1.55)	**0.02**
High CONUT (≥5)	3.25 (2.01–5.25)	<0.001	2.18 (1.29–3.68)	**0.003**

NYHA, New York Heart Association; LVEF, left ventricular ejection fraction; NT-proBNP, N-terminal pro-B-type natriuretic peptide; CONUT, controlling nutritional status. Statistically significant P-values are shown in bold.

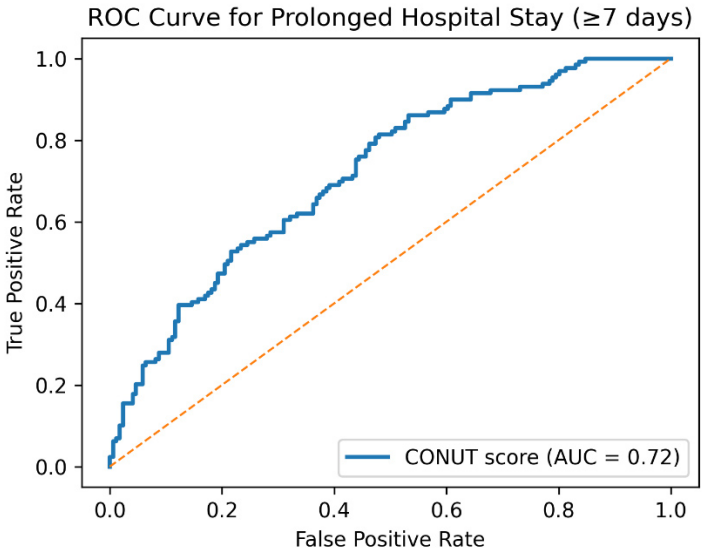

FIGURE 1. ROC curve for prolonged hospital stay (≥7 days).

OP-51.
Distinction Between Type 2 Myocardial Infarction and Myocardial Injury in Troponin Positivity: Retrospective Clinical Classification and 30-Day Prognosis

Muhammet Geneş[1]

[1]*Department of Cardiology, Sincan Training and Research Hospital, Ankara, Turkiye*

Objectives: To determine the distribution of Type 2 myocardial infarction (T2MI) and myocardial injury according to the 4th Universal Definition in patients with high-sensitivity cardiac troponin (hs-cTn) positivity and to compare their 30-day short-term outcomes.
Methods: In a single-center retrospective cohort, consecutive patients aged ≥18 years with at least one hs-cTn value above the 99th percentile upper reference limit upon admission to the emergency department or internal medicine/cardiology wards were screened. Type 1 MI/STEMI, acute myocarditis/pericarditis, isolated troponin elevation following major trauma/CPR, and missing data (lack of serial troponin measurements or insufficient ECG/clinical records) were excluded. Classification was performed according to the 4th Universal Definition: acute myocardial injury was defined by a rise/fall pattern in serial hs-cTn measurements; T2MI was defined as acute injury plus evidence of ischemia (ischemic symptoms, new ischemic ECG changes, or new regional wall motion abnormality on imaging) and a clinical context consistent with supply-demand imbalance. Patients without evidence of ischemia were classified as myocardial injury. The primary outcome was 30-day all-cause mortality; secondary outcomes were 30-day readmission (emergency/ward) and length of stay (LOS). Categorical variables were compared using Fisher's exact/chi-square tests, and continuous variables using the Mann–Whitney U test. Additionally, exploratory multivariate logistic regression for mortality was reported.
Results: Out of 237 troponin-positive admissions, 185 patients were included in the analysis after exclusions: T2MI 67 (36.2%) and myocardial injury 118 (63.8%). The most common triggers in T2MI were tachyarrhythmia (28%), severe anemia/bleeding (17%), and hypertensive emergency (14%). In myocardial injury, sepsis/infection (31%) and acute respiratory failure (19%) were more frequent. While 30-day mortality was 14/118 (11.9%) in myocardial injury and 5/67 (7.5%) in T2MI (RR 1.59, 95% CI 0.60–4.22; Fisher P=0.453), 30-day readmission was observed as 12/67 (17.9%) in T2MI and 16/118 (13.6%) in myocardial injury (RR 1.32, 95% CI 0.67–2.62; P=0.523). LOS was significantly longer in the myocardial injury group [median 7 (4–11) days vs 5 (3–9) days; P<0.001]. In exploratory multivariate analysis, age, sepsis, chronic kidney disease (CKD), and peak hs-cTn (log) were associated with 30-day mortality; the myocardial injury class maintained its association with mortality compared to T2MI (aOR 1.46, 95% CI 1.01–2.12).
Conclusions: In troponin-positive patients, myocardial injury is more frequent than T2MI and is associated with a longer length of stay. Although crude comparisons of 30-day mortality and readmission rates did not show significant differences between groups, myocardial injury may be associated with higher mortality in multivariate analysis. Structured classification based on the 4th Universal Definition at the emergency/ward level may standardize clinical communication and support close post-discharge follow-up strategies in high-risk cases.
Keywords: High-Sensitivity Troponin, Type 2 Myocardial Infarction, Myocardial Injury, Retrospective Classification, 30-Day Mortality.

OP-52.
Myocardial Contraction Fraction as an Independent Predictor of Cardiovascular Mortality in Patients with Chronic Renal Failure

Oğuz Kağan Şentürk[1], İrem Erdoğan Şentürk[1], Selvi Öztaş[1], Selma Kenar Tiryakioğlu[1], Mehmet Usta[2]

[1]Department of Cardiology, Bursa City Hospital, Bursa, Türkiye; [2]Department of Nephrology, Bursa City Hospital, Bursa, Türkiye

Objectives: In chronic renal failure, cardiovascular mortality is the main determinant of overall mortality, and early and accurate assessment of cardiac function is critically important for clinical management. The reliability of measuring the ventricular ejection fraction for assessing myocardial performance in this patient group is limited because it can be frequently affected by volume load and hemodynamic variability. The myocardial contraction fraction (MCF) is an index obtained by dividing the stroke volume by the myocardial volume. This parameter has been specifically tested in those with diseases characterized by pathological left ventricular hypertrophy, such as amyloidosis and severe aortic stenosis. However, this parameter has never been studied before in patients with chronic renal failure. In this study, we aimed to test the prognostic and clinical value of the myocardial contraction fraction by comparing it with the left ventricular EF and global ventricular strain (GLS) parameters.

Methods: We prospectively analyzed 46 patients diagnosed with chronic renal failure undergoing renal replacement therapy at our center from 2020-2025. Clinical parameters and survival rated were assessed based on a consistent follow-up duration 56 months

Results: A total of 46 patients were included in the study. These patients were followed up for approximately 56 months. Patients were divided into two groups: non-survivors and survivors. While no significant difference was observed in the left ventricular EF between the two groups (51.45±7.11 vs. 52.75±6.10, P=0.619), the MCF was significantly lower in those who died than in those who survived (18.95±7.09 vs. 29.69±12.86, P=0.038). This significant difference was detected both clinically and statistically. In addition, the left ventricular GLS was significantly lower in those who died than in those who survived (13.42±2.38 vs. 16.04± 3.04, P=0.037). On logistic regression analysis, both the MCF and GLS were identified as independent predictors of mortality. In addition, the results of the ROC curve analyses revealed that the MCF was strongly able to predict mortality (AUC: 0.853). Compared with that of the MCF, the ability of the GLS to predict mortality was relatively limited (AUC: 0.740).

Discussion: The present study demonstrated that MCF, when evaluated in conjunction with GLS, serves as a significant predictor of mortality,in contrast to LVEF. In patient groups with severe limitations in EF, especially those with pathalogical left ventricular hypertrophy, GLS and, in addition MCF provide added value in clinical risk stratification compared to traditional EF-based assesment .

Conclusions: In conclusion, the MCF is a more sensitive marker than LVEF for assessing cardiac performance in patients with chronic kidney disease undergoing renal replacement therapy. Our findings suggest that MCF serves as a robust predictor of mortality in this high-risk patient population. Larger-scale studies will more clearly establish the role of the MCF in routine cardiac assessment.

Keywords: Myocardial Contraction Fraction, Renal Replacement Therapy, Mortality, Predictors of Mortality

OP-53.
Surgical Stentectomy and Bypass in Coronary Full Metal Jacket

Demir Çetintaş[1]

[1]*Department of Cardivascular Surgery, Bursa City Hospital, Bursa, Türkiye*

Objectives: To evaluate whether stentectomy combined with coronary artery bypass grafting (CABG) is a feasible treatment option in patients with a coronary "full metal jacket," defined as overlapping stent implantation covering at least 60 mm of a coronary artery segment. Patients with a coronary full metal jacket who had coronary ischemia refractory to optimal medical therapy and in whom repeat percutaneous coronary intervention (PCI) with balloon angioplasty or stenting could not be performed due to patient refusal, anatomical unsuitability, or inability to cross the lesion were treated surgically with stentectomy and CABG.
Case Presentation: A 70-year-old male patient had a full metal jacket in the left anterior descending artery (LAD), created by multiple stents implanted at different times from the proximal LAD to the apex. The patient re-presented with acute myocardial infarction, and repeat balloon angioplasty and stenting were recommended; however, the patient declined. After surgical consultation elsewhere, the patient was considered inoperable. Upon admission to our clinic, he had intermittent chest pain, with fluctuating troponin levels between 200 and 300. Coronary angiography revealed a diminutive right coronary artery, no significant lesions in the circumflex artery, a critical proximal stenosis in the diagonal branch, and a full metal jacket in the LAD with 95–99% proximal stenosis and multiple in-stent stenoses along its course (Figures 1 and 2). After obtaining informed consent, median sternotomy was performed. The saphenous vein was harvested using the no-touch technique. On the beating heart, a longitudinal arteriotomy of approximately 6 cm was performed along the stented LAD segment, and the stents were excised via open endarterectomy. The arteriotomy was closed with a saphenous vein patch. A saphenous vein bypass graft was then placed to the diagonal branch. Under partial aortic clamping, the diagonal graft was anastomosed to the aorta, and the LAD graft was anastomosed end-to-side to the diagonal graft, creating a composite Y-graft configuration (Figures 3 and 4). The patient was transferred to the cardiovascular intensive care unit postoperatively.
Discussion: Since the first description of the full metal jacket by Fischman et al. in 1989, the use of multiple overlapping stents has increased, particularly in complex lesions and acute myocardial infarction. Although repeat PCI is often preferred in patients with a full metal jacket who are refractory to medical therapy, patient preference, anatomical limitations, and failed interventions may necessitate surgical alternatives. Within the framework of "lifetime management" of coronary artery disease, future treatment options should be carefully considered. Surgery and PCI should be regarded as complementary rather than competing strategies.
Conclusions: In patients with coronary full metal jackets and ischemia resistant to medical therapy, surgical stentectomy combined with CABG is an effective and viable treatment option.
Keywords: Full Metal Jacket, Endarterectomy, Coronary Artery Bypass Grafting

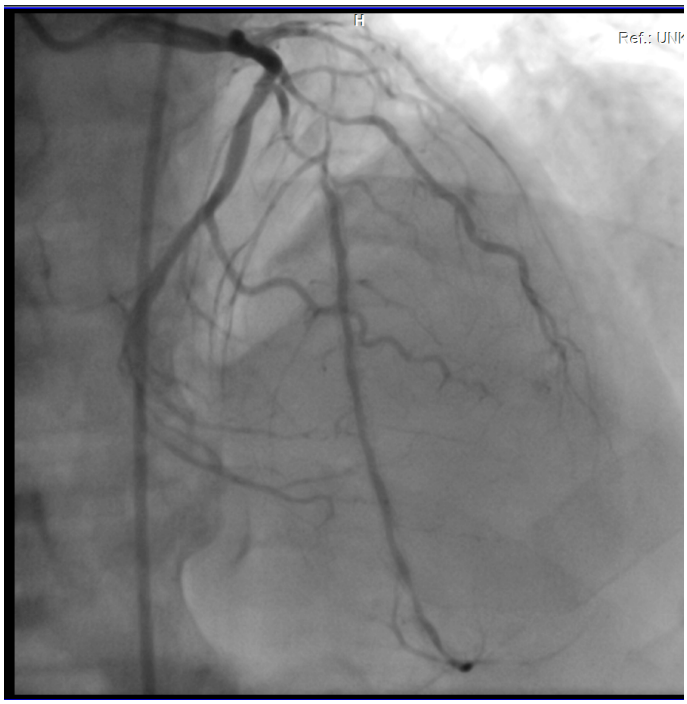

FIGURE 1. Coronary angiographic image of the patient.

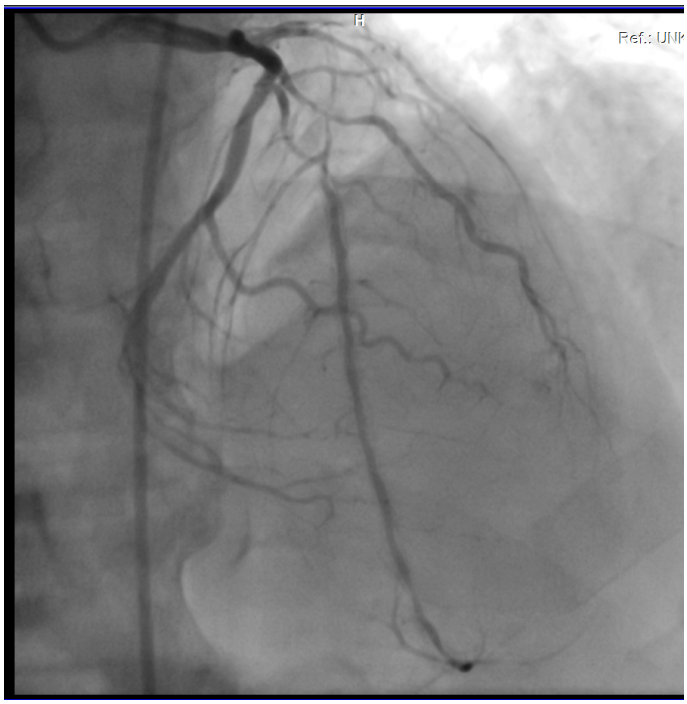

FIGURE 2. Coronary angiographic image of the patient.

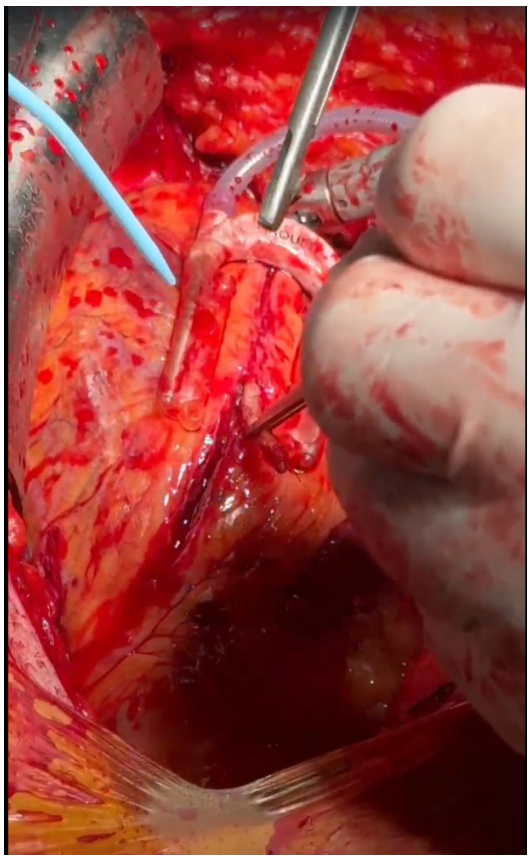

FIGURE 3. Operative image of the patient's surgical procedure.

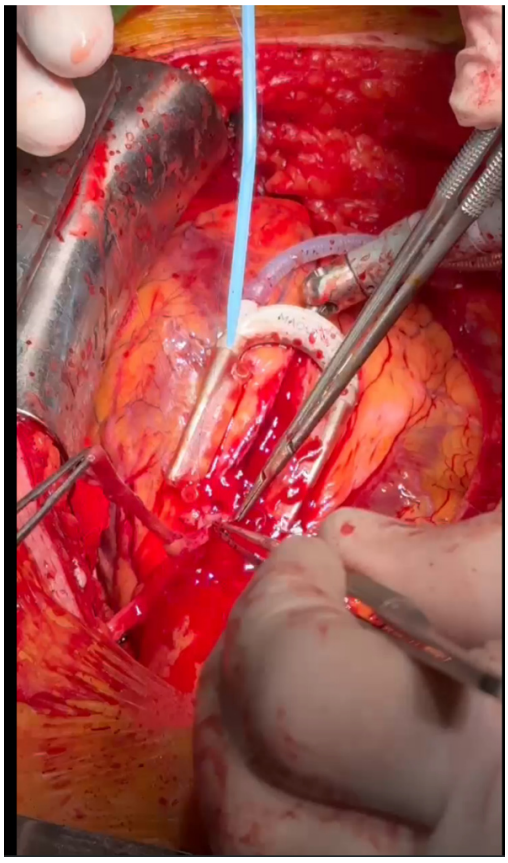

FIGURE 4. Operative image of the patient's surgical procedure.

OP-54.
AF-Ablation Performed via Transeptal Passage Through Septal Occuder Device: A Case Report.

Mustafa Karaca[1], Semih Babacan[1], Fahrettin Tuğrul Çitekçi[1], Hüseyin Sefa İnce[1]

[1]Department of Cardiology, Katip Çelebi University, İzmir Atatürk Training and Research Hospital, İzmir, Türkiye

Objectives: Atrial Septal Defect (ASD) is a common congenital heart disease often associated with late-stage complications such as atrial fibrillation (AF). While percutaneous closure is the gold standard for ASD, the presence of an occluder device complicates subsequent left-sided interventions requiring transseptal access.
Case Presentation: A 50-year-old male, who underwent percutaneous ASD closure with a 34 mm Abbott Amplatzer device in 2017, presented with symptomatic AF refractory to medical therapy. Transesophageal echocardiography confirmed a stable device with no thrombus. During the electrophysiology study, initial transseptal puncture through the inferior portion of the device using a Brockenbrough needle was unsuccessful. Access was eventually achieved using a floppy guidewire through the device fabric (Figure 1), followed by sequential balloon dilatation (PTCA and peripheral balloons) (Figure 2). A PolarX Cryoballoon catheter was then advanced through the device, and successful isolation of all four pulmonary veins was achieved (Figure 3). The patient was discharged in sinus rhythm with no residual shunt or complications (Figure 4). At the 2-month follow-up, sinus rhythm was maintained.
Conclusions: AF ablation in patients with a prior ASD occluder is technically challenging but feasible. While native septal puncture is an option, direct access through the occluder device—when guided by precise imaging and balloon dilatation—provides a safe and effective alternative for cryoballoon ablation. Long-term monitoring for device integrity and residual shunts remains essential.
Keywords: Atrial Septal Defect, AF Ablation, Passage Through Transseptal Occluder Device

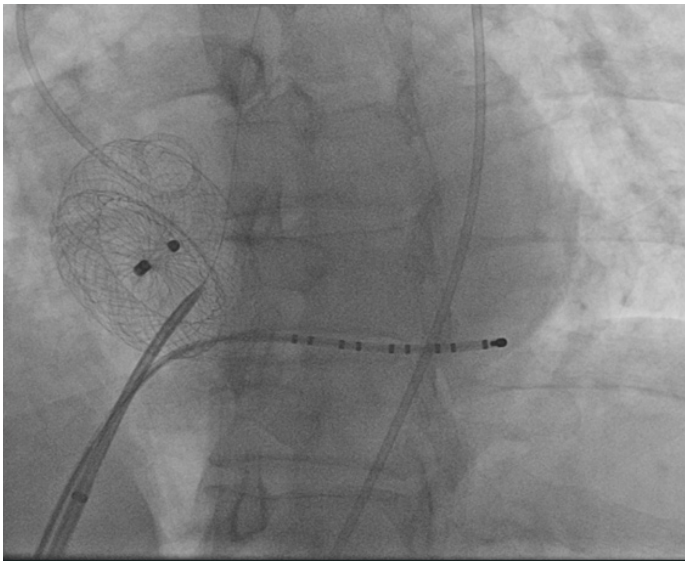

FIGURE 1. Advancement of the floppy wire through the occluder device

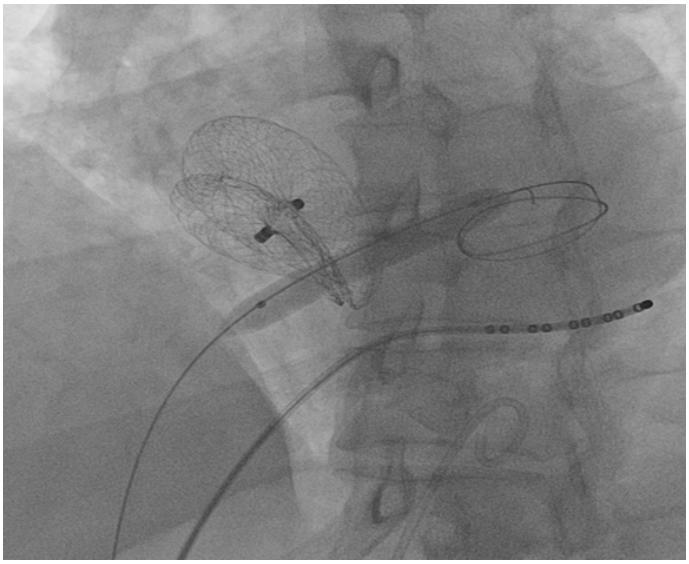

FIGURE 2. Balloon dilatation of the occluder device

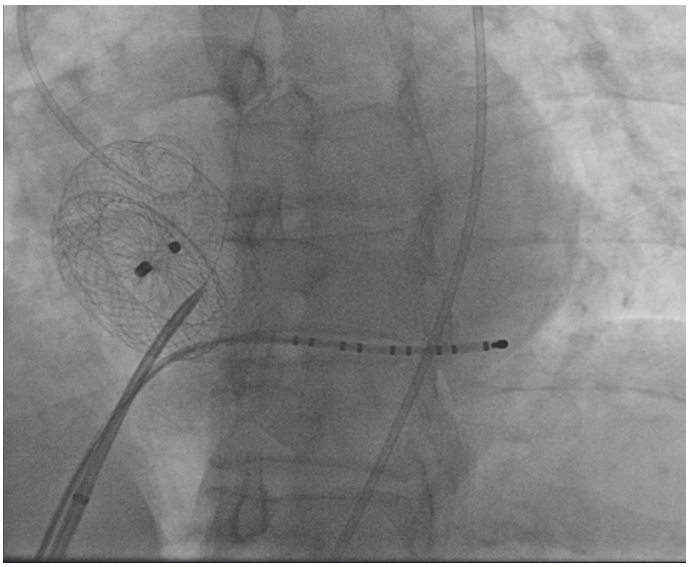

FIGURE 3. **Passage of the ablation catheter through the device**

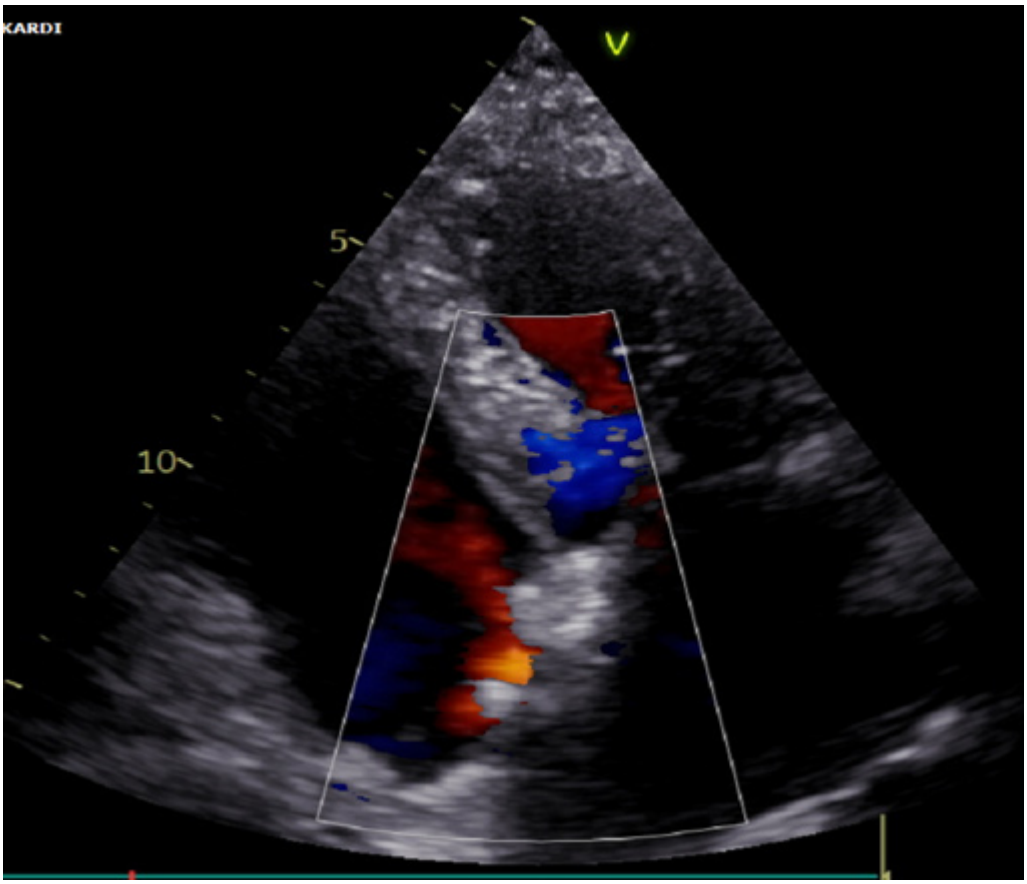

FIGURE 4. **Post-procedural control echocardiography demonstrating an intact interatrial septum**

OP-55.
Acute Axillary Artery Occlusion Following Transradial Intervention: A Case Report

Zeynep Yapan Emren[1], Sadık Volkan Emren[2], Serdar Enes Akcan[2], Fahrettin Tuğrul Çitekçi[2], Yalım Ayberk Çetin[2], Tolunay Demirbaş[2]

[1]Department of Cardiology, İzmir Bakırçay University, Faculty of Medicine, İzmir, Türkiye; [2]Department of Cardiology, İzmir Katip Celebi University, Faculty of Medicine, İzmir, Türkiye

Objectives: The transradial approach is preferred over the transfemoral approach in coronary angiography and percutaneous coronary interventions due to lower rates of bleeding and vascular complications. It is recommended in international guidelines, particularly because it has been associated with reduced mortality in patients with acute coronary syndrome. However, the growing use of transradial access has increased recognition of rare but potentially serious vascular complications. Procedural issues such as radial artery spasm, dissection, or perforation may prolong intervention time, while post-procedural complications—including radial artery occlusion, hematoma, pseudoaneurysm, and nerve injury—can lead to morbidity and upper extremity functional impairment. This report presents a case of acute radial artery occlusion after a transradial intervention, focusing on diagnostic and endovascular treatment strategies.

Case Presentation: A 70-year-old female patient presented with worsening chest pain. Her medical history included heart failure with reduced ejection fraction, left foot amputation due to diabetic complications, and coronary artery disease. One year earlier, surgical revascularization had been recommended but declined. Following coronary angiography at our center, a multidisciplinary team decided to perform percutaneous coronary intervention on the left anterior descending artery (LAD). The next day, transradial stent implantation to the LAD (Figure 1) was successfully performed, and the patient was monitored in the intensive care unit with tirofiban infusion. Approximately 20 hours later, she developed severe arm pain, and the radial pulse was absent on examination. Doppler ultrasonography revealed widespread occlusion consistent with acute thrombosis in the brachial, radial, and ulnar arteries starting from the axillary level, with no distal flow. The patient was urgently taken to the catheterization laboratory. The right femoral artery was cannulated with an 8F sheath. After angiographic confirmation of distal occlusion (Figure 2), cardiovascular surgery consultation deemed the patient unsuitable for surgery, and percutaneous endovascular treatment was planned. The occlusion was crossed retrogradely with a guiding catheter and floppy guidewire. Predilatation with a 5×60 mm balloon was followed by further dilatation using an 8×60 mm non-compliant balloon (Figure 3), restoring brachial artery flow. An 8×80 mm self-expandable stent was deployed, and thrombus aspiration achieved adequate distal perfusion (Figure 4). Heparin infusion was started post-procedure. Although the radial pulse remained absent, ulnar and brachial pulses were triphasic. With symptom resolution and no signs of limb ischemia, the patient was discharged for outpatient follow-up.

Discussion and Conclusions: Transradial interventions are generally safe; however, serious upper extremity arterial complications may occur, especially in patients with diabetes and peripheral vascular disease. While radial artery occlusion is often benign, proximal thrombus extension significantly increases the risk of acute limb ischemia. In this case, early diagnosis and timely endovascular treatment preserved limb function. This case emphasizes the importance of prompt recognition and intervention in managing vascular complications after transradial procedures.

Keywords: Transradial Approach, Radial Artery Occlusion, Endovascular Treatment

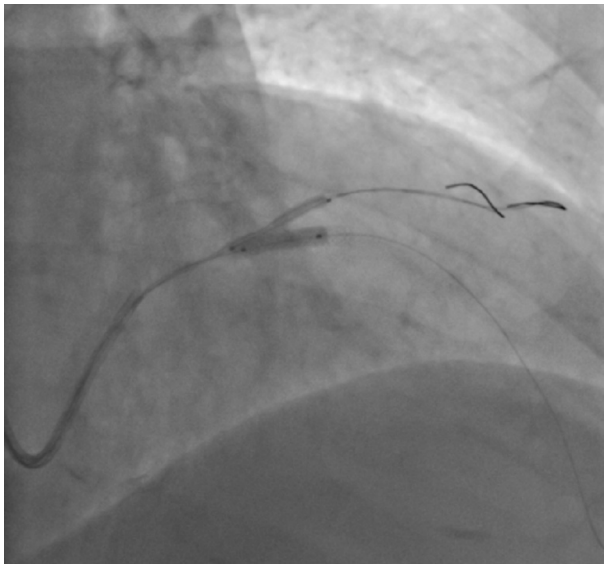

FIGURE 1. Successful stent implantation in the left anterior descending artery (LAD) via the transradial approach.

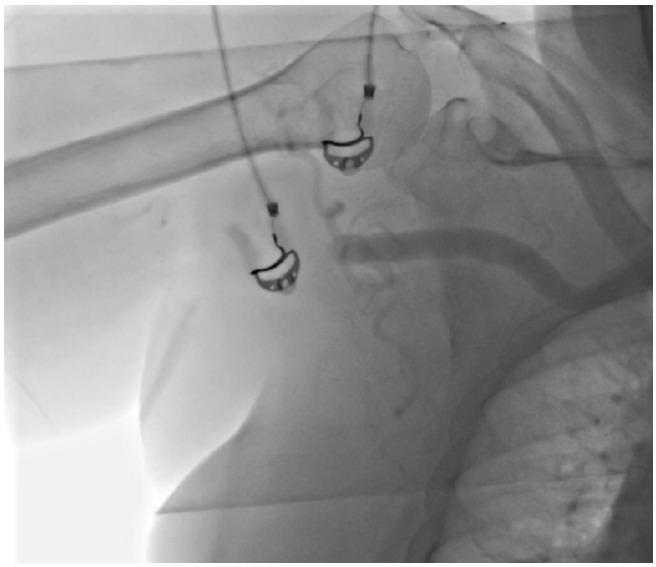

FIGURE 2. The right femoral artery was cannulated with an 8F sheath; absence of distal flow was observed from the level of the axillary artery onward.

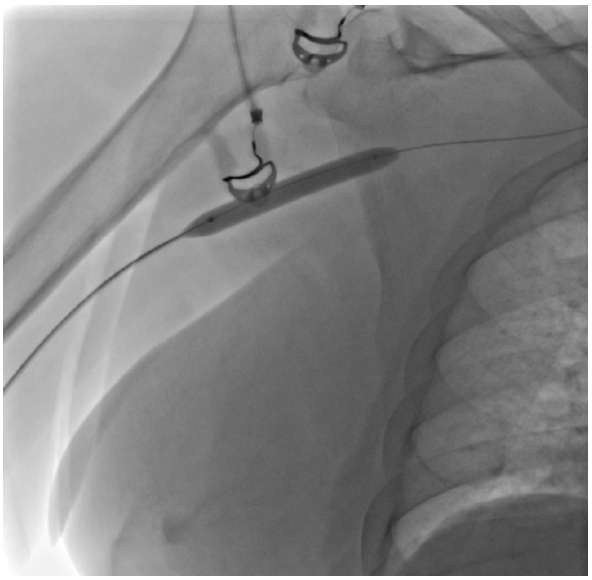

FIGURE 3. After crossing the occlusion retrogradely with a guide catheter and floppy wire, predilatation was performed using a 5×60 mm balloon; due to insufficient flow, redilatation was performed with an 8×60 mm non-compliant balloon, restoring brachial artery flow.

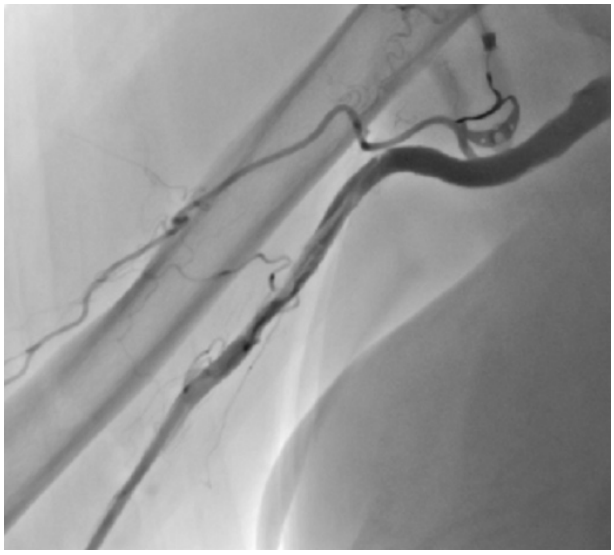

FIGURE 4. An 8×80 mm self-expanding stent was implanted in the dissected segment; additionally, thrombus aspiration was performed using a 4F sheath, achieving adequate distal perfusion in the axillary artery.

OP-56.
A Multidomain Risk Cluster for Predicting Contrast-Induced Nephropathy After Carotid Artery Stenting

Emre Yilmaz[1], Sencer Çamci[1], Aıbek Orozbaev[1]

[1]Department of Cardiology, Giresun University, Faculty of Medicine, Giresun, Türkiye

Objectives: Contrast-induced nephropathy (CIN) continues to represent an important clinical complication following carotid artery stenting (CAS), particularly in older patients with widespread atherosclerotic disease. Although conventional clinical risk factors have been well described, the role of integrated, multidomain biomarker-based risk stratification in this population has not been fully elucidated. The present study aimed to evaluate whether a multidomain risk cluster incorporating inflammatory, nutritional, and renal biomarkers is associated with the development of CIN after CAS, and to assess its predictive performance in comparison with established prognostic scoring systems.

Methods: This study included 224 consecutive patients who underwent CAS. CIN was defined according to standard diagnostic criteria. A multidomain clustering model was generated using C-reactive protein, albumin, lymphocyte count, neutrophil count, and blood urea nitrogen, classifying patients into low- and high-risk clusters. Clinical, laboratory, and procedural characteristics were compared between clusters. Independent predictors of CIN were explored using univariable and multivariable logistic regression analyses. Discriminative performance was evaluated by receiver operating characteristic (ROC) curve analysis and the area under the curve (AUC).

Results: CIN developed in 23 (10.3%) patients (Table 1). Patients assigned to the high-risk cluster exhibited a substantially higher incidence of CIN than those in the low-risk cluster (24.4% vs. 2.1%), corresponding to a markedly increased relative risk (RR) [RR: 14.94, 95% confidence interval (CI): 4.28–52.16; P<0.001] (Figure 1). After adjustment for age, diabetes mellitus, hypertension, sex, and baseline glomerular filtration rate, high-risk cluster membership remained independently associated with CIN occurrence (odds ratio: 6.00, 95% CI: 1.55–23.24; P=0.009) (Figure 2). In comparative analyses, the multidomain cluster demonstrated superior discriminative performance (AUC: 0.781) ans relative to the Osaka prognostic score (OPS) (AUC: 0.717) (Table 2).

Discussion and Conclusions: A multidomain biomarker-based risk cluster integrating inflammatory, nutritional, and renal parameters independently predicts contrast-induced nephropathy following carotid artery stenting and outperforms commonly used prognostic scores. This strategy may offer clinically relevant risk stratification beyond traditional models in patients undergoing CAS.

Keywords: Contrast-Induced Nephropathy, Carotid Artery Stenting, Multidomain Risk Stratification, Inflammation and Nutritional Biomarkers, Risk Clustering

TABLE 1. Comparison of Clinical and Laboratory Characteristics Between Low- and High-Risk Multidomain Clusters

Variables	Low risk cluster (n=142)	High risk cluster (n=82)	P-value
Age (years)	69 (6176)	71 (67 - 82)	**< 0.001**
Diabetes mellitus	62 (43.6%)	38 (46.3%)	0.104
Hypertension	120 (84.5%)	70 (85.4%)	0.272
Coronary artery diseasen	52 (36.6%)	37 (45.1%)	0.209
Smoking	41 (28.9%)	27 (32.9%)	0.512
Female gender	43 (30.3%)	22 (26.8%)	0.391
Creatinine (mg/dL)	0.9 (0.831.12)	0.93 (0.81-1.40)	0.349
GFR (mL/min/1.73 m^2)	75 (6091)	81 (49.5-89)	**0.009**
BUN (mg/dL)	17.75 (14.0121.96)	24.76 (19.15-28.50)	**< 0.001**
ALT (IU/L)	15 (1020)	19 (12-31)	0.067
AST (IU/L)	17 (1521)	22 (16-32)	**0.005**
Glucose (mg/dL)	101 (92123)	141 (101-174)	**0.002**
Total cholesterol (mg/dL)	180 (152-211)	168 (164-205)	0.719
Triglycerides (mg/dL)	145 (94-191)	123 (105-178)	0.629
HDL-C (mg/dL)	39 (35-48)	42 (31-46)	0.215
LDL-C (mg/dL)	105.72±38.93	104.89±34.72	0.885
Sodium (mmol/L)	140 (138-141)	136 (135-139)	**< 0.001**
Potassium (mmol/L)	4.44±0.47	4.27±0.48	**0.016**
Albumin (g/L)	42.91±3.49	36.92±4.53	**< 0.001**
CRP (mg/L)	2 (0.9-4.5)	34 (14-48.7)	**< 0.001**
HbA1c (%)	5.7 (5.5-6.87)	6.7 (5.82-8.25)	**< 0.001**
Hemoglobin (g/dL)	13.6 (11.1-14.9)	12 (10.9-13.5)	**< 0.001**
Platelet (×10^9/L)	235 (188-281)	300 (218-382)	0.082
Lymphocyte (×10^9/L)	2.08 (1.77-2.72)	1.48 (1.11-1.82)	**< 0.001**
Neutrophil (×10^9/L)	4.7 (3.45-5.41)	5.88 (4.24-8)	**0.001**
WBC (×10^9/L)	7.65 (6.17-8.83)	8.23 (6.19-10.82)	0.140
Hospitalization duration (days)	1 (1-3)	2 (1-10)	**< 0.001**
OPS	0 (0-1)	2 (1-2)	**< 0.001**
CVA	16 (11.3%)	6 (7.3%)	0.399
CIN	3 (2.1%)	20 (24.4%)	**< 0.001**

Data are shown as mean±standard deviation or number (percentage) or median (25th–75th percentile) where appropriate. GFR, glomerular filtration rate; BUN, blood urea nitrogen; ALT, alanine aminotransferase; AST, aspartate aminotransferase; HDL-C, high-density lipoprotein cholesterol; LDL-C, low-density lipoprotein cholesterol; CRP, c-reactive protein; WBC, white blood cell; OPS, Osaka prognostic score; CVA, cerebrovascular accident; CIN, contrast-induced nephropathy.
Statistically significant P-values are shown in bold.

TABLE 2. Diagnostic Performance of Risk Clusters and Prognostic Scores for Contrast-Induced Nephropathy

	AUC	95% CI	P-value	Sensitivity	Specificity
Multidomain Risk Cluster	0.781	0.690-0.871	**< 0.001**	87%	69%
OPS	0.717	0.589-0.845	**0.001**	60%	82%

AUC, area under the curve; CI, confidence interval; OPS, Osaka prognostic score.
Statistically significant P-values are shown in bold.

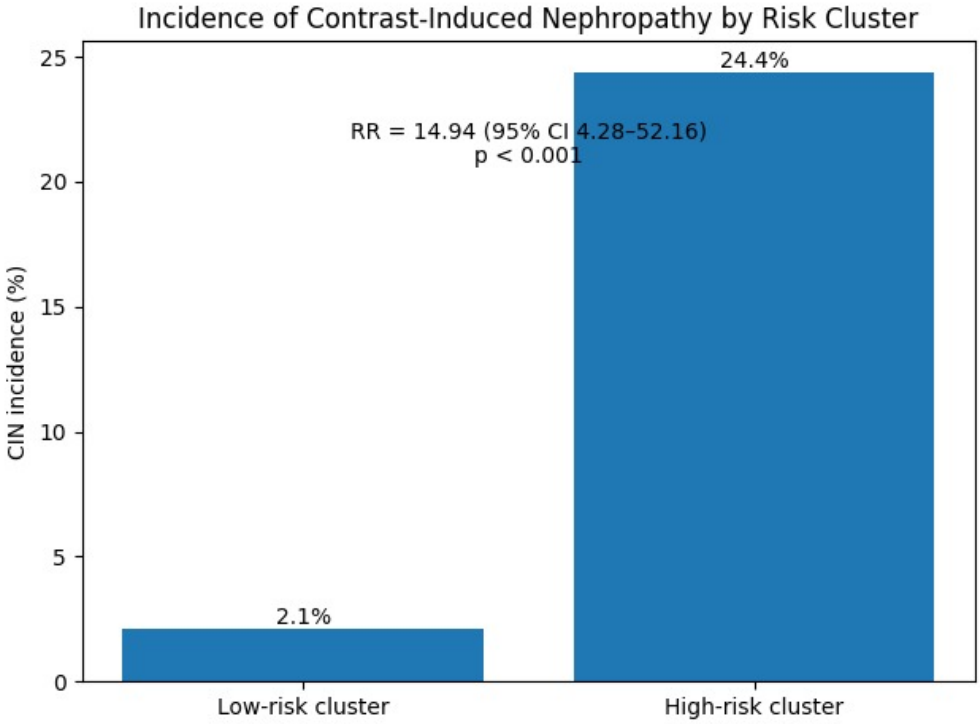

FIGURE 1. **Incidence of CIN according to multidomain risk clusters. The high-risk cluster was associated with a significantly increased risk of CIN (RR: 14.94, 95% CI: 4.28–52.16; P<0.001). CIN=contrast-induced nephropathy, RR=relative risk, CI=confidence interval.**

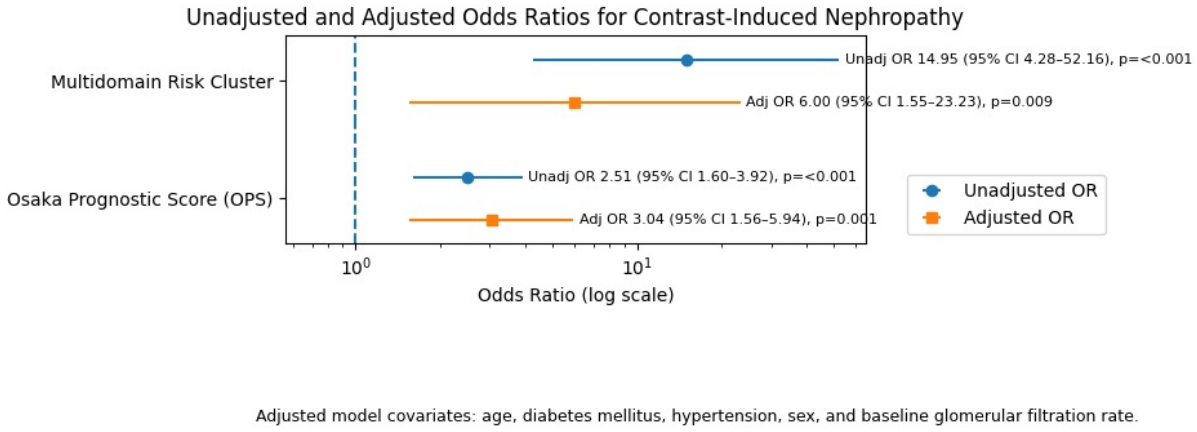

FIGURE 2. **Unadjusted and adjusted associations between multidomain risk clusters and contrast-induced nephropathy. OR, odds ratio, CI, confidence interval, OPS, Osaka prognostic score.**

OP-57.
An Overlooked Phenotype: Widespread Non-calcified Atherosclerosis Presenting with Vision Loss

Nuray Mammadova[1], Çetin Alak[1], Mustafa Yilmaz[1]

[1]Department of Cardiology, Uludağ University, Faculty of Medicine, Bursa, Türkiye

Case Presentation: We present a case of a 45-year-old male patient who developed sudden vision loss in the left eye due to central retinal artery occlusion (CRAO) and was evaluated for systemic embolic sources. The case illustrates the presence of widespread, non-calcified atherosclerotic vascular involvement despite a low Agatston score, highlighting a malignant atherosclerosis phenotype. The patient had a history of hypertension and long-standing uncontrolled diabetes (HbA1c: 11.3%). No family history of early cardiovascular disease was reported. On physical examination, the left arm pulse was weak, and a ~30 mmHg systolic blood pressure difference was observed between arms. Laboratory analysis revealed an LDL cholesterol level of 255 mg/dL. Transthoracic echocardiography (TTE) and cardiac magnetic resonance imaging (MRI) were performed to assess cardiac involvement. CT coronary angiography and conventional coronary angiography were used to evaluate coronary and systemic arteries. Genetic testing was not available; familial hypercholesterolemia (HeFH) was suspected based on clinical criteria. TTE showed concentric left ventricular hypertrophy, inferolateral wall calcification with mild motion abnormality, and nodular calcifications at the papillary muscle level (Figure 1). Cardiac MRI revealed left ventricular EF of 62%, cardiac index 3.4 L/min/m², inferolateral wall thinning and akinesia, and subendocardial late gadolinium enhancement (LGE) in basal and mid-inferolateral segments and apical lateral and anterior segments, consistent with prior myocardial infarction (Figure 3). CT coronary angiography revealed an Agatston score of 13, non-calcified atherosclerotic plaques in the carotid, subclavian, and coronary arteries, and significant stenosis in the carotid and brachiocephalic arteries (Figure 2, 5). Conventional coronary angiography demonstrated severe multi-vessel disease: LMCA 30–40%, LAD distal to D1 95%, CX proximal 80%, OM1 98%, RCA mid 40–50% (Figure 4).

Discussion: The initial CRAO presentation reflects the high sensitivity of the retinal circulation to atheroembolic events. Multimodal imaging revealed widespread non-calcified, embolic-risk plaques in coronary, carotid, subclavian, and possibly visceral arteries, despite a low calcium score. This phenotype differs from classical calcified plaque models and has been described in patients with HeFH, in whom non-calcified lipid-rich plaques may predominate. Multimodal imaging, combining TTE, MRI, CT, and angiography, provided comprehensive assessment and demonstrated strong correlation between echocardiographic, MRI, and CT findings.

Conclusions: This case highlights that sudden vision loss due to CRAO in a young patient may represent the first manifestation of a systemic malignant atherosclerosis phenotype with high embolic risk. Low Agatston scores do not exclude severe non-calcified plaque burden. Comprehensive assessment, integrating clinical, laboratory, and multimodal imaging data, is essential for accurate diagnosis and risk stratification.

Keywords: Non-calcified Atherosclerosis, Central Retinal Artery Occlusion (CRAO), Multimodal Cardiovascular Imaging

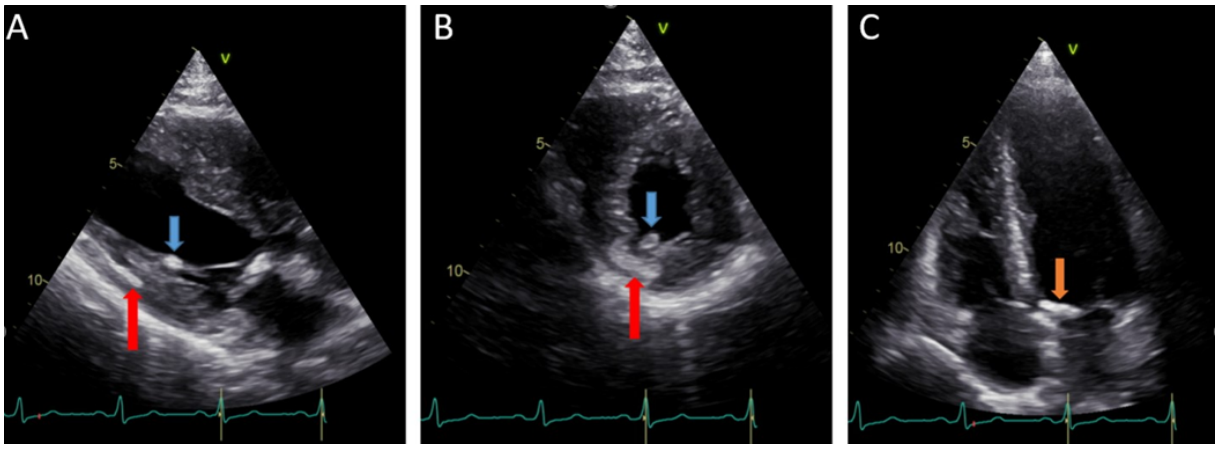

FIGURE 1. **Findings of intracardiac calcification on transthoracic echocardiography. (A) In the parasternal long-axis section, myocardial calcification (red arrow) is seen in the inferolateral wall and a calcified focus (blue arrow) is seen in the posterior papillary muscle. (B) In the parasternal short-axis section, widespread calcification (red arrow) is seen in the inferolateral segment and nodular calcification (blue arrow) is seen in the posterior papillary muscle. (C) In the apical four-chamber section, prominent calcification is noted in the posterior part of the mitral annulus (orange arrow). These findings are consistent with fibrocalcific changes that were initially confused with an intracardiac mass, but were understood to have developed secondary to a silently experienced myocardial infarction with advanced imaging techniques.**

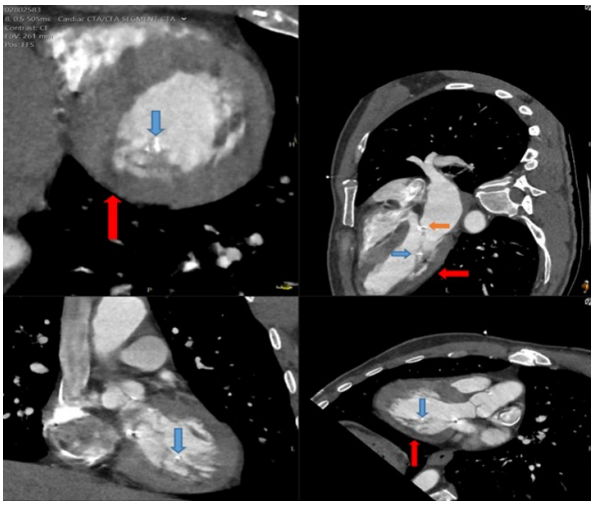

FIGURE 2. **Myocardial and valvular calcification on cardiac computed tomography. Blue arrow: Calcification localized at the level of the posterior papillary muscle. Red arrow: Thinning of the inferolateral wall and myocardial calcification secondary to a previous myocardial infarction. Orange arrow: Significant calcification at the level of the mitral annulus. CT findings show a high degree of structural correlation with the calcified nodules in the inferolateral segment, wall thinning, and echogenic foci at the level of the mitral annulus detected on echocardiography.**

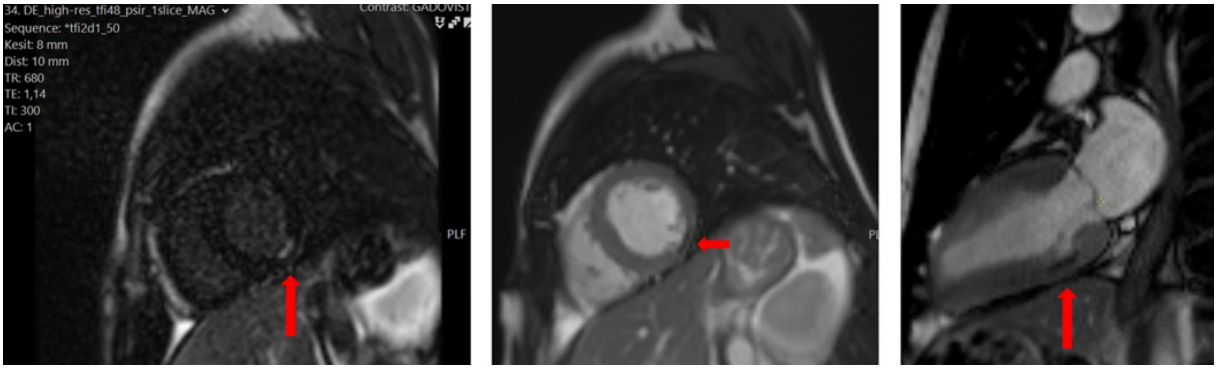

FIGURE 3. **Cardiac magnetic resonance imaging showing inferolateral wall involvement. Red arrows: Areas of delayed gadolinium uptake consistent with myocardial infarction, showing transmural delayed involvement in the inferolateral wall of the left ventricle. Wall thinning and akinetic motion pattern were observed in the same region. These findings correlate highly with calcification foci and wall motion abnormalities observed on CT and echocardiography.**

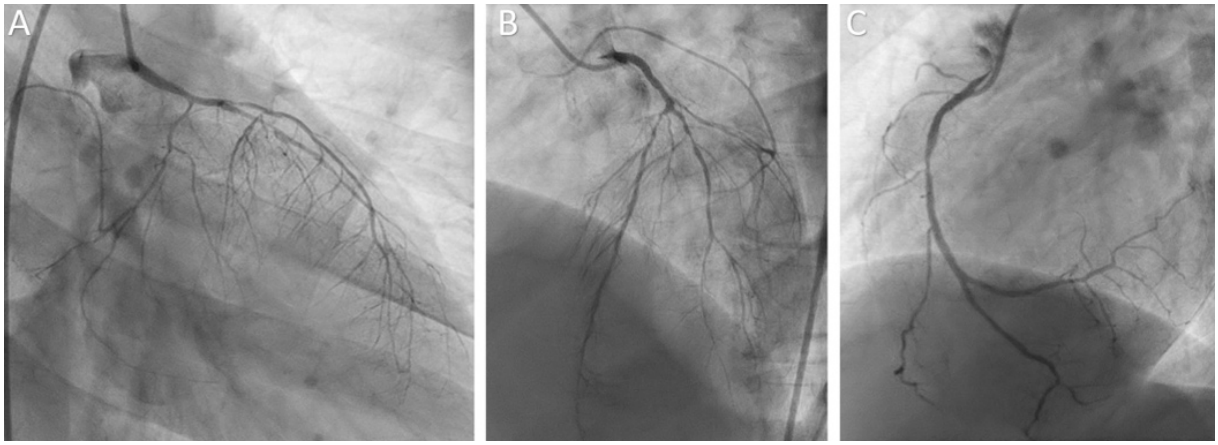

FIGURE 4. **Coronary angiography images. Multiple segmental stenoses are observed in the projections of (A) the left anterior descending artery (LAD), (B) the circumflex artery (Cx), and (C) the right coronary artery (RCA).**

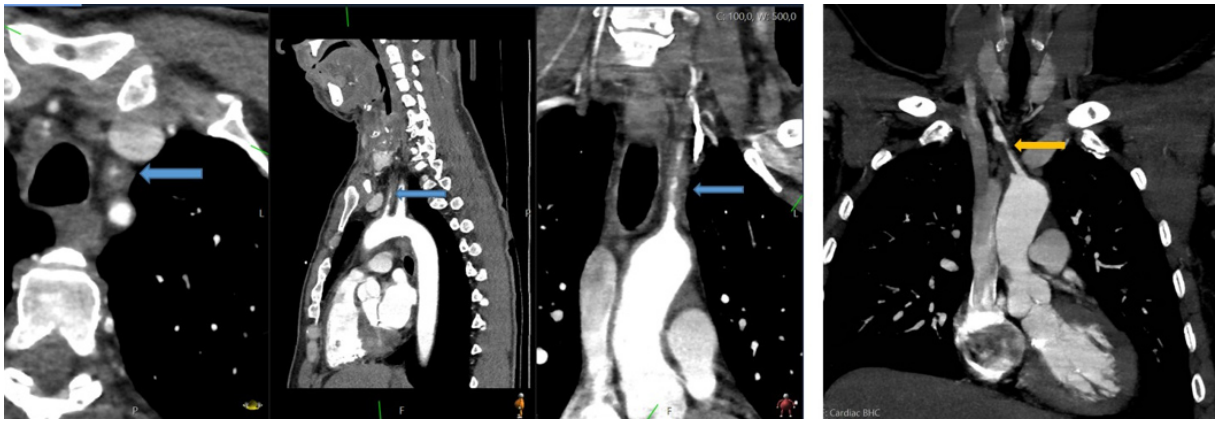

FIGURE 5. **Extracranial large vessel stenoses on thoracoabdominal CT angiography. Blue arrows: Indicate the area where the left main carotid artery is occluded. Orange arrow: Indicates the severe stenosis observed at the origin of the right main carotid artery. These findings reveal widespread atherosclerotic involvement and peripheral vascular manifestations of concomitant coronary artery disease in the patient.**

OP-58.
Safety and Efficacy of Carotid Artery Stenting Without Routine Anticholinergic Pretreatment

İbrahim AKTAŞ[1]

[1]*Department of Cardiology, Malatya Turgut Ozal University, Faculty of Medicine, Malatya, Türkiye*

Objectives: The administration of prophylactic atropine is widely regarded as a standard of care to counteract procedural hemodynamic instability during carotid artery stenting (CAS). We aimed to evaluate the clinical approach and outcomes of CAS in a setting where prophylactic atropine is not routinely administered.
Methods: The study population consisted of 120 consecutive patients who received carotid artery stent implantation in our department from 2018 to 2025. All participants were closely followed during their hospital stay for the occurrence of procedural hemodynamic depression (defined as bradycardia with a heart rate decrease to <50% of baseline or an absolute heart rate <40 bpm, and hypotension with systolic blood pressure <90 mmHg) as well as periprocedural complications, including TIA and stroke.
Results: Invasive hemodynamic monitoring during the CAS procedure demonstrated a significant reduction in both systolic and diastolic blood pressure compared to pre-procedural baseline values (mean systolic: 140.3 vs. 121.2 mmHg, P=0.001; mean diastolic: 66.4 vs. 57.0 mmHg, P=0.036). Similarly, the mean heart rate showed a statistically significant decline from 69 bpm to 61 bpm (P=0.002). Despite these fluctuations, they were clinically well-tolerated in 95% of the cases. Consequently, the requirement for atropine intervention was remarkably low, with only 6 patients (5%) necessitating treatment for significant bradycardia or hypotension. In these instances, hemodynamic parameters normalized within minutes following administration. Regarding periprocedural complications, only one stroke and one TIA were observed in the entire cohort; notably, both events occurred in the non-atropine group, and no neurological complications were recorded among patients who required atropine.
Discussion: Current guidelines often advocate for universal anticholinergic prophylaxis to mitigate the baroreceptor reflex induced by carotid bulb stretching during CAS. However, our findings suggest that clinically significant hemodynamic instability requiring intervention is relatively infrequent, occurring in only 5% of our cohort. By adopting a "wait-and-watch" approach for persistent changes (exceeding one minute), we avoided the potential side effects of unnecessary anticholinergic administration without compromising patient safety. Importantly, the rare periprocedural neurological events (n=2) were not associated with the management of hemodynamic depression, as both cases occurred in patients who remained stable throughout the procedure. This suggests that a selective intervention strategy is sufficient for maintaining procedural safety while preventing over-treatment.
Conclusions: In conclusion, a selective atropine administration strategy based on persistent hemodynamic criteria—rather than universal prophylaxis—is both feasible and safe for patients undergoing CAS. Given the low intervention rate (5%) and the rapid recovery of hemodynamic parameters when treated, routine anticholinergic pretreatment may be reserved for high-risk cases or avoided altogether to ensure a more individualized clinical approach.
Keywords: Carotid Artery Stenting, Atropine, Hemodynamic Instability

OP-59.
The Dark Path of Infective Endocarditis: Prosthetic Valve Endocarditis Unveiled by Multimodality Imaging

Muhammed Yahya Demirel[1], Çetin Alak[1], Melih İnce[1], Selin Abdu Tinaz[1], Bülent Özdemir[1]

[1]Department of Cardiology, Uludag University, Faculty of Medicine, Bursa, Türkiye

Objectives: Prosthetic valve endocarditis (PVE) is a rare but life-threatening complication associated with high morbidity and mortality. Diagnosis may be particularly challenging when clinical findings are nonspecific and transthoracic echocardiography (TTE) fails to demonstrate definitive signs of infection. In this context, multimodality imaging has emerged as a critical tool for identifying intracardiac pathology and extracardiac complications, enabling accurate diagnosis and appropriate management.
Case Presentation: A 70-year-old male with no known chronic comorbidities successfully underwent surgical aortic valve replacement with a sutureless bioprosthetic valve and ascending aorta replacement due to severe aortic regurgitation and ascending aortic aneurysm. The early postoperative course was uncomplicated. One month after surgery, the patient was hospitalized with fever and chills. Laboratory evaluation revealed elevated inflammatory markers; however, TTE demonstrated a normally functioning prosthetic valve without evidence of infective endocarditis. Based on these findings, the patient was discharged with oral antibiotic therapy.
Five months later, he was re-admitted due to persistent fatigue and anemia. Blood cultures yielded Enterococcus faecalis. Repeat TTE remained nondiagnostic, prompting further evaluation with transesophageal echocardiography (TEE), cardiac computed tomography (CT), and positron emission tomography/computed tomography (PET/CT). TEE revealed a mobile vegetation measuring 10×3 mm on the bioprosthetic aortic valve, along with a suspicious lesion originating from the left coronary cusp, consistent with a sinus of Valsalva aneurysm or abscess. Cardiac CT confirmed the presence of a sinus of Valsalva aneurysm. PET/CT demonstrated heterogeneous increased F-18 FDG uptake surrounding the aortic valve and distal aortic graft (SUVmax 4.5), suggestive of active infection. In addition, focal FDG uptake within the spleen (SUVmax 6.8) was consistent with septic embolization, compatible with splenic infarction or abscess. These multimodality imaging findings established the diagnosis of late prosthetic valve endocarditis complicated by aortic root involvement and systemic septic embolization, and the patient subsequently underwent reoperation.
Conclusions: This case underscores the diagnostic limitations of isolated echocardiographic assessment in prosthetic valve endocarditis and highlights the pivotal role of multimodality imaging in detecting clinically significant but otherwise occult complications, including aortic root involvement, sinus of Valsalva aneurysm, and septic embolization. Early and integrated use of TEE, cardiac CT, and PET/CT can substantially enhance diagnostic accuracy and guide optimal therapeutic decision-making in complex PVE cases.
Keywords: Prosthetic Valve Endocarditis, Multimodality Imaging, Sinus of Valsalva Aneurysm

OP-60.
The Cost of Pregnancy? Peripartum Cardiomyopathy Following IVF

Ayşe Nilgün Kara[1], Çetin Alak[1], Mustafa Yilmaz[1]

[1]Department of Cardiology, Uludağ University, Faculty of Medicine, Bursa, Türkiye

Case Presentation: A 36-year-old woman with no prior history of cardiac or systemic disease presented with progressive dyspnea, orthopnea, and chest pain that began during the final weeks of pregnancy and persisted after delivery. On physical examination, decreased breath sounds were noted at the lung bases, and a grade 2/6 apical systolic murmur was auscultated. Her heart rate was 120 beats/min, and blood pressure was 120/80 mmHg. Electrocardiography demonstrated sinus rhythm without ischemic changes. Laboratory evaluation revealed markedly elevated cardiac biomarkers, including a B-type natriuretic peptide level of 1285 pg/mL and a troponin level of 30.5 ng/L. Transthoracic echocardiography demonstrated a markedly dilated left ventricle with an end-diastolic diameter of 67 mm and severely reduced left ventricular ejection fraction (LVEF) of 18%. Severe mitral regurgitation and moderate-to-severe tricuspid regurgitation were also present. A detailed obstetric history revealed multiple prior in vitro fertilization (IVF) cycles, with the index pregnancy achieved through assisted reproductive technology. The patient was admitted to the intensive care unit with the diagnosis of peripartum cardiomyopathy (PPCM). On postpartum day 2, guideline-directed medical therapy for heart failure, including metoprolol, enalapril, spironolactone, and furosemide, was initiated. Despite optimal medical therapy, on postpartum day 14 she developed signs of low cardiac output, including hypotension, cold extremities, and oliguria. Intravenous dobutamine infusion was started, leading to hemodynamic stabilization, and the inotropic support was gradually tapered. After stabilization, breastfeeding was discontinued, and bromocriptine therapy was initiated on postpartum day 17. The treatment regimen consisted of 2.5 mg twice daily for the first two weeks, followed by 2.5 mg once daily for an additional two weeks, for a total treatment duration of four weeks. During therapy, the patient experienced marked clinical improvement, with resolution of dyspnea and regression of congestion. Serial echocardiographic evaluations demonstrated gradual recovery of left ventricular systolic function and reduction in chamber dimensions. At the 1-year follow-up, the patient was asymptomatic with a normal functional capacity and transthoracic echocardiography showed normalization of left ventricular size and recovery of LVEF to 52%.

Conclusions: Pregnancy achieved through IVF is associated with an increased risk of PPCM, a condition best explained by a multifactorial multiple-hit model. Factors such as advanced maternal age, cumulative exposure to supraphysiologic estrogen and progesterone levels, pregnancy-related hemodynamic overload, multiple gestations, and hypertensive disorders act synergistically to increase myocardial vulnerability. Hormonal regimens used in IVF may further impair endothelial function, promote fluid retention, and exacerbate adverse cardiac remodeling. A central pathophysiological mechanism in PPCM is oxidative stress–mediated cleavage of prolactin into a cardiotoxic 16-kDa fragment. Bromocriptine inhibits prolactin secretion and has been shown to facilitate myocardial recovery. In patients with severe left ventricular dysfunction, temporary inotropic support followed by bromocriptine therapy after hemodynamic stabilization is recommended. With the increasing use of IVF worldwide, heightened awareness of PPCM risk, close cardiovascular surveillance, and timely initiation of bromocriptine in selected patients are crucial to prevent persistent heart failure and improve long-term outcomes.

Keywords: Peripartum Cardiomyopathy, IVF, Pregnancy

OP-61.
Malignant RCA in the Shadow of Perimyocarditis

Ayşe Nilgün Kara[1], Çetin Alak[1], Nazmiye Sümeyye Güllülü[1]

[1]Department of Cardiology, Uludağ University, Faculty of Medicine, Bursa, Türkiye

Case Presentation: A 29-year-old male presented to the emergency department with pleuritic chest pain radiating to the left hemithorax that began at rest while sleeping. Symptoms developed following one-week history of sore throat and cough. There was no prior history of cardiovascular disease, syncope, or exertional symptoms. The admission electrocardiogram demonstrated incomplete right bundle branch block without ischemic ST–T segment changes. High-sensitivity cardiac troponin I levels were markedly elevated, measuring 5,881.5 ng/L initially and increasing to 9,846.3 ng/L on repeat testing (67% rise). Transthoracic echocardiography revealed preserved left ventricular systolic function with an ejection fraction of 60% and no regional wall motion abnormalities. Cardiac chamber dimensions were normal, and no pericardial effusion was detected. Given the clinical presentation and significant troponin elevation, coronary angiography was performed with a preliminary diagnosis of acute coronary syndrome. The left coronary system was angiographically normal. Selective catheterization of the right coronary artery (RCA) was unsuccessful, and non-selective imaging did not demonstrate critical stenosis. Due to suspicion of an anomalous coronary origin, coronary computed tomography angiography (CCTA) was performed. CCTA revealed an anomalous RCA originating near the left coronary sinus with an acute take-off angle and an interarterial course between the aorta and pulmonary artery, consistent with a malignant coronary variant. To evaluate a potential inflammatory etiology, cardiac magnetic resonance imaging (CMR) was performed. Left ventricular systolic function was preserved with normal segmental wall thickening, and right ventricular motion was normal. Subepicardial late gadolinium enhancement and myocardial edema were observed at the basal anterolateral, lateral, and inferolateral segments. Native T1 and T2 relaxation times were prolonged, supporting the diagnosis of acute perimyocarditis. The patient was treated with nonsteroidal anti-inflammatory drugs and colchicine. Chest pain resolved gradually, and serial troponin measurements showed a progressive decline. The patient remained hemodynamically stable and was discharged after six days of hospitalization. Six months after resolution of the acute inflammatory episode, myocardial perfusion scintigraphy was performed to assess whether the malignant interarterial RCA course was associated with inducible ischemia. The study demonstrated normal myocardial perfusion without evidence of ischemia. Despite the absence of functional ischemia, elective coronary artery bypass grafting was recommended by the heart team in accordance with the 2018 AHA/ACC Class IIb recommendation, considering the patient's young age and high-risk coronary anatomy.

Conclusions: Coronary artery anomalies are rare congenital variations associated with sudden cardiac death, particularly in young individuals. An interarterial course of the RCA between the aorta and pulmonary artery is considered a malignant variant due to potential dynamic compression during exertion. These anomalies may remain asymptomatic and become clinically evident when unmasked by inflammatory conditions. Acute perimyocarditis, typically following a viral prodrome, can closely mimic acute coronary syndrome with chest pain and elevated cardiac biomarkers. In patients with non-obstructive coronary anatomy, inflammatory myocardial injury should be considered in the differential diagnosis. Multimodal imaging using CCTA, CMR, and myocardial perfusion scintigraphy is essential for establishing the diagnosis and guiding individualized, risk-based management strategies.

Keywords: Coronary Anomaly, Perimyocarditis, Multimodal Imaging

OP-62.
One Implantation, Two Challenges: Anatomical Difficulty and Post-Cardiac Injury Syndrome

Orkhan Yunisli[1], Çetin Alak[1], Selin Abdu Tinaz[1], Tunay Şentürk[1]

[1]Department of Cardiology, Uludag University, Faculty of Medicine, Bursa, Türkiye

Objectives: Cardiac resynchronization therapy (CRT) reduces symptoms, hospitalization rates, and mortality in patients with heart failure with reduced ejection fraction and intraventricular conduction delay, particularly left bundle branch block (LBBB). Accurate coronary sinus (CS) lead positioning during CRT-D implantation is a key determinant of procedural success.
However, anatomical variations of the CS Ostium such as inferior or posterior location and marked angulation- may complicate cannulation. In such cases, advanced techniques including simultaneous coronary angiography (CAG) or steerable catheters may be required.
Cardiac tamponade after implantation is rare but potentially fatal. Early effusions are usually related to mechanical injury, whereas late-onset effusions are typically caused by an immune-mediated inflammatory response known as post-cardiac injury syndrome (PCIS).
We present a case of PCIS-related tamponade requiring surgical intervention following implantation with difficult CS cannulation necessitating simultaneous CAG.
Case Presentation: A 39-year-old man with hypertension, diabetes mellitus, heart failure presented with dyspnea. Electrocardiography showed sinus rhythm with LBBB. Transthoracic echocardiography revealed fraction of 34% with global hypokinesia, E/A reversal, mild mitral and tricuspid regurgitation, minimal aortic regurgitation, and a systolic pulmonary artery pressure of 24 mmHg. CRT-D implantation was indicated. During the procedure, CS cannulation using standard catheters was unsuccessful. Fluoroscopy demonstrated an inferio-posteriorly located CS ostium with marked angulation and hook-like configuration. Simultaneous left coronary angiography delineated the ostial orientation (Figure 1). Successful cannulation was achieved using a steerable ablation catheter (Marinr™ MC/MCXL), and the lead was placed in the posterolateral vein (Figure 2). The procedure was uneventful, and the patient was discharged the following day. Thirty days later, the patient re-presented with fatigue and presyncope. Follow-up echocardiography showed ejection fraction of 34%, paradoxical septal motion, visible pacemaker leads, and pericardial effusion with variable thickness up to 3.6 cm. Thoracic computed tomography confirmed a pericardial effusion measuring up to 5 cm, without pulmonary pathology (Figure 3). Despite colchicine and anti-inflammatory therapy the effusion progressed. Following surgical consultation, pericardial window and partial pericardiectomy were performed. Histopathology demonstrated fibrin deposition, perivascular lymphoid infiltration, mesothelial proliferation, consistent with chronic pericarditis. Postoperatively, the effusion regressed and the patient was discharged in stable condition two weeks later.
Discussion: CS lead placement is critical for CRT success. Although the CS ostium is typically located between the tricuspid septal leaflet and inferior vena cava, anatomical variations may hinder cannulation with conventional catheters. In this case, the inferio-posterior, hook-like ostium configuration rendered standard techniques ineffective. Simultaneous CAG enabled accurate visualization, allowing successful lead placement using a steerable catheter.
Pericardial effusion after CRT-D implantation is uncommon. Early effusions usually result from mechanical injury, whereas PCIS represents delayed immune-mediated inflammatory response, typically occurring within

1–12 weeks. The timing and histopathological findings in this patient support the diagnosis of PCIS. In progressive cases refractory to medical therapy, surgical pericardial window is an effective treatment.

Conclusion: Recognition of CS anatomical variations and use of adjunctive imaging can improve implantation success. Steerable catheters are valuable in challenging anatomies. Late-onset pericardial effusion should raise suspicion for PCIS and early recognition is essential for appropriate management.

Keywords: Cardiac Resynchronization Therapy, Coronary Sinus Anatomical Variation, Post-Cardiac Injury Syndrome

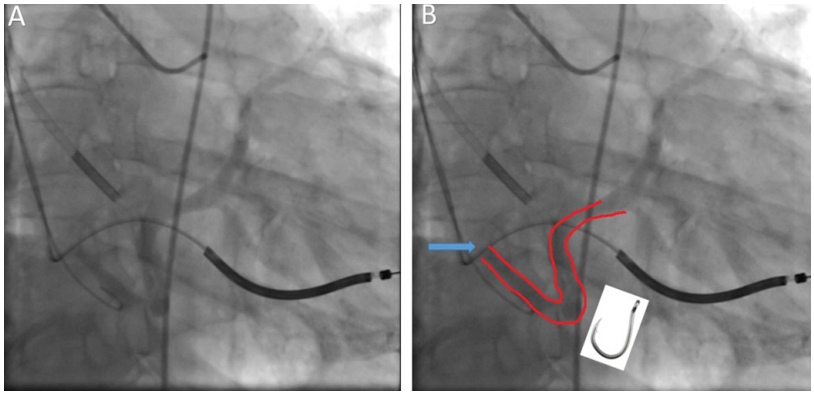

FIGURE 1. (A) The fluoroscopic image shows an inferior-posteriorly located coronary sinus ostium outlet with significant angulation. (B) The schematic contour and fishhook metaphor drawn on the same image illustrate the characteristic sharp angle of the ostium outlet and the difficulty of catheter guidance. The blue arrow indicates the coronary sinus ostium.

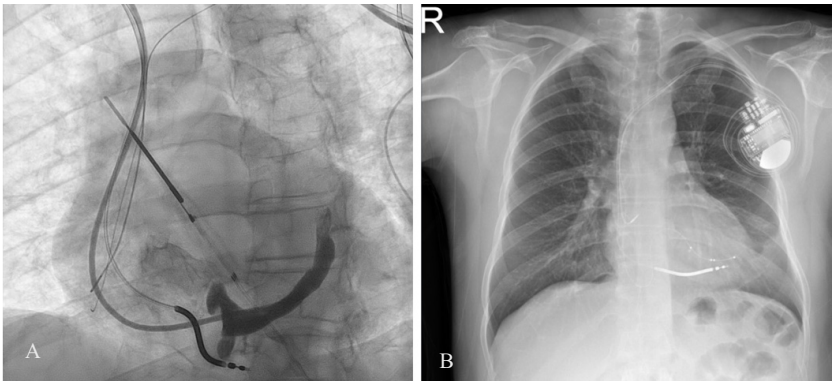

FIGURE 2. (Fluoroscopy during the procedure and post-procedure PA chest X-ray. (A) Fluoroscopy shows successful cannulation and opacification of venous anatomy in coronary sinus contrast filling. (B) Post-procedure PA chest X-ray shows the CRT-D device, lead placements, and significant angulation of the coronary sinus lead.

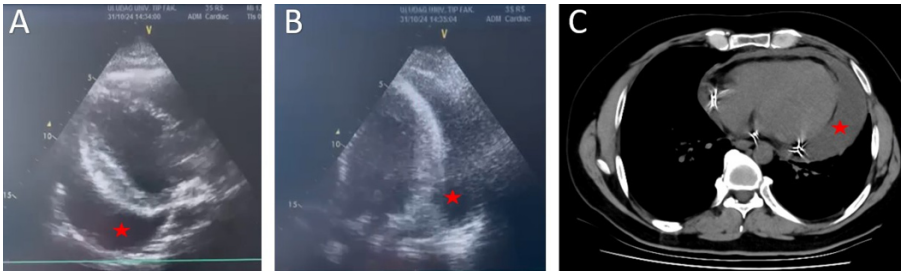

FIGURE 3. Transthoracic Echocardiography and Thoracic CT Images (A) Pericardial effusion reaching 3.6 cm at its thickest point in the parasternal long axis section. (B) Pericardial effusion appearance in the apical four-chamber section. (C) Pericardial effusion reaching up to 5 cm at its thickest point in the axial section of the thoracic CT scan. The red star indicates pericardial fluid.

OP-63.
Ozaki Procedure

Mustafa Selçuk Atasoy[1], Hakan Güven[1]

[1]*Department Of Cardiovascular Surgery, Bursa City Hospital, Bursa, Türkiye*

Objectives: Since an ideal prosthetic heart valve has not yet been achieved and valve repair has not become the standard treatment for aortic valve disease, valve replacement remains the gold standard. However, prosthetic valves are associated with several complications such as infection, patient–prosthesis mismatch, and structural degeneration. Therefore, the search for alternative solutions in aortic valve pathologies continues. As a promising alternative to conventional approaches, we aimed to highlight the "neocuspidization / Ozaki procedure." In patients with an indication for aortic valve surgery—particularly those with a small aortic annulus and an anticipated risk of patient–prosthesis mismatch—the Ozaki procedure was discussed as an alternative to conventional methods such as mechanical or bioprosthetic valve replacement, transcatheter aortic valve implantation (TAVI), and stentless valves. This technique utilizes the patient's own pericardium, eliminates patient–prosthesis mismatch, allows future management of potential complications with TAVI, and represents a cost-effective surgical option. Autologous pericardium is harvested, glutaraldehyde-treated, tailored with templates, and sutured to the aortic annulus to create a new valve.
Case Presentation: A 71-year-old female patient presented with dyspnea. Diagnostic evaluation revealed severe aortic stenosis with a left ventricular ejection fraction of 60%, an aortic valve area of 0.6 cm², a transvalvular gradient of 70/40 mmHg, and a left ventricular outflow tract diameter of 18 mm. The patient underwent the Ozaki procedure. She was monitored in the intensive care unit on postoperative day 1 and transferred to the ward on day 2. Her postoperative course was uneventful, and she was discharged with recommendations on postoperative day 5. Postoperative and 1-year follow-up echocardiography demonstrated no aortic regurgitation. The mean transvalvular gradient was 11 mmHg in the early postoperative period and 8 mmHg at 1 year. The patient remains asymptomatic during follow-up.
Discussion: The general principle in valve surgery is that "the best valve is the patient's own valve." Therefore, whenever feasible and appropriate, valve pathologies are treated with repair techniques, depending on the surgeon's experience. When repair is not possible, valve replacement is required. Available options for the aortic valve include mechanical valves, stented or stentless bioprosthetic valves, the Ross procedure, sutureless valves, and TAVI. The ideal valve should not cause tissue rejection, should not add operative risk, should be easy to implant, should function smoothly, should not require anticoagulant or antiplatelet therapy, should be cost-effective, should provide adequate blood flow without generating high gradients, and should resist lifelong structural degeneration. As no current valve fulfills all these criteria, alternative approaches continue to emerge. Over the past two decades, the Ozaki procedure has gained attention by providing a large effective orifice area without the need for aortic root enlargement, especially in patients with a small annulus. It is low-cost, does not require long-term anticoagulation, has a relatively short learning curve, and demonstrates reoperation-free rates of approximately 97% at 3 years and 92% at 10 years.
Conclusions: Although further studies are required to evaluate the long-term outcomes of the Ozaki procedure, its early and mid-term results are highly satisfactory, and favorable long-term outcomes are anticipated.
Keywords: Ozaki Procedure, Narrow Aortic Annulus, Aortic Neocuspidization

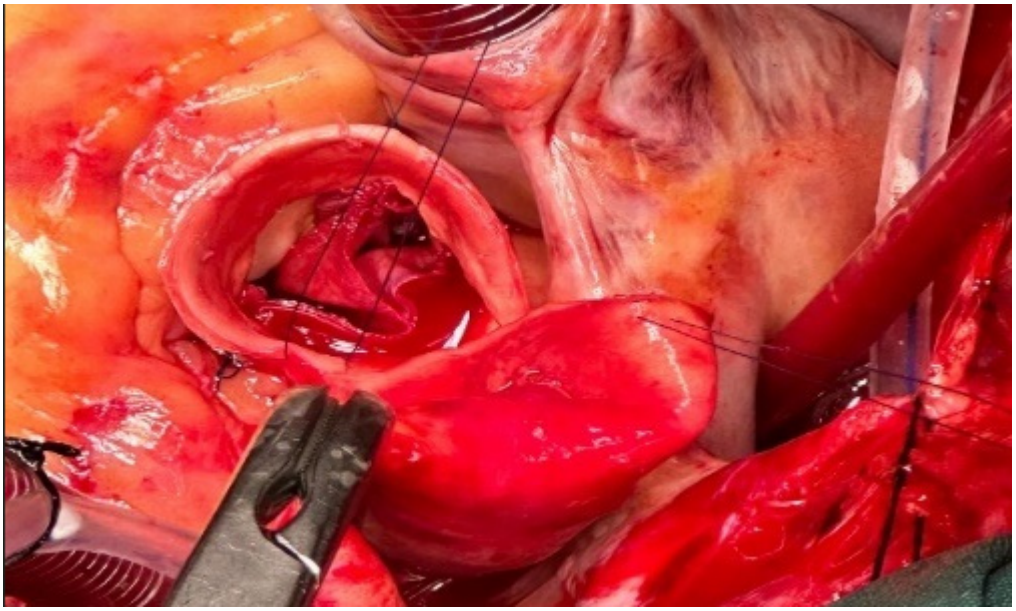

FIGURE 1. **Intraoperative steps of the Ozaki procedure: preparation of autologous pericardium and neocuspidization of the aortic valve.**

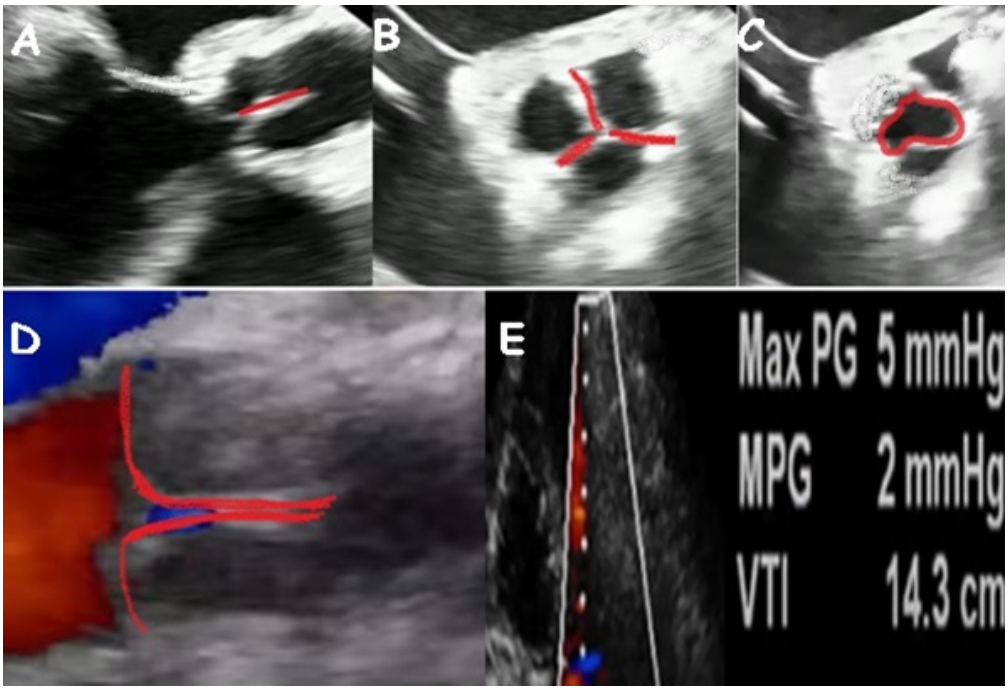

FIGURE 2. **Postoperative echocardiographic assessment showing absence of aortic regurgitation and reduced transvalvular gradient. A: A large coaptation surface when the aortic valve leaflets are closed. B: Appearance of the aortic neocuspid valve when it is closed. C: Large effective aortic orifice area D: Aortic regurgitation, underdeveloped, large coaptation surface. E: Postoperative low aortic gradient.**

OP-64.
Diagnostic Performance of Coronary CT Angiography Compared with Invasive Coronary Angiography and the Impact of Coronary Calcium Score: A Single-Center Real-World Study

Shokhzod Atashev[1], Çetin Alak[1], Alparslan Birdane[1]

[1]Department of Cardiology, Uludag University, Faculty of Medicine, Bursa, Türkiye

Objectives: Coronary artery disease (CAD) remains a leading cause of cardiovascular morbidity and mortality worldwide. Invasive coronary angiography (ICA) is considered the gold standard for evaluating coronary anatomy but carries procedural risks and resource limitations. Coronary computed tomography angiography (CCTA) has emerged as a reliable non-invasive alternative with high sensitivity and strong negative predictive value (NPV), particularly for excluding obstructive CAD. However, diagnostic accuracy may be affected by coronary calcification. This single-center real-world study aimed to evaluate the diagnostic performance of CCTA compared with ICA and to assess the impact of coronary calcium score on accuracy.
Methods: In this retrospective study conducted between January 2018 and January 2025 at Bursa Uludag University, 193 patients with suspected stable CAD who underwent both CCTA and ICA were analyzed. Demographic characteristics, cardiovascular risk factors, and imaging findings were retrieved from hospital records. CCTA examinations were performed using a 128-slice CT scanner with retrospective ECG gating, and stenosis severity was classified according to CAD-RADS. ICA findings were evaluated independently by two experienced observers blinded to CCTA results. Significant stenosis thresholds of ≥50% and ≥70% were used as reference standards. Sensitivity, specificity, positive predictive value (PPV), and negative predictive value (NPV) were calculated on a patient-, vessel-, and segment-based level. Statistical significance was set at $p<0.05$.
Results: On a patient-based analysis, CCTA demonstrated high sensitivity (92.7%) and NPV (88%) for detecting ≥50% stenosis, while specificity was lower (39.6%). For ≥70% stenosis, sensitivity remained high (88.3%) with an NPV of 91.3%, confirming strong rule-out capability for severe disease. Vessel-based analysis showed the highest sensitivity in the LAD (88.1% for ≥50% stenosis), whereas sensitivity was lower in the LCX and RCA. Negative predictive value remained high across all vessels, indicating that a normal CCTA reliably excluded significant stenosis. Segment-based analysis revealed high specificity and NPV (>92%) but lower sensitivity, likely reflecting limitations related to motion artifacts and heavy calcification in small segments. Coronary calcium score had a significant impact on diagnostic accuracy. In patients with a calcium score of zero, sensitivity, specificity, and NPV for ≥70% stenosis were all 100%, suggesting that ICA could potentially be avoided in this subgroup. Increasing calcium burden was associated with a marked decline in specificity and PPV, with the highest false-positive rate observed in the 101–300 score range. Among clinical risk factors, smoking was significantly associated with both moderate and severe stenosis ($P<0.05$). Lower HDL, higher creatinine levels, and reduced ejection fraction were more common in patients with significant disease. CCTA also detected extracardiac findings—including pulmonary nodules, pulmonary artery dilatation, and aortic calcification—that were not identified by ICA.
Conclusions: In this single-center real-world cohort, CCTA demonstrated high sensitivity and strong NPV, making it a reliable non-invasive tool for excluding obstructive CAD in patients with suspected stable disease.

Diagnostic accuracy was particularly high in patients with a zero calcium score, whereas increasing calcification reduced specificity and increased false-positive findings. Careful patient selection is essential when using CCTA as an

Keywords: Coronary Artery Disease, Invasive Coronary Angiography, Coronary Computed Angiography, Coronary Calcium Score